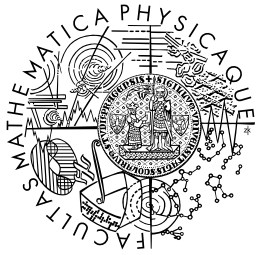

FACULTY
OF MATHEMATICS
AND PHYSICS
Charles University

DOCTORAL THESIS

Lukáš Polcar

Weyl metrics and their generalizations: classical and quantum viewpoint

Institute of Theoretical Physics

Supervisor of the doctoral thesis: RNDr. Otakar Svítek, Ph.D.

Study programme: Physics

Study branch: Theoretical Physics, Astronomy and Astrophysics

Prague 2023

I declare that I carried out this doctoral thesis independently, and only with the cited sources, literature and other professional sources. It has not been used to obtain another or the same degree.

I understand that my work relates to the rights and obligations under the Act No. 121/2000 Sb., the Copyright Act, as amended, in particular the fact that the Charles University has the right to conclude a license agreement on the use of this work as a school work pursuant to Section 60 subsection 1 of the Copyright Act.

In ..... date ....

Author's signature

First I would like to thank my supervisor Dr. Otakar Svítek for his advices and guidance during my doctoral studies. Furthermore I would like to thank Dr. Georgios Lukes-Gerakopoulos and Dr. Vojtěch Witzany for their ideas and and help during my studies of gravitational waves. My thanks also belong to Dr. Morteza Kerachian and Viktor Skoupý for their collaboration on our common publication. I would also like to express my gratitude to Dr. Niels Warburton and UCD relativity group for their hospitality during my stay in Dublin. Finally I would like to dedicate this thesis to my closest family for their continuous support throughout my entire life.

Title: Weyl metrics and their generalizations: classical and quantum viewpoint

Author: Lukáš Polcar

institute: Institute of Theoretical Physics

Supervisor: RNDr. Otakar Svítek, Ph.D., Institute of Theoretical Physics

Abstract: In this thesis, we study two distinct topics both connected to stationary axially symmetric spacetimes. The first is a study of an exact solution sourced by phantom scalar field. This solution can be derived from the well-known Curzon-Chazy metric and has several unusual features. It is a spherically symmetric wormhole which is however not symmetric with respect to its throat, it possesses a non-scalar curvature singularity and functions as a one-directional time machine. The energy content of the spacetime is examined and various other properties are discussed. The remaining parts are dedicated to extreme mass ratio inspirals in two stationary axially symmetric spacetimes, perturbed Schwarzschild and Kerr. The canonical perturbation theory was used to transform the respective geodesic Hamiltonian to action-angle coordinates allowing us to evolve flux-driven inspirals in both spacetimes.

Keywords: Weyl solutions with scalar field, wormholes, gravitational energy, gravitational waves, action-angle coordinates, canonical perturbation theory, extreme mass ratio inspiral

Contents

Introduction

For the past seven years, all of my research in general theory of relativity had a single common denominator, stationary axially symmetric spacetimes. This started already during my bachelor and master studies where I encountered the Weyl metric for the first time. The focus of my work at that time was motion of test particles in spacetimes describing superposition of Schwarzschild black hole with various discs or rings using analytical methods capable of detecting onset of chaotic behaviour. The results were then published in the form of two papers, [67] and [66] (which are naturally not part of this thesis). It was during that times that I became familiar with some parts of the theory of dynamical systems.

The aim of this thesis was to build upon this knowledge of Weyl solutions and expand my study of theses spacetimes beyond the motion of test particles following geodesics. One of the directions I wanted to pursue was studying spacetimes with test-fields or spacetimes directly sourced by matter fields. After some considerations I settled on the solutions sourced by scalar field. While I was studying exact solutions of the Einstein's equations I returned to the test particles, this time using the methods of canonical perturbation theory which eventually led me to gravitational waves and extreme mass ratio inspirals (EMRI).

The final part of this dissertation was supposed to concern a quantization of axially symmetric spacetimes. For that purpose I was studying literature on loop quantum gravity with a plan to formulate the constraints of general relativity in reduced Ashtekar variables adapted to the axial symmetry as was done in [28] and [29] but this time with inclusion of scalar field. Unfortunately I was unable to realize these plans as my attention gradually shifted more and more towards studies of gravitational inspirals. The original results of this thesis were thus obtained in the field of exact spacetimes (summarized in publication [68]) and in the area of gravitational waves where two papers were produced, [69] and [46].

Let us now return to the exact solutions with scalar field, in my studies of these solutions I was greatly inspired by the paper [32] which reviews many of the known Weyl metrics as well as techniques of finding new solutions sourced by minimally coupled scalar field and its counterpart with negative energy density (called phantom scalar field) using the symmetries of the field equations. After examining different configurations of Curzon-Chazy-type solutions with scalar field, a particular limit in one of the parameters captured my attention. The resulting metric produced in that limit had finite curvature scalars at the coordinate location $r = 0$ yet the phantom scalar field was unmistakeably diverging there. On first sight it looked like that the metric may be extendible through the null hypersurface $r = 0$ but eventually we showed that it is a non-scalar curvature singularity which is something not commonly discussed in the literature. It was also clear that this solution derived from a single Curzon-Chazy "particle" was a spherically symmetric traversable wormhole (not surpirsing when the source was scalar field with negative energy density) which was however not symmetric with respect to its throat unlike the typical wormholes introduced in [60] which became apparent when an embedding diagram was constructed. In contrast to that, the conformal diagram looks symmetric with respect to the throat, looking like two asymptotically flat regions connected by the wormhole. Yet due to

the non-scalar singularity it is possible to reach future timelike infinity in a finite proper time when we approach it from the region containing the singularity which is also very unintuitive result. The energy of the scalar field is negative but the total energy of the spacetime is positive. This prompted me to study different definitions of quasilocal energy to get an insight on the energy content of the spacetime. It was shown that one such energy concept has a reasonable Newtonian interpretation in relation to the geodesic equation yet this description is not without problems. This wormhole solution can be generalized to multiple Curzon-Chazy particles [31] forming a class of solutions that is static but besides that lacking any other symmetry in general. This class of solutions is analogous to the Majumdar-Papapetrou class of electrovacuum solutions. It is thus interesting to observe that the phantom scalar class of solutions is composed of wormholes each with a region equipped with a singularity analogously to the electromagnetic class is containing extreme Reissner-Nordström black holes which have singularity as well.

The other results of this thesis are in the field of gravitational waves which has undergone rapid development over the past years starting from their first historical detection [1] by the ground based LIGO detector in 2015. From that moment astrophysicists are no longer reliant predominantly on the electromagnetic spectrum but can now study the universe using signals in the form of gravitational waves which enables them to test general relativity itself in the strong field regime. So far the detectors observed gravitational waves from inspiraling binaries (of black holes or neutron stars) with comparable masses, a new generation of space based detectors such as LISA [3] (expected to launch in 2030s) should be able to detect the so called extreme mass ratio inspirals (EMRI) where the ratio of masses $\varepsilon = m/M$ of the two objects is less than 10^{-4}. Space based detectors are constructed for detecting lower frequencies of gravitational waves from EMRIs. Additionally, these inspirals will take much longer (number of orbital cycles is proportional to ε^{-1}), this has a great implication for modelling these events using numerical relativity, which becomes computationally expensive. This is the reason why other approaches such as post-Newtonian (PN) expansions, black hole perturbation theory or effective one-body (EOB) formalism are being developed.

Over the last few decades a substantial progress has been made by reaching higher and higher orders in PN expansions while investigating second-order self-force contribution in the perturbation theory. On this journey more effects such as spin of the secondary body [79] have been incorporated to the models with other possible influences (presence of other fields [53]) being considered recently. What is however often omitted from the debate is an astrophysical perturbation to the spacetime in which we study the inspiral, this may have a form of ring, disc, dark matter halo etc. This was the motivation of my work. The inspirals were modelled using the adiabatic approximation which means solving the geodesic equation of the background and calculating the fluxes of constants of motion. As a perturbed spacetime may not have a complete set of integrals of motion we chose to solve this problem by approximately transforming the corresponding Hamiltonian into action-angle coordinates by the means of canonical perturbation theory. The resulting integrable Hamiltonian thus approximates the original non-integrable one and the solution to the geodesic equation can be explicitly written using analytical formulas as $x^i = x^i(t, J^k)$ where J^k are the action vari-

ables whose fluxes we may then compute. The action-angle coordinates are often discussed in literature in the context of two-timescales [38] but are rarely used in practice. One of the few examples where they were used to study perturbation (without calculating the fluxes) was in [62] where the implementation was mostly numerical.

My first work on inspirals is summarized in [69] where the background spacetime was described by Schwarzschild metric perturbed by presence of distant matter while the fluxes were calculated using quadrupole formalism. Although it was in a sense a simple model we could qualitatively study the effect of distant matter located at the equatorial plane on the inspiralling body. The next plan was to use black hole perturbation theory, with which I was unfamiliar at that time. However, I obtained the necessary knowledge during my four-month stay with the relativity group at University College Dublin where I studied the Teukolsky formalism (which included solving the radial Teukolsky equation using the Sasaki-Nakamura approach) and even caught a small glimpse of self-force in the form of a scalar toy model from the paper [91] whose results I reproduced. The resulting paper [46], on which I collaborated mostly with Morteza Kerachian, was focusing on EMRI in Kerr spacetime where we tried to test the geodesic approximation to its limits showing that the Teukolsky amplitudes and fluxes calculated from the perturbatively obtained geodesics are not accurate for large eccentricities.

The rest of this thesis is organized as follows. The first chapter introduces the stationary axially symmetric metric and its special static case, the Weyl metric. Various spacetimes belonging to this class are discussed as well as some methods of generating new solutions such as the Janis-Newman algorithm. The second chapter reviews various concepts of energy in general relativity, the stress-energy pseudotensors, the quasi-local energy and finally the energy carried by the gravitational waves. The third chapter focuses on the canonical perturbation theory and extreme mass ratio inspirals or to be more specific it presents the two timescales approach and the adiabatic approximation which requires only the knowledge of the gravitational-wave fluxes to evolve an EMRI. Two methods to calculate the fluxes are then discussed in the remaining parts of the chapter. The last three chapters contain three of our publications, each of which is accompanied by a brief summary/commentary at the beginning of the respective chapter.

1. Stationary and axially symmetric spacetimes

In this chapter we will introduce a general form of stationary and axially symmetric metric and review some spacetimes belonging to this class of solutions of Einstein's equation. Then we will restrict ourselves to the static subclass of solutions described by the Weyl metrics. We will also mention the Janis-Newman algorithm as a bridge between static and stationary solutions. The spacetimes discussed here are mostly those relevant to our three papers [68], [69] and [46].

1.1 General stationary and axially symmetric metric

1.1.1 Postulating two symmetries

We will start this general section by establishing the notion of two symmetries which shall from now on be imposed on our spacetime manifold $\mathcal{M}$. The spacetimes studied in this thesis are stationary and axially symmetric. The symmetries will let us express the general form of metric describing them.

When speaking of spacetime symmetries what we have in mind is that our spacetime metric $g_{\mu\nu}$ is invariant under the action of a one-dimensional Lie group G parametrized by s. The action of the group on the metric is called pullback which can be expressed using the Lie derivative $\mathcal{L}_\xi$ with respect to the vector field ξ

$$\Phi_* = \exp(s\mathcal{L}_\xi). \tag{1.1}$$

The vector field ξ then in turn represents the Lie algebra of G. By requiring that $\Phi_* g_{\mu\nu} = g_{\mu\nu}$ we obtain the equation for ξ

$$\mathcal{L}_\xi g_{\mu\nu} = 0 \tag{1.2}$$

which is the definition of a Killing vector field.

For the spacetime to be stationary it must possess a timelike Killing field $\xi^{(t)}$. The associated group G_t is the group of time translation. A set of orbits $\gamma_x(t)$ representing action of the group G_t on the spacetime $\mathcal{M}$ are then elements of a 3-dimensional manifold Σ_3. This can be characterized by a map Ψ

$$\Psi : \mathcal{M} \to \Sigma_3, \;\; x \to \Psi(x), \tag{1.3}$$

which associates orbit γ_x to each point x in spacetime. This splitting of our manifold $\mathcal{M}$ (as described in [81]) into orbits of time translation group and to the quotient space $\Sigma_3 = \mathcal{M} \setminus G$ can be followed by splitting the metric into the metric $h_{\mu\nu}$ on Σ_3 and the part given by the Killing field

$$g_{\mu\nu} = h_{\mu\nu} + f^{-1}\xi^{(t)}_{\mu}\xi^{(t)}_{\nu}, \;\; f = \xi^{(t)}_{\mu}\xi^{(t)\mu}. \tag{1.4}$$

where $h_{\mu\nu}$ satisfies $\xi^{(t)\mu}h_{\mu\nu} = 0$ and $\mathcal{L}_{\xi^{(t)}}h_{\mu\nu} = 0$. This definition can be extended to general tensors on Σ_3.

By defining the time coordinate t as the Killing time which means that $\xi^{(t)} = \partial_t$, or rather $\xi^{(t)\mu} = \delta^{\mu}_0$, the general stationary metric has the form

$$\begin{aligned} \mathrm{d}s^2 &= f(\mathrm{d}t + A_i\mathrm{d}x^i)^2 + h_{ij}\mathrm{d}x^i\mathrm{d}x^j \\ \xi^{(t)}_0 &= g_{00} = f, \;\; \xi^{(t)}_i = g_{0i} = fA_i \end{aligned} \tag{1.5}$$

where all metric functions depend only on the three remaining coordinates x^i.

We can now add axial symmetry to the picture. This time the symmetry is with respect to G_ϕ which is a rotation group isometric to $SO(2)$. Following [52] we can describe the action of the group by the map Φ.

$$\Phi : G_\phi \times \mathcal{M} \to \mathcal{M}, \;\; (\phi, x) \to \Phi(\phi, x) \tag{1.6}$$

The map also defines the set of fixed points which is the axis of symmetry W_2

$$\exists W_2, \;\; q \in W_2 : \Phi(\phi, q) = q \;\; \forall \phi \in G_\phi. \tag{1.7}$$

The related Killing field is now $\xi^{(\phi)\mu}$ which generates closed orbits around the axis of symmetry and can be shown to be spacelike close to W_2.

One of the common requirements on the metric is the regularity of the axis. This condition means that the square of the norm of the Killing vector $X = \xi^{(\phi)\mu}\xi^{(\phi)}_{\mu}$ satisfies $X \approx \rho_c^2$ at a point close to the axis with ρ_c being the distance from the point to the axis. Only then can the length of the orbit generated by $\xi^{(\phi)\mu}$ be equal to $2\pi\rho_c$. If this is not true it would introduce a deficit angle and a conical singularity at the axis. This type of singularity differs from a curvature singularity in the fact that all tetrad components of the Riemann tensor along any curve approaching the axis are continuous (and therefore finite). Yet the general definition of a spacetime singularity is based on the inability to extend curves (or more specifically geodesics) through a certain point(s) of the spacetime which is what happens here as well. The simplest example of this is the cone which is everywhere flat but one cannot globally extend it past its vertex. These quasi-regular singularities are discussed in detail in [23].

The regularity at the axis is assured if the Killing field has this expansion around the axis

$$\xi^{(\phi)\mu}(x^\nu) = (x^\nu - q^\nu)\nabla_\nu\xi^{(\phi)\mu}|_q + \mathcal{O}((x-q)^2) \tag{1.8}$$

where $q \in W_2$. The squared norm X is then

$$X = (x^\mu - q^\mu)(x^\nu - q^\nu)\mathcal{H}_{\mu\nu} + \mathcal{O}((x-q)^3) \tag{1.9}$$

where the tensor $\mathcal{H}_{\mu\nu} = \nabla_\mu \xi^{(\phi)\rho} \nabla_\nu \xi^{(\phi)}_\rho$ can be shown to have a property of being a metric on the vector space orthogonal to the axis when evaluated on the axis (see [52]). The regularity condition can be expressed in a covariant form as

$$\lim_{x \to q} \frac{\nabla_\mu(X) \nabla^\mu(X)}{4X} = 1. \tag{1.10}$$

Since the Killing vectors $\xi^{(t)\mu}$ and $\xi^{(\phi)\mu}$ commute, there exists a surface to which they are both tangent. If in addition the following algebraic property of the Ricci tensor is satisfied

$$\xi^{(t)\mu} R_{\mu[\nu} \xi^{(t)}_\rho \xi^{(\phi)}_{\lambda]} = \xi^{(\phi)\mu} R_{\mu[\nu} \xi^{(t)}_\rho \xi^{(\phi)}_{\lambda]} = 0 \tag{1.11}$$

then it can be shown that the spacetime manifold admits a surface orthogonal to the one spanned by the Killing vectors. (This condition is easy to verify in the vacuum or scalar case.)

Using the orthogonality and associating the coordinate $\phi \in (0, 2\pi)$ with the Killing vector $\xi^{(\phi)} = \partial_\phi$, the metric can then be put into the form

$$\mathrm{d}s^2 = f(\mathrm{d}t + A\mathrm{d}\phi)^2 - f^{-1}(\gamma_{IJ}\mathrm{d}x^I\mathrm{d}x^J + W^2\mathrm{d}\phi^2) \tag{1.12}$$

where everything now depends on the remaining two coordinates x^I. Since any two-dimensional metric is conformally flat we can use the parametrization

$$f = -e^{2U}, \;\; \gamma_{IJ} = e^{2k}\delta_{IJ} \tag{1.13}$$

denoting the coordinates as z and ρ as common in cylindrical coordinates we arrive at the metric at Weyl canonical coordinates (t, ρ, z, ϕ)

$$\mathrm{d}s^2 = -e^{2U}(\mathrm{d}t + A\mathrm{d}\phi)^2 + e^{-2U}(e^{2k}(\mathrm{d}\rho^2 + \mathrm{d}z^2) + \rho^2\mathrm{d}\phi^2) \tag{1.14}$$

with three independent metric functions $U(\rho, z), k(\rho, z)$ and $A(\rho, z)$.

The regularity of the axis in this coordinates is then expressed simply as $\lim_{\rho \to 0} k = 0$.

1.1.2 Field equations and selected solutions

We can now formulate the field equations of stationary axially symmetric spacetime (details can be found in [35] or [81].).

Inserting the metric (1.14) or even the more general form (1.12) into Einstein equations we obtain a system of partial differential equations for the three undetermined metric functions (U, A, k). First we shall restrict ourselves to the vacuum solutions since in that case the field equations have a particularly compact form.

By taking the following parametrization ($f = -e^{2U}$) and using the complex (Ernst) potential $\mathcal{E}$

$$\mathcal{E} = f + \mathrm{i}\varphi, \quad \varphi_{,\rho} = -\rho^{-1} f^2 A_{,z}, \quad \varphi_{,z} = \rho^{-1} f^2 A_{,\rho} \tag{1.15}$$

one can write down the system of equations for U and A as a single covariant equation

$$(\mathcal{E}+\bar{\mathcal{E}})\nabla^2\mathcal{E} = 2(\nabla\mathcal{E})^2. \tag{1.16}$$

This is the Ernst equation and by covariant we mean that the d'Alembert (or in this case Laplace) operator and gradient are defined using the covariant derivative with respect to the metric (1.14). The last metric function k (its gradient to be precise) is then completely determined by the Ernst potential

$$k_{,\rho} = \frac{1}{4}\rho f^{-2}(\mathcal{E}_{,\rho}\bar{\mathcal{E}}_{,\rho} + \mathcal{E}_{,z}\bar{\mathcal{E}}_{,z}) \qquad k_{,z} = \frac{1}{4}\rho f^{-2}(\mathcal{E}_{,\rho}\bar{\mathcal{E}}_{,z} - \mathcal{E}_{,z}\bar{\mathcal{E}}_{,\rho}), \tag{1.17}$$

These equations are integrable and the metric function k can be written as a line integral (often with the regularity condition $k|_{\rho=0} = 0$). The procedure to find a vacuum solution is then to first solve the Ernst equation (1.16) and then obtain $k = k(U,\omega)$ from (1.17) which is a straightforward task.

Let us now briefly touch solutions which were relevant in our research. The first one is the Kerr solution which is to this day the most astrophysically significant model of a black hole. The metric is most commonly expressed in the Boyer-Lindquist coordinates which are related to the Weyl coordinates by

$$\rho = \sqrt{r^2 - 2Mr + a^2}\sin(\theta), \qquad z = (r-M)\cos(\theta). \tag{1.18}$$

The BL coordinates cover the entire spacetime manifold unlike the Weyl coordinates and the metric (1.14) which describes only the stationary region of the spacetime or to be more specific, the part located above the (outer) horizon which is a segment on the axis in the Weyl coordinates. The Kerr metric is then

$$\begin{aligned} ds^2 = &-\left(1 - \frac{2Mr}{\Sigma}\right)dt^2 + \frac{\Sigma}{\Delta}\,dr^2 + \Sigma\,d\theta^2 \\ &+\left(r^2 + a^2 + \frac{2Ma^2r}{\Sigma}\sin^2\theta\right)\sin^2\theta\,d\phi^2 \\ &-\frac{4Mar}{\Sigma}\sin^2\theta\,dt\,d\phi, \end{aligned} \tag{1.19}$$

where a is the Kerr parameter corresponding to the spin of the black hole J by relation $a = \frac{J}{M}$ and M is its mass, while

$$\Delta = r^2 - 2Mr + a^2, \qquad \Sigma = r^2 + a^2\cos^2\theta. \tag{1.20}$$

It was shown that this is the only vacuum solution describing an asymptotically flat stationary black hole spacetime with nondegenerate horizon [72]. The Kerr metric is also algebraicly special (type D), its curvature tensor can be written using a single Weyl scalar, Ψ_2. In addition to the symmetries of the stationary axially symmetric spacetimes, the Kerr solution possesses a Killing tensor. The contraction of the four-momenta vectors with this tensor gives an integral of geodesic motion, the famous Carter constant [77]. This allows for the separability

of the geodesic equation but this also applies for the equation governing the linear perturbations around the Kerr background (Teukolsky equation). This greatly simplifies the calculations as is discussed in the chapter 3 and our submitted publication [46]

Apart from the Kerr metric we have also encountered the setting in which a Schwarzschild black hole was perturbed by a surrounding matter in the form of a ring or a disc. Even though the black hole itself is static the surrounding matter consists of particles orbiting the black hole and so they necessarily have a non-zero angular momentum. It is thus natural to study this in the framework of stationary and axially symmetric spacetimes.

Such spacetimes were considered in [22] and [92], where a different form of metric was adopted, the so-called Carter-Thorne-Bardeen form

$$\mathrm{d}s^2 = -e^{2\nu}\mathrm{d}t^2 + \rho^2 B^2 e^{-2\nu}(\mathrm{d}\phi + \omega \mathrm{d}t)^2 + e^{2\xi - 2\nu}(\mathrm{d}\rho^2 + \mathrm{d}z^2) \tag{1.21}$$

with an additional function B present. Although the metric possesses the same symmetries as (1.14) one should keep in mind that the coordinates ρ and z are different from the Weyl canonical coordinates while the functions ν and ξ are analogous to U and k respectively. It is interesting to note that in these ρ and z coordinates the Schwarzschild metric is spherically symmetric which means we can use the euclidean transformation relations $\rho = r\sin(\theta)$, $z = r\cos(\theta)$ instead of (1.18) (The coordinate r here corresponds to isotropic coordinates).

The system of field equations is then (considering only a ring or disc located at the equatorial plane)

$$\begin{aligned} \nabla \cdot (\rho \nabla B) &= 0, \\ \nabla \cdot (B \nabla \nu) - 2B^3 \rho^2 e^{-4\nu}(\nabla \omega)^2 &= 4\pi B e^{2k-2\nu}(T^\phi_\phi - 2\omega T^t_\phi - T^t_t), \\ \nabla \cdot (B^3 \rho^2 e^{-4\nu} \nabla \omega) &= -16\pi B e^{2k-2\nu} T^t_\phi. \end{aligned} \tag{1.22}$$

The metric function ξ is, like k, fully determined by the other two metric functions and can be written as a line integral.

In [22] and [92] it was shown that these equations can be solved using a perturbative expansion around the Schwarzschild solution. For that reason they chose B to be a spherically symmetric function

$$B = 1 - \frac{M^2}{4r^2}. \tag{1.23}$$

They then expanded the metric functions in the mass ratio $\varepsilon = m/M$ where m is the mass of the ring/disc. The two independent functions $F^1 = \nu$ and $F^2 = \omega$ are then inserted in the form $F^I = \sum_n \varepsilon^n F^I_n$ into the system (1.22).

The zeroth order corresponds to the Schwarzschild solution ($\omega_0 = 0$). For the first order contributions F^I_1 the equations (1.22) for ν and ω decouple from each other and since they are also linear, it is possible to find the Green's function for each metric function F^I_1.

The solution using the Green's function G^I can be expressed as

$$F_1^I(x,\theta) = \int_1^\infty \int_{-1}^1 S^I(x_0,\theta_0) G^I(x,\theta,x_0,\theta_0) \mathrm{d}x_0 \mathrm{d}(\cos(\theta_0)) \tag{1.24}$$

where S^I is a source term given by the components of stress-energy tensor while the new coordinate x is related to r as $x = \frac{r}{M}\left(1 + \frac{M^2}{4r^2}\right)$. The particular form of the Green's function is quite long and it is expressed using elliptic integrals so we will not include them here but they are written explicitly in [22].

In our particular case [69] we chose the perturbing matter to be a ring for simplicity, which means that the resulting metric functions ν and ω are proportional to their respective Green's functions ($F_1^I(x,\theta) = K^I G^I(x,\theta,x_0,\frac{\pi}{2})$) with the coefficients K^I being given by the mass and angular momentum of the ring respectively.

Our aim was to include the influence of the ring, located far from the black hole, on the geodesic motion close to it. For simplicity the ring was placed at the infinity which enabled us to asymptotically expand the Green's functions and compare the contributions to ν and ω. In that analysis it turned out that the first non-constant term of ν is of the order x_0^{-3} while for ω it is $x_0^{-9/2}$ which allowed us to neglect the non-constant part of ω and consider only ν. The constant terms were then eliminated by a coordinate transformation into co-rotating coordinates leaving us with a static metric. The Hamiltonian associated with this metric was then sufficiently simple to implement the approximate transformation to action-angle coordinates (as discussed in chapter 3).

1.1.3 Janis-Newman algorithm

Before closing this section let us discuss a method which could in principle serve as a technique for generating stationary axially symmetric metric from a spherically symmetric metric. This trick was first employed by Janis and Newman in [61] to successfully recover the Kerr metric (1.19) from its static limit, the Schwarzschild metric. They then proceeded to do the same for the Reissner-Nordström solution and obtained its rotating counterpart, the Kerr-Newman solution. Since its initial success however there were numerous attempts to employ the method but the results were questionable to say the least.

We are now going to present a generalized form of Janis-Newman algorithm (as described in [24]) which starts from the following seed metric which is static and spherically symmetric

$$\begin{aligned} \mathrm{d}s^2 = -f_t(r)\mathrm{d}t^2 + f_r(r)\mathrm{d}r^2 + f_\Omega(r)\mathrm{d}\Omega^2. \\ \mathrm{d}\Omega^2 = \mathrm{d}\theta^2 + (H(\theta))^2\mathrm{d}\phi^2 \end{aligned} \tag{1.25}$$

where $H(\theta)$ can be equal to $\sin(\theta)$ or $\sinh(\theta)$. Let us mention that there exists an extension for the case when a gauge field is present (like in the Reissner-Nordström case) but we will only include scalar fields which are treated like the metric functions $f_i(r)$.

The next step is to transform to null coordinates

$$\mathrm{d}t = \mathrm{d}u - \sqrt{\frac{f_r}{f_t}}\mathrm{d}r \tag{1.26}$$

to eliminate the metric component g_{rr}

$$\mathrm{d}s^2 = -f_t \mathrm{d}u^2 - 2\sqrt{f_r f_t}\mathrm{d}u\mathrm{d}r + f_\Omega \mathrm{d}\Omega^2. \tag{1.27}$$

Now comes the crucial and non-trivial step, complexification of coordinates r and u and transformation of the form

$$r = r' + \mathrm{i}F(\theta), \;\; u = u' + \mathrm{i}G(\theta). \tag{1.28}$$

where the functions $F(\theta)$ and $G(\theta)$ are to be determined later (In the original J-N trick, i.e. in the Kerr case, we had $F(\theta) = -G(\theta) = a\cos(\theta)$). Now, the original form of the trick involved expressing the metric in the Newman-Penrose tetrad which itself is complex but still transforms as vectors when we perform the change of coordinates (1.28). We can however simply avoid this by using the ansatz by Giampieri which was proved to be completely equivalent to it according to [24]

$$\mathrm{i}\mathrm{d}\theta \to H(\theta)\mathrm{d}\phi. \tag{1.29}$$

This is then combined with the differentiated form of the transformation relations (1.28). Apart from the tensorial structure of the metric (1.25) we also have to transform the metric functions $f_i(r)$ in such a way that they remain real since in the end we would like to obtain a real metric. There is no unique way how to do it but for simple functional forms we can use the following prescriptions

$$\begin{aligned} r &\to \frac{1}{2}(r + \bar{r}) \\ \frac{1}{r} &\to \frac{1}{2}\left(\frac{1}{r} + \frac{1}{\bar{r}}\right) \\ r^2 &\to r\bar{r} \end{aligned} \tag{1.30}$$

where $\bar{r}$ is complex conjugate to r. The new metric functions obtained in this fashion are denoted as $\bar{f}$. If a scalar field is present then the same transportation applies to it as well, $\Phi \to \bar{\Phi}$. Putting all this together we obtain a new metric in null coordinates. We can then proceed by eliminating the $g_{u'r'}$ and $g_{r'\phi}$ components of the metric by the transformations $u' \to t'$ and $\phi \to \phi'$ which are analogous to (1.26). These are the Boyer-Lindquist coordinates in which the result reads

$$\mathrm{d}s^2 = -\bar{f}_t(\mathrm{d}t' + \omega H \mathrm{d}\phi')^2 + \frac{\bar{f}_\Omega}{\Delta}\mathrm{d}r'^2 + \bar{f}_\Omega(\mathrm{d}\theta^2 + \sigma^2 H^2 \mathrm{d}\phi'^2) \tag{1.31}$$

$$\omega = \frac{\mathrm{d}G}{\mathrm{d}\theta} + \sqrt{\frac{\bar{f}_r}{\bar{f}_t}}\frac{\mathrm{d}F}{\mathrm{d}\theta}, \quad \sigma^2 = 1 + \frac{\bar{f}_r}{\bar{f}_\Omega}\left(\frac{\mathrm{d}F}{\mathrm{d}\theta}\right)^2, \quad \Delta = \frac{\bar{f}_\Omega}{\bar{f}_r}\sigma^2. \tag{1.32}$$

We have thus obtained a metric which is stationary and axially symmetric, in ideal case it is a rotating counterpart of the original metric (1.25) but the problem is that this is not in general an on-shell transformation i.e. it does not map a

solution to a solution. While the form of the algorithm remains the same the matter content of the spacetime or even the gravitational theory (the equations of motion) can be vastly different. It is not clear how should the field equations enter the picture so it cannot be ensured that they can be satisfied even for the general ansatz (1.28). It was shown in [18] however that for the Einstein-Maxwell theory the only type D solution that can be found using the algorithm is the Kerr-Newman solution while for the perfect fluid the only possible solution is the Kerr metric (which implies vacuum solution only).

In our calculation we wanted to apply this to scalar field spacetime, instead of the most famous JNW we opted for one of its limits belonging to a class of solutions derived in [31] sourced by a minimally-couple massless scalar field (This solution is in detail discussed in our publication [68].) .

$$\mathrm{d}s^2 = -e^{-\frac{2m}{r}}\mathrm{d}t^2 + e^{\frac{2m}{r}}(\mathrm{d}r^2 + r^2\mathrm{d}\Omega^2), \qquad \Phi = \pm\frac{m}{r} \tag{1.33}$$

on which I tried to apply the Janis-Newman trick since it is quite a simple solution when compared to the more general Janis-Newman-Winicour solution. If we perform the transformations discussed above, we can actually use the Einstein's equations and determine the functions F and G to be

$$F(\theta) = 0, \qquad G(\theta) = a\ln\left(\frac{1-\cos(\theta)}{\sin(\theta)}\right) + b \tag{1.34}$$

which means that the new metric

$$\mathrm{d}s^2 = -e^{-\frac{2m}{r}}(\mathrm{d}t + a\mathrm{d}\phi)^2 + e^{\frac{2m}{r}}(\mathrm{d}r^2 + r^2\mathrm{d}\Omega^2), \qquad \Phi = \pm\frac{m}{r} \tag{1.35}$$

is a solution. The scalar field and the metric functions depending on r are unchanged due to the trivial solution $F(\theta) = 0$. After a quick review however we can see that we obtained the same spacetime but in a rotating frame, using the transformation $t = t' - a\phi$ we get the original metric (1.33), a similar case to the Minkowski metric which is mapped on itself as well by the algorithm. This is then just one of many unsuccessful attempts to obtain a new solution using the J-N trick, according to the summary in [24] very few new solutions apart from the Kerr-Newman metric were found using the algorithm, most of them were derived from the Schwarzschild metric in higher dimension or by adding non-minimally coupled scalar fields (axion–dilaton) or by adding other gauge fields (Einstein-Yang-Mills theory).

1.2 Static case: Weyl metrics

We can now restrict ourselves to the case of static axially symmetric spacetimes which are commonly described by the Weyl family of metrics. In physics, the term static usually means that the system is time-independent (stationary) and also symmetric with respect to the time reversal. In the general-relativistic formalism this means that there exists a time-like Killing vector field $\xi^{(t)}_\mu$ which is hypersurface-orthogonal, this means the vector field is proportional to a gradient of a function [81] or alternatively that the vorticity of the congruence defined by

$\xi^{(t)}_\mu$ is zero. In coordinates adapted to the problem this means $g_{0i} = 0$ and for our stationary axially symmetric metric (1.14) this yields $A = 0$ leaving us with the Weyl metric

$$\mathrm{d}s^2 = -e^{2U}\mathrm{d}t^2 + e^{-2U}(e^{2k}(\mathrm{d}\rho^2 + \mathrm{d}z^2) + \rho^2\mathrm{d}\phi^2). \tag{1.36}$$

The metric contains two functions which are to be determined by the field equations. The function U is often called gravitational potential as it has that very meaning in the Newtonian limit of the geodesic equation and also due to the fact that in vacuum it is a solution to the Laplace equation (this is case also for a general static spacetime [32].

It is not surprising that the functions k is fully determined by U. The field equations for the spacetime then read

$$U_{,\rho\rho} + \frac{1}{\rho}U_{,\rho} + U_{,zz} = 0, \tag{1.37}$$

$$k_{,\rho} = \rho\Big((U_{,\rho})^2 - (U_{,z})^2\Big), \quad k_{,z} = 2\rho U_{,\rho}U_{,z}. \tag{1.38}$$

A key aspect of the equation (1.37) is the fact that they are linear which allows for straightforward superposition of two solutions in U. The nonlinearity of the Einstein's equations is however preserved in the other metric function k which however can be calculated as a quadrature once U is found. Thus when superposing two sources the result is $U = U_1 + U_2$ and $k = k_1 + k_2 + k_{12}$ where k_{12} is often called the interaction part of k.

1.2.1 Vacuum solutions: rods and point particles

In the vacuum the first step is to solve the Laplace equation (1.37), this can be done using the same methods as in Newtonian case since the equation is the same as in cylindrical coordinates of a flat space. One of the approaches is to solve equation (1.37) in spherical coordinates using separation of variables. The angular part is then solved using the spherical harmonics which in this (real) case are given by the Legendre polynomials P_n evaluated at $\cos(\theta)$ while the radial part can be written for an asymptotically flat spacetime as $r^{-(n+1)}$. A general solution vanishing at the infinity is then a linear combination of such solutions

$$U = \sum_{n=0}^{\infty} a_n r^{-(n+1)} P_n(\cos(\theta)), \tag{1.39}$$

the corresponding k is then

$$k = -\sum_{l,m=0}^{\infty} a_l a_m \frac{(l+1)(m+1)}{l+m+2}\frac{P_l P_m - P_{l+1}P_{m+1}}{r^{l+m+2}}. \tag{1.40}$$

Similarly to the previous section on stationary and axially symmetric spacetimes we shall now go through solutions which were relevant (or have some connections) to our research. The first is the Curzon-Chazy solution which is given by the first

term in the expansion (1.39). The function U is thus just a Newtonian potential of a point particle the metric however is not spherically symmetric since the corresponding k function in (1.40) depends on θ as well. In Weyl coordinates the solution is then

$$U = -\frac{m}{r}, \quad k = -\frac{m^2\rho^2}{2r^4} = -\frac{m^2\sin^2(\theta)}{2r^2}, \qquad r = \sqrt{\rho^2 + z^2}. \tag{1.41}$$

The most characteristic property of this spacetime is the direction-dependent singularity located at $r = 0$. When this coordinate point is approached by a geodesic from the equatorial plane ($z = 0$) it can be shown that it encounters a curvature singularity and cannot be extended beyond this point. On the other hand if approached along the axis of symmetry, it is possible to pass through the point and enter a new region of the spacetime. This dependence on direction is evident already at the level of Kretschmann scalar

$$K = 8\exp\left(\frac{2m^2\rho^2}{r^4} - \frac{4m}{r}\right)\left(\frac{2m^4\rho^2}{r^{12}}(m^2 - 3mr + 3r^2) + \frac{6m^2}{r^8}(m - r)^2\right). \tag{1.42}$$

To test how the curvature singularity behaves we can calculate the limit $r \to 0^+$ of the expression from different directions. When the origin is approached from the equatorial plane, we have $\rho = r$ which means that the argument of the exponential unction tends to $+\infty$ and K diverges. On the other hand if we go along the axis ($\rho = 0$), the limit of the exponential function as well as that of K is zero.

This points to the fact that the Weyl coordinates are not suitable to describe this part of the spacetime. It is thus convenient to find a new set of coordinates to fully unveil the structure of the singularity. This was done for example by Taylor [85] who used a new pair of coordinates instead of (ρ, z), one of which was the Kretschmann scalar to better visualise a $t, \phi = const.$ plane. In addition Morgan and Szekeres [84] found a transformation to comoving coordinates and subsequently obtained a regular metric when approaching along the axis and showed that the metric can be smoothly connected to the Minkowski metric after passing through this ring-like singularity.

Since the field equation for U is linear one can imagine superposing several Curzon-Chazy particles with each of them lying on the axis of symmetry. The simplest such solution consists of two particles located at $z = \pm m$ which is given by [32]

$$U = -\frac{m_+}{r_+} - \frac{m_-}{r_-}, \quad k = -\frac{m_+^2\rho^2}{2r_+^4} - \frac{m_+^2\rho^2}{2r_-^4} + \frac{m_+m_-}{2m^2}\left(\frac{\rho^2 + z^2 - m^2}{r_+r_-} - 1\right). \tag{1.43}$$

where $r_\pm = \sqrt{\rho^2 + (z \pm m)^2}$. This solutions had similar properties to the single-particle one, the singularities are direction-dependent in a similar fashion but the part of the axis between the two particles is occupied by a conical singularity since the regularity condition on the axis is not satisfied, this suggests an existence of a strut that makes the static two particle-system stable.

Apart from the point-particle solutions we can also consider the spherically symmetric Schwarzschild solution whose metric functions are

$$U = \frac{1}{2}\ln\left(\frac{d_1 + d_2 - 2M}{d_1 + d_2 + 2M}\right), \qquad k = \frac{1}{2}\ln\left(\frac{(d_1 + d_2)^2 - 4M^2}{4d_1 d_2}\right), \tag{1.44}$$

where $d_{1,2} = \sqrt{\rho^2 + (z \mp M)^2}$. The metric function U represents a gravitational potential of a rod located at the axis between $z = -M$ and $z = M$. The Weyl coordinates obviously cover only the static part of the spacetime, the transformation to the spherical Schwarzschild coordinates is given by (1.18) with $a = 0$. From the transformation relations we can see that the horizon of the black hole is represented by the above-mentioned finite rod. This solution can be generalized by assigning an arbitrary "density" to the rod or to be more precise by rescaling the metric functions as $U \to \lambda U$, $k \to \lambda^2 k$. The class of metrics produced by this rescaling is known as Zipoy-Voorhees solution. Unlike its special case, the Schwarzschild metric, the singularity at the rod is not a horizon thorough which we can extend the spacetime but a curvature singularity. By taking an appropriate limit which reduces the rod to a single point of mass m one can recover also the Curzon- Chazy solution (1.41). From the Zipoy-Voorhees metric one can derive another solution by complexifying the mass M and the parameter λ (This means $\lambda \to \mathrm{i}\lambda$.), such a spacetime has a structure of a wormhole [32].

Of course like in the previous case with the Curzon-Chazy solution one can add other rods on the axis and get solutions analogical to (1.43) but what is really important is the fact that we can superpose the Schwarzschild solution with other axially symmetric sources such as rings or discs, the only tricky part here may be finding the function k analytically. One such a notable example is the Bach-Weyl ring whose function U is just a Newtonian potential of a ring with radius b and mass m

$$U = -\frac{2mK(x)}{\pi\sqrt{(\rho + b)^2 + z^2}}. \tag{1.45}$$

where $K(x)$ is the elliptic integral of the first kind,

$$K(x) = \int_0^{\frac{\pi}{2}} \frac{\mathrm{d}\phi}{\sqrt{1 - x^2 \sin^2\phi}}, \qquad x = \sqrt{\frac{4\rho b}{(\rho + b)^2 + z^2}}.$$

It is worth noting that the function (1.45) is the Green's function G^ν in (1.24) which is the consequence of the decoupling of ω and ν at the first order of perturbative expansion of equations (1.22). In our previous studies we have encountered several of these rings and discs when studying geodesic motion in Weyl spacetimes ([67] and [66]) some of which had peculiar properties, for example the proper distance to the Bach-Weyl ring from the region $\rho < b$ is infinite [78]. Overall, while it is possible to take a Newtonian potential and find a corresponding Weyl metric the symmetries and other geometrical properties may not be what one would intuitively expect as was demonstrated on the examples above.

1.2.2 Solutions with scalar field

In our studies we concentrated on solutions sourced by a minimally coupled scalar field, the Lagrangian density of the theory is then

$$\mathcal{L} = (\mathcal{R} - 2\varepsilon\nabla_\mu\Phi\nabla^\mu\Phi)\sqrt{-g} \tag{1.46}$$

where $\varepsilon = \pm 1$ represents the sign of energy density of the field (for $\varepsilon = -1$ the scalar field is often called "phantom"). The vacuum field equations (1.37) and (1.38) are now modified due to the presence of the scalar field

$$U_{,\rho\rho} + \frac{1}{\rho}U_{,\rho} + U_{,zz} = 0, \qquad \Phi_{,\rho\rho} + \frac{1}{\rho}\Phi_{,\rho} + \Phi_{,zz} = 0 \tag{1.47}$$

$$k_{,\rho} = \rho\{\Big[(U_{,\rho})^2 - (U_{,z})^2\Big] + \varepsilon\Big[(\Phi_{,\rho})^2 - (\Phi_{,z})^2\Big]\}, \qquad k_{,z} = 2\rho(U_{,\rho}U_{,z} + \varepsilon\Phi_{,\rho}\Phi_{,z}). \tag{1.48}$$

One of the reasons this theory with scalar field is special is the symmetry of the field equations which allow to easily generate new solutions with scalar field from vacuum solutions. The field equations are symmetric [32] with respect to the rotations for $\varepsilon = 1$ i.e. the (U, Φ) pair is rotated by an angle α while the function k is preserved

$$U \to \cos(\alpha)U + \sin(\alpha)\Phi, \qquad k \to k, \qquad \Phi \to \cos(\alpha)\Phi - \sin(\alpha)U, \tag{1.49}$$

while for the scalar field with negative energy density the equations are invariant under boosts

$$U \to \cosh(\alpha)U + \sinh(\alpha)\Phi, \qquad k \to k, \qquad \Phi \to \cosh(\alpha)\Phi + \sinh(\alpha)U. \tag{1.50}$$

The new solutions thus have one additional parameter α.

In the theory with scalar field it is possible to have only one of the two metric functions (U, k) non-vanishing, which is something that cannot be achieved in the vacuum case where having one of the functions zero means that the spacetime is flat. If $U = 0$, the metric becomes ultrastatic (the hypersurface-orthogonal Killing vector is also covariantly constant). From a vacuum spacetime we can obtain an ultrastatic solution by $\alpha = \frac{\pi}{2}$ in (1.49) for $\varepsilon = 1$ or by using the swap symmetry

$$U \to \Phi, \qquad k \to -k, \qquad \Phi \to U. \tag{1.51}$$

which exists only in the phantom field as is evident by looking at the right-hand side of the equations (1.48). Thus there exist twice as many solutions in the phantom case due to this symmetry [32]. The other interesting limit is when the metric function k is zero which can be achieved in the phantom case by setting $\Phi = U$ (not swapping the two), in such a case the metric can be written in the form

$$\mathrm{d}s^2 = -e^{2U}\mathrm{d}t^2 + e^{-2U}\mathrm{d}l^2 \tag{1.52}$$

where $\mathrm{d}l^2$ is a metric of three-dimensional Euclidean space. From this form it is apparent that this goes beyond the scope of axially symmetric spacetimes. This means that we can superpose solutions to the Laplace equations located anywhere not just on the axis of symmetry. One can thus for example have several Curzon-Chazy particles located anywhere, with their mutual attraction being compensated by the repulsive scalar field. An analogical class of solutions exists in the electro-vacuum case known as the Majumdar-Papapetrou solution [35] whose line element can also be written in the form (1.52).

To give a simple example, consider the Janis-Newman-Winicour solution, a general spherically symmetric solution with minimally coupled scalar field, which can be naturally extended to the phantom case as well. This phantom version then has a special limit with $k = 0$ which is the spherical Curzon-Chazy spacetime (1.33) while the classical scalar field version includes the ultrastatic limit $U = 0$ which after complexifying its mass is in fact the Bronnikov-Ellis wormhole (See our publication [68].).

2. Energy in general relativity

When analysing physical interpretation of the solutions of Einstein's equations one would like to employ tools and concepts established in other branches of physics. One such important concept is energy, a conserved quantity that is associated with time-translation symmetry of the corresponding theory. Since it is related to time it encodes the dynamics of the system in the Hamiltonian formulation thus making it a key piece in studying most physical systems.

Since the conception of general relativity there have been numerous attempts and approaches inspired by the conservation laws in other established field theories. Despite the effort there has been no widely accepted approach to this day, this again underlines the unique position of gravity among other field theories. In the following we will review some of the most important proposals but also summarize the energy-momentum associated with matter fields. We will however not discuss in detail the conservation laws for point particles in general relativity. Suffice to say that for a geodesic motion characterized by four-momentum p^μ, the conserved quantities associated with symmetries of the spacetime can be found by projecting p^μ on a Killing vector or more generally on a Killing tensor (a totally symmetric tensor of rank n satisfying $\nabla_{(\mu}K_{\mu_1\dots\mu_n)} = 0$ [90]).

As mentioned in the previous chapter, in stationary axially symmetric spacetimes there are always two Killing vectors, $\xi^{(t)}$, $\xi^{(\phi)}$ with corresponding integrals of motion, the energy $E = -\xi^{(t)}_\mu p^\mu$ and z-component of angular momentum $L_z = \xi^{(\phi)}_\mu p^\mu$. The most famous solution with a Killing tensor is the Kerr metric with the integral of motion known as the Carter constant. The motion in Kerr spacetime is consequently fully integrable (three independent integrals of motion) which is very useful for calculations as demonstrated in our paper [46].

Let us now return to the realm of field theory. We will consider the gravitational field described by the Einstein-Hilbert action and a matter field φ^A with Lagrangian density $\mathfrak{L}_M = L_M\sqrt{-g}$

$$S = S_{EH}[g_{\mu\nu}] + S_M[\varphi^A, g_{\mu\nu}] = \frac{1}{2\kappa}\int_\Omega R\sqrt{-g}\mathrm{d}x^4 + \int_\Omega \mathfrak{L}_M \mathrm{d}x^4 \tag{2.1}$$

with $\kappa = 8\pi$ in our units. For simplicity we shall assume that $\mathfrak{L}_M$ depends only on the first derivatives of φ^A. From the variational principle $\delta S = 0$ we can derive the equations of motion (Euler-Lagrange equations) for the metric and the field φ^A

$$G_{\mu\nu} = \kappa T_{\mu\nu}, \qquad \frac{\delta S_M}{\delta \varphi^A} = 0. \tag{2.2}$$

From the variational formulation of a theory one can not only obtain the field equations (in this case the Einstein's equations and equations of motion for the matter fields) but also conservation laws provided that the action possesses a symmetry with respect to a continuous group. This is the consequence of the Noether's (first) theorem and is a natural way how to search for conserved quantities which is what we are going to do now starting with the matter fields.

2.1 Energy of matter fields

We shall first look at the action S_M corresponding to a field φ^A in (2.1). In a special-relativistic set-up (i. e. with a fixed Minkowski background) we assume the action to be invariant with respect to the Poincaré group which also means invariance to its subgroup of spacetime translation. To be more specific we consider a transformation of the form $x^\mu \to x'^\mu = x^\mu - K^\mu$ where K^μ is a constant four-vector, the corresponding field then transforms as $\varphi^A(x^\mu) \to \varphi'^A(x'^\mu) = \varphi^A(x^\mu + K^\mu)$. What we have in mind here is an active transformation, not a change of coordinates. An infinitesimally small translation (infinitesimal K^μ) of the field is then $\varphi'^A = \varphi^A + \delta\varphi^A$ with $\delta\varphi^A(x^\nu) = K^\mu \partial_\mu \varphi^A$. The assumption of invariance of the action then means $\delta S_M = S'_M[\varphi'^A(x'^\mu)] - S_M[\varphi^A(x)] = 0$. After a lengthy procedure (expanding the Lagrangian in $\delta\varphi^A$ and using integration by parts) described in many field-theory textbooks (for example in [82]) we arrive at

$$\delta S_M = \frac{\delta S_M}{\delta \varphi^A}\delta\varphi^A + \partial_\mu J^\mu[K] = 0. \tag{2.3}$$

The first term in (2.3) corresponds to the Euler-Lagrange equations and if they are satisfied we are left with $\partial_\mu J^\mu[K] = 0$ which is a continuity equation for a current $J^\mu[K]$ with associated conserved charge given as an integral of $J^0[K]$ over a constant-time surface. The current can be expressed as $J^\mu[K] = \theta^\mu{}_\nu K^\nu$ where $\theta^\mu{}_\nu$ is the canonical stress-energy tensor

$$\theta^\mu{}_\nu = \frac{\partial \mathfrak{L}_M}{\partial(\partial_\mu \varphi^A)}\partial_\nu \varphi^A - \mathfrak{L}_M \delta^\mu{}_\nu. \tag{2.4}$$

Since the translation four-vector is constant and arbitrary, the stress-energy tensor itself satisfies $\partial_\mu \theta^{\mu\nu} = 0$. The choice of the vector K^μ selects the specific conservation law, for a timelike K^μ the conserved quantity is the energy while in the spacelike case it is a component of the momentum vector, thus the equation $\partial_\mu \theta^{\mu\nu} = 0$ describes the conservation of the four-momentum with respect to the basis given by $K^\mu_i = \delta^\mu{}_i$. So we can see that already at this level the right quantity to describe the conservation of energy and momentum is the stress-energy tensor whose components give the densities of these quantities while the integrals give the total four-momentum in a finite volume of the whole spacetime.

This stress-energy tensor is in general not symmetric which is a requirement for conservation of angular momentum but this can be changed by adding a divergence-free vector field to the current (using the Belinfante procedure). In fact when discussing the angular momentum we should mention that the procedure leading to the derivation of (2.3) can be extended to other continuous symmetries like rotation symmetry by applying the Noether theorem, however we shall go one step further by including the gravitational part of the action.

In general relativity not only the Einstein-Hilbert action but also the action for matter fields are constructed in such a way that they are invariant under a general one-parametric diffeomorphism ("active coordinate transformation") which can be represented using integral curves of a generating vector field

$K^\mu(x)$. To clarify this we will assume that $\mathfrak{L}_M$ is a scalar density constructed only from φ^A and $g_{\mu\nu}$ and also that $K^\mu(x)|_{\partial\Omega} = 0$. The coordinate transformation can be written using Lie flow with infinitesimal transformation of the coordinates being $x'^\mu = x^\mu - K^\mu(x^\nu)$. The infinitesimal shift of the field is then $\varphi'^A = \varphi^A + \mathcal{L}_K\varphi^A$ where the Lie derivative of the field can be decomposed as $\mathcal{L}_K\varphi^A = K^\mu\nabla_\mu\varphi^A + S_\mu{}^{\nu A}{}_B\varphi^B\nabla_\nu K^\mu$ where $S_\mu{}^{\nu A}{}_B$ depends on the nature of the field φ^A. This transformation of the fields can be found by linearising the transformation of the field φ^A under this active transformation (linearising pullback and pushforward), the finite transformation can be expressed using exponential of $\mathcal{L}_K$ as mentioned in the chapters 1 and 3.

By employing a useful identity $\mathcal{L}_K(\mathfrak{L}_M) = \nabla_\mu(\mathfrak{L}_M K^\mu)$ ($\mathfrak{L}_M$ is a scalar density), we can derive the generally covariant Noether identity [83]

$$\frac{\delta S_M}{\delta\varphi^A}\mathcal{L}_K\varphi^A + T^{\mu\nu}\mathcal{L}_K g_{\mu\nu} + \nabla_\mu J^\mu[K] = 0 \tag{2.5}$$

where the current $J^\mu[K]$ is given by

$$J^\mu[K] = \theta^\mu{}_\nu K^\nu + (\sigma^{\mu[\rho\nu]} + \sigma^{\rho[\mu\nu]} + \sigma^{\nu[\mu\rho]})\nabla_\rho K_\nu. \tag{2.6}$$

The current has the same form as in the previous case, it contains the canonical stress energy tensor (2.4) where the partial derivatives of the field are now replaced by covariant derivatives. Since the variation of the field discussed now is a general diffeomorphism, there is also another contribution to the current coming from the spin tensor $\sigma^{\mu\rho\nu}$ which is zero only for the scalar field. By including it in the current we can properly formulate the conservation of total angular momentum. The presence of the spin tensor is due to the terms of the Lie derivative involving $\nabla_\nu K^\mu$, the spin tensor then reads [10]

$$\sigma^{\mu\alpha}{}_\beta = \frac{\partial\mathfrak{L}_M}{\partial(\nabla_\mu\varphi^A)}S^\alpha{}_\beta{}^A{}_B\varphi^B. \tag{2.7}$$

The identity (2.5) differs from the original one (2.3) not only by the presence of covariant derivative and spin tensor but also by variation with respect to the metric which produces the tensor

$$T^{\mu\nu} = -\frac{2}{\sqrt{-g}}\frac{\delta S_M}{\delta g_{\mu\nu}}. \tag{2.8}$$

This is the symmetric stress energy tensor used in general relativity which represents the matter in the Einstein equations (2.2) and which is also symmetric. To see how this tensor is connected to the canonical stress-energy tensor we have to look what happens on shell. When the equations of motion are satisfied we arrive at [83]

$$\nabla_\mu T^{\mu\nu} = 0, \;\; T^{\mu\nu} = \theta^{\mu\nu} + \nabla_\rho(\sigma^{\mu[\nu\rho]} + \sigma^{\rho[\mu\nu]} + \sigma^{\nu[\mu\rho]}). \tag{2.9}$$

Both stress-energy tensors ($\theta^{\mu\nu}$ and $T^{\mu\nu}$) are thus related but the partial derivative in the divergence of $T^{\mu\nu}$ is now replaced with covariant one which is the reason

it does not lead to any conservation law as it does not have a form of continuity equation. This can be seen when the divergence is expressed using a partial derivative in some coordinates [54]

$$\nabla_\mu T^\mu{}_\alpha = \frac{1}{\sqrt{-g}}\partial_\mu(\sqrt{-g}T^\mu{}_\alpha) - \frac{1}{2}T_{\mu\nu}\, g^{\mu\nu}_{,\alpha} = 0. \tag{2.10}$$

The first term containing the partial derivative is the desired one and had it not been for the presence of the other term we could have used the Gauss theorem and express the conservation law in its integral form. The special-relativistic form is recovered (as can be expected) only in a local inertial frame where $g^{\mu\nu}_{,\alpha} = 0$. The diffeomorphism invariance thus does not produce any conservation law but it is still possible to have conserved currents in curved spacetime if the spacetime metric possesses a symmetry i.e. if there exists a Killing vector field. In that case we have a conserved current in the form $\partial_\mu(T^{\mu\nu}\xi_\nu) = 0$ which is a direct consequence of the Killing equation$\nabla_{(\mu}\xi_{\nu)} = 0$. Due to the correspondence in (2.9) the current $J^\mu[\xi]$ defined in (2.6) is conserved as well.

We may thus define a quantity $Q[K]$ [44] as an integral over space-like hypersurface Σ with metric γ and normal n_ν

$$Q[K] = \int_\Sigma T^{\mu\nu}K_\mu n_\nu \sqrt{\gamma}\mathrm{d}x^3. \tag{2.11}$$

As discussed above Q represents a conserved quantity only if $Q = Q[\xi]$, ξ being a Killing vector. In particular if it is timelike, than Q is interpreted as energy while inserting a spacelike Killing field would give a component of (angular) momentum. In absence of Killing vectors it is still possible to define energy and momentum even if they are not conserved. For example by inserting the normal n_μ we get $Q[n]$ which is understood as total energy seen by family of observers with fourvelocity n^μ with $T^{\mu\nu}n_\mu n_\nu$ being the energy density at a given point.

2.2 Stress-energy pseudotensors

While the picture for matter is quite clear, in fact it is a straightforward generalization of the special-relativistic approach, we can now look at the identities (2.9) to see what happens for gravity (without matter) as described by the Einstein-Hilbert action in (2.1) which depends only on the spacetime metric. This means that $\theta^\mu{}_\nu = 0$ and $\sigma^{\mu\alpha}{}_\beta = 0$. The result is then

$$\nabla_\mu G^{\mu\nu} = 0. \tag{2.12}$$

These are just the contracted Bianchi's identities (which are already automatically satisfied so it does not provide us with a new information). This means that there is no gravitational stress-energy tensor for gravitational field or, if we take into account matter, that the gravitational field stress energy tensor is just a sum of the matter stress energy tensors which is basically a different statement of Einstein's equations. While the repetition of the procedure described in the previous section does not lead to a stress-energy tensor, we would still like to have an object

representing energy (and momentum) of a gravitational field, even for a spacetime with no Killing vectors as it is precisely this situation in which one would expect a transfer of energy (and momentum) between matter and the gravitational field. If we want to stick to the intuition that the energy and momentum are conserved we would like to preserve the form of continuity equation. This leads us to the concept of gravitational pseudotensors (or complexes) which are typically constructed from the first derivatives of the metric (or equivalently from the Christoffel symbols). This non-tensorial character means that these objects are fully coordinate-dependent and in particular in the inertial frame they vanish which is an expected consequence of the equivalence principle.

We can rewrite the covariant divergence (2.10) as

$$\partial_\mu(\sqrt{-g}T^\mu{}_\alpha) - k_\alpha = 0, \qquad k_\alpha = \frac{1}{2}\sqrt{-g}T_{\mu\nu}\, g^{\mu\nu}_{,\alpha} \tag{2.13}$$

where k_α is the second term which should in principle correspond to gravity however it does not have the form of a divergence. Adopting a fixed (but arbitrary) coordinate system we can rewrite the equation using Einstein's equations into the desired form [58]

$$\theta^\mu{}_\nu = \sqrt{-g}(T^\mu{}_\nu + \tau^\mu{}_\nu), \qquad \partial_\mu\theta^\mu{}_\nu = 0 \tag{2.14}$$

where the conserved quantity $\theta^\mu{}_\nu$ is called energy-momentum complex and describes the total energy and momentum density while the gravitational part of it is covered by the energy-momentum pseudotensor $\tau^\mu{}_\nu$. The most direct way to find $\theta^\mu{}_\nu$ would be using the same procedure as for the matter fields in special relativity which means using the Noether identity (2.3) with $\theta^\mu{}_\nu$ corresponding to the canonical stress-energy tensor, this approach [58] leads to the Einstein energy complex

$$\Theta^\mu{}_\nu = \frac{1}{16\pi}H^{\mu\alpha}_{\nu,\alpha} \qquad H^{\mu\alpha}_\nu = \frac{g_{\nu\beta}}{\sqrt{-g}}[-g(g^{\mu\beta}g^{\alpha\lambda} - g^{\alpha\beta}g^{\mu\lambda})]_{,\lambda}. \tag{2.15}$$

where the conserved complex is itself expressed as a divergence of an antisymmetric superpotential $H^{\mu\alpha}_\nu = -H^{\alpha\mu}_\nu$ which ensures that the complex is automatically a conserved current. This allows for generalising the approach by constructing a superpotential from the metric and its first derivatives to obtain new stress-energy complexes and consequently gravitational pseudotensors. Since we demand that τ vanishes in a local inertial frame it has to depend only on the first derivatives of $g_{\mu\mu}$ (second derivatives are associated with curvature which does not vanish in any frame). This effectively means that the second derivatives from $\Theta^\mu{}_\nu$ cancel the second derivatives in $G^\mu{}_\nu$ which is indeed true in (2.15). Speaking of the coordinates, a fairly common problem of the gravitational complexes (and pseudotensors) is the dependence of the result on coordinates, for instance the Einstein complex is zero in Minkowski spacetime in Cartesian coordinates while it gives a non-zero result in the same spacetime when spherical coordinates are used [58]. The same happens in the Schwarzschild spacetime where a correct result for the total mass is recovered only in the Cartesian-type coordinates. To

rectify this issue Møller [58] derived a new superpotential $\chi^{\mu\alpha}_{\nu,\alpha}$ whose divergence gives the Møller energy complex $\theta^{\mu}{}_{\nu}$

$$\theta^{\mu}{}_{\nu} = \frac{1}{8\pi}\chi^{\mu\alpha}_{\nu,\alpha} \qquad \chi^{\mu\alpha}_{\nu} = \sqrt{-g}(g_{\nu\rho,\lambda} - g_{\nu\lambda,\rho})g^{\mu\rho}g^{\alpha\lambda}. \tag{2.16}$$

To give just one last example, one of the most famous results in this area is due to Landau and Lifshitz who defined [54] a superpotential

$$h^{\mu\nu\alpha} = \frac{1}{4\kappa}\partial_{\beta}[(-g)g^{\mu\nu}g^{\alpha\beta} - g^{\mu\alpha}g^{\nu\beta}]. \tag{2.17}$$

The corresponding conserved quantity is again given as a divergence

$$\theta^{\mu\nu} = \partial_{\alpha}h^{\mu\nu\alpha} = ((-g)(T^{\mu\nu} + \tau^{\mu\nu})) \tag{2.18}$$

where $\tau^{\mu\nu}$ is the Landau-Lifshitz pseudotensor. The main benefit of this pseudotensor is that it is symmetric which is a natural requirement for stress energy tensors since it is a condition for conservation of angular momentum. However by looking at the superpotential in (2.17) one notices that it does not have a correct weight as a tensor density which makes it in a sense incompatible with $\sqrt{-g}T^{\mu\nu}$ (see [83]) and it also suffers from the same coordinate dependence defect as the Einstein complex.

In our studies we concentrated mostly on highly symmetric (spherically or axially symmetric) spacetimes and in particular for the scalar Curzon-Chazy counterpart (1.33) the gravitational stress-energy complexes give zero energy density outside the origin while giving the correct result for the total mass. A good review of results for spherically symmetric spacetimes can be found in [56] or [89]. There are also examples of axially symmetric spacetimes where the energy-momentum pseudotensors have been used. For our purpose it was interesting to see the results for the axially symmetric Curzon-Chazy spacetime which are given in [27] where five different pseudotensors where employed each giving a different result, for example the Møller complex even vanishes.

There are many other pseudotensors which will not be mentioned here, suffice to say that each of them gives some reasonable results in certain situation while they do not have all the properties one would expect.

As was mentioned above, the equivalence principle leads to the pseudotensorial description of gravitational energy which can lead to vastly different results in different coordinates which is one of the reasons to avoid using the pseudotensors altogether as the very concept of gravitational energy-momentum density may be meaningless. An alternative is then using a quasi-local notion of energy where the energy and momentum is assigned to a finite region of space and not a single point. This will be discussed in the next part.

To conclude this section it is worth noting that there were some attempts of deriving a tensorial expression for gravitational energy and momentum, a notable one is the Bel-Robinson tensor [73] which is constructed entirely from the Weyl tensor in the same way as the electromagnetic stress energy tensor is constructed from the Faraday tensor. This is however a fourth-rank tensor so it is not clear how it corresponds to the matter represented by $T^{\mu\nu}$.

2.3 Quasi-local energy

In this section we are going to present several concepts of quasilocal mass/energy which resigns on the notion of density located at each point (or stress-energy tensor) but tries to define how much mass-energy is located in a region of spacetime, the definition is typically covariant in nature.

The first one is the well-known Komar mass which can be derived in several different ways but we can start from an interesting analogy with Newton's gravitation where the total mass in a region with closed surface S being its boundary can be calculated using the Gauss law as

$$M = \frac{1}{4\pi}\int_S \vec{\nabla}\Phi \cdot \mathrm{d}\vec{S} \tag{2.19}$$

The gradient of the gravitational potential Φ represents gravitational field intensity or acceleration exerted on a test particle. In a stationary spacetime with a timelike Killing field ξ, we have a natural choice for static observers whose acceleration we can easily calculate as

$$a^\nu = (\xi^\mu/F)\nabla_\mu(\xi^\nu/F), \qquad F = (-\xi_\mu\xi^\mu)^{1/2}. \tag{2.20}$$

In our spacetime with spacelike hypersurface Σ with boundary S the analogue of (2.19) would then be [90]

$$M = \int_S s^\nu(\xi^\mu/F)\nabla_\mu\xi_\nu \mathrm{d}S \tag{2.21}$$

where the vector s^ν is tangent to Σ and normal to S. Let us note that from now on we may also write $\mathrm{d}S$ in an alternative form $\mathrm{d}S = \sqrt{q}\mathrm{d}^2x$ where q_{ij} is the metric on the surface S.

After absorbing the vectors contracted with $\nabla_\mu\xi_\nu$ into $\mathrm{d}S^{\mu\nu}$ or the Levi-Civita tensor we get the two common forms for the Komar mass

$$M_K = -\frac{1}{8\pi}\int_S \nabla_\mu\xi_\nu \mathrm{d}S^{\mu\nu} = -\frac{1}{2}\int_S \varepsilon_{\alpha\beta\mu\nu}\nabla^\mu\xi^\nu \tag{2.22}$$

Using the Stokes theorem for differential forms we can convert the integral over S to an integral over Σ using the identity satisfied by Killing vectors

$$\Box\xi^\mu = -R^\mu{}_\nu\xi^\nu \tag{2.23}$$

and using Einstein's equations we get the Komar mass in terms of the stress-energy tensor

$$M_K = 2\int_\Sigma (T_{\mu\nu} - \frac{1}{2}Tg_{\mu\nu})n^\mu\xi^\nu \mathrm{d}V. \tag{2.24}$$

From this formula, one may notice that the total mass inside two closed surfaces S_1 and S_2 is the same if there is no matter in-between them which is a reasonable conclusion. This may however also seem counter-intuitive (from the Newtonian perspective) if the integrand is zero while $T_{\mu\nu} \neq 0$ which means that the Komar mass is insensitive to some configurations of matter fields. This happened for example in our studies of spherically symmetric solution with scalar field [68]

where only the $r-r$ component of $T_{\mu\nu}-\frac{1}{2}Tg_{\mu\nu}$ was non-zero. Of course the total mass-energy of an isolated system is calculated when S is placed at the (spacelike) infinity.

When discussing the Komar integral (2.22) we should note that this integral can be defined for other conserved quantities when the timelike Killing vector is replaced by other Killing vectors. In that case the factor in front of the integral is different, for example in the case of angular momentum where $\xi=\xi^{(\phi)}$, the factor is $(16\pi)^{-1}$ instead of $(-8\pi)^{-1}$. It is also interesting to remark on how Arthur Komar [47] originally derived the expression (2.22). He started from the Møller's prescription of the superpotential (2.16) contracted with a vector field ξ (not necessary a Killing vector),the divergence of such quantity ($D^{\mu}=(\chi^{\mu\alpha}_{\nu}\xi^{\nu})_{,\alpha}$) is of course a conserved current ($\partial_{\mu}D^{\mu}=0$ as $\chi^{\mu\alpha}_{\nu}=\chi^{[\mu\alpha]}_{\nu}$) but it is not a covariant expression, to mend this he added another identically conserved current and arrived at $J^{\mu}=4\nabla_{\nu}(\nabla^{[\mu}\xi^{\nu]})$ which is covariantly conserved but it also can be used in the form of a continuity equation with its respective conserved total mass. On the other hand if ξ is not a Killing vector we lose the formula (2.24) and the analogy with the Gauss law as described above.

Another concept of mass-energy commonly used in general relativity is the ADM energy (or in general we speak of ADM quantities). This is based on the Hamiltonian approach to the Einstein's theory (ADM formalism [7]) which utilizes 3+1 splitting of spacetime which is foliated by spacelike hypersurfaces Σ_t parametrized by a coordinate time t. The tangent vector to the time coordinate is then decomposed using the lapse N and shift vector N^{μ} (tangent to Σ_t) as $t^{\mu}=Nn^{\mu}+N^{\mu}$ where n^{μ} is normal to Σ_t.

Now assuming that Σ has a boundary and also taking into account the Gibbons–Hawking boundary term which is commonly absent in the variational formulation of GR (2.1) one can derive the gravitational Hamiltonian as [44], [14]

$$H_G=\frac{1}{2\kappa}\int_{\Sigma}\Big[NC_0(p^{ij},h_{ij})+N^kC_k(p^{ij},h_{ij})\sqrt{h}\Big]\mathrm{d}^3x+H_{\partial\Sigma}. \tag{2.25}$$

The Hamiltonian is written as a functional of the canonical variables h_{ij},the metric on Σ, and its conjugate momentum p^{ij} which is associated with extrinsic curvature of Σ and also of the lapse-shift vector $N^{\mu}=(N,N^k)$, N^k are components of the shift vector in the coordinates x^i parametrizing Σ. The first part of H_G is the one from which the equations of motion can be derived and is entirely constructed from constraints. They are the Hamiltonian constraint C_0 and momentum constraint C_k. Without going into details it is important to realize that when evaluated on the solution to the equations of motion the constraints by definition vanish and the only part of the Hamiltonian that is left is $H_{\partial\Sigma}$ which is evaluated only on the boundary of Σ. The boundary $S=\partial\Sigma$ has a normal vector s^{ν} (tangent to Σ) and is equipped with metric $q_{\mu\nu}$. The on-shell Hamiltonian then reads

$$H_{\partial\Sigma}=-\frac{1}{8\pi}\int_{\partial\Sigma}N(k-k_0)-N^i(K_{ij}-Kh_{ij})s^j\mathrm{d}S. \tag{2.26}$$

Here the quantity $k=q^{\mu\nu}\nabla_{\mu}s_{\nu}$ is the trace of the extrinsic curvature of the surface S while K_{ij} is the extrinsic curvature of Σ (and $K=h^{\mu\nu}\nabla_{\mu}n_{\nu}$ is its

trace), in fact the second term is the momentum p_{ij} contracted with N^i and the normal s^j. The term containing k_0 is the the trace of the extrinsic curvature of S as embedded in the Minkowski spacetime and it is added to the Hamiltonian as a constant because the Hamiltonian is normalized to be zero in flat space (It would also produce an infinite result for Minkowski space which is also the reason why this constant is subtracted.)

Like in other theories, the Hamiltonian evaluated on-shell is a natural candidate for energy of the system. For an asymptotically flat spacetime we can define the ADM energy as

$$E_{ADM} = -\frac{1}{8\pi}\int_{S(t,r\to\infty)}(k-k_0)\sqrt{q}\mathrm{d}^2x \tag{2.27}$$

where the surface S is pushed to the spatial infinity. The energy is obtained from (2.26) by a specific choice $N = 1$, $N^i = 0$ while ADM (angular) momentum can be found using other choices (see [44] or [14]) which naturally correspond to the symmetries associated with each quantity.

There exists another expression for ADM energy which can be shown to be equivalent to (2.27)

$$E_{ADM} = \frac{1}{16\pi}\int_{S(t,r\to\infty)}(D^i h_{ij} - D_j h)s^j\sqrt{q}\,\mathrm{d}^2x \tag{2.28}$$

where D is the Levi-Civita derivative in Minkowski space, similarly the trace h is calculated with respect to the three dimensional flat metric.

So far we have mostly discussed the notion of energy and partially also momentum but in the asymptotically flat space we can also define the mass using the standard relation from special relativity

$$M = \sqrt{E^2 - P^i P_i}. \tag{2.29}$$

In such a case one can derive mass using the ADM approach or using the Komar formulas and see that they coincide in a stationary asymptotically flat spacetimes [44]. As we considered (in [68]) primarily spacetimes where $P^i = 0$ (static) we interchangeably used the terms mass and energy.

While the ADM mass in an asymptotically flat spacetime is conserved (even if the spacetime is not stationary) there is another concept of mass/energy defined using an almost identical formula called Bondi-Sachs energy

$$E_{BS} = -\frac{1}{8\pi}\int_{S(u,v\to\infty)}(k-k_0)\sqrt{q}\mathrm{d}^2x \tag{2.30}$$

where the only difference is that the surface over which the extrinsic curvature is integrated is located at the future null infinity ((u, v) is the pair of null coordinates). The energy defined in this way is not constant as there is a radiation flux to the infinity to which the ADM mass is not sensitive [44].

The ADM energy is closely connected to the Brown-York energy which is derived using Hamilton-Jacobi formalism. When evaluating the action functional on the solution of the equations of motion one obtains the Hamilton's principal function S_{cl} which is a function of the boundary conditions (initial and final sets

of values λ_i and λ_f). Varying a simple action describing a motion of a particle one obtains the result

$$\delta S_{cl} = (p\delta q)|_{\lambda_i}^{\lambda_f} - (H\delta t)|_{\lambda_i}^{\lambda_f} \tag{2.31}$$

if the equations of motion are satisfied. From this expression we can see that the momenta and the energy (Hamiltonian) can be obtained simply by partial differentiation.

Using the same technique as for the action (2.1) leads to an analogical result [15]

$$\delta S_{cl} = \frac{1}{2\kappa}\int_{\Sigma_f} P^{ij}\delta h_{ij}\sqrt{h}\mathrm{d}^3x - \frac{1}{2\kappa}\int_{\Sigma_i} P^{ij}\delta h_{ij}\sqrt{h}\mathrm{d}^3x - \frac{1}{2\kappa}\int_B \tau^{ij}\delta\gamma_{ij}\sqrt{\gamma}\mathrm{d}^3x \tag{2.32}$$

where the boundary is composed of spacelike hypersurfaces Σ_i and Σ_f (with metric h_{ij}) and timelike hypersurface(s) B (equipped with metric γ_{ij}). By comparing this with (2.31) we can deduce that the relevant quantity representing energy is

$$\tau^{ij} = -\frac{2}{\sqrt{-\gamma}}\frac{\delta S_{cl}}{\delta\gamma_{ij}} = \frac{1}{8\pi}(\Theta^{ij} - \Theta\gamma^{ij}) \tag{2.33}$$

which is called the surface stress-energy tensor where Θ^{ij} is the extrinsic curvature of B. This definition has the very same form as the one for the matter stress-energy tensor (2.8) so one could naturally ask what is the covariant divergence of τ^{ij}. Using the covariant derivative $\mathcal{D}$ compatible with γ_{ij} (τ^{ij} is a tensor on B) one has [15]

$$\mathcal{D}_i\tau^{ij} = -\sqrt{-\gamma}n_\mu T^{\mu\nu}\gamma^j_\nu. \tag{2.34}$$

Thus in the absence of matter or more generally when the right-hand side is zero we get $\mathcal{D}_i\tau^{ij} = 0$ as for $T^{\mu\nu}$ itself. If in addition there exists a Killing vector ξ tangent to B we can define a conserved "charge" in much the same way as for the matter field in (2.11)

$$Q[\xi] = \int_S \tau^{ij}\xi_i\bar{t}_j\sqrt{q}\mathrm{d}^2x. \tag{2.35}$$

Here the surface S is $S = B \cap \Sigma_t$ for arbitrary t while $\bar{t}_j$ is its normal lying in B. In the special case $\xi_i = \bar{t}^i$ one gets a "density" in the form

$$\varepsilon = \tau_{ij}\bar{t}^i\bar{t}^j = -\frac{1}{8\pi}k \tag{2.36}$$

where k is the trace of the extrinsic curvature of S encountered already at (2.26). If we then subtract the flat-space contribution so that we have a reasonable normalization one obtains the Brown-York energy as

$$E_{BY} = -\frac{1}{8\pi}\int_S (k - k_0)\sqrt{q}\mathrm{d}^2x \tag{2.37}$$

where S is unlike in the ADM not considered to be located at the infinity but can be a boundary of a compact Σ_t. For a general Killing field ξ the conserved quantity would have a momentum contribution and the result would depend on the 2+1 decomposition of ξ on B (see [15] and [83]). There are several other definitions of energy relying on extrinsic curvature of surfaces like the Kijowski energy or Epp energy [44].

So far we have discussed the concepts of energy in a general spacetime but there are some approaches derived solely for spacetimes with particular symmetries. One of them is the Misner-Sharp energy which is defined only for spherically symmetric spacetime. We consider a spherically symmetric metric

$$\mathrm{d}s^2 = -2e^{-f}\mathrm{d}\xi_+\mathrm{d}\xi_- + r^2\mathrm{d}\Omega^2, \tag{2.38}$$

where f is the function of the null coordinates $\xi_\pm$ (The coordinates used here are $(\xi_+, \xi_-, \theta, \phi)$.).

The Misner-Sharp energy can be defined by multiple expressions as [37]

$$E_{MS} = \frac{1}{2}r(1 - g^{-1}(\mathrm{d}r, \mathrm{d}r)) = \frac{1}{2}r + e^f r\partial_+(r)\partial_-(r) = \frac{1}{2}r + \frac{1}{4}e^f r^3\theta_+\theta_- \tag{2.39}$$

Starting from the first expression, it may look like it is purely coordinate dependent but we have to keep in mind that r is not just any radial coordinate but the areal radius of the sphere whose metric is invariant with respect to the $SO(3)$ group. The tensor g^{-1} is just an inverse of our spherically symmetric metric (with contravariant indices) so one can easily check that it gives the correct result for the Schwarzschild solution. The second expression is of course defined using the coordinates and functions present in metric (2.38) while the third form is given in terms of expansion of ingoing and outgoing null geodesics. There is yet another form of the Misner-Sharp energy which employs the Riemann curvature tensor and the two normals to the sphere (n timelike and s spacelike) [83],[44]

$$E_{MS} = \frac{1}{8}r^3 R_{\mu\nu\rho\sigma}\epsilon^{\mu\nu}\epsilon^{\rho\sigma}, \qquad \epsilon_{\mu\nu} = \epsilon_{\mu\nu\rho\sigma}n^\rho s^\sigma. \tag{2.40}$$

The Misner-Sharp energy is a widely established quasilocal notion of energy in spherically symmetric spacetime. If we use the orthogonal $t - r$ coordinates instead of $\xi_\pm$, the interpretation of the M-S energy $E_{MS}(t, r)$ is the total energy inside the sphere of radius r at the time t. The M-S energy coincides with the ADM energy (2.27) and Bondi-Sachs energy (2.30) when the sphere is located at the spatial and null infinity respectively [37].

Despite the fact that Misner-Sharp energy is quasilocal it is interesting to note that it is associated with a conserved current known as the Kodama vector which is given in the null coordinates as

$$j = \frac{e^f}{4\pi r^2}\Big(\partial_+(E_{MS})\partial_- - \partial_-(E_{MS})\partial_+)\Big). \tag{2.41}$$

It can be shown that like for the above-mentioned currents we can define a charge for j which is exactly the M-S energy.

There are several other quasilocal energy approaches which reduce to the Misner-Sharp energy in the spherically symmetric case, an example of this is the Hawking or Hayward energy which is also defined using expansion of null geodesics. Another interesting aspect of the M-S energy is that it reproduces the Newtonian limit. It is possible to derive an implicit expression for the Misner-Sharp energy in the form [37]

$$E_{MS} = c^2 \int_\Sigma \rho \left(1 + \frac{\dot{r}^2}{c^2} - \frac{2E_{MS}}{c^4 r}\right)^{\frac{1}{2}} \mathrm{d}V \tag{2.42}$$

where the density ρ is given by the matter stress-energy tensor and the expression is in the $t-r$ coordinates (c is the speed of light). By Taylor-expanding the square root ($c \to \infty$) we can see that the leading contritions in the integrand are from the density of the matter ρ, its kinetic energy $\frac{1}{2}\rho\dot{r}^2$ and potential energy $-\frac{\rho E_{MS}}{c^2 r}$.

Speaking of the Newtonian limit there is another energy which has a reasonable Newtonian interpretation but it also has a resemblance to the Maxwell theory of electromagnetism. This energy was derived by Katz, Lynden-Bell and Bičák with the assumption that the spacetime is stationary and asymptotically flat [45],[51]. As we have seen in the first chapter the stationary metric can be put into the form

$$\mathrm{d}s^2 = -\xi^2(\mathrm{d}t + \mathcal{A}_i \mathrm{d}x^i)^2 + h_{ij}\mathrm{d}x^i\mathrm{d}x^j. \tag{2.43}$$

where all the metric functions are independent of t. The total mass of the system M is then decomposed into the matter part and gravitational part

$$M = E_M + E_G. \tag{2.44}$$

The concept of total mass M is clearly defined in an asymptotically flat spacetime while the energy E_M is computed using the formula (2.11) from the point of view of static observers whose fourvelocity is proportional to the Killing vector ∂_t (with normalization to -1 of course). Subsequently we can define "equivalents" of electric and magnetic field using the metric functions as

$$\mathcal{B} = \nabla \times \mathcal{A}, \quad \mathcal{E} = -\nabla(\ln(\xi)) \tag{2.45}$$

the curl and gradient operators are defined here with respect to the spatial part of the metric h_{ij}.

Now comes the crucial part of defining the gravitational potential. It is important to notice here that the equivalent of Newtonian gravitational potential is given by h_{ij} and not by ξ which determines the "electric field". The term gravitational potential in GR is indeed often associated with the logarithm of the g_{tt} component but this is only due to its role in the Newtonian limit of the geodesic equation. On the other hand the g_{rr} term is often associated with mass (This can be seen in the definition of the Misner-Sharp energy (2.39)) which is why it is related to the gravitational energy. Only in specific spacetimes (for example when $g_{tt}g_{rr} = -1$) can these two potentials coincide. The gravitational potential as defined in [51] is given by a conformal factor in the following transformation

$$\bar{h}_{ij} = e^{-2\Phi} h_{ij} \tag{2.46}$$

where the 3-metric $\bar{h}_{ij}$ is defined by having zero scalar curvature. This was inspired by the static Newtonian limit of a metric where the two potentials are the same and the metric $\bar{h}_{ij}$ is flat (see for example [44]). After expressing M and E_M using integrals and some manipulations we get a generalized version of the Gauss law

$$\nabla \cdot \mathcal{D} = \kappa(T_0^0 + \rho_G) \tag{2.47}$$

where divergence of a vector field $\mathcal{D}$ is equal to a contribution from matter (T_0^0) and the density of the gravitational energy which is given by the field itself which is how the non-linnearity of the Einstein's equations manifests. The field $\mathcal{D}$ and the density ρ_G are then specifically given as [51]

$$\mathcal{D} = \frac{1}{2}\xi^2 \mathcal{A} \times \mathcal{B} - 2\nabla\Phi \tag{2.48}$$

$$\kappa\rho_G = -\frac{1}{4}\xi^2\mathcal{B}^2 - |\nabla\Phi|^2 - \frac{1}{2}\xi^2\mathcal{A}\cdot(\mathcal{E}\times\mathcal{B}). \tag{2.49}$$

We can observe that there is a gradient of the potential present in $\mathcal{D}$ while there is also another term which does not have any analogy in the Maxwell theory. Similarly we can see quadratic terms from $\mathcal{B}$ and $\nabla\Phi$ as in the electromagnetic case but there is also the last term which is absent in the Maxwell case. It is worth noting that at least in the static case the gravitational energy density is negative which means it has a repulsive effect as the source on the right-hand side of (2.47). The vector $\mathcal{D}$ should in principle correspond to the intensity of gravitational field which is demonstrated in equation (2.47), however it is not directly related to the geodesic motion as that role is played by $\mathcal{E}$.

Apart from the equation (2.48) there are also equations containing the other components of $T^\mu{}_\nu$ for example we can find that $\nabla \times \mathcal{B}$ is equal to the momentum density T_0^i plus a gravitational term which is a nonlinear equivalent of the Ampère's law.

2.4 Gravitational waves

The final part of our discussion of energy in General relativity will be mainly concerned with stress-energy carried by gravitational waves but this section will also serve as a bridge between this chapter and the following one concerned with inspirals due to emission of gravitational waves. Here we shall sketch the derivation of the stress energy tensor for gravitational waves propagating on a background spacetime with metric $g^{(B)}_{\mu\nu}$. The total metric is then decomposed into the background part and the perturbation $h_{\mu\nu}$ which represents the gravitational wave

$$g_{\mu\nu} = g^{(B)}_{\mu\nu} + h_{\mu\nu}, \qquad h_{\mu\nu} = \mathcal{O}(\varepsilon). \tag{2.50}$$

Let us now describe the nature of ε. We will assume that ε captures the smallness of the perturbing metric with respect to the background $g^{(B)}_{\mu\nu}$ which means smallness of the amplitude of the wave in these coordinates ($g^{(B)}_{\mu\nu} \gg h_{\mu\nu}$). In addition we shall also assume a high frequency regime akin to that in geometrical

optics, this means that the size of the perturbation parameter is given by the ratio of the wavelength λ to the characteristic length R on which the background curvature changes($\varepsilon \sim \frac{\lambda}{R}$). To summarize it, the metric part $h_{\mu\nu}$ is $\mathcal{O}(\varepsilon)$ small but rapidly oscillating on the scale of its short wavelength λ ($\frac{\lambda}{R} = \mathcal{O}(\varepsilon)$).

By inserting the metric into the vacuum Einstein's equations $R_{\mu\nu} = 0$ and naively expanding it in ε we get

$$R_{\mu\nu} = R^B_{\mu\nu} + R^{(1)}_{\mu\nu} + R^{(2)}_{\mu\nu} \approx 0 \tag{2.51}$$

where $R^{(1)}_{\mu\nu}$ and $R^{(2)}_{\mu\nu}$ are linear and quadratic in $h_{\mu\nu}$ respectively while all the remaining terms are neglected. So far we considered only the size of the perturbing metric $h_{\mu\nu}$ itself but not the size of its derivatives. The first derivatives of the metric are of the order $\mathcal{O}(\varepsilon^{-1})$ while the second derivatives are $\mathcal{O}(\varepsilon^{-2})$. This is not that surprising when we imagine a decomposition into plane waves with frequencies inversely proportional to λ. When we take this into account we can see that the second term of the expansion (2.51) is actually dominant as it contains second derivatives of the metric which means it is of the order $\mathcal{O}(\varepsilon^{-1})$. The field equations (2.51) can then be split according to [42] and [57] as

$$R^{(1)}_{\mu\nu} = 0, \qquad R^B_{\mu\nu} = -\langle R^{(2)}_{\mu\nu} \rangle. \tag{2.52}$$

The equation on the left contains all the $\mathcal{O}(\varepsilon^{-1})$ oscillating terms while the other equation is of the order $\mathcal{O}(1)$ but it contains only the averaged part of $R^{(2)}_{\mu\nu}$ which is consistent with the fact that $R^B_{\mu\nu}$ varies on the scale R. It is easy to imagine this splitting in case of a plane-wave solution with frequency ω for which the second order Ricci tensor $R^{(2)}_{\mu\nu}$ contains terms with frequency 2ω as well as constant terms as it is quadratic in $h_{\mu\nu}$. All the other parts of the Ricci tensor are neglected (details in [57], [25]). The gravitational waves thus contribute to the background curvature.

Let us now discuss both equations separately. It is first useful to study the metric perturbation in the "trace-reversed" form

$$\bar{h}_{\mu\nu} = h_{\mu\nu} - \frac{1}{2} h g^{(B)}_{\mu\nu}. \tag{2.53}$$

After some manipulation the equation $R^{(1)}_{\mu\nu} = 0$ reads

$$\begin{aligned} \Box^B \bar{h}_{\mu\nu} + 2R^B_{\alpha\mu\beta\nu} \bar{h}^{\alpha\beta} + g_{\mu\nu} \nabla^B_\alpha \nabla^B_\beta \bar{h}^{\alpha\beta} \\ -2\nabla^B_{(\mu} \nabla^{B\alpha} \bar{h}_{\nu)\alpha} - 2R^B_{\alpha(\mu} \bar{h}_{\nu)}{}^{\alpha} = 0 \end{aligned} \tag{2.54}$$

where all the covariant derivatives are with respect to $g^{(B)}_{\mu\nu}$ as is the d'Alembertian $\Box^B = g^{(B)\mu\nu} \nabla^B_\mu \nabla^B_\nu$. Raising and lowering indices as well as calculating traces is also done by $g^{(B)}_{\mu\nu}$. This is the dynamical equation governing the propagation of the gravitational waves on the background spacetime. This equation can be simplified further. Firstly we can choose a suitable gauge condition. The gauge transformation of $h_{\mu\nu}$ is associated with an infinitesimal coordinate transformation $x'^\mu = x^\mu - \xi^\mu$ (ξ^μ is not a Killing vector). The field is then transformed by

applying the Lie derivative on the metric $g_{\mu\nu}$ (as was discussed at the beginning of this chapter) and neglecting the $\varepsilon\xi$ terms

$$h'_{\mu\nu} = h_{\mu\nu} + 2\nabla_{(\mu}\xi_{\nu)}. \tag{2.55}$$

W shall now impose the Lorenz gauge condition along with tracelessness

$$\nabla^B_\mu \bar{h}^{\mu\nu} = 0 = \bar{h}, \tag{2.56}$$

this then means $\bar{h}_{\mu\nu} = h_{\mu\nu}$. In the linearisation around Minkowski background it is common to adopt the transverse-traceless (TT) gauge which in addition to (2.56) demands that $u^\mu h_{\mu\nu} = 0$ for an observer with four-velocity u^μ, this condition however cannot be imposed globally together with (2.56) in a curved spacetime [25],[57].

The choice of the Lorenz gauge eliminates the third and fourth term in (2.54), we can however also get rid of the terms with Ricci tensor which were produced by using the commutation relations for the covariant derivatives. While the averaged part of the gravitational waves ($\langle R^{(2)}_{\mu\nu}\rangle$ varying over large scales) contributes to the background curvature in (2.52) we can neglect it when compared to the curvature produced by a background source (like a black hole). This effectively means treating $h_{\mu\nu}$ as a test field without any influence on the background curvature. With that in mind we can consider $g^{(B)}_{\mu\nu}$ to be almost a vacuum solution then the background Ricci tensor vanishes, $R^B_{\mu\nu} \approx 0$. An alternative decomposition is presented in [25] while in [42] the Ricci terms are not neglected at all.

Putting all this together we get a much simpler equation

$$\Box^B h_{\mu\nu} + 2R^B_{\alpha\mu\beta\nu} h^{\alpha\beta} = 0. \tag{2.57}$$

This is a generalization of the wave equation with an additional term due to the background curvature. As was stated above, this equation by itself describes only the effect of the background on the propagation of waves but in this approximation we neglect the effect of the wave on the spacetime geometry itself which is what the second equation of (2.52) describes. This is the consequence of the nonlinear nature of Einstein's equations which means that while at the leading order we could treat $h_{\mu\nu}$ as a test field obeying eq. (2.57), at the higher orders in ε we have to treat (2.52) as a system and not two independent decoupled equations.

We can now switch our attention to the second equation $R^B_{\mu\nu} = -\langle R^{(2)}_{\mu\nu}\rangle$. Now, for reasons discussed above, an averaging is used on the terms quadratic in $h_{\mu\nu}$. A detailed approach called Brill-Hartle averaging scheme is given in [43]. It involves averaging over spacetime with a suitable weighting function which eliminates the high-frequency oscillations. Particularly the averaging also eliminates the terms containing second derivatives of the perturbation metric contained in $R^{(2)}_{\mu\nu}$. This is due to the fact that they can be written as total divergence and by using the Gauss theorem we get a vanishing surface integral (see [43]). The equation can then be put in the form of Einstein's equations for background metric and a source which is then interpreted as the stress-energy tensor of gravitational waves

$$R^{(1)}_{\mu\nu} = 0 \qquad R^B_{\mu\nu} - \frac{1}{2} R^B g^B_{\mu\nu} = \kappa T^{GW}_{\mu\nu} \tag{2.58}$$

where $8\pi T^{GW}_{\mu\nu} = \langle R^{(2)}_{\mu\nu}\rangle - \frac{1}{2}\langle R^{(2)}\rangle g^B_{\mu\nu}$ is explicitly

$$T^{GW}_{\mu\nu} = \frac{1}{32\pi}\left\langle \nabla^B_\mu \bar{h}_{\alpha\beta}\nabla^B_\nu \bar{h}^{\alpha\beta} - \frac{1}{2}\nabla^B_\mu \bar{h}\nabla^B_\nu \bar{h} - 2\nabla^B_\beta \bar{h}^{\alpha\beta}\nabla^B_{(\mu}\bar{h}_{\nu)\alpha}\right\rangle. \tag{2.59}$$

The gravitational-wave stress energy tensor is symmetric and satisfies $\nabla^B_\mu T^{\mu\nu} = 0$ which is in accordance with equation (2.58). While the stress-energy tensor (2.59) depends only on the first derivatives, it can be show it is a gauge-invariant quantity because of the averaging in its definition. In the transverse-traceless gauge (2.56) the stress energy tensor reads

$$T^{GW}_{\mu\nu} = \frac{1}{32\pi}\left\langle \nabla^B_\mu h_{\alpha\beta}\nabla^B_\nu h^{\alpha\beta}\right\rangle. \tag{2.60}$$

The gravitational-wave stress-energy tensor is of great importance when calculating fluxes of energy and angular momentum at infinity from an inspiraling particle which will be discussed in the following chapter.

3. Geodesics and extreme mass ratio inspiral

This chapter is concerned with describing the theory on which our papers [69] and [46] are built upon. The physical model studied in both of those papers is a special case of a relativistic two-body problem known as extreme mass ratio inspiral (EMRI). As the name suggests the mass ratio characterizing the system is extremely small, $\varepsilon = m/M \leq 10^{-4}$. The two orbiting bodies are often considered to be black holes (with the primary one being supermassive obviously) making it a relativistic problem by definition. Naturally one could approach this by formulating an initial value problem for the full Einstein's equations or more specifically solve the field equations using the ADM formalism [7]. This is the numerical relativity approach. However, for an EMRI the number of orbital cycles the system undergoes is proportional to ε^{-1} which makes it very computationally expensive. For that reason, perturbation methods are used to model the system until the final stages of its evolution when the two black holes merge (here the full theory is necessary to use).

The first is the post-Minkowskian (weak field) or post-Newtonian expansion (weak field, slow motion) [12], which is used for binaries with comparable masses as well, the key assumption of these methods is a sufficient separation of the two bodies. An alternative is a fully relativistic treatment in the form of black hole perturbation theory based on expansion in the small mass ratio ε. This covers primarily the gravitational self-force [9] and other techniques like the Teukolsky or Regge-Wheeler formalism. Then there is the effective one body formalism [16] which aims to describe all the stages of the binary evolution using information from the other methods.

The Newtonian one-body problem is fairly simple, the test body follows a Keplerian ellipse. In the relativistic one-body problem, a test particle follows a geodesic of the background spacetime, in our models an exact solution describing a black hole (Schwarzschild or Kerr). If the particle is no longer massless then it also affects the geometry of spacetime, the result is the gravitational self-force acting on the particle. This causes the orbit to decay, this dissipation is then associated with loss of energy and angular momentum carried away in the form of gravitational waves. In an even more realistic model one should take into account the spin of the secondary body since even a test particle with spin does not follow a geodesic (the spin is coupled to the background curvature). This was explored for example in [79] or [20]. One could also study how a presence of additional matter surrounding the central black hole (ring or disc) influences an EMRI. This environmental effect was discussed in [80] but it was also the main motivation behind our publications [69] and [46] and the reason we chose to implement the action-angle formalism in the geodesic part of the problem.

Our strategy in both papers was similar.

1. Transform the Hamiltonian describing geodesic motion into action-angle coordinates using the methods of canonical perturbation theory.

2. Calculate the gravitational-wave fluxes on a three-dimensional grid in the

space of slowly varying variables (actions or orbital parameters).

3. Adiabatically evolve the inspiral and produce gravitational waveforms.

The action-angle coordinates go hand in hand with the two-timescales approach to EMRI separating the variables to two groups, slow and fast. In addition, the actions may play the role of orbital parameters (and integrals of motion) in nearly integrable systems which can be approximated by Hamiltonian systems in action-angle form. This enabled us to calculate an inspiral in [69] where the axially symmetric spacetime lacks a complete set of integrals of motion. It is worth mentioning that an analogical method involving elimination of fast variables in a perturbative expansion was also used in the context of self-force-driven inspiral [50] where the system considered was not Hamiltonian (it included the self-force) unlike ours which was restricted only to geodesics.

3.1 Canonical perturbation theory

As already mentioned, and as is clear from its name the canonical perturbation theory is built upon the Hamiltonian canonical formalism where the concept of conjugated action-angle coordinates can be defined. Since the Hamiltonian formalism is one of the basic pillars of theoretical physics we shall first go very briefly through some of the basic definitions which are described in details in [2], [6] or [49]. Particularly we shall employ the geometrical perspective which will however not be exactly a mathematically rigorous one, we will only define objects we need for the formulation of canonical perturbation theory.

The first object usually defined is the $2n$-dimensional manifold M^{2n} with a differential 2-form ω known also as a symplectic 2-form with following properties

- It is closed, $\mathrm{d}\omega = 0$ (d is the exterior derivative).
- It is non-degenerate, $\forall e_1, e_2 \in TM^{2n}, e_1 \neq 0,\ \omega(e_1, e_2) = 0 \Rightarrow e_2 = 0$..

While this symplectic structure can stand on its own, from the physical perspective one arrives at the symplectic structure when constructing the phase-space manifold as a cotangent bundle of the configuration manifold Q, i.e. we have $M^{2n} = T^*Q$. The original coordinates $q^i, i = 1..n$ on Q can be extended to its cotangent bundle by the coordinates called momenta p_i. Using the $2n$ coordinates $\mathbf{z} = (\mathbf{q}, \mathbf{p})$ we can define the canonical one-form

$$\Theta = \sum_{i=1}^{n} p_i \mathrm{d}q^i \tag{3.1}$$

using which we can obtain the symplectic two-form on our phase-space symplectic manifold by applying the exterior derivative on it

$$\omega = \mathrm{d}\Theta = \sum_{i=1}^{n} \mathrm{d}p_i \wedge \mathrm{d}q^i. \tag{3.2}$$

Thus in this phase-space formulation the 1-form Θ plays the role of a potential for ω which automatically satisfies $\mathrm{d}\omega = 0$ while the explicit form (3.2) can also be shown to satisfy the requirement of non-degeneracy.

Now the coordinates $(\mathbf{q}, \mathbf{p})$ in which ω has the particular simple form (3.2) are called canonical as is the transformation between two sets of canonical coordinates $(\mathbf{q}, \mathbf{p}) \to (\mathbf{Q}, \mathbf{P})$, this means that it is a transformation preserving the components of the symplectic 2-form, i.e. $\omega'_{ij} = \omega_{ij}$. Instead of focusing directly on ω , whose components transform properly as a tensor, we can formulate the canonical transformation on the level on Θ and Θ' as

$$\sum_{i=1}^{n} p_i \mathrm{d}q^i = \sum_{i=1}^{n} P_i \mathrm{d}Q^i + \mathrm{d}S \tag{3.3}$$

where S is a function on the phase-space manifold. We can thus see that the potential form is not uniquely determined and is given up to a gradient which is a relation identical to that describing gauge freedom in electromagnetism. The function S can then be expressed using functions of four different combinations of new and old canonical coordinates thus giving rise to the generating function approach.

The 2-form ω on a symplectic manifold plays a role similar to that of a space-time metric in Riemannian geometry, raising and lowering indices, for that we also need a tensor with components ω^{ij} which is a matrix inverse to ω_{ij}. A vector field of a particular importance is the one constructed from a function f by taking its gradient and then raising its index. Explicitly the vector field X_f associated with function f is then defined as

$$X_f^i = \omega^{ij} \mathrm{d}_j f, \qquad \omega^{ij}\omega_{jk} = \delta^i{}_k. \tag{3.4}$$

Naturally, the definition of the Poisson brackets of two functions f and g is then

$$\{f, g\} = \omega(X_g, X_f) = \mathrm{d}_i f \omega^{ij} \mathrm{d}_j g = X_g^i \mathrm{d}_i f = \mathcal{L}_{X_g} f \tag{3.5}$$

where $\mathcal{L}_{X_g}$ is the Lie derivative with respect to the vector field X_g. The reason why the vector fields of the form (3.4) have an important role is the identity

$$\mathcal{L}_{X_f} \omega = 0 \tag{3.6}$$

which means that the symplectic 2-form is preserved under the flow generated by X_f for some function f. This result is the basis for the Liouville theorem and any vector field satisfying this equation is called symplectic (The vector field X_H constructed from the Hamiltonian is just a one special example.). From now on we shall utilize $\mathcal{L}_{X_g} = \mathcal{L}_g$ as a simplified notation .

The dynamics is encoded in the vector field X_H associated with the Hamiltonian, the Hamilton's canonical equations can then be written as

$$\dot{z}^i = \mathcal{L}_H z^i. \tag{3.7}$$

The space of solutions of these equations consists of integral curves of the field X_H. A solution with initial condition z_0^i can then be written as an exponential of the Lie derivative $\mathcal{L}_H$

$$z^i(t) = \exp(t\mathcal{L}_H) z_0^i, \qquad z^i(0) = z_0^i \tag{3.8}$$

where the Hamiltonian H is a function on the space of initial conditions $H(z_0^i)$.

Integrable systems and action-angle coordinates

We can now proceed by shifting our focus to integrable systems which is a small but significant subset of dynamical systems. These systems posses symmetries which manifest in the form of integrals of motion $F(\mathbf{q}, \mathbf{p})$ which are functions on the phase-space manifold invariant under the dynamical flow generated by the vector field X_H, this can be mathematically expressed as $\{F, H\} = \mathcal{L}_H F = 0$, i.e. their Poisson bracket with Hamiltonian vanishes identically. Consequently an integral of motion is a constant of motion $F(\mathbf{q}(t), \mathbf{p}(t)) = f$. In the case where multiple integrals of motion are present we say that integrals of motion are in involution if $\{F_i, F_j\} = 0$. Two integrals of motion are independent if their differentials $\mathrm{d}F_i$ are linearly independent. If the number of independent integrals of motion in involution is equal to the number of degrees of freedom, then the system with Hamiltonian $H = F_1$ is said to be (completely) integrable.

With all the preliminary definitions behind us we can state the Liouville-Arnold theorem which applies to the integrable systems.

Theorem (Liouville-Arnold)**.** *Suppose that*

- *The $2n$-dimensional phase-space manifold M^{2n} admits n independent integrals of motion F_i in involution with $F_1 = H$ (the integrability assumption).*
- *By fixing the values of integrals of motion we define*

$$M_f = \{z \in M^{2n}, F_i(z) = f_i, i = 1, ..., n\}.$$

Then the theorem concludes that

1. *M_f is a manifold invariant under dynamical flow generated by the vector field X_H*
2. *If in addition M_f is compact and connected then it is diffeomorphic to n-dimensional torus T^n.*
3. *The torus can be parametrized by n angles $(\psi_1, .., \psi_n)$, $\psi_i \in (0, 2\pi)$ with evolution equations in the form $\frac{\mathrm{d}\psi_i}{\mathrm{d}t} = \Omega_i(\mathbf{f})$.*
4. *The equations of motion can be integrated by quadratures.*

The key result of the theorem is the fact that the motion is constrained to a submanifold M_f which if compact (like in the example of bound orbits in Kerr spacetime), corresponds to a torus which can be parametrized by angles whose evolution is linear in time and is given by $\Omega_i(\mathbf{f})$ which are the fundamental frequencies whose value is given solely by the values of integrals of motion which select the specific torus from the phase-space manifold.

The phase space of an integrable system thus has a simple structure, it is foliated by invariant tori. While we could treat ψ_i and f_i as phase-space coordinates they are not canonically conjugate. It can be shown [2], [6] that there exist momenta conjugate to the angles called actions J_i, the phase-space is thus parametrized by action-angle (AA) coordinates $(\boldsymbol{\psi}, \mathbf{J})$. The actions are defined as

$$J_i = \frac{1}{2\pi} \oint_{\gamma_i(\mathbf{f})} \Theta. \tag{3.9}$$

The actions are calculated by first choosing a torus (by fixing f_i) and on the torus we find n closed curves γ_i which form the basis of the first homotopy group (fundamental group) on the torus and then integrate the canonical one-form Θ along these curves to obtain the actions. Here we can see the invariant nature of the action defined using purely geometrical means. The freedom of choosing Θ (or the coordinates) does not affect the integral (3.9) as the $\mathrm{d}S$ term in (3.3) gives a vanishing contribution since $\oint \mathrm{d}S = 0$. Similarly if one would use a curve γ_i' homotopic to γ_i one would get using the Stokes theorem

$$\oint_{\gamma_i(\mathbf{f})} \Theta - \oint_{\gamma_i'(\mathbf{f})} \Theta = \int_{\partial\Gamma(\mathbf{f})} \Theta = \int_{\Gamma(\mathbf{f})} \omega = 0 \tag{3.10}$$

where $\partial\Gamma = \gamma_i' \cup \gamma_i$ and $\Gamma \subset M_f$. The last equality is due to $\omega|_{M_f} = 0$ which is shown in [2], this is compatible with the fact that in action-angle coordinates we have $\omega = \sum_{i=1}^{n} \mathrm{d}J_i \wedge \mathrm{d}\psi^i$. Still the action-angle coordinates are not uniquely determined, one can perform a transformation to a new set of action angle coordinates using a matrix with integer matrix elements (since we require the 2π-periodicity of the angles), this is described in [4].

The integral (3.9) gives us the relation $J_i = J_i(\mathbf{f})$ (actions are thus integrals of motion as well) which can be inverted and specifically since the first integral of motion is the Hamiltonian we get $H = H(\mathbf{J})$ where the actions are no longer fixed by $\mathbf{f}$ and the Hamiltonian is thus a phase-space function independent of angles. The Hamilton's equation expressed in action-angle coordinates are then solved trivially

$$\psi_i(t) = \Omega_i t + \psi_{0i}, \qquad J_i(t) = \text{constant}, \qquad \Omega_i(\mathbf{J}) = \frac{\partial H(\mathbf{J})}{\partial J_i}. \tag{3.11}$$

The nature of the motion is determined by the fundamental frequencies Ω_i. The crucial part of that is the question whether the frequencies are rationally independent or if they satisfy the resonance condition

$$\mathbf{k} \cdot \boldsymbol{\Omega} = 0, \qquad \mathbf{k} \in \mathbb{Z}^n \setminus \{\mathbf{0}\}. \tag{3.12}$$

If this is not satisfied then the torus is called non-resonant. While the solution (3.12) is a one-dimensional curve in the phase space, it densely fills the torus, the motion is then called quasiperiodic. In the resonant case (3.12), the motion is restricted to a lower-dimensional torus not uniquely specified by fixing the actions and if all the frequencies are commensurate with each other then the motion is confined to a one-dimensional torus and is consequently periodic.

Now that we know the relations between actions and the original integrals of motion, we would also like to have a canonical transformation between old set of the coordinates and the AA coordinates $(\mathbf{q}, \mathbf{p}) \to (\boldsymbol{\psi}, \mathbf{J})$. This can be done using a generating function of second type $S(\mathbf{q}, \mathbf{J})$ which is given by the integral (3.9) but with the curves γ_i now not being loops but having endpoints

$$S(\mathbf{q},\mathbf{J}) = \int_{\mathbf{q_0}}^{\mathbf{q}} \sum_{i=1}^{n} p_i(\mathbf{q}',\mathbf{J}) \mathrm{d}q'^i. \tag{3.13}$$

This line integral is then path-independent as the curve over which we integrate lies in M_f where $\mathrm{d}\Theta = 0$. The transformation relations are then $p_i = \frac{\partial S}{\partial q^i}$ and $\psi_i = \frac{\partial S}{\partial J_i}$.

One of the advantages of this theoretical approach is that finding the transformation relation to action angle coordinates is equivalent to solving the original equations of motion. The solution is then $\mathbf{q}(t) = \mathbf{q}(\boldsymbol{\psi}(t),\mathbf{J})$ where $\boldsymbol{\psi}(t)$ is given by (3.11).

There are very few integrable Hamiltonians that can be put into action-angle form using only elementary functions. We will mention two significant examples, the first is the linear harmonic oscillator whose Hamiltonian in original coordinates and after transformation to action-angle coordinate takes form

$$H(q,p) = \frac{p^2}{2m} + \frac{1}{2} m\Omega^2 q^2 \rightarrow \quad H(\psi, J) = \Omega J. \tag{3.14}$$

Here the transformation can be found in a simple form that as well provides the solution of the equations of motion

$$q = \sqrt{\frac{2J}{m\Omega}} \sin(\psi), \qquad p = \sqrt{2J\Omega\, m} \cos(\psi). \tag{3.15}$$

Another example from Newtonian mechanics is the Kepler Hamiltonian

$$H_{Kepler} = \frac{1}{2m}\left[p_r^2 + \frac{1}{r^2}\left(p_\theta^2 + \frac{p_\phi^2}{\sin^2\theta}\right)\right] - \frac{k}{r}. \tag{3.16}$$

while in action-angle coordinates we have [49]

$$H_{Kepler}(J_r, J_\theta, J_\phi) = -\frac{mk^2}{2(J_r + J_\theta + J_\phi)^2}. \tag{3.17}$$

where we assume without loss of generality that $J_\phi > 0$. The system has three degrees of freedom, namely (r,θ,φ) but the Hamiltonian (3.17) is degenerate, all three fundamental frequencies are identical. Consequently the motion is periodic unlike in the Schwarzschild case where $\Omega_r \neq \Omega_\theta = \Omega_\phi$ and the Kerr spacetime where all three frequencies are in general different (Obviously there are some exceptions like circular orbits but in general the Kerr frequencies are not commensurable and the motion is not periodic). Alternatively the Kepler Hamiltonian is often treated using another set of action-angle coordinates called Delaunay variables where we can use the symmetry of the Hamiltonian and replace the sum of actions in the denominator of (3.17) with a single action corresponding to a single non-zero frequency.

Lie series and Birkhoff normalization

Unfortunately, very few Hamiltonian systems are integrable. However, we can still use those few as a starting point of a perturbation expansion. Let us consider a Hamiltonian as an expansion in a small perturbation parameter ε

$$H(\psi, \mathbf{J}) = H_{int}(\mathbf{J}) + \sum_{n=1}^{\infty} \varepsilon^n H_n^{(0)}(\psi, \mathbf{J}) = H_{int}(\mathbf{J}) + P(\psi, \mathbf{J}) \tag{3.18}$$

where we express everything using action-angle coordinates of the integrable Hamiltonian H_{int} (with frequencies Ω_i) and furthermore assume that $H_n^{(0)}(\psi, \mathbf{J})$ are 2π-periodic functions in ψ.

We say that the Hamiltonian(3.18) is in Birkhoff normal form up to the order N if $\{H_{int}, P\} = \mathcal{O}(\varepsilon^{N+1})$. This thus means eliminating all the oscillatory terms from the Hamiltonian up to ε^N.

Starting from the first order in the expansion, perhaps the oldest approach is averaging the term $H_1^{(0)}(\psi, \mathbf{J})$ over the angles, which results in the new action being conserved while the fundamental frequencies are altered by the averaged $\mathcal{O}(\varepsilon)$ term. This approach is viable also for non-Hamiltonian systems as is the case of the adiabatic approximation presented in the following section. Other methods rely on generating functions which are combinations of new and old variables as was already mentioned above (the function S in (3.3)) , these are the Lindstedt method and its generalization, the von Zeipel method (both described in [5]). However a superior formulation exists which does not involve inverting partial derivatives of generating functions defining the transformation relation. This method also provides us with a simple framework that naturally extends to arbitrarily high orders in ε. This is the method of Lie transform or Lie series which was introduced in [17]. The Lie transformation $z^i \to Z^i$ is defined as a flow generated by a symplectic vector field X_χ

$$Z^i = z^i(\varepsilon) = \exp(\varepsilon \mathcal{L}_\chi) z^i \tag{3.19}$$

where χ is a function on the phase space. This form of transformation is essentially a generalization of the time evolution given in (3.8) with exchanging $t \leftrightarrow \varepsilon$ and $H \leftrightarrow \chi$. This transformation can be shown to be canonical as the Poisson brackets are preserved as a consequence of the following identity

$$\{\exp(\mathcal{L}_\chi) f, \exp(\mathcal{L}_\chi) g\} = \exp(\mathcal{L}_\chi)\{f, g\} \tag{3.20}$$

which can be proved simply by inserting the relations (3.19) into the Poisson brackets. Alternatively one can deduce the canonicity of the transformation from the equation (3.6) which means that

$$\exp(\varepsilon \mathcal{L}_\chi)\omega = \omega. \tag{3.21}$$

This formula is analogous to the pullback given by a Killing vector (1.1) preserving the spacetime metric. The symplectic vectors are generators of canonical transformation in the same fashion as the Killing vectors are generators of isometries in Riemannian or Lorentzian geometry.

As we already mentioned above, the Lie series transformation has several advantages when compared to the ordinary generating function method. The inverse of (3.19) can be obtained by simply acting with the inverse operator, that is

$$z^i = \exp(-\varepsilon \mathcal{L}_\chi) Z^i \tag{3.22}$$

where we obviously have to exchange the coordinates in the function χ, which means that $z^i \to Z^i$. Transforming a function to new coordinates is also straightforward

$$f(Z^i) = f(\exp(\varepsilon \mathcal{L}_\chi) z^i) = \exp(\varepsilon \mathcal{L}_\chi) f(z^i) \tag{3.23}$$

this is just a pullback of the function f. Now that we know how to Lie-transform functions we can return to the perturbed Hamiltonian (3.18) and try to eliminate the angle variables from the $\mathcal{O}(\varepsilon)$ part of the Hamiltonian. Recall that we assumed the 2π-periodicity in angles which means we can do a Fourier series decomposition of the Hamiltonian

$$H_1^{(0)}(\boldsymbol{\psi}, \mathbf{J}) = \sum_{\mathbf{k}} h_1^{(0)}(\mathbf{J}, \mathbf{k}) e^{\mathrm{i}\mathbf{k}\cdot\boldsymbol{\psi}} = h_1^{(0)}(\mathbf{J}, \mathbf{0}) + \tilde{H}_1^{(0)}. \tag{3.24}$$

The only term from $H_1^{(0)}$ which we would like to preserve is $h_1^{(0)}(\mathbf{J}, \mathbf{0})$. By acting with the Lie-series operator (3.19) on (3.18) we obtain up to the linear order in ε

$$H^{(1)} = \exp(\varepsilon \mathcal{L}_\chi) H = H_{int} + \varepsilon \{H_{int}, \chi\} + \varepsilon H_1^{(0)} + \mathcal{O}(\varepsilon^2). \tag{3.25}$$

To eliminate the oscillating terms from the first-order Hamiltonian we need to find the so far undetermined function χ this means solving the homological equation

$$\{H_{int}, \chi\} + \tilde{H}_1^{(0)} = 0 \Rightarrow \chi = \sum_{\mathbf{k} \neq \mathbf{0}} \frac{h_1^{(0)}(\mathbf{J}, \mathbf{k})}{\mathbf{k} \cdot \boldsymbol{\Omega}(\mathbf{J})} e^{\mathrm{i}\mathbf{k}\cdot\boldsymbol{\psi}}. \tag{3.26}$$

As we can see the solution has a simple form but crucially we have so far omitted a key assumption that is the fact that the frequency vector $\boldsymbol{\Omega}(\mathbf{J})$ (whose presence in the solution comes from the Poisson bracket containing H_{int}) is nonresonant (it does not satisfy condition (3.12)) so that the denominators in the function χ are not zero. By denoting $h_1^{(0)} = Z^{(1)}$, the Hamiltonian after the first canonical transformation has the desired form

$$H^{(1)}(\boldsymbol{\psi}^{(1)}, \mathbf{J}^{(1)}) = H_{int}(\mathbf{J}^{(1)}) + \varepsilon Z^{(1)}(\mathbf{J}^{(1)}) + \sum_{n=2}^{\infty} \varepsilon^n H_n^{(1)}(\boldsymbol{\psi}^{(1)}, \mathbf{J}^{(1)}). \tag{3.27}$$

In the second order we proceed in the same manner which means eliminating oscillating terms from $H_2^{(1)}$ by solving the homological equation (3.26) for a generating function $\chi_{(2)}$, with ε replaced by ε^2 in (3.25) because we now want to eliminate

$\mathcal{O}(\varepsilon^2)$ terms. By applying multiple Lie transforms we can reach arbitrary high order N

$$H^{(N)} = \exp(\varepsilon^N \mathcal{L}_{\chi_{(N)}}) \dots \exp(\varepsilon^2 \mathcal{L}_{\chi_{(2)}}) \exp(\varepsilon \mathcal{L}_{\chi_{(1)}}) H = \mathcal{U}^{(N)}(\boldsymbol{\chi}) H. \tag{3.28}$$

The Hamiltonian then separates into the desired part depending on the actions only and a small remainder $R = \mathcal{O}(\varepsilon^{N+1})$

$$H^{(N)} = H_{int}(\mathbf{J}^{(N)}) + \sum_{n=1}^{N} \varepsilon^n Z^{(n)}(\mathbf{J}^{(N)}) + R(\boldsymbol{\psi}^{(N)}, \mathbf{J}^{(N)}) \tag{3.29}$$

We have thus found the Birkhoff normal form of the order N. By applying the same transformation $\mathcal{U}^{(N)}(\boldsymbol{\chi})$ we can derive the relations between the original and new coordinates

$$\psi_i = \mathcal{U}^{(N)}(\boldsymbol{\chi}) \psi_i^{(N)}, \qquad J_i = \mathcal{U}^{(N)}(\boldsymbol{\chi}) J_i^{(N)}. \tag{3.30}$$

If we now neglect the remainder the solution of the Hamilton's equations is simple (3.11), the solution in the original coordinates is $\psi_i(t) = \psi_i(\boldsymbol{\psi}^{(N)}(t), \mathbf{J}^{(N)})$ and $J_i(t) = J_i(\boldsymbol{\psi}^{(N)}(t), \mathbf{J}^{(N)})$. A natural question would now be how it is with the convergence of this perturbation scheme. Generally the answer is that one can reach an optimal order at which the remainder is smallest and the approximation is the most faithful to the original system. By proceeding to higher orders, the effect of accumulation of small divisors becomes prevalent and the approximation tends to be less and less reliable even if there is no nontrivial $\mathbf{k}$ satisfying $\mathbf{k} \cdot \boldsymbol{\Omega} = 0$ exactly [21].

In higher orders, higher harmonics are present in the Hamiltonian (3.18) which means that $\mathbf{k_0} \cdot \boldsymbol{\Omega}$ can be very small for some $\mathbf{k_0}$. A small divisor first encountered in an order n is then propagated to higher orders. This happens due to the action of the Lie series operator with function $\chi_{(n)}$ (with a $\mathbf{k_0}$ term) on the non-oscillating terms (with $\mathbf{k} = 0$) of order higher than n which produces a new oscillating term containing $(\mathbf{k_0} \cdot \boldsymbol{\Omega})^{-1} e^{\mathrm{i}\mathbf{k_0} \cdot \psi}$ which then needs to be eliminated by a generated function of higher order than n containing a term proportional to $(\mathbf{k_0} \cdot \boldsymbol{\Omega})^{-2}$. The normalisation procedure thus in general creates more divergent terms in the remainder which are proportional to $(\mathbf{k_0} \cdot \boldsymbol{\Omega})^{-r}$, with positive integer exponent r. So far we have discussed only the Ansatz (3.18) which assumes expansion in a small perturbation parameter ε (like the quadrupole moment in our publication [69] or the Kerr parameter in [46]). What if the expansion was in a close neighbourhood of a point in the phase space instead of some fixed parameter. This is the case covered by the Birkhoff Normal Form Theorem (BNFT) which will be stated just a few lines below.

The starting point for the formulation of BNFT is an elliptic equilibrium point where dynamics is governed by the harmonic oscillator Hamiltonian or in the more general case of n degrees of freedom the Hamiltonian describing n independent harmonic oscillators

$$H_0 = \sum_{i=1}^{n} \Omega_i \frac{(p_i)^2 + (q_i)^2}{2} = \mathbf{J} \cdot \boldsymbol{\Omega}. \tag{3.31}$$

where we used the slightly altered definition (3.14) by setting the mass of each oscillator as $m = \Omega^{-1}$. Also like in the previous discussion of small divisors we will assume that the frequencies Ω_i are non-resonant. We will now consider a perturbed version of (3.31)

$$H(\mathbf{q}, \mathbf{p}) = H_0(\mathbf{q}, \mathbf{p}) + P(\mathbf{q}, \mathbf{p}), \quad P = \mathcal{O}(\|\mathbf{q}, \mathbf{p}\|^3) \tag{3.32}$$

where P is a smooth function whose expansion from the origin starts with cubic terms thus acting as a small perturbation close to $\mathbf{z} = (\mathbf{q}, \mathbf{p}) = (\mathbf{0}, \mathbf{0})$. We can now state the BNF theorem according to [34]

Theorem (Birkhoff Normal Form Theorem)**.** *For any positive integer N, there exists a neighbourhood $\mathcal{U}_N$ of the origin and a canonical transformation $\mathcal{T}_N : (\mathbf{q}', \mathbf{p}') \in \mathcal{U}_N \to (\mathbf{q}, \mathbf{p}) \in \mathcal{V}_N$ which puts the non-resonant Hamiltonian* (3.32) *into Birkhoff normal form up to the order N*

$$H^{(N)} := H \circ \mathcal{T}_N = H_0 + Z^{(N)} + \mathcal{R}^{(N)} = H_{(N)} + \mathcal{R}^{(N)} \tag{3.33}$$

and

1. *$Z^{(N)}$ is a polynomial of degree $N + 2$ satisfying $\{Z^{(N)}, H_0\} = 0$*
2. *The remainder R is a C^∞ function bounded as $|\mathcal{R}^{(N)}| \leq C_N \|z'\|^{N+3}, \quad \forall z' \in \mathcal{U}_N$,*
3. *$T_N(z')$ is close to identity near origin $\mathcal{T}_N(z') = z' + \mathcal{O}(\|z'\|^2)$*
4. *$Z^{(N)}$ depends only on the new actions $J_i' = \frac{(p_i')^2 + (q_i')^2}{2}$, $Z^{(N)} = Z^{(N)}(\mathbf{J}')$.*

We can thus conclude that when staying close to the origin $\mathbf{z} = 0$, the dynamical flow generated by $H_{(N)}$ approximates the real dynamics more faithfully the larger the number of normalisation steps we take. This is due to the fact that the norm of the remainder shrinks with N.

The importance of the expansion (3.32) around an elliptic fixed point lies in the fact that this corresponds to stable circular orbits in Schwarzschild or, more generally, Kerr spacetime. These are effectively one-degree-of-freedom systems which is why we did not have to worry about the non-resonance condition (and consequently the small divisors). We thus employed this scheme in our publications [69] and [46] where we started by expanding from a stable circular orbit in those spacetimes with the dynamics being reliable for small eccentricities while in the normal-form approximation for eccentric orbits the error grows with order of approximation N, which is in agreement with the BNF theorem. One can notice that the deviation in action is largest close to the apocenter while in the neighbourhood of the stable circular orbit the action seems to be converging to its theoretical value.

Ultimately the question of convergence of the Birkhoff normalization (and the convergence of the normal form itself) in various situations is still a subject of mathematical research (see [48]), nevertheless this does not change the practical usefulness of obtaining an approximate Hamiltonian in action-angle coordinates.

Apart from the Birkhoff normal form there exist other normal forms of Hamiltonians useful for various reasons. One such an example is the Kolmogorov normal form

$$H_K = \mathbf{J}\cdot\boldsymbol{\Omega} + Z(J) + H_1(\boldsymbol{\psi},\mathbf{J}), \quad Z(J), H_1 = \mathcal{O}(\mathbf{J}^2) \tag{3.34}$$

where the functions $Z(J)$ and H_1 are at least quadratic in actions. Thus even if the angles are not removed from the perturbation Hamiltonian entirely, one can still have a motion restricted to an invariant torus specified by $\mathbf{J} = 0$ with frequencies Ω_i even if a perturbation is present which is easy to see from the Hamilton's equations. The principal difference here is that the normalization procedure is convergent with the obstacle in small divisors avoided [21]. It is thus possible to normalize Hamiltonians in the form (3.34) under some assumptions (details in [33]). The construction of this normal form was used to prove the KAM theorem thus showing that non-resonant tori can survive under small perturbation.

To conclude this section there exist also other normal-forms such as the resonant normal form which allows us to study the dynamics created by the breakup of resonant tori, or the hyperbolic normal form covering the neighbourhood of an unstable fixed point with asymptotic manifold emanating from it (summarised in [21]).

3.2 The two timescales and adiabatic approximation

In this section we shall briefly introduce the concept of the two timescale formulation of extreme mass ratio inspiral. We will follow the treatment of Hinderer and Flanagan [38] as they summarize this approach in a comprehensive manner. The aim of this method is to describe the EMRI evolution in time using the action-angle formulation. The equations governing the motion of an inspiraling body are expressed as a perturbative expansion around the geodesic motion with the mass ratio $\varepsilon = \frac{\mu}{M}$ being the perturbation parameter

$$\frac{\mathrm{d}\psi_i}{\mathrm{d}t} = \Omega_i(\mathbf{J}) + \varepsilon g^{(1)}(\boldsymbol{\psi},\mathbf{J}) + \mathcal{O}(\varepsilon^2) \tag{3.35}$$

$$\frac{\mathrm{d}J_i}{\mathrm{d}t} = \varepsilon G^{(1)}(\boldsymbol{\psi},\mathbf{J}) + \varepsilon^2 G^{(2)}(\boldsymbol{\psi},\mathbf{J}) + \mathcal{O}(\varepsilon^3). \tag{3.36}$$

For $\varepsilon = 0$ the equations reduce to the Hamilton's equations for geodesics discussed in previous sections. The functions $g^{(i)}$ and $G^{(i)}$ represent the gravitational self-force driving the inspiral. Due to the nature of the AA coordinates one assumes that both sets of the perturbing functions are 2π-periodic in angles ψ_i.

For inspiral in Kerr spacetime we typically assume that $\boldsymbol{\psi} = (\psi_r, \psi_\theta)$ as the motion in the coordinates (t, ϕ) is trivial due to the symmetries generated by the Killing vectors. As for the actions one can naturally use the definitions presented in the previous sections $\mathbf{J} = (J_r, J_\theta, J_\phi)$ or alternatively use the integrals of motion $\mathbf{J} = (E, L_z, Q)$ (energy, z-component of the angular momentum and Carter constant) or the commonly used Keplerian orbital parameters $\mathbf{J} = (e, p, \mathcal{I})$. The evolution parameter t is typically the coordinate (Boyer-Lindquist) time but one can use another definition like the Mino time [55]. Apart from the action-angle form (3.35) one can also start directly from geodesic equation and promote

the integrals of motion or orbital elements to functions of time with their evolution being governed by the self-force four-acceleration thus going through a sequence of geodesics parametrized by the aforementioned parameters which is analogical to what we discuss here (see method of osculating geodesics in details in [70]).

Now comes the crucial observation coming directly from the equations (3.35). Judging by the leading term we can see that the rate of change of the angles ψ_i is dominated by the fundamental frequencies whose size is given by the mass of the central black hole M. This is the dynamical or orbital timescale characterized by the periods of the bound geodesic motion which are of order $\mathcal{O}(1)$. In contrast to that we have the inspiral timescale, this timescale is $\mathcal{O}(\varepsilon^{-1})$ long as this is the typical duration over which the actions J_i change significantly ($\dot{J} \sim \varepsilon$ in (3.35)). Consequently we can separate variables into two categories, the first are the slow variables whose change is often measured in the slow time parameter $\tilde{t} = \varepsilon t$, these are the actions (orbital parameters) and other quantities dependent on them such as the fundamental frequencies which are no longer constant or the amplitudes of the emitted gravitational waves. The other group consists of fast variables, these are the angles and the phases of the gravitational waves.

The concept of two timescales now manifests in a new parametrization. In addition to the already defined slow time $\tilde{t}$, the variables are now required to depend also on the fast phases Φ_i which generalize the notion of angle variables. The phase-space coordinates are then expanded in ε as

$$\psi_i(\mathbf{\Phi}, \tilde{t}) = \sum_{k=0}^{\infty} \varepsilon^{k/2} \psi_i^{(k/2)}(\mathbf{\Phi}, \tilde{t}), \qquad J_i(\mathbf{\Phi}, \tilde{t}) = \sum_{k=0}^{\infty} \varepsilon^{k/2} J_i^{(k/2)}(\mathbf{\Phi}, \tilde{t}) \tag{3.37}$$

where the dependence on Φ_i is naturally 2π-periodic with the exception $\psi_i^{(0)}(\mathbf{\Phi} + 2\pi\mathbf{k}, \tilde{t}) = \psi_i^{(0)}(\mathbf{\Phi}, \tilde{t}) + 2\pi k_i$, this requirement becomes clear when analysing the first order in the perturbative expansion. The rapidly changing phases can themselves be expanded in ε using slowly varying angular frequencies $\bar{\Omega}_i$

$$\frac{\mathrm{d}\Phi_i}{\mathrm{d}t} = \sum_{k=0}^{\infty} \varepsilon^{k/2} \bar{\Omega}_i^{(k/2)}(\tilde{t}). \tag{3.38}$$

By integrating this equation term by term we get the expansion in the phases as

$$\Phi_i(\tilde{t}) = \frac{1}{\varepsilon}\phi^{(0)}(\tilde{t}) + \frac{1}{\sqrt{\varepsilon}}\phi^{(1/2)}(\tilde{t}) + \phi^{(1)}(\tilde{t}) + \sqrt{\varepsilon}\phi^{(3/2)}(\tilde{t}) + \varepsilon\phi^{(2)} + \mathcal{O}(\varepsilon^{3/2}). \tag{3.39}$$

We can now analyse the equations of motion (3.35) and expansions (3.37) order by order but what we will concentrate on is the leading order in ε which is called adiabatic (or adiabatic approximation). At the adiabatic order one can find that by inserting (3.39) into equations (3.37) and some manipulations [38] we obtain the following result

$$\psi_i^{(0)} = \Phi_i, \qquad J_i^{(0)}(\mathbf{\Phi}, \tilde{t}) = J_i^{(0)}(\tilde{t}), \qquad \bar{\Omega}_i^{(0)}(\tilde{t}) = \Omega_i(\mathbf{J^{(0)}}(\tilde{t})) \tag{3.40}$$

The angle variable is equal to the fast phase which corresponds to the fact that the latter is an extension of the former while the slowly evolving actions do

not depend on the phases whose time derivatives are given by the fundamental frequencies.

By averaging out the rapidly oscillating angles $\psi_i^{(0)}$ from the forcing term $G^{(1)}$ (with the averaged part denoted as $\bar{G}^{(1)} = \langle G^{(1)} \rangle$) we arrive at two sets of differential equations governing the motion [38]

$$\frac{\mathrm{d}\psi_i^{(0)}(\tilde{t})}{\mathrm{d}\tilde{t}} = \frac{1}{\varepsilon}\Omega_i(\mathbf{J}^{(0)}(\tilde{t})), \qquad \frac{\mathrm{d}J_i^{(0)}(\tilde{t})}{\mathrm{d}\tilde{t}} = \bar{G}_i^{(1)}(\mathbf{J}^{(0)}(\tilde{t})). \tag{3.41}$$

This allows us to first solve the equations for actions $J_i^{(0)}(\tilde{t})$, which are depended on the mass ratio only through the slow time $\tilde{t}$, and subsequently we can find $\psi_i^{(0)}(\tilde{t})$ by a simple quadrature.

The averaging itself is done over invariant torus specified by fixing the actions

$$\bar{G}_i^{(1)}(\mathbf{J}) = \left\langle G_i^{(1)}(\boldsymbol{\psi}, \mathbf{J}) \right\rangle = \frac{1}{(2\pi)^n} \int_0^{2\pi} G_i^{(1)}(\boldsymbol{\psi}, \mathbf{J}) \mathrm{d}^n\psi. \tag{3.42}$$

We should stress at this point that this averaging is done under the assumption that the fundamental frequencies are not in resonance ($\mathbf{k} \cdot \boldsymbol{\Omega} \neq 0$). In the particular case of Kerr spacetime this is equivalent to the statement that Ω_r and Ω_θ are not commensurate. In the resonant case the motion in $\psi_r - \psi_\theta$ space is periodic and does not densely cover the torus. Alternatively one can also do the averaging by calculating a one-dimensional integral along a geodesic which gradually fills the invariant torus,if the time over which we integrate is very long (ideally infinite). We used this type of averaging in [69]. The treatment of resonances requires a more delicate approach than the two methods mentioned above [80].

The function $G_i^{(1)}(\boldsymbol{\psi}, \mathbf{J})$ represents the self-force at the first order in ϵ, it can be split into two parts [38], the first is dissipative which is responsible for the decay of the actions (constants of motion) and the conservative part (there is a Hamiltonian formulation of this part of the self-force [13]) which only slightly alters the geodesic motion (the fundamental frequencies). The conservative part of $G_i^{(1)}(\boldsymbol{\psi}, \mathbf{J})$ does not survive the averaging so only the averaged dissipative part plays a role in the adiabatic equations of motion (3.41). There is yet another simplification in the adiabatic order which allows us to calculate $\left\langle G_i^{(1)}(\boldsymbol{\psi}, \mathbf{J}) \right\rangle$ using the gravitational-wave fluxes of $J_i^{(0)}$ to infinity (and horizon). This straightforward approach was used in our papers [69] and [46]

We can now briefly mention the higher orders in the phase expansion (3.39). It can be shown that in the absence of resonances the terms of the order $\mathcal{O}(\varepsilon^{-1/2})$ can be set to zero (the actions $J_i^{(1/2)}$ can be absorbed into $J_i^{(0)}$). These terms thus play an important role in the resonant case where their contribution to the resulting phase of the gravitational wave is substantial. The first post-adiabatic order is much harder to calculate as one has to take into consideration both parts of the first-order self-force as well as the averaged part of the second order self-force, this means including $G^{(1)}$, $g^{(1)}$ and $\left\langle G^{(2)} \right\rangle$. While the inclusion of the first post-adiabatic terms is essential in producing accurate waveforms, it goes beyond the limits of our calculation which is why we shall focus on describing the methods of calculating fluxes of constants of motion using quadrupole formalism and black hole perturbation theory in the following two sections.

3.3 Quadrupole formalism

The first method of calculating the gravitational wave fluxes necessary for evolving adiabatic inspirals, which we are going to discuss, is the quadrupole formalism. This approach is actually the oldest one but we present it here as it was used in our publication [69]. We will be interested in the metric describing the gravitational wave perturbation at the infinity from which we can calculate the fluxes using the stress-energy tensor (2.60). During the derivation, the assumption of nearly Newtonian source and field is used, which is why we shall restore the two fundamental constants of general relativity c and G.

Following [8] we define the field variable $\bar{h}^{\mu\nu}$ without any assumption apart from the following gauge condition

$$\bar{h}^{\mu\nu} = \sqrt{-g}g^{\mu\nu} - \eta^{\mu\nu}, \qquad \partial_\mu \bar{h}^{\mu\nu} = 0. \tag{3.43}$$

This condition is the harmonic gauge condition and is equivalent to the relation $\Box x^\mu = 0$. The Einstein's equation can then be recast as

$$\Box \bar{h}_{\mu\nu} = \frac{16\pi G}{c^4}\Lambda_{\mu\nu}, \qquad \Lambda_{\mu\nu} = (-g)(T_{\mu\nu} + \tau^{LL}_{\mu\nu} + \tau^{H}_{\mu\nu}) \tag{3.44}$$

where the d'Alembertian on the left side is just $\Box = \eta^{\mu\nu}\partial_\mu\partial_\nu$. On the right hand side we have the sum of matter stress-energy tensor, the Landau-Lifshitz pseudotensor (defined by (2.17)) and another symmetric pseudotensor defined by a superpotential whose form stems from our choice (3.43). Given the properties of both sides of the equation (3.44) it is not surprising that $\partial_\mu\Lambda^{\mu\nu} = 0$. The flat-space d'Alembertian can then be inverted using its Green's function which leaves us with

$$\bar{h}_{\mu\nu}(t,x) = -\frac{4G}{c^4}\int \frac{\Lambda_{\mu\nu}(x', t - |x-x'|/c)}{|x-x'|}\mathrm{d}^3x'. \tag{3.45}$$

Using $\partial_\mu\Lambda^{\mu\nu} = 0$ we can transform Λ^{ij} into the form

$$\Lambda^{ij} = \frac{1}{2}\partial_{00}(\Lambda^{00}x^i x^j) + \partial_k F^{kij}. \tag{3.46}$$

Now comes the crucial assumption about the spacetime to be a small perturbation of the Minkowski space and by assuming the Newtonian character of the source ($T^{00} \gg |\tau^{LL}_{\mu\nu} + \tau^{H}_{\mu\nu}|$, $T^{00} \gg |T^{ij}|$) we can neglect the contribution of the gravitational field in $\Lambda_{\mu\nu}$ which is now fully given by the matter stress-energy tensor. This allows us to do several simplifications (see [57]). Firstly we can eliminate the term $\partial_k F^{kij}$ using a surface integral at the infinity (It involves only gravitational $\mathcal{O}(G)$ terms which we neglect), secondly we can express our spacetime in Cartesian coordinates at infinity ($\sqrt{-g} = 1$) and lastly perform a multipole expansion far from the source (the wave zone $r \gg \lambda$, $r = \sqrt{\delta_{ij}x^i x^j} \to \infty$) which gives us at the leading order

$$h_{ij}(t, r\to\infty) = \frac{2G}{c^4}\frac{1}{r}\frac{\mathrm{d}^2 I_{ij}(t - r/c)}{\mathrm{d}t^2}. \tag{3.47}$$

The quantity I_{ij} is the quadrupole moment of the source given by integral

$$I^{ij}(t) = \int_{source} T^{00}(x,t)x^i x^j \mathrm{d}^3x. \tag{3.48}$$

Having obtained the metric perturbation,it is customary to work in the transverse-traceless (TT) gauge with respect to a static observer at the infinity. As the metric (3.47) is already the transverse part of $h_{\mu\nu}$, we only need to subtract the trace part to obtain the TT gauge. This can be done on the level of I_{ij} by defining the reduced quadrupole moment by

$$\mathit{I}^{ij}(t) = \int_{source} T^{00}(x,t)\left(x^i x^j - \frac{1}{3}x^k x_k \delta^{ij}\right)\mathrm{d}^3x \tag{3.49}$$

which then gives us the desired result in the form [57]

$$h_{ij}^{TT}(t,r) = \frac{2G}{c^4}\frac{1}{r}\frac{\mathrm{d}^2\mathit{I}_{ij}(t-r/c)}{\mathrm{d}t^2}. \tag{3.50}$$

While this metric already has two independent components it is common to also work with two polarizations h_+ and $h_\times$. These can be recovered by employing two projection tensors and contracting them with h_{ij}^{TT} this is described for example in [59] and was also used in our paper [69].

With the metric known we can proceed by calculating the loss of energy and angular momentum due to radiation. The averaged flux of an integral of motion I (associated with a Killing vector ξ) to the infinity is then given by an integral over sphere located at the infinity

$$\left\langle \frac{\mathrm{d}I}{\mathrm{d}t} \right\rangle^{\infty} = \int_{S(t,r\to\infty)} \xi^\mu T_{\mu\nu}^{GW} s^\nu \mathrm{d}S \tag{3.51}$$

where the gravitational-wave stress-energy tensor (2.60) was discussed in previous chapter (as before s^ν is the normal vector to the sphere). By plugging in the expression (3.50) we get the well known results for energy and the three components of angular momentum (detailed derivation in [64])

$$\left\langle \frac{\mathrm{d}E}{\mathrm{d}t} \right\rangle = \frac{G}{5c^5}\sum_{i,j=1}^{3}\left\langle \left(\frac{\mathrm{d}^3\mathit{I}_{ij}}{\mathrm{d}t^3}\right)^2 \right\rangle, \quad \left\langle \frac{\mathrm{d}L_i}{\mathrm{d}t} \right\rangle = \frac{2G}{5c^5}\sum_{j,k,l=1}^{3}\epsilon_{ijk}\left\langle \left(\frac{\mathrm{d}^3\mathit{I}_{jl}}{\mathrm{d}t^3}\frac{\mathrm{d}^2\mathit{I}_{kl}}{\mathrm{d}t^2}\right) \right\rangle. \tag{3.52}$$

Obviously the rate of change of energy and angular momentum of an inspiraling particle is given with negative sign.

As a complement to the above mentioned results of the quadrupole formalism one can derive a radiation-reaction potential

$$\Phi^{react} = -\frac{1}{2}h_{00}^{react} = \frac{G}{5c^5}\frac{\mathrm{d}^5\mathit{I}_{ij}(t)}{\mathrm{d}t^5}x^i x^j. \tag{3.53}$$

whose gradient gives the force acting on the particle due to the radiation. This potential can be obtained by finding the component h_{00} from the transverse part of the metric $h_{\mu\nu}$ given by (3.47) using the gauge condition (3.43). After some manipulations and gauge transformations (as shown in [57]) one can extract the part h_{00}^{react} of h_{00} responsible for the gravitational backreaction (other parts are

non-dynamical like the Coulombic potential). The force obtained from the potential then provides alternative means of deriving the fluxes (3.52).

Let us note before concluding this section that the quadrupole formalism is only a starting point in a much larger landscape called post-Newtonian (PN) expansion. This approximation assumes the gravitational field to be weak and the motion of the source to be slow. The expansion itself is performed in powers of $(\frac{v}{c})^{2n}$ with n being the order of the approximation. For example by looking at the powers of c one can recognize that the potential (3.53) as well as the fluxes (3.52) are of the 2.5PN order. In the PN approximation both the metric $h_{\mu\nu}$ and the stress-energy tensor are expanded in the powers of c which allows us to compute the generalizations of the potential (3.53) (the radiative force is no longer fully scalar but contains also a purely vector part) as well as the fluxes (3.52). The definition of the quadrupole moment (3.48) is now also different as it contains contributions from the T^{0i} components of the stress energy tensor which are at the leading order neglected when compared with T^{00}. A similar approach to the PN expansion is the post-Minkowskian expansion [65] which starts from Minkowski spacetime by expanding the metric in the powers of the Newton gravitational constant G. All these techniques are beyond the scope of this thesis and we will not discuss them further, a comprehensive review can be found in [12].

3.4 The Teukolsky formalism

In the previous section we have discussed the lowest order of the post-Newtonian expansion, in the following we shall dive into the area of black hole perturbation theory or more specifically into the Teukolsky formalism. The methods of the black hole perturbation theory are fully relativistic meaning that they expand the full Einstein's equations in powers of a perturbation parameter ε (which is not a physical constant like c or G) and solve them order by order. The zeroth order (the background) typically corresponds to a black-hole exact solution like the Kerr or Schwarzschild solution. An example of a perturbation scheme was the high frequency approximation performed in the expansion of the Ricci tensor (2.51) where we used two different lengthscales, each associated with either the background or the gravitational waves. In the case of the extreme mass ratio inspiral the perturbation parameter is naturally the ratio of the two masses $\varepsilon = m/M$.

The most straightforward approach is to expand the metric

$$g_{\mu\nu} = g^{(B)}_{\mu\nu} + \varepsilon h^{(1)}_{\mu\nu} + \mathcal{O}(\varepsilon^2) \tag{3.54}$$

but even in the first order the linearised Einstein's equations for $h^{(1)}_{\mu\nu}$ may be difficult to solve. An alternative is to formulate the linearised equations in a more simple form involving only scalars and take advantages of symmetries of the background if they are present. Once the equations for the scalars are solved one can reconstruct the corresponding metric $h^{(1)}_{\mu\nu}$ from them. This program was first successfully implemented in the Schwarzschild spacetime by using the Regge-Wheeler-Zerilli formalism [71] [93]. In this approach the metric perturbation is decomposed into a basis of tensor spherical harmonics which separates the radial and angular dependence of the metric. Following a Fourier transform in time

we are left with ordinary differential equations in the radial coordinate r which can be formulated in terms of master scalars. These are the Regge-Wheeler and Zerilli equations. This RWZ formalism can describe not only the gravitational perturbations but also perturbation of fields corresponding to a different spin than $s = 2$ like scalar ($s = 0$) or electromagnetic ($s = 1$) using a single second-order partial differential equation depending on s. While this formalism has become very popular, it cannot be extended beyond spherical symmetry, most notably to the Kerr black hole. In that case one can instead turn to the Teukolsky formalism as we did in our paper [46].

The Teukolsky equation introduced in [87] is based on the Newman-Penrose (NP) formalism which enables us to write the field equations for gravitational or electromagnetic field using scalars defined by projecting the curvature tensor and covariant derivatives onto a NP tetrad (see below). From this we can derive the Teukolsky master equation which is a partial differential equation for a single scalar describing perturbation of a field with spin s (this includes also Weyl spinors with $s = 1/2$). The scalar function solving the Teukolsky equation thus has a mathematical meaning, it is a curvature scalar describing dynamical degrees of freedom (in the gravitational case the scalars constructed from the Weyl tensor). It can be shown that the scalar is gauge invariant, it does not depend on coordinates, nor the particular NP tetrad [87] which is a useful property.

Since we are concerned only with adiabatic order (3.41), we only need the gravitational-wave fluxes as was the case in the previous section. This time however we will have to consider fluxes to the horizon as well as we are perturbing a black hole spacetime. The fact that we only need the fluxes and the waveforms at infinity and on the horizon greatly simplifies the calculations as the source of the perturbation has a singular nature, it is a point particle with mass m described by stress energy tensor

$$T^{\mu\nu} = m\frac{u^\mu(\tau)u^\nu(\tau)}{u^0(\tau)\sqrt{-g}}\delta^3(x^i - x^i(\tau)) \tag{3.55}$$

where $x^i(\tau)$ is the geodesic trajectory in the spacelike coordinates x^i, u^μ is the four-velocity and δ^3 is an ordinary three-dimensional delta function. We thus do not have to perform any regularization at the location of the particle as is done in the self-force calculations.

The method of solving the Teukolsky equation described in the following subsections uses complete separability of the equation in the Kerr spacetime, it is a frequency-domain method. An alternative to this mode decomposition is the time-domain approach [36] [63].

3.4.1 The NP formalism and the Teukolsky equation

The important result was derived by Teukolsky in [87] using the Newman-Penrose formalism. The Newman-Penrose tetrad consists of two null vectors l and n and two complex-conjugated vectors m and $\bar{m}$ satisfying the following normalization

$$l^\mu n_\mu = -1, \qquad m^\mu \bar{m}_\mu = 1 \tag{3.56}$$

while the other scalar products are zero. Consequently the metric can be expressed using the NP tetrad as

$$g_{\mu\nu} = -2l_{(\mu}n_{\nu)} + 2m_{(\mu}\bar{m}_{\nu)}. \tag{3.57}$$

When introducing the NP formalism one proceeds by defining the covariant derivatives in direction of the tetrad field like $D = l^\mu \nabla_\mu$ and spin coefficients such as $\kappa = -l^\mu m^\nu \nabla_\mu l_\nu$ but we will not discuss that in detail.

As we have mentioned above, the Teukolsky equation was found for field perturbations with various spins. For instance for the spin $s = 0$ we have a single scalar field while the electromagnetic field ($s = 1$) is described by three complex scalars Φ_0, Φ_1 and Φ_2 each of which is obtained by projecting the electromagnetic tensor on the NP tetrad. In the gravitational case ($s = 2$) the Riemann curvature tensor is decomposed into the Ricci tensor which is completely determined by the matter content ($T_{\mu\nu}$) and the Weyl tensor $C_{\mu\nu\lambda\rho}$ which contains the two degrees of freedom of gravitational field (the two polarizations of gravitational waves).

There are five Weyl scalars Ψ in total but only three of them are relevant in our discussion

$$\Psi_0 = C_{\mu\nu\lambda\rho}l^\mu m^\nu l^\lambda m^\rho, \quad \Psi_2 = C_{\mu\nu\lambda\rho}l^\mu m^\nu \bar{m}^\lambda n^\rho, \quad \Psi_4 = C_{\mu\nu\lambda\rho}n^\mu \bar{m}^\nu n^\lambda \bar{m}^\rho. \tag{3.58}$$

The scalar Ψ_2 is the only nonzero Weyl scalar for the Petrov type D spacetime which is an algebraically special class of spacetime to which the Kerr solution belongs. While the scalar Ψ_2 describes the Coulombic part of the field the scalars Ψ_0 and Ψ_4 correspond to the transverse components of gravitational waves propagating in the null directions l and n [35].

The aim of the Teukolsky formalism is to find a perturbation ${}_s\psi$ to a field with spin weight s. The concept of spin weight comes from the Geroch-Held-Penrose (GHP) formalism [30] and it is defined by transformation properties of scalars when NP basis is changed using complex rotation. The NP scalars are thus split into the background and perturbation part and the field equations are linearised which leads to the Teukolsky equation in the form

$$\mathfrak{L}_s\psi = 8\pi\mathfrak{T} \tag{3.59}$$

where $\mathfrak{L}$ is a linear differential operator and $\mathfrak{T}$ is the source of the perturbation. The key in the derivation is the decoupling of the various NP scalars so that we are left with an equation for a single scalar ${}_s\psi$, this is discussed in [87] or by using the GHP formalism in [71]. One should keep in mind that the particular form of the source $\mathfrak{T}$ as well as the linear operator $\mathfrak{L}$ depends on the spin weight of the particular scalar ${}_s\psi$. We shall now turn our attention to the Kerr spacetime as this is probably the most significant black-hole solution where perturbation can be studied while it was also the focus of our paper [46].

3.4.2 Teukolsky equation in Kerr spacetime

Since the Kerr metric (1.19) is algebraically special, many spin coefficients vanish and we are also left with a single Weyl scalar $\Psi_2^{(0)} = -M\xi^{-3}$ where $\xi = r -$

$\mathrm{i}a\cos(\theta)$. The NP tetrad originally used to derive the Teukolsky equation [87] in Kerr spacetine is the Kinnersley tetrad [19]

$$\begin{aligned} l &= \frac{(r^2+a^2)}{\Delta}\partial_t + \partial_r + \frac{a}{\Delta}\partial_\phi \\ n &= \frac{(r^2+a^2)}{2\Sigma}\partial_t - \frac{\Delta}{2\Sigma}\partial_r + \frac{a}{2\Sigma}\partial_\phi \\ m &= -\frac{\rho}{\sqrt{2}}\left(\mathrm{i}a\sin\theta\partial_t + \partial_\theta + \frac{\mathrm{i}}{\sin\theta}\partial_\phi\right) \end{aligned} \tag{3.60}$$

alternatively one can also use the Carter tetrad which is related to the Kinnersley tetrad by rescaling the tetrad vectors with Kerr metric functions. The abstract equation (3.59) now takes a concrete form

$$\begin{aligned} &\left[\frac{(r^2+a^2)^2}{\Delta} - a^2\sin^2\theta\right]\frac{\partial^2{}_s\psi}{\partial t^2} + \frac{4Mar}{\Delta}\frac{\partial^2{}_s\psi}{\partial t\partial\phi} + \left[\frac{a^2}{\Delta} - \frac{1}{\sin^2\theta}\right]\frac{\partial^2{}_s\psi}{\partial\phi^2} \\ &-\Delta^{-s}\frac{\partial}{\partial r}\left(\Delta^{s+1}\frac{\partial_s\psi}{\partial r}\right) - \frac{1}{\sin\theta}\frac{\partial}{\partial\theta}\left(\sin\theta\frac{\partial_s\psi}{\partial\theta}\right) - 2s\left[\frac{a(r-M)}{\Delta} + \frac{\mathrm{i}\cos\theta}{\sin^2\theta}\right]\frac{\partial_s\psi}{\partial\phi} \\ &-2s\left[\frac{M(r^2-a^2)}{\Delta} - r - \mathrm{i}a\cos\theta\right]\frac{\partial_s\psi}{\partial t} + (s^2\cot^2\theta - s){}_s\psi = 4\pi\Sigma\mathcal{T}. \end{aligned} \tag{3.61}$$

This is the Teukolsky (master) equation in Kerr spacetime for a perturbation ${}_s\psi$. It is a second-order linear partial differential equation which closely resembles the wave equation. This becomes more apparent if it is expressed as [11]

$$[(\nabla^\mu + s\Gamma^\mu)(\nabla_\mu + s\Gamma_\mu) - 4s^2\Psi_2^{(0)}]{}_s\psi = 4\pi\mathcal{T}. \tag{3.62}$$

From this form it is clear that it reduces to the wave equation in the scalar ($s = 0$) case. The right-hand side of the equation is given by the source $\mathcal{T}$ which is given by a differential operator acting on the tetrad components of the corresponding source (stress-energy tensor in the gravitational case, the electric four-current in the electromagnetic case etc.). The source and the perturbation ${}_s\psi$ depend also on the choice of a particular NP scalar for which we are trying to solve the Teukolsky equation. As was discussed in the previous section we have two Weyl scalars describing radiation each associated with a value of spin weight, we can thus have either ${}_2\psi = \psi_0$ or ${}_{-2}\psi = \xi^4\psi_4$ [87]. One should also note that in the absence of source the two Weyl scalars are not independent but are related by the Teukolsky-Starobinsky identities [71]. In electromagnetic case the situation is analogous with two scalars Φ_0 and Φ_2 corresponding to the spin weights 1 and -1 respectively.

While we can in principle solve the Teukolsky equation (3.61) using numerical methods it is possible to employ a semi-analytical approach as well by using the fact that it is separable in the radial and angular variables. This is due to the symmetries of the Kerr spacetime which allows for the separation of the geodesic equation using the Carter constant. A perturbation with spin weight s can thus be decomposed as

$$ {}_s\psi = \int_{-\infty}^{\infty} \sum_{l,m} {}_sR_{lm\omega}(r) {}_sS_{lm}(\theta,\phi,a\omega) e^{-\mathrm{i}\omega t} \mathrm{d}\omega \tag{3.63} $$

where the angular functions ${}_sS_{lm}(\theta,\phi,a\omega)$ are called spin-weighted spheroidal harmonics satisfying the eigenfunction problem for the angular part of the Teukolsky equation

$$ \frac{\mathrm{d}}{\mathrm{d}\chi}\left((1-\chi^2)\frac{\mathrm{d}_s S_{lm}}{\mathrm{d}\chi}\right) + \left(a^2\omega^2\chi^2 - \frac{(m+s\chi)^2}{1-\chi^2} - 2as\omega\chi + s + A\right){}_sS_{lm} = 0 \tag{3.64} $$

where $\chi = \cos\theta$, $A = \lambda_{lm} + 2am\omega - a^2\omega^2$ and λ_{lm} is the eigenvalue. The functions ${}_sS_{lm}(\theta,\phi,a\omega)$ form a complete basis which is orthogonal with respect to a scalar product given by integration over a sphere [71]. The spin-weighted spheroidal harmonics reduce to spin-weighted spherical harmonics ${}_sY_{lm}(\theta,\phi)$ for $a\omega = 0$ and if also $s = 0$ the resulting functions are the standard spherical harmonics $Y_{lm}(\theta,\phi)$ present already in the solution of the flat-space Laplace equation (1.39). As in the case of spherical harmonics, the ϕ-dependence is trivial (${}_sS_{lm}(\theta,\phi,a\omega) = {}_sS_{lm}(\theta,0,a\omega)e^{\mathrm{i}m\phi}$).

The eigenvalue λ_{lm} is like other quantities a function of $a\omega$ and it is also the separation constant in the equation (3.61) which is the reason it is also present in the radial Teukolsky equation

$$ \Delta^{-s}\frac{\mathrm{d}}{\mathrm{d}r}\left(\Delta^{s+1}\frac{\mathrm{d}_s R_{lm\omega}}{\mathrm{d}r}\right) + \left(\frac{K^2 - 2\mathrm{i}s(r-M)K}{\Delta} + 4\mathrm{i}sr - \lambda_{lm}\right){}_sR_{lm\omega} = {}_s\mathcal{T}_{lm} \tag{3.65} $$

where $K = (r^2+a^2)\omega - am$.

3.4.3 Solving the Teukolsky radial equation

We shall now discuss some approaches to solving the radial Teukolsky equation (3.65). As the equation is linear we first solve the homogeneous problem before adding the source term ${}_s\mathcal{T}_{lm}$. The fundamental solution is given by a linear combination of two independent basis solutions which are often found by reformulating the equation by replacing the radial coordinate r with tortoise coordinate r_* and by imposing certain boundary conditions at the infinity and on the horizon located at r_+. The resulting pair of solutions can then be expressed using ingoing and outgoing waves, the solutions with their boundary forms are [40],[71]

$$ {}_sR^{(H)}_{lm\omega}(r \to r_+) \sim {}_sB^{hole}_{lm\omega}\Delta^{-s}e^{-\mathrm{i}pr_*}, \tag{3.66} $$

$$ {}_sR^{(H)}_{lm\omega}(r \to \infty) \sim {}_sB^{out}_{lm\omega}r^{-1-2s}e^{\mathrm{i}\omega r_*} + {}_sB^{in}_{lm\omega}r^{-1}e^{-\mathrm{i}\omega r_*} \tag{3.67} $$

$$ \tag{3.68} $$

and

$$ {}_sR^{(\infty)}_{lm\omega}(r \to r_+) \sim {}_sD^{out}_{lm\omega} e^{\mathrm{i}pr_*} + {}_sD^{in}_{lm\omega} \Delta^{-s} e^{-\mathrm{i}pr_*}, \tag{3.69} $$

$$ {}_sR^{(\infty)}_{lm\omega}(r \to \infty) \sim {}_sD^{\infty}_{lm\omega} r^{-1-2s} e^{\mathrm{i}\omega r_*} \tag{3.70} $$

where $p = \omega - m\Omega_+$ with Ω_+ being the angular velocity of the horizon $\Omega_+ = \frac{a}{2Mr_+}$. The reflection/transmission coefficients B and D are determined by (3.65). Once setting these boundary conditions one can in principle numerically integrate the equation to obtain the solutions $R^{(H)}$ and $R^{(\infty)}$ for $r \geq r_+$. So one can for example start with $R^{(H)}$ at the horizon (and freely choose the coefficient B^{hole}) and integrate up to the infinity. In doing so one may encounter numerical difficulties for a large value of r because there is r^{-s} difference between the ingoing and outgoing wave which means that one of them will be (depending on the value of s) suppressed which may lead to numerical errors for $r \to \infty$. An analogous situation arises for the $R^{(\infty)}$ when close to the horizon, as $\Delta(r_+) = 0$. One of the approaches to circumvent this issue is to relate the solution of Teukolsky equation to a solution of another equation which does not have the same problem. Such an equation was found by Sasaki and Nakamura [75].

Though there exists a generalization for an arbitrary spin [39] we shall stick with the $s = -2$ case for simplicity. A solution $R(r)$ to the equation (3.65) can be mapped onto the function $\chi(r)$

$$ \chi(r) = \alpha(r) R(r) + \frac{\beta(r)}{\Delta} R'(r) \tag{3.71} $$

which itself is related to X defined as $\chi = X\Delta/\sqrt{r^2 + a^2}$. This X is then the solution to the Sasaki-Nakamura equation

$$ \frac{\mathrm{d}^2 X}{\mathrm{d}r^{*2}} - F(r) \frac{\mathrm{d}X}{\mathrm{d}r^*} - U(r) X = 0. \tag{3.72} $$

We will not include the functions $\alpha(r)$ and $\beta(r)$ nor the potentials $F(r)$ and $U(r)$ (they can be found in [40] or [75]), what is important however is the fact that these potentials asymptotically behave like $F(r) \sim r^{-2}$ and $U(r) = -\omega^2 + \mathcal{O}(1/r^{-2})$. This is in contrast to the Teukolsky potentials (when the Teukolsky equation is put into a form similar to (3.72)) with asymptotics of r^{-1} . This long-distance nature of the Teukolsky potentials is associated with the suppression of one of the complex exponentials. This is absent in the Sasaki-Nakamura solution X which is just a linear combination of an ingoing and outgoing wave so that no part of the solution is numerically suppressed. The procedure would thus be to first solve the Sasaki-Nakamura equation (using the Teukolsky boundary conditions) and then transform the solution X to the solution R using a relation inverse to (3.71) (see [40]).

Another method commonly used to solve the radial Teukolsky equation is the Mano–Suzuki–Takasugi (MST) method. In that scheme one again reformulates the equation (3.65) by inserting an ansatz containing an undetermined function $p(x)$ (see [76]). The equation for $p(x)$ can then be solved perturbatively with an expansion parameter $\varepsilon = 2M\omega$. For $\varepsilon = 0$, $p(x)$ is given by a hypergeometric

function but even if the perurbative part is present one can express the complete solution $p(x)$ as a series in hypergeometric functions with coefficients satisfying a recurrence relation. We will not however discuss this method here further (details are in [76]).

Having found the homogeneous solution we can now derive a general solution when a source term is present. This can be done by employing the variations of constants which yields a general solution

$$ {}_sR_{lm\omega}(r) = {}_sC^{(H)}_{lm\omega}(r){}_sR^{(\infty)}_{lm\omega}(r) + {}_sC^{(\infty)}_{lm\omega}(r){}_sR^{(H)}_{lm\omega}(r) \tag{3.73} $$

where $C^{(H)}$ and $C^{(\infty)}$ are given by an integral over the source $\mathcal{T}_{lm}$ and the respective homogeneous solution

$$ {}_sC^{(H)}_{lm\omega}(r) = \int_{r_+}^{r} \frac{{}_sR^{(H)}_{lm\omega}(r')}{W(r')\Delta(r')}{}_s\mathcal{T}_{lm}(r')\mathrm{d}r' \quad {}_sC^{(\infty)}_{lm\omega}(r) = \int_{r}^{\infty} \frac{{}_sR^{(\infty)}_{lm\omega}(r')}{W(r')\Delta(r')}{}_s\mathcal{T}_{lm}(r')\mathrm{d}r'. \tag{3.74} $$

In this expression $W(r)$ is the Wronskian of the equation (3.65). When calculating the integrals (3.74) one can use the fact that $\Delta^{s+1}(r)W(r) = const.$ [71] (a consequence of the Abel identity).

We can now turn our attention to the source which we will assume to be a point particle following a bound Kerr geodesics parametrized here by the coordinate time $(r(t), \theta(t), \phi(t))$. We shall restrict ourselves only to the ψ_4 Weyl scalar which means that $s = -2$ (in principle one can use the scalar ψ_0 instead of ψ_4). The radial part of the source $\mathcal{T}_{lm}$ can be found using the Fourier transform in time and also using the orthogonality condition of the spin-weighted spheroidal harmonics

$$ \mathcal{T}_{lm}(r,\omega) = \int_{-\infty}^{\infty}\int_{S} \Sigma\mathcal{T}\bar{S}_{lm}(\theta,\phi,a\omega)e^{\mathrm{i}\omega t}\mathrm{d}\Omega\mathrm{d}t. \tag{3.75} $$

The decomposition of the source is thus analogical to the solution ψ_4 itself. As was already stated in the previous sections the source $\mathcal{T}$ is given by NP diferential operators acting on tetrad components of $T_{\mu\nu}$ [87]. Since the source is localized, meaning the stress-energy tensor has the form $T_{\mu\nu} \sim \delta(r - r(t))\delta(\theta - \theta(t))\delta(\phi - \phi(t))$, the integration over the angular coordinates is trivial as is the integration over r in (3.74) which produces a Heaviside step function $\Theta(r - r(t))$ for C^H or $\Theta(r(t) - r)$ in the case of C^∞. We are thus left with only a single integral over t

$$ C^{H/\infty}_{lm\omega}(r) = \int_{-\infty}^{\infty} I^{H/\infty}_{lm}(r, r(t), \theta(t))e^{\mathrm{i}\omega t - \mathrm{i}m\phi(t)}\mathrm{d}t. \tag{3.76} $$

The function $I^{H/\infty}$ depends on r only through the step function while it contains first and second derivatives of the homogeneous solution [19]. We can now use the fact that the motion in $r(t)$ and $\theta(t)$ is periodic with frequencies Ω_r and Ω_θ respectively. The integrands $I^{H/\infty}$ can then be written as a Fourier series in phases $\psi_r = \Omega_r t$ and $\psi_\theta = \Omega_\theta t$ which means that the coefficients $C^{H/\infty}$ are just a sum of delta functions

$$ C^{H/\infty}_{lm}(r,\omega) = \sum_{nk} C^{H/\infty}_{nkml}(r)\delta(\omega - \omega_{nkm}). \tag{3.77} $$

Since we have only discrete frequencies $\omega_{nkm} = n\Omega_r + k\Omega_\theta + m\Omega_\phi$ we can replace the integral in time (3.76) with integrals over respective angle (phase) variables ψ_i to obtain the Fourier coefficients $C^{H/\infty}_{nkml}$ (see [19] and [41]). The complete solution (3.63) is then a sum of individual modes

$$\xi^4\psi_4 = \sum_{nklm} R_{nklm}(r)S_{lm}(\theta)e^{\mathrm{i}m\phi - \mathrm{i}\omega_{nkm}t}, \tag{3.78}$$

here we again extracted the ϕ exponential from S_{lm}. This solution has a particularly simple form at the infinity where C^∞ vanishes and the asymptotic form of R^∞ is given simply by (3.69). Putting this all together, one obtains

$$\psi_4(r \to \infty) = \frac{1}{r}\sum_{nklm} C^H_{nkml}S_{lm}(\theta)e^{\mathrm{i}m\phi - \mathrm{i}\omega_{nkm}(t-r)} \tag{3.79}$$

where $C^H_{nkml} = C^H_{nkml}(\infty)$ which is just the value of the coefficients for $r > r(t)$ while the tortoise coordinate asymptotically behaves as $r_*(r \to \infty) = r$.

3.4.4 The gravitational wave metric and fluxes

A relevant question at this point is, how does the metric perturbation $h_{\mu\nu}$ describing gravitational wave relate to the Weyl scalar ψ_4 (or ψ_0). This can be done in the radiation gauge which is analogical to the TT gauge since it demands that $h^\mu{}_\mu = 0$ and either $l^\mu h_{\mu\nu} = 0$ in the case of ingoing radiation gauge (IRG) or $n^\mu h_{\mu\nu} = 0$ for the outgoing radiation gauge (ORG). The metric in these gauges can be reconstructed using the so called Hertz potential.

There are in fact two Hertz potentials ψ^{IRG} and ψ^{ORG} which are scalars with the same spin weights as ψ_4 and ψ_0 respectively. For instance in the IRG gauge the metric tetrad components can be found by applying a second order differential operator on the Hertz potential ψ^{IRG}: $h^{IRG}_{\mu\nu} = F(\psi^{IRG})_{\mu\nu}$ a similar relation holds true also for the ORG Hertz potential [71]. One significant property of ψ^{IRG} is the fact that it satisfies the Teukolsky equation $\mathfrak{L}\psi^{IRG} = \eta^{IRG}(\mathfrak{T})$ but with a different source term η^{IRG} than in equation (3.59), this source term however is determined by the stress-energy tensor as well.

One can thus find ψ^{IRG} by solving the Teukolsky equation with this modified source or alternatively one can obtain it from one of the two Weyl scalars $\psi_{0/4} = G(\psi^{IRG})$ where G represents a fourth-order differential operator. Since the Hertz potential is also a solution to the Teukolsky equation it can be decomposed into modes similarly to (3.78) one can thus functionally relate the Weyl-scalar radial modes to those of the Hertz potential $R^{IRG}_{lm\omega} = H(R_{lm\omega})$, his was done for example in [88] for the ORG potential. Since we have not introduced here any spin coefficients or NP derivatives we will not discuss the particular form of all these linear relations (hence using just letters F, G and H)

Without dwelling any deeper into this let us finally discuss a useful formula which relates the Weyl scalar ψ_4 to the tetrad component of the metric perturbation $h_{m\bar{m}}$ at the infinity

$$\psi_4(r \to \infty) = \frac{1}{2}\frac{\mathrm{d}^2}{\mathrm{d}t^2}h_{m\bar{m}}, \quad h_{m\bar{m}} = h_+ - \mathrm{i}h_\times \tag{3.80}$$

where the two independent polarizations h_+ and $h_\times$ are recovered from the complex component $h_{m\bar{m}}$. By twice integrating the formula (3.79) we arrive at

$$h_{m\bar{m}}(r\to\infty) = -\frac{2}{r}\sum_{nklm}\frac{C^H_{nkml}}{\omega^2_{nkm}}S_{lm}(\theta)e^{\mathrm{i}m\phi-\mathrm{i}\omega_{nkm}(t-r)} \tag{3.81}$$

which is a simple and important formula as an observer detecting a gravitational waveform is commonly located at the infinity (we used this formula in [46]).

Now that we have explicit formulas for gravitational perturbations (Weyl scalars and the metric) we can try to calculate the fluxes of integrals of motion which drive the evolution of orbital parameters in the adiabatic approximation (3.41). This was an essential part of our calculations in [46]. As was already mentioned in the previous sections the gravitational waves have their own effective stress-energy tensor (2.60) which can be written using the two polarizations h_+ and $h_\times$ as [19]

$$T^{GW}_{\mu\nu} = \frac{1}{16\pi}\left\langle \frac{\partial h_+}{\partial x^\mu}\frac{\partial h_+}{\partial x^\nu} + \frac{\partial h_\times}{\partial x^\mu}\frac{\partial h_\times}{\partial x^\nu}\right\rangle. \tag{3.82}$$

Recall that the formula for fluxes of quantities associated with Killing vectors is

$$\left\langle \frac{\mathrm{d}I}{\mathrm{d}t}\right\rangle^\infty = \int_{S(t,r\to\infty)}\xi^\mu T^{GW}_{\mu\nu}s^\nu \mathrm{d}S. \tag{3.83}$$

The Kerr spacetime has two Killing vectors corresponding to the energy E and the z-component of the angular momentum L_z. In the BL coordinates at the infinity the integrand is just $T^r{}_t\, r^2\mathrm{d}\Omega$ for the energy and $T^r{}_\phi\, r^2\mathrm{d}\Omega$ for the angular momentum. The integration over the sphere is straightforward as it uses the orthogonality and normalization of spin-weighted spheroidal harmonics S_{lm} while the time oscillations are averaged-out which leads to the following results [19] in terms of the amplitudes C^H

$$\left\langle \frac{\mathrm{d}E}{\mathrm{d}t}\right\rangle^\infty = \sum_{nklm}\frac{|C^H_{nkml}|^2}{4\pi\omega^2_{nkm}} \quad \left\langle \frac{\mathrm{d}L_z}{\mathrm{d}t}\right\rangle^\infty = \sum_{nklm}\frac{m|C^H_{nkml}|^2}{4\pi\omega^3_{nkm}}. \tag{3.84}$$

While most of the radiation ends up in the future null infinity it can also pass through the horizon into the Kerr black hole. We would thus need to calculate the gravitational wave fluxes through the horizon $\left\langle \frac{\mathrm{d}E}{\mathrm{d}t}\right\rangle^H$ and $\left\langle \frac{\mathrm{d}L_z}{\mathrm{d}t}\right\rangle^H$. The approach to derive them does not rely on the stress-energy tensor (3.82), instead one starts with the area of the Kerr horizon given by its mass and angular momentum

$$A = 8\pi(M^2 + \sqrt{M^4 - J^2}). \tag{3.85}$$

By differentiating this expression with respect to the Boyer-Lindquist time t and realizing that gravitational radiation absorbed by the black hole changes its parameters which means $\mathrm{d}E^H = \mathrm{d}M$ and $\mathrm{d}L^H_z = \mathrm{d}J$ (due to the conservation of energy and angular momentum). When the radiation is decomposed into modes it can be assumed that for each mode the following equality holds $\mathrm{d}L^H_z = \frac{m}{\omega_{nkm}}\mathrm{d}E^H$

[86] ($\mathrm{d}L_z^H$ and $\mathrm{d}E^H$ are not independent), this allows us to calculate the rate of change of energy or angular momentum from the rate of change of the horizon area whose change due to the radiative perturbation was found using the Hawking-Hartle tetrad

$$\frac{\mathrm{d}^2 A}{\mathrm{d}t\mathrm{d}\Omega} = \frac{2Mr_+}{\varepsilon}|\sigma^{HH}|^2 \tag{3.86}$$

where $\varepsilon = \sqrt{M^2 - a^2}/4Mr_+$ and σ^{HH} is the perturbation of the shear associated with the l^μ vector of the HH tetrad which is the generator of the horizon. This shear can be expressed [86] using the Weyl scalar ψ_0 as $\sigma^{HH} = -\psi_0/(\mathrm{i}p_{nkm} + 2\varepsilon)$ where $p_{nkm} = \omega_{nkm} - m\Omega_+$. The rate of change of A is thus directly linked to the Weyl scalar ψ_0 evaluated on the horizon. By transforming ψ_0 from the HH tetrad to the Kinnersley tetrad (3.60), using the horizon boundary conditions (3.66) and averaging one can derive the horizon fluxes

$$\left\langle \frac{\mathrm{d}E}{\mathrm{d}t} \right\rangle^H = \sum_{nklm} \alpha_{nkml} \frac{|C^\infty_{nkml}|^2}{4\pi\omega^2_{nkm}} \quad \left\langle \frac{\mathrm{d}L_z}{\mathrm{d}t} \right\rangle^H = \sum_{nklm} \alpha_{nkml} \frac{m|C^\infty_{nkml}|^2}{4\pi\omega^3_{nkm}}. \tag{3.87}$$

where the coefficients α_{nkml} can be found in [19].

So far we have not discussed the fluxes of the last integral of motion in the Kerr spacetime, the Carter constant. The fluxes formulas for Q were derived considerably later than those for E and L_z. In addition to the Teukolsky formalism, the self-force approach is used to calculate the averaged decrease of Carter constant due to radiation (See [74] for the derivation). As this goes beyond the scope of this thesis we shall just include the resulting fluxes written in terms of the Teukolsky amplitudes [41]

$$\left\langle \frac{\mathrm{d}Q}{\mathrm{d}t} \right\rangle^\infty = \sum_{nklm} \frac{|C^H_{nkml}|^2}{2\pi\omega^3_{nkm}} (\mathcal{L}_{nkm} + k\Upsilon_\theta) \tag{3.88}$$

$$\left\langle \frac{\mathrm{d}Q}{\mathrm{d}t} \right\rangle^H = \sum_{nklm} \alpha_{nkml} \frac{|C^\infty_{nkml}|^2}{2\pi\omega^3_{nkm}} (\mathcal{L}_{nkm} + k\Upsilon_\theta). \tag{3.89}$$

The coefficients $\mathcal{L}_{nkm}$ are given by $\mathcal{L}_{nkm} = m\langle\cot^2\theta\rangle L_z - a^2\omega_{nkm}\langle\cos^2\theta\rangle E$ where the averaging is done over the complete period of motion in the θ-coordinate.

With all the flux formulas known the total change of the integrals of motion of the particle due to gravitational radiation is

$$\left\langle \frac{\mathrm{d}I}{\mathrm{d}t} \right\rangle^{particle} = -\left\langle \frac{\mathrm{d}I}{\mathrm{d}t} \right\rangle^\infty - \left\langle \frac{\mathrm{d}I}{\mathrm{d}t} \right\rangle^H. \tag{3.90}$$

This result can then be used to calculate an adiabatic evolution (3.41) of a flux-driven extreme mass ratio inspiral.

4. Phantom scalar field counterpart to Curzon-Chazy spacetime (paper 1)

- Polcar, L. and Svítek, O. Phantom scalar field counterpart to Curzon–Chazy spacetime. *Classical and Quantum Gravity*, 39(18):185002, Aug 2022

This chapter is concerned with our study [68] of a particular solution to the Einstein's equations which is related to the well-known Curzon-Chazy solution and is sourced by the phantom scalar field. The relation to the Weyl metrics with scalar field is described in last section of chapter 1 while the gravitational energy widely discussed in the paper is the topic of chapter 2.

The investigated solution which we have called spherical Curzon-Chazy or scalar Curzon-Chazy solution (SCC) can be obtained from the Curzon-Chazy solution by adding a massless scalar field with negative energy density and demanding that the Weyl metric function k (see chapter 1) vanishes. In addition to belonging to the Weyl metrics and spherically symmetric solutions with scalar field, this solution belongs to the static spacetimes describing "particles" whose gravitational attraction is compensated by the repulsive nature of the phantom scalar field. This is similar to the Majumdar-Papapetrou (MP) class of electrovacuum solutions. In this analogy our SCC spacetime describes the single-particle solution corresponding to the extreme Reissner-Nordström black hole in the MP class.

The solution itself has a structure of a traversable wormhole which however is not symmetric with respect to its throat. This wormhole connects two different regions of spacetime. The first region is asymptotically simple (but not asymptotically empty) while the other one contains a curvature singularity which can be reached in a finite proper time. This singularity is associated with the divergence of the scalar field on this null hypersurface and is non-scalar meaning that while the curvature invariants are finite (in fact they vanish), the tetrad components of the Riemann tensor associated with geodesic observers are divergent. The spacetime is also a one-directional time machine, observers can get very far to the future if they enter the region with singularity, in the most extreme case one can reach future timelike infinity in a finite proper time when approaching it from this region.

To better understand the spacetime, we tested various concepts of gravitational energy. From the quasilocal definitions, the Misner-Sharp energy turned out to be the most useful while the Katz-Lynden-Bell-Bičák approach allowed us to reasonably define energy density of gravitational field which had a Newtonian interpretation. Finally we briefly examined the spacetime with $m < 0$ and also the case where electromagnetic field is present as well but the structure of these spacetimes is not as rich as in the SCC spacetime.

Phantom scalar field counterpart to Curzon–Chazy spacetime

Lukáš Polcar and Otakar Svítek

Institute of Theoretical Physics, Faculty of Mathematics and Physics, Charles University, V Holešovičkách 2, 180 00 Prague 8, Czech Republic

E-mail: polcar.vm@seznam.cz, ota@matfyz.cz

Abstract. We derive and analyze phantom scalar field counterpart to Curzon–Chazy spacetime. Such solution contains a wormhole throat while the region inside the throat behaves like a one-directional time machine. We describe its conformal structure and non-scalar singularity hidden inside the wormhole. We examine the results provided by different definitions of mass of the spacetime to understand their value in the presence of phantom matter. The electromagnetic generalization of this spacetime is as well briefly considered.

1. Introduction

Scalar field provides a canonical source for spacetime since it is both sufficiently simple and reasonably realistic source. The simplicity enables one to employ analytical methods more thoroughly and also presents much cleaner picture of potential physical effects. At the same time there is both experimental verification of the role of scalar fields in nature (Higgs field) and an extensive theoretical use in modeling of various phenomena (inflation, dark energy/matter).

Substantial interest has been naturally devoted to spherically symmetric solutions of gravity coupled to scalar field with the no-hair theorems being one of the main focus (e.g. see recent review [1]). Obviously, one would like to analytically investigate solutions with less symmetry. Natural candidate in this regard is the Weyl family of metrics and its generalizations including scalar field (both standard and phantom) which was recently studied in [2]. One aim of this analysis was to uncover the role these geometries might play in building wormholes. Even more ambitious generalizations of spherically symmetric solutions with scalar fields have been performed recently (e.g. towards dynamical spacetimes without symmetries [3, 4]) however in these generic situations explicit analysis of basic properties becomes extremely complicated (e.g. even the proof of the existence of horizon demands lengthy mathematical analysis).

The simplest solution of the Weyl class [5] is from a certain point of view the Curzon–Chazy spacetime [6] since it produces Newtonian potential. On the other hand it contains directional singularity at the origin. Naturally, one would like to obtain similarly simple scalar field solution. After recalling the general solution for Curzon–Chazy geometry with minimally coupled massless scalar field we investigate a specific limit (made possible in the presence of phantom scalar field) that reduces this two-parametric solution to one-parametric. In this solution the Newtonian potential is preserved and is apparently sourced by the scalar field which has Newtonian character

as well. In this solution the singularity at the origin is removed and moreover the spacetime becomes spherically symmetric.

At the same time, this solution represents certain limit of the famous Janis–Newman–Winicour (JNW) solution [7] (when generalized to phantom scalar field) which was however initially discovered by Fisher [8]. JNW solution with standard scalar field serves as a prime example of how the scalar field spoils regularity of a horizon or leads to naked singularities. This behavior of scalar field is hard to tame even when invoking other sources (see [9]).

In this paper, we derive the phantom scalar field version of Curzon–Chazy spacetime and proceed to study its features. Namely we show that it contains a wormhole throat and works as a one-directional time machine. We analyze its conformal structure, discover non-scalar singularity hidden on the other side of wormhole throat and devote substantial effort to understand the value of different definitions for energy of the spacetime and analyze the interplay of scalar field and gravitational parts of the total energy. Note, that the wormhole we are having in mind is of the bridge type (with general prototype being discussed at the end of [4]) as opposed to the thin-shell type (e.g. [10]). Finally, we use a recently published study [11] about generating techniques to obtain electromagnetic generalization of the solution and analyze its drastically modified conformal structure.

We do realize that having a solution with phantom scalar field is hard to justify physically. In particular the system has energy unbounded from below which would lead to instability, see e.g. [12] for the discussion of serious quantum instabilities affecting such matter systems. This work was motivated purely theoretically, that is, by a particular limit of the well-known Curzon-Chazy solution generalized to contain scalar field. However, we briefly analyze some astrophysically relevant properties, e.g. gravitational lensing.

2. Obtaining the solution

We consider a massless scalar field minimally coupled to gravity described by action

$$S = \int (\mathcal{R} - 2\varepsilon \nabla_\mu \Phi \nabla^\mu \Phi) \sqrt{-g}\, \mathrm{d}^4 x. \tag{1}$$

where the parameter ε enables us to describe either the conventional scalar field ($\varepsilon = 1$) or the so called phantom scalar field ($\varepsilon = -1$) which has negative energy density. The scalar field Φ is related to its usual definition Ψ by $\Phi = \sqrt{\frac{\kappa}{2}}\Psi$ where the Einstein gravitational constant is $\kappa = 8\pi$, with $G = 1$ and $c = 1$. The equations of motion then take form

$$R_{\mu\nu} = 2\varepsilon \partial_\mu \Phi \partial_\nu \Phi, \qquad \Box \Phi = 0. \tag{2}$$

We will now restrict ourselves to a static axially symmetric spacetime with a line element in the form introduced by Weyl [5]

$$\mathrm{d}s^2 = -e^{2U(\rho,z)}\mathrm{d}t^2 + e^{2k(\rho,z)-2U(\rho,z)}(\mathrm{d}\rho^2 + \mathrm{d}z^2) + \rho^2 e^{-2U(\rho,z)}\mathrm{d}\phi^2. \tag{3}$$

This metric is determined by only two functions $U(\rho, z)$ and $k(\rho, z)$.

The field equations (2) are then reduced to [2]

$$U_{,\rho\rho} + \frac{1}{\rho}U_{,\rho} + U_{,zz} = 0, \qquad \Phi_{,\rho\rho} + \frac{1}{\rho}\Phi_{,\rho} + \Phi_{,zz} = 0 \tag{4a}$$

$$k_{,\rho} = \rho\{\left[(U_{,\rho})^2 - (U_{,z})^2\right] + \varepsilon\left[(\Phi_{,\rho})^2 - (\Phi_{,z})^2\right]\}, \qquad k_{,z} = 2\rho(U_{,\rho}U_{,z} + \varepsilon\Phi_{,\rho}\Phi_{,z}). \tag{4b}$$

Since equations (4a) are Laplace equations in flat 3-dimensional space expressed for axially symmetric situation in polar coordinates, the first solution that may come to one's mind is that of a Newtonian gravitational potential of a point particle located at the origin. For the vacuum case $\Phi = 0$ we can solve the corresponding $k(\rho, z)$ using (4b) arriving at

$$U = -\frac{M}{r}, \qquad k = -\frac{M^2\rho^2}{2r^4}, \qquad r = \sqrt{\rho^2 + z^2}. \tag{5}$$

This is the (single-particle) Curzon–Chazy solution [6]. The most striking feature of this solution is the direction-dependent singularity at $r = 0$. When one approaches the origin from the equatorial plane ($z = 0, \rho \to 0^+$) the Kretschmann scalar diverges. On the other hand if one approaches the origin along the z-axis using an appropriate worldline the singularity can be avoided and the spacetime can be extended beyond $r = 0$. The structure of the singularity was studied in [13] and more recently in [14].

We can now add the scalar field and see how it affects the singularity. The equations (4b) possess a rotation ($\varepsilon = 1$) or a boost symmetry ($\varepsilon = -1$) for the pair (U, Φ) while preserving the function k (details in [2]). This together with the fact that Φ satisfies the same equation as U allows us to generate a solution with scalar field from the vacuum solution (5). A solution with scalar field is then

$$U = -\frac{1}{s}\frac{M}{r}, \qquad k = -\frac{M^2\rho^2}{2r^4}, \qquad \Phi = \pm\frac{\sqrt{\varepsilon(s^2-1)}}{s}\frac{M}{r} \tag{6}$$

where the new parameter s satisfies $|s| > 1$ for $\varepsilon = 1$ while for the phantom scalar field we have $|s| < 1$.

The solution (6) has two interesting limits. The first is the ultrastatic limit $|s| \to \infty$ which eliminates the function U completely. The Kretschmann scalar is then

$$K^{ustat} = \frac{12M^4}{r^8}\mathrm{e}^{\frac{2M^2\rho^2}{r^4}}. \tag{7}$$

It is clear that $K^{ustat} \to \infty$ for $r \to 0$ and the corresponding singularity is thus no longer direction-dependent.

The other limit (described in [2]) eliminates the metric function k. This can be done by reparametrizing M and evaluating the following limit

$$M = ms \quad , \quad s \to 0 \ , \tag{8}$$

while keeping $m > 0$ fixed. The Kretschmann scalar now reads

$$K^{scc} = \frac{4\mathrm{e}^{\frac{-4m}{r}}m^2\left(7\,m^2 - 16\,mr + 12\,r^2\right)}{r^8}. \tag{9}$$

We have thus managed to seemingly remove the curvature singularity at $r = 0$ where K^{scc} is zero in the sense of the corresponding limit. In addition, the spacetime is now spherically symmetric. Using the transformation to spherical coordinates in

much the same way as in the Euclidean space we arrive at the Spherical Curzon–Chazy spacetime (SCC)

$$\mathrm{d}s^2 = -e^{-\frac{2m}{r}}\mathrm{d}t^2 + e^{\frac{2m}{r}}(\mathrm{d}r^2 + r^2\mathrm{d}\Omega^2), \qquad \Phi = \pm\frac{m}{r}. \tag{10}$$

Although the initial idea was to figure out how the presence of scalar field affects the singularity, the SCC can be also obtained from the Janis–Newman–Winicour (JNW) solution

$$\mathrm{d}s^2 = -\left(1-\frac{2M}{r}\right)^{\frac{1}{s}}\mathrm{d}t^2 + \left(1-\frac{2M}{r}\right)^{-\frac{1}{s}}\mathrm{d}r^2 + \left(1-\frac{2M}{r}\right)^{-\frac{1}{s}}(r^2-2Mr)\mathrm{d}\Omega^2, \tag{11a}$$

$$\Phi = \pm\frac{1}{2}\frac{\sqrt{|1-s^2|}}{s}\ln\left(1-\frac{2M}{r}\right). \tag{11b}$$

The JNW solution [7] is a famous static spherically symmetric solution with a free scalar field which was initially discovered by Fisher [8] but later rediscovered several times. The intervals of s corresponding to the conventional or the phantom scalar field are the same as above. If we perform the limit (8) we again recover the SCC solution (10).

There is yet another class of solutions to which the SCC spacetime belongs. This solution was found by Gibbons in [15] where the corresponding metric reads

$$\mathrm{d}s^2 = -e^{2U(X)}\mathrm{d}t^2 + e^{-2U(X)}\mathrm{d}l^2, \qquad \Phi = \pm U(X). \tag{12}$$

The line element $\mathrm{d}l^2$ is that of flat space while the function $U(X)$ satisfies ordinary flat-space Laplace equation $\triangle U(X) = 0$. We can thus have multi-particle solution where the gravitational attraction is compensated by the repulsion due to the presence of the phantom scalar field. This class of solution is analogical to the Majumdar–Papapetrou class [16] where the extremely charged particles mutual gravitational attraction is balanced by their electric repulsion. In this analogy the Spherical Curzon–Chazy spacetime corresponds to the extreme Reissner–Nordström black hole.

3. Basic properties and geodesics

The SCC metric asymptotically behaves like the Schwarzschild solution. This becomes clear when using the areal radius defined below by expression (13) as a coordinate instead of r. Naturally, in the limit $r \to \infty$ the solution reduces to the Minkowski metric. The key point of our investigation thus lies on the other side, at $r = 0$ where (at the least) a coordinate singularity is present. The limits $r \to 0$ of g_{tt} and g_{rr} are the same as in the case of the Schwarzschild horizon where the singularity can be eliminated when using suitable coordinates. Since the Kretschmann scalar (9) is zero at $r = 0$ one would naively expect the same can be done for the SCC spacetime.

On the other hand, not everything is similar to the Schwarzschild metric. One obvious difference that one may notice is the divergence of the areal radius of the sphere centered at $r = 0$

$$R_A(r) = re^{\frac{m}{r}}. \tag{13}$$

The radius reaches its minimum at $r = m$ and then grows again to infinity. This behaviour is often typical for wormholes and it will be discussed in the following sections.

We shall now try to reach $r = 0$ using various radial geodesics. Starting from $r = r_0 > 0$ the proper distance to the origin along a spacelike geodesic given by $t = const.$ is

$$d(0, r_0) = \int_0^{r_0} e^{\frac{m}{r}} \mathrm{d}r = +\infty. \tag{14}$$

This is in direct contrast to Schwarzschild where the distance to the horizon is finite. For an ingoing null radial geodesic parametrised by an affine parameter λ the tangent vector reads

$$l^\mu = \frac{\mathrm{d}x^\mu}{\mathrm{d}\lambda} = (e^{\frac{2m}{r}}, -1, 0, 0), \tag{15}$$

which shows that $r = 0$ can only be reached in infinite coordinate time t. On the other hand light arrives at $r = 0$ in a finite value of λ. The same conclusions apply also for the timelike geodesics with four-velocity in the form

$$U^\mu = (Ee^{\frac{2m}{r}}, \pm\sqrt{E^2 - e^{\frac{-2m}{r}}}, 0, 0) \tag{16}$$

where E is the energy with respect to the timelike Killing field $\xi^{(t)}_\mu$

$$E = -U^\mu \xi^{(t)}_\mu = -g_{tt} U^t.$$

The proper time to reach $r = 0$ is then finite

$$\tau = \int_{r_0}^{0} -\frac{\mathrm{d}r}{\sqrt{E^2 - e^{\frac{-2m}{r}}}} < +\infty. \tag{17}$$

This creates a counter-intuitive notion that an infinite distance can be covered in a finite proper time. It also points to the geodesic incompleteness of the spacetime.

As was already mentioned above the finiteness of the Kretschmann scalar (9) at $r = 0$ could indicate that the coordinate singularity can be removed. For the radial part of the metric it is indeed so and for that we can use the proper time τ of timelike radial geodesics as one coordinate while for the other coordinate l we find the corresponding tangent vector L^μ satisfying (we use $[\cdot, \cdot]$ to denote a commutator of two vector fields)

$$[U, L] = 0, \qquad U^\mu L_\mu = 0. \tag{18}$$

The simplest form of L^μ is then

$$L^\mu = (\pm(Ee^{\frac{2m}{r}} - \frac{1}{E}), \sqrt{E^2 - e^{\frac{-2m}{r}}}, 0, 0) \tag{19}$$

The metric in the new coordinates reads

$$\mathrm{d}s^2 = -\mathrm{d}\tau^2 + \frac{E^2 - e^{\frac{-2m}{r}}}{E^2}\mathrm{d}l^2 + R_A^2(r)\mathrm{d}\Omega^2. \tag{20}$$

We can see that g_{ll} is finite and non-zero for any value of r, for $r = 0$ the radial part of the metric even reduces to the Minkowski line element.

The transformation relations $x^\mu = (t, r) \to (\tau, l)$ can be found by solving

$$\frac{\partial x^\mu}{\partial \tau} = U^\mu, \qquad \frac{\partial x^\mu}{\partial l} = L^\mu. \tag{21}$$

We now have to choose our geodesic observers. For $E > 1$ the geodesics have no turning point and can reach $r = \infty$. We can further choose between ingoing observers coming from infinity to $r = 0$ or outgoing ones going in the opposite direction. We then get the transformation in the form

$$t = \frac{\tau}{E} + f(\tau_\pm), \qquad r = R(\tau_\pm) \tag{22a}$$

$$\frac{\mathrm{d}f}{\mathrm{d}\tau_\pm} = E e^{\frac{2m}{R(\tau_\pm)}} - \frac{1}{E}, \qquad \frac{\mathrm{d}R}{\mathrm{d}\tau_\pm} = \pm\sqrt{E^2 - e^{\frac{-2m}{R(\tau_\pm)}}}, \quad \tau_\pm = \tau \pm l \tag{22b}$$

where the $+$ sign corresponds to the outgoing observers while $-$ to the ingoing ones. If we choose for example the ingoing observers we can depict the neighbourhood of $r = 0$ better in these new coordinates than in t, r as is illustrated in figure 1.

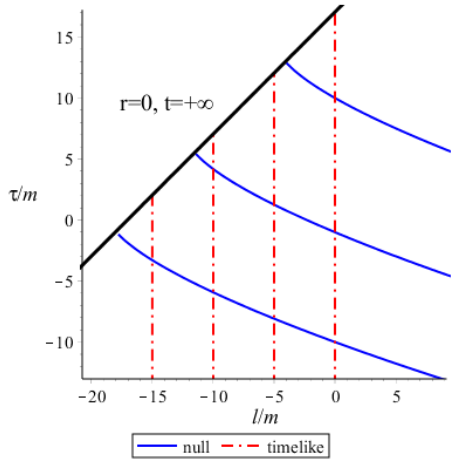

Figure 1: Null and timelike geodesic observers arriving at $r = 0$. The energy of timelike observers satisfies $E > 1$, see (22).

The null and timelike geodesics terminate at $\tau - l = R^{-1}(0)$ clearly displaying the geodesic incompleteness. At this point one would start to think about extending the metric beyond $r = 0$ and it is really possible to smoothly extend it to Minkowski space if we could somehow discard the problematic angular part.

Even though the coordinates (τ, l) provide us with a new insight they fail to properly cover some parts of the spacetime. If we choose the ingoing observers in (22) the set $(t = -\infty, r = 0)$ is not well described in the new coordinates while for the outgoing observers the same can be said for $(t = +\infty, r = 0)$, in both cases $(|t| < \infty, r = 0)$ is missing as it is inaccessible to timelike observers.

There is yet another choice of geodesic observers which leads to new coordinates. The geodesics with $E < 1$ are travelling from $r = 0$ to their turning point $r_{max} =$

$-\frac{m}{\ln(E)}$ after which they arrive back to the origin. This coordinate chart then contains $(t = \pm\infty, r = 0)$ but the part of the spacetime with $r > r_{max}$ is not covered at all.

Let us now briefly cover the non-radial motion, in particular the circular orbits. From the normalization of four-velocity $g^{\mu\nu}u_\mu u_\nu = \varepsilon$ (where $\varepsilon = -1$ or $\varepsilon = 0$) we get the equation defining effective potential

$$u_r^2 e^{-\frac{4m}{r}} = E^2 - V_{eff}(r) \tag{23}$$

where the effective potential itself is

$$V_{eff}(r) = \frac{L^2}{r^2} e^{-\frac{4m}{r}} - \varepsilon\, \mathrm{e}^{-\frac{2m}{r}}. \tag{24}$$

For massive particles ($\varepsilon = -1$) the potential looks similar to that of the Schwarzschild black hole. It has a stable and an unstable circular orbit for a sufficiently large angular momentum L. This can be seen in the figure 2 where we can notice that the potential is everywhere finite and tends to zero for $r \to 0$.

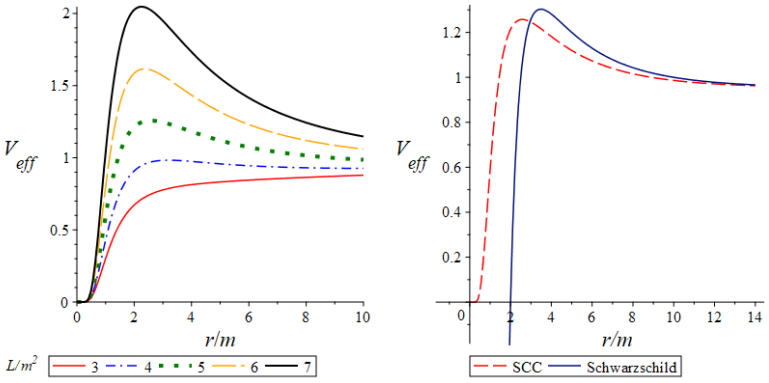

(a) (b)

Figure 2: (a) Plots of the effective potential V_{eff} (in the case of massive particles) for several different values of the angular momentum L. (b) Comparison with the Schwarzschild potential for a fixed value of $L = 5m^2$.

In order to find circular orbits we need to solve the equation $V'_{eff}(r) = 0$. Here we will only mention the significant ones, the innermost stable circular orbit (ISCO) for the massive particles and the photon unstable circular orbit in the massless case. While the photon sphere can be easily located the ISCO had to be found numerically

$$r_{photon} = 2m, \qquad r_{ISCO} \approx 5.263m. \tag{25}$$

We can compare that to the Schwarzschild case where $r^{Sc}_{photon} = 3m$ and $r^{Sc}_{ISCO} = 6m$. At this point it is worth pointing out that the actual counterpart of the Schwarzschild coordinate r is the areal radius defined in equation (13) since it has the same geometrical meaning. In this coordinate the values are actually larger in our spacetime than in Schwarzschild

$$R_{photon} \approx 3.297m, \qquad R_{ISCO} \approx 6.3643m. \tag{26}$$

While studying geodesics we can also compute the deflection angle for null geodesics to see how our spacetime behaves as a gravitational lens. Similarly to the Schwarzschild case described in [17] we can calculate the angle by formula

$$\delta\psi = 2\int_{r_0(m)}^{\infty} \frac{b}{r\sqrt{\mathrm{e}^{\frac{4m}{r}} r^2 - b^2}}\mathrm{d}r - \pi \tag{27}$$

where $b = \frac{L}{E}$ is the impact parameter and $r_0(m)$ is the turning point of our null geodesic. We can expand this integral to obtain a result for small masses (or large impact parameters)

$$\delta\psi = \frac{4m}{b} + \frac{4\pi\, m^2}{b^2} + \mathcal{O}(m^3). \tag{28}$$

The same expansion done for Schwarzschild yields

$$\delta\psi_{Schw} = \frac{4m}{b} + \frac{15\pi\, m^2}{4b^2} + \mathcal{O}(m^3). \tag{29}$$

We can see that while the first term is the same (and corresponds to the famous formula derived already by Einstein) the second term is slightly larger in our spacetime indicating modified lensing signature.

4. Conformal structure

We shall now take a look at the global structure of the spacetime. In an approach similar to that used in the Schwarzschild spacetime we first express the metric in null coordinates using the tortoise coordinate $r^*(r)$

$$t^{\pm} = t \pm r^*(r), \qquad r^*(r) = \int_m^r e^{\frac{2m}{r'}}\,\mathrm{d}r'. \tag{30}$$

we chose to have $r^*(m) = 0$ as this is the location of the soon to be investigated wormhole throat (see the following section). The metric is then

$$\mathrm{d}s^2 = -e^{-\frac{2m}{r}}\mathrm{d}t^+\mathrm{d}t^- + R_A^2(r)\mathrm{d}\Omega^2. \tag{31}$$

At this point one would probably ask whether it is possible to have a finite and nonzero metric coefficient $g_{t^+t^-}$ at $r = 0$. As the coefficient depends only on r we have to use a transformation relations such that the multiplication factor produced by the transformation is independent of t while the metric remains in null coordinates. This can be done (up to some multiplicative constants) using exponentials

$$u = \pm e^{\pm t^+}, \qquad v = \mp e^{\mp t^-}. \tag{32}$$

These are the familiar null Kruskal coordinates. The metric then becomes

$$\mathrm{d}s^2 = -e^{\mp 2r^* - \frac{2m}{r}}\mathrm{d}u\mathrm{d}v + R_A^2(r)\mathrm{d}\Omega^2. \tag{33}$$

It is clear that we cannot make the radial part of the metric regular as g_{uv} is either zero (the + sign in (33)) or diverges as $r \to 0^+$ (the − sign).

Despite this setback the metric in null coordinates is still useful for plotting the conformal diagram. It is easier to perform the compactification using the form (31).

Using the Kruskal coordinates (33) directly would lead to the same picture with only the intervals of our new coordinates (T, R) being modified. For the compactification we use the same functions as in Minkowski spacetime (here $[\cdot, \cdot]$ denotes a closed interval)

$$t^+ = \tan\left(\frac{1}{2}(T+R)\right), \qquad t^- = \tan\left(\frac{1}{2}(T-R)\right), \qquad T, R \in [-\pi, \pi]. \tag{34}$$

The metric in the new coordinates reads

$$\mathrm{d}s^2 = \frac{e^{-\frac{2m}{r}}}{4\cos^2\left(\frac{1}{2}(T+R)\right)\cos^2\left(\frac{1}{2}(T-R)\right)}(-\mathrm{d}T^2 + \mathrm{d}R^2) + R_A^2(r)\mathrm{d}\Omega^2. \tag{35}$$

The conformally conjugated metric can then be obtained as $\widetilde{g}_{\mu\nu} = \Omega^2 g_{\mu\nu}$ where the conformal factor Ω is given by

$$\Omega^2 = 4e^{\frac{2m}{r}}\cos^2\left(\frac{1}{2}(T+R)\right)\cos^2\left(\frac{1}{2}(T-R)\right). \tag{36}$$

It can be shown that the conformally related metric $\widetilde{g}_{\mu\nu}$ has all coefficients finite. The boundary of the physical spacetime is of course given by $\Omega = 0$ which is also the boundary of the corresponding conformal diagram as depicted in figures 3 and 4.

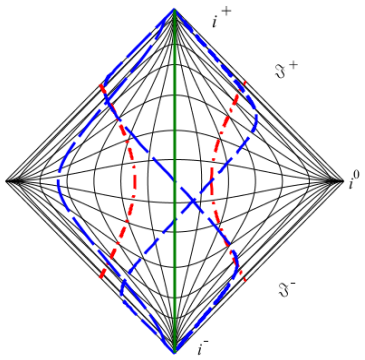

Figure 3: The Penrose conformal diagram with timelike curves. The potential wormhole throat or the radius of minimal area ($r = m$) is marked in green (solid line), geodesics in blue (dashed line) and constantly accelerated observers in red (dash-dotted line).

When looking at the diagrams in figures 3 and 4 we notice that they look like two copies of the Minkowski spacetime compactified using spherical coordinates (t, r) and glued together along $r = 0$. On the right side we have the usual structure of the asymptotically flat spacetime with infinities i^0, $i^\pm$ and $\mathscr{I}^\pm$. Since the left side boundary looks indistinguishable one would think that it could also have its own space and null infinities. As was already stated the spacetime can be interpreted as a wormhole and indeed the conformal diagram looks like that of a static spherically symmetric wormhole connecting two asymptotically flat regions (see for example [18] or [19]).

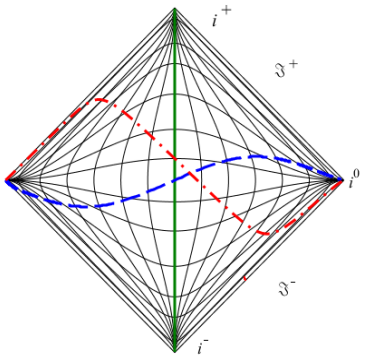

Figure 4: The Penrose conformal diagram with spacelike curves. The wormhole throat ($r = m$) is marked in green (solid line), a spacelike geodesic in blue (dashed line) and a $\tau = const.$ curve (see (22)) in red (dash-dotted line).

The figure 3 features all three types of geodesics (ingoing, outgoing and those with $E < 1$) while it also includes two constantly accelerated (Rindler-like) observers ($a_\mu a^\mu = const.$). The way the worldlines approach infinity is the same at both sides of the diagram (apart from the $E < 1$ geodesics) but what is really different from an ordinary wormhole is the asymmetry with respect to its throat which is marked in green. The motion on the left side of the diagram ($r < m$) takes only a finite amount of proper time. This was already mentioned in the previous section but what is really unintuitive here is the fact that the future time infinity i^+ can be reached in a finite proper time provided that we travel there along a geodesic that approaches it from the left (the same obviously applies for i^-).

This means that the region inside the wormhole throat works as a one-directional time machine enabling travel to infinitely distant future (as perceived by observers outside of the wormhole throat) in finite time by entering the wormhole for certain time.

This strange finiteness is present in the case of spacelike curves as well. Some of the spacelike curves can be seen in figure 4. While the spacelike geodesics $t = const.$ (in black) reach the "left spatial infinity" (the point $(|t| < \infty, r = 0)$) after an infinite distance (see (14)) the radial geodesics not confined in a $t = const.$ plane need to cover only a finite distance to reach the point. The same can be also said for the coordinate line $\tau = const.$ in the comoving coordinates (22). This is again valid only for the left side and the distance to right i^0 is obviously infinite no matter which curve we choose.

As was already stated above the conformal structure looks identical to that of the Minkowski spacetime and so it is not surprising that the spacetime is asymptotically simple which means that Ω satisfies [20]

$$\mathrm{d}\Omega(\mathcal{I}^\pm) \neq 0, \qquad \mathrm{d}\Omega(i^0) = 0. \tag{37}$$

The same is surprisingly true also for the infinities on the left. On the other hand the spacetime is not asymptotically empty as it is filled with the phantom scalar field (the condition $T_{\mu\nu} = \mathcal{O}(\Omega^3)$ given in [20] is not satisfied). It is thus not correct to call the spacetime asymptotically flat even though it possesses the same asymptotic structure.

Apart from the finite lengths of the worldlines in the $r < m$ part the spacetime looks like a generic static wormhole [19]. The biggest difference however is the presence of a curvature singularity in $r = 0$ which will be discussed further in the section 7 of this paper. The conformal structure of the spacetime is then depicted in the figure 5.

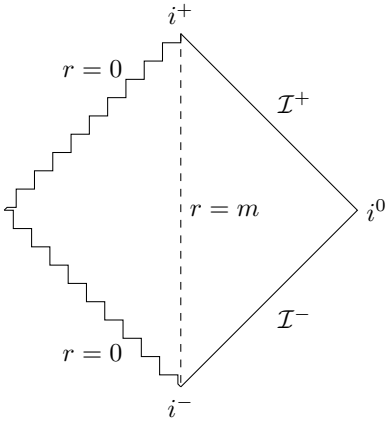

Figure 5: Schematically drawn Penrose conformal diagram including the singularity, the throat and the asymptotic infinities

5. The wormhole

The wormhole structure of the spacetime becomes evident when studying null congruences. The two independent future-pointing radial null vectors (an outgoing k and an ingoing l) can be written as

$$k^\mu = k^t(x^\mu)(1, e^{-\frac{2m}{r}}, 0, 0), \qquad l^\mu = \frac{1}{k^t(x^\mu)}(e^{\frac{2m}{r}}, -1, 0, 0) \tag{38}$$

where $k^t(x) > 0$ is a function of all coordinates while the vectors satisfy the normalization condition $k^\mu l_\mu = -2$. Using the metric on the sphere $\sigma_{\mu\nu}$ we can compute the expansion using the formula

$$\theta^{(k)} = \sigma^{\mu\nu} \nabla_\mu k_\nu. \tag{39}$$

The resulting expansions then read

$$\theta^{(k)} = \frac{2\,(r-m)\,k^t(x^\mu)e^{-\frac{2m}{r}}}{r^2}, \qquad \theta^{(l)} = -\frac{2(r-m)}{r^2 k^t(x^\mu)}. \tag{40}$$

For $r > m$ the outgoing and the ingoing expansion have expected signs $\theta^{(k)} > 0$ and $\theta^{(l)} < 0$. This changes at the minimum of the areal radius R_A located at $r = m$ where the expansions vanish and then flip signs for $r < m$. This is consistent with the notion of a wormhole with a throat at $r = m$.

In order to obtain a better insight it is useful to compare our spacetime to a more simple one such as the Bronnikov–Ellis (BE) wormhole [21] which is the simplest static spherically symmetric wormhole given by metric

$$\mathrm{d}s^2_{BE} = -\mathrm{d}t^2 + \mathrm{d}x^2 + (x^2 + m^2)\mathrm{d}\Omega^2. \tag{41}$$

The convenience of the coordinates used in the BE wormhole stems from the form of the areal radius ($g_{\theta\theta}$) which is a symmetric function with respect to the throat at $x = 0$. In our case we can also find analogous coordinate $x \in (-\infty, \infty)$ which can be defined as

$$x(r) = \mathrm{signum}\,(r - m)\sqrt{\mathrm{e}^{\frac{2m}{r}} r^2 - m^2\mathrm{e}^2}. \tag{42}$$

The inverse transformation is then

$$r(x \neq 0) = -\frac{m\,\Theta\,(x)}{W\left(-\sqrt{\frac{m^2}{x^2+m^2\mathrm{e}^2}}\right)} - \frac{m\,\Theta\,(-x)}{W\left(-1, -\sqrt{\frac{m^2}{(x^2+m^2\mathrm{e}^2)}}\right)}; \qquad r(0) = m \tag{43}$$

where $\Theta(x)$ is the step function while $W(x)$ and $W(-1, x)$ are the branches of Lambert W-function. The metric then has the desired form

$$\mathrm{d}s^2 = g_{tt}(x)\mathrm{d}t^2 + g_{xx}(x)\mathrm{d}x^2 + (x^2 + m^2e^2)\mathrm{d}\Omega^2. \tag{44}$$

The functions $g_{tt}(x)$ and $g_{xx}(x)$ are rather lengthy expressions and so it serves no purpose to actually write them down here when it is easy to plot them (see figure 6).

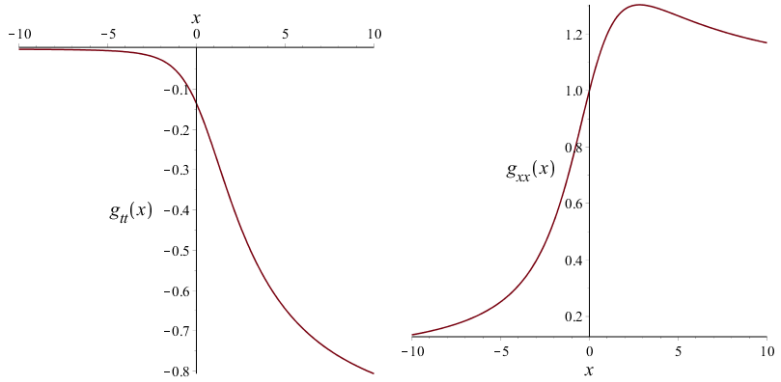

Figure 6: The functions $g_{tt}(x)$ (left) and $g_{xx}(x)$ (right) of the metric (44) for $m = 1$.

It is clear from the plots that the metric functions are not symmetric with respect to $x = 0$ with the metric (44) approaching Minkowski for $x \to \infty$ while for $x \to -\infty$ both $g_{tt}(x)$ and $g_{xx}(x)$ vanish.

When studying wormholes it is common to perform embedding of the plane $t = const., \theta = \frac{\pi}{2}$ to illustrate how two asymptotically flat universes are connected by its funnel-like structure. In our case the cylindrical coordinate ρ in the euclidean space is connected to the coordinate r as

$$\rho = r\mathrm{e}^{\frac{m}{r}} \tag{45}$$

which is in fact the already mentioned areal radius. To find the embedding diagram $z(\rho)$ (z also being an euclidean coordinate) we can easily derive the well known formula

$$\frac{\mathrm{d}z}{\mathrm{d}\rho} = \pm\sqrt{g_{\rho\rho}(\rho) - 1}. \tag{46}$$

To get the function $g_{\rho\rho}$ one must invert the relation (45). However, this is only possible for each interval $r > m$ or $r < m$ separately. So instead of applying (46) globally we use different $g_{\rho\rho}$ for each interval

$$\frac{\mathrm{d}z}{\mathrm{d}\rho} = \sqrt{g^{(1)}_{\rho\rho}(\rho) - 1} \qquad r > m \tag{47a}$$

$$\frac{\mathrm{d}z}{\mathrm{d}\rho} = -\sqrt{g^{(2)}_{\rho\rho}(\rho) - 1} \qquad r < m. \tag{47b}$$

The functions $g^{(i)}_{\rho\rho}$ on the respective intervals can again be expressed using the Lambert functions. This allows us to compute $z(\rho)$ which in turn can be used to plot the embedding diagram in the figure 7.

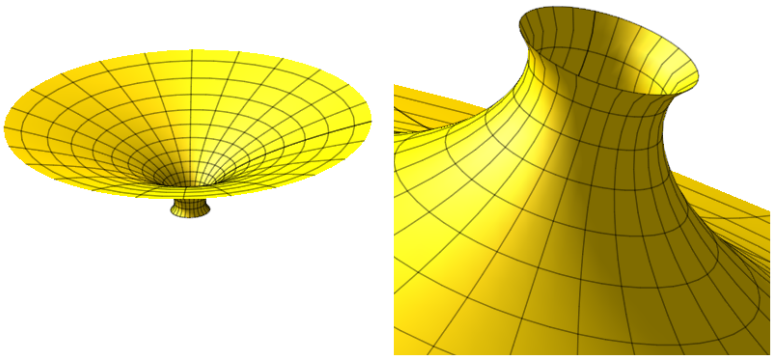

Figure 7: Embedding of the equatorial plane into the Euclidean space

When looking at the diagram we can once again see the asymmetry with respect to the throat. The embedded surface gradually approaches the plane $z = 0$ in the limit $r \to \infty$ which is an expected behaviour. On the other side of the throat however the diagram ends abruptly before reaching $r = 0$ (at the point ρ_0 for which $g^{(2)}_{\rho\rho}(\rho_0) = 1$). This can be interpreted by saying that after passing through the throat the space expands so quickly that it no longer fits into the euclidean space. This is closely connected to the problem of reaching i^+ via the $r < m$ region in a finite time which was discussed above.

So far we have been describing our spacetime as if it were a wormhole without proving that it satisfies any formal definition of wormhole. Let us now briefly examine two such definitions both of which define wormholes as spacetimes with a throat but without an event horizon in the vicinity of the throat. The definitions differ in their conditions for a throat. The first definition, due to Morris and Thorne [22], employs the equation of the embedded surface $z = z(\rho)$ and states that at the throat $\rho = \rho_0$ the following condition are to be satisfied

$$\lim_{\rho\to\rho_0}\frac{\mathrm{d}z}{\mathrm{d}\rho}=\infty \tag{48a}$$

$$\lim_{\rho\to\rho_0}\frac{\mathrm{d}^2\rho}{\mathrm{d}z^2}>0. \tag{48b}$$

Both of these conditions of course apply only for the positive branch of $z(\rho)$ in (46) as both of them are identical in case of the Morris-Thorne wormhole (determined by the shape function $b(\rho)$ in [22]). Our spacetime is not symmetric with respect to the throat at $\rho_0 = me$ so we have to verify the conditions for each branch separately. The first condition clearly holds true as can be seen from the embedding diagrams. The second condition (eq. (48b)) is the so called flare-out condition which is again satisfied with an identical result for both branches

$$\lim_{\rho\to\rho_0}\frac{\mathrm{d}^2\rho}{\mathrm{d}z^2}=2me.$$

An alternative definition of wormhole was introduced by Visser [23]. It defines a wormhole throat as a spacelike surface with two null congruences normal to it. In our case it is the surface $t = const., r = m$ with congruences k and l as defined in (38). The expansion scalar should then satisfy

$$\theta^{(k)}|_{r_0}=0 \tag{49a}$$

$$\dot{\theta}^{(k)}|_{r_0}=\mathcal{L}_k\theta^{(k)}|_{r_0}\geq 0. \tag{49b}$$

The second equation is again called flare-out condition. The same conditions are also supposed to hold true for the congruence l. Using the expressions (40) one can easily check that both conditions are satisfied. It is not even necessary to compute the derivatives one can simply use the Raychaudhuri equation for null geodesics

$$\dot{\theta}=-\frac{1}{2}\theta^2-\sigma_{\mu\nu}\sigma^{\mu\nu}+\omega_{\mu\nu}\omega^{\mu\nu}-T_{\mu\nu}k^\mu k^\nu. \tag{50}$$

Since the expansion at the throat vanishes and the other optical scalars are identically zero we are left with

$$\dot{\theta}^{(k)}|_{r_0}=-(T_{\mu\nu}k^\mu k^\nu)|_{r_0}>0 \tag{51}$$

which is just a consequence of the violation of the null energy condition which is a generic feature of static wormholes [2]. As the absence of an event horizon in our spacetime is evident we can conclude that it is indeed a wormhole.

6. Mass-energy of the spacetime

We would now like to examine the mass/energy content of the spacetime. Since the spacetime has the same structure as an asymptotically flat one the notion of total mass is well defined. Taking advantage of the existence of Killing vector $\xi^{(t)}_\nu$ we can easily compute the Komar mass [24] as a surface integral over a sphere located at the infinity

$$M_K = -\frac{1}{8\pi}\int_{S\to\infty} \nabla_\mu \xi^{(t)}_\nu \mathrm{d}S^{\mu\nu} = \frac{1}{4\pi}\int_S m\mathrm{d}\Omega = m \tag{52}$$

where $\mathrm{d}S_{\mu\nu} = \sqrt{-g}\,\mathrm{d}\theta\,\mathrm{d}\phi\;\; \mathrm{d}t\wedge\mathrm{d}r$. The result is m and gives an expected interpretation to the metric parameter. What may be confusing is that the total mass is positive while the spacetime is filled with a scalar field with negative energy density. However, one must realize that the result is in perfect accordance with the behavior of geodesic observers who are attracted to $r = 0$ which would not be the case if $M_K < 0$. This leads us to conclude that the negative energy of the scalar field is somehow compensated by positive energy of the gravitational field. In order to study this further we can try to use several concepts of quasi-local energy to find out how much energy/mass is located inside a sphere of a given radius $r = const.$ (finding the function $E(r)$).

We can obviously start from the Komar energy but it turns out that when evaluating the expression (52) for an arbitrary sphere the result is the same (m).

Another concept of energy that can be applied is the Brown–York (BY) energy which can be obtained from the canonical (ADM) formalism (derived for example in [20]). It is derived based on the on-shell boundary contribution to the total hamiltonian and provides evolution hamiltonian for canonical boundary data (the bulk constraints vanish for a solution of Einstein equations). We can again compute it as an integral over a sphere

$$E_{BY} = -\frac{1}{8\pi}\int_S (k - k_0)\sqrt{\det\sigma}\,\mathrm{d}^2x \tag{53}$$

where σ is the restriction of the metric to the sphere ($\sigma = g|_S$) and k is the trace of extrinsic curvature of the sphere (as a slice in a spatial hypersurface) while k_0 refers to the extrinsic curvature of the same sphere as embedded in the flat space which ensures that $E_{BY} = 0$ for the Minkowski spacetime. If we compute the BY energy we indeed obtain a non-trivial function $E_{BY}(r)$ but with a wrong asymptotics $E_{BY}(\infty) = M_{BY} = 2m$. This result is clearly not consistent with the Komar mass (52). To understand this discrepancy let us first move to next concept of energy. The Brown–York mass is often confused with the ADM mass which is given by

$$M_{ADM} = \frac{1}{16\pi}\int_{S\to\infty} (D^i\gamma_{ij} - D_j\gamma)r^j\sqrt{\det\sigma}\,\mathrm{d}^2x \tag{54}$$

where γ is the difference between the spatial part of the metric (h) of the spacetime in question and the spatial part of the Minkowski metric ($h^{(0)}$) given in the same type of coordinates ($\gamma_{ij} = h_{ij} - h^{(0)}_{ij}$). The derivative D is the flat-space covariant derivative and r^j is the normal to the sphere. The ADM mass of course gives the correct result $M_{ADM} = m$. Brown–York mass coincides with the ADM mass only if the metric restricted to our sphere is the same as in the reference flat space i. e. $\gamma_{ij}|_S = 0$ (as was shown in [25]). We are thus forced to compute the BY mass in coordinates in which r is replaced by the areal radius according to the transformation (45). If we use this transformation we then obtain the correct result for mass but as in the case of the Komar mass we get $E_{BY}(\rho) = m$ which does not give us any information about how the energy is distributed in the spacetime.

The final concept of energy we use is the Misner–Sharp energy [26] which can be defined as

$$E_{MS}(r) = \frac{1}{8}R_A^3 R_{\mu\nu\rho\sigma}\epsilon^{\mu\nu}\epsilon^{\rho\sigma}, \qquad \epsilon_{\mu\nu} = \epsilon_{\mu\nu\rho\sigma}n^\rho r^\sigma \tag{55}$$

where n^ρ is the normal to $t = const.$ hypersurface while r^σ is a spatial normal to the sphere. This energy can only be used in the spherically symmetric case and it again tells us how much energy is located inside a sphere given by the coordinate r. Application to the SCC spacetime gives the following result

$$E_{MS}(r) = -\frac{m\,(m-2\,r)\,e^{\frac{m}{r}}}{2r}. \tag{56}$$

This function has the correct asymptotic behaviour $E_{MS}(\infty) = m$ and in contrast to the previous energies it is a non-constant function. By taking the limit $r \to 0^+$ we can see that the energy located at $r = 0$ is $-\infty$ which again supports the presence of the singularity there and it is in fact not that surprising since the scalar field is divergent there.

We can also compute the total energy of the scalar field itself from its stress-energy tensor which has a familiar form

$$T_{\mu\nu} = -\left(\nabla_\mu\Phi\nabla_\nu\Phi - \frac{1}{2}g_{\mu\nu}(\nabla\Phi)^2\right). \tag{57}$$

Let us note that this stress-energy tensor clearly violates null energy condition (and therefore all the stronger ones) everywhere in our spacetime. To restore the gravitational constant $\kappa = 8\pi$ which was absorbed into the scalar field in the action (1) we compute the energy for the scalar field $\Phi \to \sqrt{\frac{2}{\kappa}}\Phi$

$$E_{scalar} = \int_{t=const.} n_\mu T^{\mu\nu} n_\nu \sqrt{h}\mathrm{d}^3x = \int_0^\infty -\frac{m^2 e^{\frac{m}{r}}}{r^2}\mathrm{d}r = -\infty. \tag{58}$$

This gives us again an infinite result due to the singular behaviour in $r = 0$. We would now like to avoid the infinities in the energies and instead switch to the energy densities. For the scalar field (as for any matter field) we already have an explicit formula while the total energy density is in principle obtained from $E_{MS}(r)$. There is however a slight complication as we have $E_{MS}(0) = -\infty$ in contrast to the usual $E_{MS}(0) = 0$. This strange behaviour leads us to define the density using an integration from the actual zero point of $E_{MS}(r)$ at $r = \frac{m}{2}$

$$E_{MS} = \int_{\frac{m}{2}}^\infty \varrho_{MS}(r) 4\pi\sqrt{g_{rr}g_{\theta\theta}^2}\mathrm{d}r. \tag{59}$$

The densities can then be computed using the formulas

$$\varrho_{MS}(r) = \frac{1}{4\pi\sqrt{g_{rr}g_{\theta\theta}^2}}\frac{\mathrm{d}E_{MS}(r)}{\mathrm{d}r}, \qquad \varrho_{scalar}(r) = n_\mu T^{\mu\nu} n_\nu \tag{60}$$

and after the evaluation we get

$$\varrho_{MS}(r) = -\frac{1}{8\pi}\,\frac{m^2\,(r-m)}{r^5}\mathrm{e}^{-\frac{2m}{r}}, \qquad \varrho_{scalar}(r) = -\frac{1}{8\pi}\,\frac{m^2}{r^4}\mathrm{e}^{-\frac{2m}{r}}. \tag{61}$$

When looking at the figure 8 depicting Misner–Sharp energy and energy density we can again see the asymmetry with respect to the throat. For $r < m$ the total energy density is positive while in the asymptotically flat (or rather simple) part the energy density is negative.

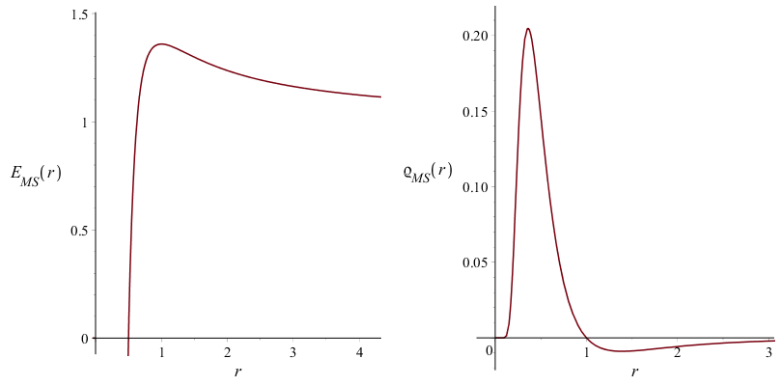

(a) (b)

Figure 8: The Misner–Sharp energy $E_{MS}(r)$ and the corresponding energy density $\varrho_{MS}(r)$ for $m = 1$.

As was stated above the negative energy of the scalar field should be somehow compensated by the positive energy of the gravitational field. To get some further insight into it we would like to find the gravitational energy density. We are fully aware of the ambiguity of the definition of this the concept. Often defined in terms of various pseudo-tensors there are disputes whether any meaningful definition of localized gravitational energy even exists. However, in our simple case of a spherically symmetric spacetime there is a way how to define a notion of gravitational energy density with reasonable properties. The naive approach would be to simply subtract the scalar field energy density from the total (in our case Misner–Sharp) energy density

$$\varrho_{gravity}(r) = \varrho_{MS}(r) - \varrho_{scalar}(r) = \frac{1}{8\pi}\,\frac{m^3}{r^5}\mathrm{e}^{-\frac{2m}{r}}. \tag{62}$$

There is however a principal problem with this straightforward approach. Although the volume integral of a quantity over a given region of space gives us the total gravitational energy it does not mean that the quantity is the gravitational energy density. In the Newtonian theory the correct expression for energy density is $\frac{1}{2}E^2$ not $\frac{1}{2}\rho\Phi$. This was correctly pointed out by Katz, Lynden-Bell and Bičák (KLB) in [27] who managed to find a prescription for the energy density in the form of a quadratic expression as in the Newtonian case. They considered a spherically symmetric metric in the form

$$\mathrm{d}s^2 = -\xi^2(\rho)\mathrm{d}t^2 + \frac{1}{1-\frac{2m(\rho)}{\rho}}\mathrm{d}\rho^2 + \rho^2\mathrm{d}\Omega^2, \tag{63}$$

where the function $m(\rho)$ gives us the total energy inside a sphere with the areal radius ρ. It can be shown that the function $m(\rho)$ is in fact the Misner–Sharp energy of the spacetime. The metric (63) uses the areal radius ρ as a coordinate but in our case we have two different spheres with the same radius ρ. This was already discussed in the previous section concerning the wormhole embedding (see equation (47)). We will now restrict ourselves to the region $r > m$ which has a regular behaviour at the infinity. Subsequently, we will briefly describe the situation for $r < m$.

KLB managed to find their expression for gravitational energy density in the desired form $\frac{1}{2}F^2$ where in analogy with Newtonian theory they define gravitational intensity F with a corresponding potential Φ

$$F = -\frac{1}{\rho}\left[1 - \left(1 - \frac{2m(\rho)}{\rho}\right)^{\frac{1}{2}}\right], \qquad F = -(g_{\rho\rho})^{-\frac{1}{2}}\frac{\mathrm{d}\Phi}{\mathrm{d}\rho} \tag{64}$$

For convenience we added a minus sign to the original KLB definition of F. The resulting intensity and potential in the region $r > m$ are then

$$F^{(1)} = -\frac{m}{r^2}\mathrm{e}^{-\frac{m}{r}}, \qquad \Phi^{(1)} = -\frac{m}{r}. \tag{65}$$

This result can be well-interpreted in the Newtonian perspective. If we write down the Newtonian limit of the geodesic equation (for a radial geodesic) we find that the radial component of four-velocity satisfies

$$\frac{\mathrm{d}u_r}{\mathrm{d}t} = -\frac{m}{r^2}\mathrm{e}^{-\frac{m}{r}} + \mathcal{O}(p_r^2) \tag{66}$$

This was expected as the potential $\Phi^{(1)}$ is also the gravitational potential in the Newtonian limit. Naturally the gravitational energy density is then

$$\varrho^{(1)}_{KLB}(r) = -\frac{1}{8\pi}\frac{\mathrm{d}\Phi^{(1)}}{\mathrm{d}\rho}g^{\rho\rho}\frac{\mathrm{d}\Phi^{(1)}}{\mathrm{d}\rho} = -\frac{1}{8\pi}\left(F^{(1)}\right)^2 = -\frac{1}{8\pi}\,\frac{m^2}{r^4}\mathrm{e}^{-\frac{2m}{r}}. \tag{67}$$

Following the results of KLB we can apply the spatial Laplace operator on $\Phi^{(1)}$

$$\triangle\Phi^{(1)} = \frac{1}{r^2 e^{\frac{3m}{r}}}\frac{\mathrm{d}}{\mathrm{d}r}\left(r^2 e^{\frac{m}{r}}\frac{\mathrm{d}}{\mathrm{d}r}\Big(-\frac{m}{r}\Big)\right) = -\frac{m^2}{r^4}\mathrm{e}^{-\frac{2m}{r}} \tag{68}$$

and see that the Poisson equation is satisfied

$$\triangle\Phi^{(1)} = 4\pi(\varrho_{scalar} + \varrho^{(1)}_{KLB}). \tag{69}$$

Here we can see that the gravitational energy (67) contributes to the right hand side of (69) the same as the energy of the scalar field (61).

It is important to remark here that for a general spherically symmetric spacetime the potential Φ does not reduce to the gravitational potential in the Newtonian limit. As KLB found out the potential has a geometric meaning, $e^{2\Phi}$ is a conformal factor of a transformation between the spatial part of the metric and the flat space.

On the other hand, the Newtonian gravitational potential is given by the metric component g_{tt} but none of the quantities derived by KLB depend on the function $\xi(\rho)$. The fact that the potential $\Phi^{(1)}$ not only satisfies the Poisson equation but also plays the role of gravitational potential in the geodesic equation is given solely by the particular form of our metric (or more generally by the metric (12)).

We can now turn to the region $r < m$. Using the same definition (64) as in $r > m$ we obtain the respective intensity along with the corresponding potential

$$F^{(2)} = \frac{m - 2\,r}{r^2}\mathrm{e}^{-\frac{m}{r}}, \qquad \Phi^{(2)} = -\frac{m}{r} - 2\ln(r). \tag{70}$$

As in the previous case this potential satisfies the Poisson equation (69) but other than that this result has some strange properties. The first thing one may notice is

the fact that both the intensity and the potential do not vanish for $m \to 0$. This may be the consequence of the usage of the coordinate ρ (the areal radius (45)) in the region $r < m$. The metric in these coordinates does not converge to the Minkowki metric when $m \to 0$ because the region $r < m$ gradually shrinks and then disappears in the limit $m \to 0$.

Another important aspect is the fact that $F^{(2)}$ flips sign at $r = \frac{m}{2}$. This is consistent with the behaviour of the Misner–Sharp energy (56) which also changes sign there. However, this is not reflected by the geodesic motion. The point $r = \frac{m}{2}$ is not a local minimum of the effective potential (24) while the test particles are attracted to $r = 0$ whatever their location. We can thus conclude that the behaviour of the intensity, potential, as well as the Misner–Sharp energy in this region is very non-intuitive and cannot be interpreted from a Newtonian viewpoint.

Apart from the issues described in the previous paragraph the main problem of the KLB approach is the fact that the integral of the total energy density fails to give us the total mass m

$$\int_{\frac{m}{2}}^{\infty} (\varrho_{scalar}(r) + \varrho_{KLB}(r)) 4\pi \sqrt{g_{rr} g_{\theta\theta}^2} \mathrm{d}r \neq m. \tag{71}$$

As already mentioned above the negative energy of the scalar field should be compensated by a positive energy of the gravitational field. But the density $\varrho_{KLB}(r)$ is defined with a negative sign (equation (67)) so it is clear that we cannot get a positive total mass m. When KLB derived their expression for energy density they subtracted the matter energy from the total (Misner–Sharp) energy. After that they performed an integration by parts where the surface term vanished. This surface term is however non-zero in our spacetime which is the reason that the integral (71) is not equal to m.

To summarize, the advantage of the KLB approach is its Newtonian interpretation which in our spacetime also includes the potential in the geodesic equation. On the other hand the integral (71) is not equal to the total mass/energy of the spacetime. The naive gravitational energy density (62) obtained as a simple difference has exactly opposite problems.

7. The non-scalar singularity

The original motivation when deriving the metric (10) was to eliminate the direction-dependent curvature singularity of the original Curzon–Chazy spacetime. It turns out that the Kretschman scalar (9) is finite if the metric function k vanishes so this seems to be the right path to a singularity-free spacetime. Not only the Kretschmann scalar but also other invariants constructed from the Riemann tensor are finite which holds also for the Newman-Penrose scalars Ψ_a and Φ_{ab}.

On the other hand as was shown in the section 3 the spacetime is geodesically incomplete, the null hypersurface $r = 0$ can be reached in a finite proper time. A question stands however. Can the spacetime be extended beyond $r = 0$? In the original Curzon–Chazy spacetime the answer is positive. If one approaches the origin $\rho^2 + z^2 = 0$ properly (along the z-axes) one can then pass through the ring-like singularity and enter Minkowski space which can be smoothly connected to the Curzon–Chazy spacetime. This was shown by Morgan and Szekeresz [28] and naively it seems that it should also be possible in the SCC spacetime whose curvature invariants

are everywhere finite. However the finiteness of curvature scalars does not mean an absence of a curvature singularity. If a component of the Riemann tensor with respect to a parallel-propagated orthonormal frame diverges we can also speak of a curvature singularity which is then called non-scalar. This is well described in [29].

Recalling the fact that the radial timelike geodesics are incomplete we may find a free-falling frame $\{e^\mu_\nu\}_{\nu=0\ldots3}$ where e^μ_0 is the four-velocity of the radial geodesic (16). The orthonormal frame is then

$$\begin{aligned} e^\mu_0 &= (Ee^{\frac{2m}{r}}, -\sqrt{E^2 - e^{\frac{-2m}{r}}}, 0, 0), \qquad e^\mu_1 = (e^{\frac{m}{r}}\sqrt{E^2\mathrm{e}^{\frac{2m}{r}} - 1}, -E, 0, 0) \\ e^\mu_2 &= (0, 0, \frac{1}{r}\mathrm{e}^{-\frac{m}{r}}, 0), \qquad e^\mu_3 = (0, 0, 0, \frac{1}{r\sin(\theta)}\mathrm{e}^{-\frac{m}{r}}). \end{aligned} \tag{72}$$

The frame is indeed parallel-propagated along the geodesic as it satisfies the equation $e^\alpha_0 \nabla_\alpha e^\mu_\nu = 0$. We can then compute the frame components of the Riemann tensor and find out that many of them indeed diverge in the limit $r \to 0$. In particular two components of the electric part of the Riemann tensor tensor have the form

$$R_0{}^2{}_{02} = R_0{}^3{}_{03} = -\frac{m}{r^4}\left(mE^2 - r\mathrm{e}^{-\frac{2m}{r}}\right). \tag{73}$$

These components play role in the geodesic deviation equation which can be written in our frame as

$$\frac{\mathrm{d}^2 n^i}{\mathrm{d}\tau^2} = -R_0{}^i{}_{0j} n^j. \tag{74}$$

We can thus conclude that the free falling observer would experience infinite tidal forces in the directions tangent to the sphere $r = const.$ when approaching $r = 0$. This is consistent with the behaviour of the areal radius (13) which grows to the infinity in the limit as well. When examining the situation more closely we found out that the frame components of the Weyl tensor are perfectly finite. It is therefore the Ricci part of the curvature which is singular. In the limit $r \to 0$ all the nonzero components of the Ricci tensor tend to

$$R_{00}, R_{10}, R_{11} \to -\frac{2E^2m^2}{r^4}. \tag{75}$$

This is not very surprising as the Ricci tensor is given by the matter filling the spacetime and in our case the scalar field diverges in $r = 0$. For illustration we can compute the components of the Ricci tensor in a different frame. We know that the distance along a spatial geodesic located at $t = const.$ is infinite (equation (14)). Avoiding the geodesic incompleteness here should yield finite curvature components. And it is indeed so. If we use

$$\hat{e}^\mu_0 = (e^{\frac{m}{r}}, 0, 0, 0), \qquad \hat{e}^\mu_1 = (0, e^{-\frac{m}{r}}, 0, 0) \tag{76}$$

together with e_2 and e_3 from (72) where $\hat{e}_1$ is the tangent vector we obtain the only nonzero Ricci component

$$\hat{R}_{11} = -\frac{2m^2}{r^4}\mathrm{e}^{-\frac{2m}{r}} \tag{77}$$

which is finite. The parallel transport equations are again satisfied for this frame ($\hat{e}^\alpha_1 \nabla_\alpha \hat{e}^\mu_\nu = 0$).

The hypersurface $r = 0$ is then a Ricci curvature singularity which is encountered in some frames while in others the curvature is regular. We can even find coordinates in which the Ricci tensor is finite. For $x = e^{\frac{m}{r}}$ the scalar field is $\Phi = \mp \ln(x)$ and $R_{11} \sim \frac{1}{x^2}$ which is zero for $x \to \infty$. The scalar field is however singular no matter which frame we use and therefore it would be surprising if the hypersurface $r = 0$ were regular and we could extend the spacetime beyond this boundary. In fact, even without considering the scalar field, the divergent components of the Riemann curvature tensor (as seen in (73)) in the parallel-propagated frame (72) rule out the existence of any extensions (see [30]).

8. A note on $m < 0$ case

Finally, let us briefly comment on the case of $m < 0$ which we have disregarded so far. Examining (9) we immediately see that curvature singularity at $r = 0$ is now a simple scalar one since Kretschmann scalar diverges. Additionally, the character of the singularity ($r = 0$ hypersurface) changed from null to timelike and it has repulsive nature since m characterizes asymptotic mass of the spacetime. The singularity is practically inaccessible for timelike observers because it is surrounded by infinitely high potential barrier and therefore only observers accelerated to attain $E = \infty$ could reach $r = 0$. The null observers can reach the singularity without any problem. Also the radial distance to it $d(r_0, 0)$ is finite as well as the coordinate time t it takes to reach $r = 0$, in fact these quantities are finite for all radial geodesics. The wormhole structure is absent completely as there is no throat (the expansions of relevant congruences are nonzero everywhere). Overall, the spacetime has a conformal structure of a simple timelike naked singularity (see figure 9).

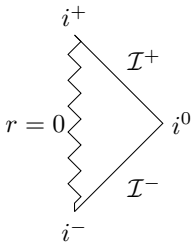

Figure 9: Penrose conformal diagram for $m < 0$ case.

9. The Maxwell-scalar solution

When considering the metrics of the form (12) one can generalize the method of generating new solutions to also include the electromagnetic field. This was done for example in [11]. The action (1) is then extended by including the Lagrangian density of the Maxwell field

$$\mathcal{L}_{\mathrm{EM}} = -\frac{1}{4} F_{\mu\nu} F^{\mu\nu} \tag{78}$$

which means adding the stress-energy tensor

$$T^{(\mathrm{EM})}_{\mu\nu} = F_{\mu\rho} F_{\nu}{}^{\rho} + \mathcal{L}_{\mathrm{EM}}\, g_{\mu\nu} \tag{79}$$

to the right-hand side of the Einstein equations. Based on [11], the solution generated from our SCC spacetime by including the electromagnetic field has the following form

$$\begin{aligned} \mathrm{d}s^2 &= -\frac{1}{\sinh^2(\frac{m}{r})}\mathrm{d}t^2 + \sinh^2\left(\frac{m}{r}\right)(\mathrm{d}r^2 + r^2\mathrm{d}\Omega^2), \\ \Phi &= \pm\frac{m}{r}, \qquad F_{tr} = \pm\frac{m}{r^2\sinh^2(\frac{m}{r})}. \end{aligned} \tag{80}$$

The relation to the SCC spacetime becomes clear when looking at the the dependence of the metric on the radial coordinate r. For $r \to 0$ the dominant source is the scalar field while the Maxwell field vanishes in the limit. Thus in the neighborhood of $r = 0$ the metric (80) reduces to the SCC metric (10). On the other hand as $r \to \infty$ the strength of the electromagnetic field grows to $F_{tr} = \pm\frac{1}{m}$. This in turn has effect on energy conditions as a timelike observer would measure a positive energy density while the null energy condition remains unaffected by $T^{(\mathrm{EM})}_{\mu\nu}$.

The areal radius $R_A(r)$ is a decreasing function of r which means that no wormhole is present in this case (The expansions of null radial geodesics do not change their signs as well.). Since the electromagnetic field does not vanish at the infinity it is clear that the spacetime is not asymptotically flat which is also apparent from its conformal diagram (figure 10) where the infinity ($|t| < \infty, r = \infty$) is a timelike hypersurface. On the other hand the left part of the diagram including the non-scalar singularity is the same as in the SCC spacetime.

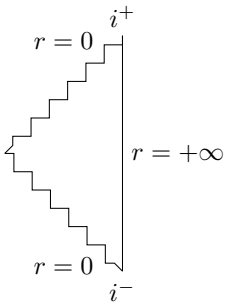

Figure 10: The conformal diagram of the SCC spacetime with electromagnetic field.

The timelike character of the infinity looks similar to an asymptotically anti-de Sitter spacetime that is however not the case here as the scalar curvature vanishes at infinity. When looking at the metric (80) at $r = \infty$ we can see that the areal radius reaches its minimal value m while the other metric components do not converge to a finite nonzero value. It is important to stress however that nothing suggests that there is a spacetime singularity at $r = \infty$. Firstly none of the timelike geodesics can reach it due to the presence of an infinite potential barrier. As for the spacelike and null geodesics, all of them reach it at an infinite value of their affine parameter, in addition all components of the Riemann tensor remain finite in the limit.

Since the spacetime is not asymptotically flat (or even simple) the concept of total mass-energy of the spacetime is ambiguous. One can use the Brown–York energy and evaluate the integral (53) at infinity. As in the SCC case however it is necessary to use the areal radius as a radial coordinate to get a meaningful result (the coordinate

ρ in (45)). One then gets the expected result $M_{BY} = m$. If one uses the Misner–Sharp energy (which is a coordinate-independent quantity), one arrives at $M_{MS} = \frac{m}{2}$. The difference between the two masses is not that surprising since they coincide for a general spherically symmetric spacetime only at such ρ_0 for which $g_{\rho\rho}(\rho_0) = 1$. This can be seen from the general forms of both masses (see for example [31]) and it is the reason why they give the same result for a metric converging to Minkowski one. The Komar mass (52) is of no use here as it produces an infinite result in this case.

10. Conclusion

We have seen that the solution we examined is behaving both as a wormhole and a time machine. However, neither of these characterisations are fully attained by our solution. Although we have a wormhole throat satisfying all the standard conditions it connects asymptotically flat region to a region whose border is a non-scalar singularity of null character. This strange region enables travelling to future timelike infinity in finite time thus essentially being a one-directional time machine. Overall picture of the geometry was provided by analysing conformal structure.

The parameter m characterising the solution can be interpreted as a mass of the spacetime as confirmed by using several definitions. The Misner–Sharp energy turned out to be a good tool for localization of the energy distribution in the spacetime. These results were compared with Katz, Lynden-Bell and Bičák approach [32].

A brief study of the case $m < 0$ revealed that it results in a spacetime that looks conformally as a standard timelike naked singularity. However, this singularity is surrounded by infinite potential barrier making it inaccessible to observers. Finally, a generalization including electromagnetic field was obtained by applying a generating technique leading to a spacetime with radically different conformal structure and without wormhole throat.

The non-scalar singularity is rather undesirable feature of our spacetime but one expects that quantum gravity effects would remove it as is the case for the timelike naked singularity sourced by scalar field [33]. Another interesting aspect would be a potential generalization including rotation. Considering the one-directional time machine character of our solution it might be interesting to analyze if the extra positive time gained by passing in and out of the wormhole might help in protecting causality in systems composed from several such wormholes.

Acknowledgements

The research was supported by the Czech Science Foundation Grant No. 22-14791S and the Charles University project GAUK No. 906419.

References

[1] Herdeiro C A R and Radu E 2015 *Int. J. Mod. Phys. D* **24** 1542014 (*Preprint* arXiv:1504.08209) URL http://www.worldscientific.com/doi/abs/10.1142/S0218271815420146?src=recsys
[2] Gibbons G W and Volkov M S 2017 *JCAP* **05** 039 (*Preprint* arXiv:1701.05533) URL https://iopscience.iop.org/article/10.1088/1475-7516/2017/05/039
[3] Tahamtan T and Svítek O 2015 *Phys. Rev.* **D91** 104032 (*Preprint* arXiv:1503.09080) URL https://journals.aps.org/prd/abstract/10.1103/PhysRevD.91.104032
[4] Tahamtan T and Svítek O 2016 *Phys. Rev.* **D94** 064031 (*Preprint* arXiv:1603.07281) URL https://journals.aps.org/prd/abstract/10.1103/PhysRevD.94.064031

[5] Weyl H 1917 *Annalen der Physik* **359** 117–145 (*Preprint* https://onlinelibrary.wiley.com/doi/pdf/10.1002/andp.19173591804) URL https://onlinelibrary.wiley.com/doi/abs/10.1002/andp.19173591804

[6] Curzon H E J 1925 *Proceedings of the London Mathematical Society* **s2-23** 477–480 (*Preprint* https://londmathsoc.onlinelibrary.wiley.com/doi/pdf/10.1112/plms/s2-23.1.477) URL https://londmathsoc.onlinelibrary.wiley.com/doi/abs/10.1112/plms/s2-23.1.477

[7] Janis A I, Newman E T and Winicour J 1968 *Phys. Rev. Lett.* **20**(16) 878–880 URL https://link.aps.org/doi/10.1103/PhysRevLett.20.878

[8] Fisher I 1948 *Zh.Eksp.Teor.Fiz.* **18** 636–640 (*Preprint* https://arxiv.org/abs/gr-qc/9911008)

[9] Tahamtan T 2020 *Phys. Rev. D* **101** 124023 (*Preprint* arXiv:2006.02810) URL https://journals.aps.org/prd/abstract/10.1103/PhysRevD.101.124023

[10] Svítek O and Tahamtan T 2018 *European Physical Journal C* **78** 167 URL https://link.springer.com/article/10.1140/epjc/s10052-018-5628-0

[11] Maeda H and Martínez C 2019 *Classical and Quantum Gravity* **36** 185017 ISSN 1361-6382 URL http://dx.doi.org/10.1088/1361-6382/ab293a

[12] Cline J M, Jeon S and Moore G D 2004 *Phys. Rev. D* **70** 043543 (*Preprint* hep-ph/0311312) URL https://journals.aps.org/prd/abstract/10.1103/PhysRevD.70.043543

[13] Scott S M and Szekeres P 1986 *Gen. Rel. Grav.* **18** 557–570 URL https://link.springer.com/article/10.1007/BF00769924

[14] Taylor J P W 2005 *Class. Quant. Grav.* **22** 4961–4971 URL https://iopscience.iop.org/article/10.1088/0264-9381/22/23/003

[15] Gibbons G W 2003 (*Preprint* arXiv:hep-th/0302199) URL https://arxiv.org/abs/hep-th/0302199

[16] Majumdar S D 1947 *Phys. Rev.* **72**(5) 390–398 URL https://link.aps.org/doi/10.1103/PhysRev.72.390

[17] Iyer S V and Petters A O 2007 *General Relativity and Gravitation* **39** 1563–1582 URL https://doi.org/10.1007%2Fs10714-007-0481-8

[18] Simpson A and Visser M 2019 *Journal of Cosmology and Astroparticle Physics* **2019** 042–042 ISSN 1475-7516 URL http://dx.doi.org/10.1088/1475-7516/2019/02/042

[19] Hayward S A 1999 *International Journal of Modern Physics D* **08** 373–382 ISSN 1793-6594 URL http://dx.doi.org/10.1142/S0218271899000286

[20] Bojowald M 2010 *Canonical Gravity and Applications: Cosmology, Black Holes, and Quantum Gravity* (Cambridge University Press) URL https://www.cambridge.org/core/books/canonical-gravity-and-applications/88843142AC5617F84ED0E1FE2742E9C3

[21] Ellis H G 1973 *Journal of Mathematical Physics* **14** 104–118 (*Preprint* https://doi.org/10.1063/1.1666161) URL https://doi.org/10.1063/1.1666161

[22] Morris M S and Thorne K S 1988 *American Journal of Physics* **56** 395–412 (*Preprint* https://doi.org/10.1119/1.15620) URL https://doi.org/10.1119/1.15620

[23] Hochberg D and Visser M 1998 *Phys. Rev. Lett.* **81**(4) 746–749 URL https://link.aps.org/doi/10.1103/PhysRevLett.81.746

[24] Komar A 1959 *Phys. Rev.* **113**(3) 934–936 URL https://link.aps.org/doi/10.1103/PhysRev.113.934

[25] Hawking S W and Horowitz G T 1996 *Classical and Quantum Gravity* **13** 1487–1498 ISSN 1361-6382 URL http://dx.doi.org/10.1088/0264-9381/13/6/017

[26] Misner C W and Sharp D H 1964 *Phys. Rev.* **136**(2B) B571–B576 URL https://link.aps.org/doi/10.1103/PhysRev.136.B571

[27] Lynden-Bell D, Katz J and Bičák J 2007 *Phys. Rev. D* **75** 024040 URL https://journals.aps.org/prd/abstract/10.1103/PhysRevD.75.024040

[28] Szekeres P and Morgan F H 1973 *Commun. Math. Phys.* **32** 313–318 URL https://link.springer.com/article/10.1007/BF01645612

[29] Ellis G F R and Schmidt B G 1977 *Gen. Rel. Grav.* **8** 915–953 URL https://link.springer.com/article/10.1007/BF00759240

[30] Clarke C J S 1973 *Communications in Mathematical Physics* **32** 205–214 URL https://link.springer.com/article/10.1007/BF01645592

[31] Blau M and Rollier B 2008 *Classical and Quantum Gravity* **25** 105004 ISSN 1361-6382 URL http://dx.doi.org/10.1088/0264-9381/25/10/105004

[32] Katz J, Lynden-Bell D and Bičák J 2006 *Classical and Quantum Gravity* **23** 7111–7127 ISSN 1361-6382 URL http://dx.doi.org/10.1088/0264-9381/23/23/030

[33] Svítek O, Tahamtan T and Zampeli A 2020 *Annals Phys.* **418** 168195 (*Preprint* arXiv:1606.05635) URL https://www.sciencedirect.com/science/article/abs/pii/S0003491620301287

5. Extreme mass ratio inspirals into black holes surrounded by matter (paper 2)

- Polcar, L., Lukes-Gerakopoulos, G., and Witzany, V. Extreme mass ratio inspirals into black holes surrounded by matter. *Physical Review D*, 106(4), Aug 2022

This chapter is based on our paper [69] whose aim was to calculate an adiabatic inspiral in the spacetime of Schwarzschild black hole surrounded by additional matter. The theoretical background for this publication can be found in chapter 3 (Canonical perturbation theory and Quadrupole formalism) but also in chapter 1 (Field equations and selected solutions).

In the existing literature the extreme mass ratio inspirals are studied predominantly in the Schwarzschild or Kerr spacetime without taking into account the potential environmental effects. What we had in mind during our calculations was a ring or disc located in the equatorial plane but far from the central black hole. To capture that idea with a sufficiently simple model we represented the matter using an external quadrupole with a nonzero angular momentum which is a solution to the Einstein's equations linearised around the Schwarzschild metric. The external quadrupole is then the first non-trivial terms in expansion of the Green's functions (1.24). To simplify the solution further we performed a transformation to the frame co-rotating with the matter close to the black hole and neglected all the non-trivial term in the expansion of the dragging function ω as they were much smaller than the quadrupole gravitational potential. We were then left with a static axially symmetric solution.

We then proceeded with the canonical transformations using the Lie series. We applied only two transformations in the Schwarzschild spacetime and one for the superposition. This means that the approximation was reliable only close to the stable Schwarzschild circular orbit (as stated by the Birkhoff normal form theorem). Unlike in the Kerr paper [46] we had to be careful in close vicinity of some Schwarzschild resonances where the approximation ceases to be valid. This is the problem of small divisors discussed in chapter 3.

Finally when the geodesic problem is solved we can calculate the gravitational-wave fluxes which was in this paper done by using the simple quadrupole formalism which was also used for generating the waveforms. At that point the reason why we used the canonical perturbation theory becomes apparent. The adiabatic approximation requires the separation of variables into two groups, slow and fast. In the geodesic limit the slow variables are three independent constants of motion. Our perturbed spacetime however is not integrable and we only have two integrals of motion. This problem may be however circumvented by our application of canonical perturbation theory which allows us to approximate the non-integrable system by an integrable one with actions playing the role of slow variables which are constant in the geodesic limit. The results are then illustrated on the phase shifts due to the presence of the additional matter and on the evolution of inclination which is not constant already at the geodesic level.

Extreme mass ratio inspirals into black holes surrounded by matter

Lukáš Polcar[1,2], Georgios Lukes-Gerakopoulos[1,*] and Vojtěch Witzany[3]
[1] *Astronomical Institute of the Czech Academy of Sciences, Boční II 1401/1a, CZ-141 00 Prague, Czech Republic*
[2] *Institute of Theoretical Physics, Faculty of Mathematics and Physics, Charles University in Prague, 18000 Prague, Czech Republic and*
[3] *School of Mathematics and Statistics, University College Dublin, Belfield, Dublin 4, D04 V1W8, Ireland*

Inspirals of stellar-mass compact objects into massive black holes, known as extreme mass ratio inspirals (EMRIs), are one of the key targets for upcoming space-based gravitational-wave detectors. In this paper we take the first steps needed to systematically incorporate the effect of external gravitating matter on EMRIs. We model the inspiral as taking place in the field of a Schwarzschild black hole perturbed by the gravitational field of a far axisymmetric distribution of mass enclosing the system. We take into account the redshift, frame-dragging, and quadrupolar tide caused by the enclosing matter, thus incorporating all effects to inverse third order of the characteristic distance of the enclosing mass. Then, we use canonical perturbation theory to obtain the action-angle coordinates and Hamiltonian for mildly eccentric precessing test-particle orbits in this background. Finally, we use this to efficiently compute mildly eccentric inspirals in this field and document their properties. This work shows the advantages of canonical perturbation theory for the modeling EMRIs, especially in the cases when the background deviates from the standard black hole fields.

I. INTRODUCTION

Extreme mass ratio inspirals (EMRIs) are one of the most complex sources of gravitational waves that we expect to be observed by the Laser Interferometer Space Antenna (LISA) [1]. These binary sources are composed of a primary supermassive black hole and a secondary much lighter compact object, such as a black hole or a neutron star. These systems are called extreme mass ratio (EMR), because the mass ratio between the secondary and the primary is below 10^{-4}. Such a small mass ratio allows us to approach the contribution of the secondary object to the binary system in a perturbative way, i.e. to treat the secondary as a perturbation to a given black hole background. In particular, by expanding the background metric in terms of the mass ratio, we can calculate the gravitational self-force [2, 3]. The respective radiation reaction carries away from the binary energy and angular momentum in the form of gravitational waves causing the secondary to inspiral towards the primary.

The aforementioned dissipation due to radiation reaction is actually slow when compared to the orbital motion of the secondary around the primary. This allows us to use a two timescale approach to model an EMRI [4, 5]. The slow time scale is concerned with the evolution of the constants of motion, which correspond to the action variables of the system, while the fast time scale is concerned with the orbital phases (or "orbital anomalies") of the secondary, which correspond to the angle variables of the system [6]. Hence, expressing an EMR system in action angle variables is a natural way to capture its dynamics.

In Ref. [7], following the action-angle line of thought, Schmidt was able to compute the fundamental orbital frequencies of a body moving on geodesics in a Kerr black hole background. Ref. [8] went one step further the above work in the direction of EMRIs, when the authors used the fundamental frequencies to efficiently decompose the Teukolsky equation [9] in the frequency domain in order to find the energy and angular momentum fluxes emitted by the secondary. Many other works employed the idea that the system describing an EMR should be, in principle, reexpressed in action-angle variables [4, 10–14]. Refs. [15, 16] derived integral and special-function formulas for the transformation to action-angle coordinates for bound geodesics in Kerr space-time, but no work expressed the full *closed-form* transform to *and from* action-angle coordinates for black hole geodesics. This was only achieved in Ref. [17] and the present work. In Ref. [17] a Taylor series like approach has been used to find the action-angle variables for bound geodesics as a function of the energy and the angular momentum on a Schwarzschild background, while in the present work we employ a Lie series approach based on canonical perturbation theory (see, e.g., [18, 19] for a comprehensive introduction into this theory).

Canonical perturbation theory has a long history of successes, such as the celebrated Kolmogorov-Arnold-Moser (KAM) theorem [20] or the computation of asymptotic manifolds [21] (for more see, e.g., [22, 23]). Our study uses the framework of this theory to address the problem of EMRIs in a background dominated by a Schwarzschild black hole and perturbed by a surrounding matter field. The Lie series approach simplifies the system and allows us to have the respective Hamiltonian expressed purely in terms of actions. This implies that we have all the important quantities, such as the characteristic frequencies of motion in closed form. The Lie series approach also provides a canonical transformation to the action-angle variables, which implies that we have at hand the invertible mapping between the original coordinates and the action-angle ones.

The perturbed black hole field that we study here can serve as a model for a broad range of physical scenarios. Massive black holes in the centers of galaxies are well known to be surrounded by dense nuclear star clusters and other molecular and dust structures [24, 25]. Other possibilities of exter-

* gglukes@gmail.com

nal gravitational perturbations come from more exotic sources such as dark matter [26, 27] or scalar fields [28]. On the other hand, various physical effects such as tidal forces, increasing rotational shearing and the associated instabilities, or gravitational radiation lead to the evacuation of the immediate vicinity of the black hole with only a few massive objects remaining in the inner few hundred Schwarzschild radii [29]. This motivates our approach, where the external matter distribution is considered as far from the black hole and its field expanded only to a handful of leading external multipoles.

To date, the motion in the fields of black holes with external gravitational perturbations was mostly studied through the methods of numerical integration. Refs [30, 31] showed that the motion of free test particles in black hole fields superposed with external multipoles (exactly as we study here) corresponds to a weakly non-integrable system with the appearance of resonances and chaos. Several other works have since documented these properties for various exact matter sources outside of the black hole and by using a number of methods of numerical analysis [32–38]. Our work stands out by using an analytical method, while we have to be aware of its limitations due to the weak non-integrability of the system proven by the large body of numerical studies.

All the advantages of using the Lie series approach come with the cost that the new system is faithful to the original one only up to a certain accuracy. Nevertheless, every model has such flaws, the true issue is whether the approximation used is accurate enough for the purpose it will be used for. In this sense, this work provides a proof of principle that by using the Lie series approach one is able to compute fast adiabatic EMRIs with fair accuracy even in the case of more complex black hole backgrounds.

The rest of the article is organized as follows. Sec. II briefly introduces the perturbation theory method. Sec. III describes the background on which the inspirals evolve in our study, and details the methodology we followed to describe the geodesic motion on this background using the Lie series method. Sec. IV discusses the techniques used to generate the inspirals, while Sec. V presents our numerical results. Finally, Sec. VI discusses our main conclusions, and refinements and further steps that will be needed for applications of this approach in contexts such as the production of waveforms for LISA.

II. CANONICAL PERTURBATION THEORY

In this section we summarize the general method that will be used to cast the conservative dynamics in action-angle coordinates in Section III.

A. Action-angle coordinates

Consider a Hamiltonian system of N degrees of freedom with the Hamiltonian $H(q_i, p_i)$ satisfying the following conditions:

1. The system possesses N linearly independent isolating integrals of motion I_i, $\{I_i, I_j\} = 0$, $i, j = 1, \ldots N$
2. Motion in the phase space is bounded.

According to the Liouville-Arnold theorem (see for example [6, 39]), the motion is then confined to an N-dimensional subset of the phase space diffeomorphic to the torus $\mathbb{T}^N$. The particular torus on which the selected trajectory lies is defined by N parameters J_i called actions and can be parametrized by N periodic angles $\psi_i \in (0, 2\pi)$. Angles are canonically conjugate to actions and together they are known as action-angle coordinates.

If we perform a canonical transformation to action-angle coordinates we find that the new form of the Hamiltonian has one remarkable property, it depends only on the actions

$$(q_i, p_i) \to (\psi_i, J_i), \quad H(q_i, p_i) \to H(J_i)\,.$$

Consequently the solution to Hamilton equations is trivial

$$\begin{aligned} J_i(t) &= \text{constant}, \\ \psi_i(t) &= \Omega_i t + \psi_{0i}, \end{aligned} \tag{1}$$

where $\Omega_i = \frac{\partial H(J_j)}{\partial J_i}$ are the frequencies of motion. Inserting the solution (1) into the transformation relations we obtain

$$q_i = q_i(\psi_j(t), J_j), \quad p_i = p_i(\psi_j(t), J_j)\,. \tag{2}$$

Thus, finding the transformation from action-angle coordinates to the original coordinates is equivalent to solving the Hamilton equations of motion in the original coordinates (q_i, p_i).

In the particular case of a separable system, in which the motion is periodic in coordinate q_i, the corresponding action can be computed using the formula [40]

$$J_i = \frac{1}{2\pi} \oint p_i \mathrm{d}q_i\,, \tag{3}$$

where the integral is taken along a complete time period of the motion.

Unfortunately, there are very few examples in which the integral (3) can be evaluated in a closed form. One such example is the harmonic oscillator whose Hamiltonian can be transformed as

$$H(q, p) = \frac{p^2}{2m} + \frac{1}{2} m\Omega^2 q^2 \to \quad H(\psi, J) = \Omega J\,, \tag{4}$$

while the transformation relations are given by

$$q = \sqrt{\frac{2J}{m\Omega}} \sin(\psi)\,, \qquad p = \sqrt{2J\Omega m} \cos(\psi)\,. \tag{5}$$

In these relations one can clearly see the familiar solution to the harmonic oscillator problem.

At this point one can surely ask whether it is possible to perform such a transformation in case of a more complicated integrable system or even in a case of a slightly perturbed integrable system. This question leads us directly to the Lie series formalism.

B. Lie series

The Lie series are a class of canonical transformations defined by an arbitrary generating function $\omega(q_i, p_i)$ (details in Refs [18, 19, 41]). We will first describe this on the best known case of time evolution. Denoting z_i as the phase space coordinates, the evolution equation can be written as

$$\frac{\mathrm{d}z_i}{\mathrm{d}t} = \{z_i, H\}. \tag{6}$$

The solution to this equation can then be found using the Taylor expansion where the time derivative is replaced by the Poisson bracket with the Hamiltonian, which is a consequence of eq. (6). Denoting $z_i(0) = z_i$ we have

$$\begin{aligned} z_i(t) = z_i + \{z_i, H\}t + \frac{1}{2}\{\{z_i, H\}, H\}t^2 + \ldots = \\ = \exp(t\mathscr{L}_H) z_i \,, \end{aligned} \tag{7}$$

where the operator $\mathscr{L}_g$ is defined as $\mathscr{L}_g f = \{f, g\}$. The operator $\mathscr{L}_g$ is called Lie derivative because in the geometrical formulation of Hamiltonian mechanics we have $\mathscr{L}_g = \mathscr{L}_{X_g}$ where X_g is the Hamiltonian vector field associated with the function g.

If we now make an exchange: $H \leftrightarrow \omega(q_i, p_i)$, $t \leftrightarrow \varepsilon$ where ε is a small parameter, we can define a new transformation

$$Z_i = z_i(\varepsilon) = \exp(\varepsilon \mathscr{L}_\omega) z_i \,. \tag{8}$$

This transformation is indeed canonical as the Poisson brackets are preserved due to the following identity [41]:

$$\{\exp(\mathscr{L}_\omega) f, \exp(\mathscr{L}_\omega) g\} = \exp(\mathscr{L}_\omega)\{f, g\}, \tag{9}$$

which leads to $\{z_i, z_j\} = \{Z_i, Z_j\}$. Another useful identity is the inverse relation for the Lie operator

$$\big(\exp(\varepsilon \mathscr{L}_\omega)\big)^{-1} = \exp(-\varepsilon \mathscr{L}_\omega). \tag{10}$$

Having introduced the Lie series formalism, we can now use it to approximately transform a Hamiltonian into action-angle coordinates, or to be more specific, to find the so called Birkhoff normal form of a Hamiltonian.

C. Birkhoff normal form

Assume we have a Hamiltonian in the form:

$$H^{(0)} = H_0(J_i) + \sum_{j=1} \varepsilon^j H_j^{(0)}(\psi_i, J_i) \,, \tag{11}$$

where $H_0(J_i)$ is a well known integrable Hamiltonian already expressed in the action-angle form while the other part is expanded in a small perturbation parameter ε. Computing the Birkhoff normal form of $H^{(0)}$ actually means eliminating the angle variables from the Hamiltonian.

Starting from the first order of the perturbation we decompose the Hamiltonian $H_1^{(0)}$ into the part which does not depend on the angles and the other which does: $H_1^{(0)} = Z_1(J_i) + h_1(\psi_i, J_i)$. If we then act with the Lie operator on $H^{(0)}$ we get

$$\exp(\varepsilon \mathscr{L}_{\omega_1}) H^{(0)} = H_0 + \varepsilon Z_1 + \varepsilon\{H_0, \omega_1\} + \varepsilon h_1 + \mathscr{O}(\varepsilon^2). \tag{12}$$

Since h_1 is to be eliminated, the terms proportional to ε have to satisfy:

$$\{H_0, \omega_1\} + h_1 \stackrel{!}{=} 0. \tag{13}$$

This is called homological equation which has to be solved for the so far unknown generating function ω_1. Once we have found ω_1 we can compute a new form of our Hamiltonian

$$H^{(1)} = \exp(\varepsilon \mathscr{L}_{\omega_1}) H^{(0)} = H_0(J_i) + \varepsilon Z_1(J_i) + \mathscr{O}(\varepsilon^2). \tag{14}$$

Thus, we have our Hamiltonian in the action-angle variables up to the first order in ε. We can now proceed in a similar fashion, i.e., solving another homological equations and so on until arriving at a desired order n in which the Hamiltonian reads

$$\begin{aligned} H^{(n)} = \exp(\varepsilon^n \mathscr{L}_{\omega_n}) \exp(\varepsilon^{n-1} \mathscr{L}_{\omega_{n-1}}) \ldots \exp(\varepsilon \mathscr{L}_{\omega_1}) H^{(0)} = \\ = U(\omega_i) H^{(0)}, \end{aligned} \tag{15}$$

where the notation $U(\omega_i)$ is used just for brevity to represent the n canonical transformations applied. Furthermore, $H^{(n)}$ can be decomposed into

$$\begin{aligned} H^{(n)} &= H_{NF}(J_i) + R^{(n)}(\psi_i, J_i) \,, \\ H_{NF}(J_i) &= H_0(J_i) + \sum_{j=1}^{r} \varepsilon^j Z_j(J_i); \;\; R^{(n)}(\psi_i, J_i) = \mathscr{O}(\varepsilon^{n+1}), \end{aligned} \tag{16}$$

where H_{NF} is the Birkhoff normal form of nth order, while $R^{(n)}$ is a remainder which can be neglected as ε^{n+1} is a sufficiently small number. The Birkhoff normal form now allows us to compute the frequencies of motion which tell us how the new angles evolve (see Eq. (1)). The old coordinates can now be expressed in terms of the new ones

$$\psi^{(0)} = U(\omega_i)\psi, \;\; J^{(0)} = U(\omega_i) J \,. \tag{17}$$

Inserting Eq. (1) into the transformation relation (2) gives us an approximative solution to the equation of motion with the error given by the size of the remainder $R^{(n)}$.

The Lie series is generally only asymptotic; there may exist a maximum order above which the approximation becomes less and less precise. The question of convergence of canonical perturbation theory is tied to the existence of small divisors and resonances, and the Lie series is not guaranteed to converge everywhere even in fully integrable systems (see, e.g., Refs [6, 18]). We shall demonstrate the issues with resonances also in Sec. III D.

III. TIDALLY PERTURBED BLACK HOLE ORBITS

Here we compute the conservative evolution of mildly eccentric orbits of test particles near black holes perturbed by a faraway gravitating ring surrounding the system. We first introduce the metric field and then apply the Lie series method to obtain action-angle coordinates of near-circular geodesics in this field. Consequently, we apply another round of canonical perturbation theory to obtain the approximate solution of these orbits under the tidal perturbation by the ring. This will be a basis for the adiabatic inspirals computed in Sec. IV.

A. A black hole perturbed by a ring-like source

Picture a black hole of mass M encircled by a rotating gravitating ring with mass $\mathscr{M}_{\rm r}$ and radius $r_{\rm r} \gg M$ much larger than the black hole horizon. What are going to be the leading-order effects of the ring on the gravitational field near the black hole? It was found already by Thirring in 1918 [42, 43] that the local inertial system inside a light, thin rotating shell is rotating with respect to the inertial system at infinity with an angular velocity

$$\Omega_{\rm Thir} = \frac{2\mathscr{J}_{\rm sh}}{r_{\rm sh}^3}\,, \tag{18}$$

where $\mathscr{J}_{\rm sh}, r_{\rm sh}$ are the total angular momentum and radius of the shell. Similarly, the rate of time inside the shell is redshifted with respect to observers at infinity by the gravitational potential on the surface of the shell

$$z_{\rm sh} = \frac{\mathscr{M}_{\rm sh}}{r_{\rm sh}}\,, \tag{19}$$

where $\mathscr{M}_{\rm sh}$ is the total mass of the shell.

Based on the works of Refs [44, 45], we show in Appendix A that a similar effect occurs in the case of the ring-hole system. Specifically, the inertial frame near the center of a ring of angular momentum $\mathscr{J}_{\rm r}$ and Schwarzschild radius $r_{\rm r}$ rotates, to leading order in $r_{\rm r} \gg M \gg \mathscr{M}_{\rm r}$, with an angular velocity

$$\Omega_{\rm in} = \frac{2\mathscr{J}_{\rm r}}{r_{\rm r}^3} + \mathscr{O}(r_{\rm r}^{-5})\,. \tag{20}$$

We assume that the ring-like structure is moving approximately as a test body in the black-hole field, so to leading order we have $\mathscr{J}_{\rm r} = \mathscr{M}_{\rm r}\sqrt{Mr_{\rm r}^2/(r_{\rm r}-3M)}$ and we can write

$$\Omega_{\rm in} = 2\mathscr{M}_{\rm r}\sqrt{\frac{M}{r_{\rm r}^5}}\left(1+\frac{3M}{2r_{\rm r}}\right) + \mathscr{O}(r_{\rm r}^{-9/2})\,. \tag{21}$$

Additionally, the internal frame is redshifted by a factor

$$z_{\rm in} = \frac{\mathscr{M}_{\rm r}}{r_{\rm r}}\left(1+\frac{M}{r_{\rm r}}\right) + \mathscr{O}(r_{\rm r}^{-3})\,. \tag{22}$$

Finally, the gravitational field near the black hole will also have a tidal contribution from the ring. Apart from assuming that the black hole is static in the "internal" inertial frame, we also truncate the tides to leading quadrupolar order. Then we obtain the metric valid near the black hole (see Appendix A for details):

$$\begin{aligned} {\rm d}s^2_{r\ll r_{\rm r}} = &-\left(1-\frac{2M}{r}\right)(1+2\nu_Q){\rm d}t^2 + \frac{1+2\chi_Q-2\nu_Q}{1-2M/r}{\rm d}r^2 \\ &+(1-2\nu_Q)r^2\left[(1+2\chi_Q){\rm d}\vartheta^2 + \sin^2\vartheta\,{\rm d}\varphi^2\right], \end{aligned} \tag{23}$$

$$\nu_Q \equiv \frac{Q}{4}\left[r(2M-r)\sin^2\vartheta + 2(M-r)^2\cos^2\vartheta - 6M^2\right], \tag{24}$$

$$\chi_Q \equiv QM(M-r)\sin^2\vartheta\,, \tag{25}$$

where $Q \equiv \mathscr{M}_{\rm r}/r_{\rm r}^3$ is the quadrupole perturbation parameter and t, r, ϑ, ϕ are Schwarzschild-like coordinates in the local frame. The local metric is approximately vacuum, static and axisymmetric with respect to the local time and azimuthal angle t, φ with corresponding Killing vectors $\xi^\mu_{(t)} = \delta^\mu_t$, $\xi^\mu_{(\varphi)} = \delta^\mu_\varphi$. As such, it is an approximate Weyl metric [46, 47].

The form (23) of the metric is valid only for $r \ll r_{\rm r}$ and rings that are not compact, $\mathscr{M}_{\rm r} \ll r_{\rm r}$. Specifically, it neglects all terms starting from $\mathscr{O}(r_{\rm r}^{-4})$ and $\mathscr{O}(\mathscr{M}_{\rm r}^2)$. Also, as already discussed, the local coordinates are related to the coordinate time and azimuthal angle T, ϕ of static observers at infinity as

$${\rm d}T = (1+z_{\rm in}){\rm d}t\,, \tag{26}$$

$${\rm d}\phi = {\rm d}\varphi + \Omega_{\rm in}{\rm d}t\,. \tag{27}$$

This has to be taken into account when predicting observations from the dynamics in the metric field (23).

Note that this framework is very flexible, since it does not necessarily fix the relationship between $z_{\rm in}, \Omega_{\rm in}$ and Q. For more general matter distributions than a thin ring, these parameters can be computed separately and fed into the formalism the same way as it is done here. However, one case which we do not treat are time-dependent and non-axisymmetric perturbations which would correspond to perturbers orbiting our EMR binary at intermediate distances. The possibility of inclusion of this case is discussed in Sec. VI.

B. Quasi-circular Schwarzschild geodesics

We would now like to apply the aforementioned theory to the Hamiltonian

$$H_{\rm tot} = \frac{1}{2}g^{\mu\nu}p_\mu p_\nu\,, \tag{28}$$

where $g^{\mu\nu}$ is our background metric (23) and the four-momentum p_μ is normalized to unity, i.e. $g^{\mu\nu}p_\mu p_\nu = -1$. We will first start with the well known Schwarzschild Hamiltonian ($Q = 0$)

$$H_{\rm Schw} = \frac{1}{2}\left[\frac{-1}{1-\frac{2M}{r}}p_t^2 + \left(1-\frac{2M}{r}\right)p_r^2 + \frac{1}{r^2}\left(p_\theta^2 + \frac{p_\phi^2}{\sin^2\theta}\right)\right]. \tag{29}$$

Unfortunately this Hamiltonian cannot be put exactly into the action-angle variables like the Kepler Hamiltonian. Nevertheless $H_{\rm Schw}$ remains separable which means that by adopting a new evolution parameter λ defined as $\mathrm{d}\tau = r^2\mathrm{d}\lambda$ we can separate our Hamiltonian to a radial and an angular part. The parameter λ is a special case of the Carter-Mino time [48, 49] used for similar reasons in the Kerr spacetime. The Hamiltonian generating evolution in λ (see Appendix B) can be written as

$$H_{\rm Schw(\lambda)} = \frac{1}{2}r^2(g_S^{\mu\nu}p_\mu p_\nu + 1) = H_{\rm rad} + H_{\rm ang}\,, \tag{30}$$

where

$$H_{\rm rad} = \frac{1}{2}r^2\left[-\frac{1}{1-\frac{2M}{r}}p_t^2 + \left(1-\frac{2M}{r}\right)p_r^2 + 1\right], \tag{31}$$

is the radial part and

$$H_{\rm ang} = \frac{1}{2}\left(p_\theta^2 + \frac{p_\phi^2}{\sin^2\theta}\right)$$

is the angular part of the Hamiltonian.

Having separated our Hamiltonian we can now perform the transformation of the respective parts into action-angle coordinates. Since the metric does not depend on ϕ, the specific angular momentum $p_\phi = J_\phi = L_z$, i.e. the z-component of the angular momentum per unit mass, is already an action variable while for the θ part we have

$$J_\theta = \frac{1}{2\pi}\oint p_\theta \mathrm{d}\theta = L - J_\phi \tag{32}$$

where L is the specific total angular momentum. The action J_θ, thus, describes the part of angular momentum associated with non-equatorial motion.[1] The angular part of the Hamiltonian in the action-angle coordinates reads

$$H_{\rm ang} = \frac{1}{2}(J_\theta + J_\phi)^2\,. \tag{33}$$

The conjugate angles ψ_θ and ψ_ϕ to the actions J_θ and J_ϕ are obtained by canonical transformations, which can be found in Appendix B.

Let us now discuss the more difficult part, which involves the radial part $H_{\rm rad}$. In Eq. (31) we replace the p_t component of the four-momentum by the specific energy of the system $E = -p_t$ and we perform an expansion of the system around a stable circular orbit ($r = r_c, p_r = 0, E = E_c$). The perturbation parameter along which the expansion takes place is the distance from the circular orbit (something akin to the eccentricity). We assume that the relevant phase space coordinates deviate from those corresponding to the circular orbit like

$$r - r_{\rm c} = \mathscr{O}(\varepsilon) = p_r,\;\; E - E_c = \delta E = \mathscr{O}(\varepsilon^2)\,, \tag{34}$$

where ε is a book-keeping parameter telling us how big each term in our expansion is. Keep in mind that ε is not the perturbation parameter, after the computation we can just set it to $\varepsilon = 1$.

As the radius $r_{\rm c}$ is the minimum of the effective potential $V_{\rm eff} = H_{\rm rad}$ (see, e.g., [50]), the first post-circular approximation is the harmonic oscillator. After performing a transformation similar to Eq. (4) (details in Appendix B) we get the radial part in the form

$$H_{\rm rad} = K_0 + K_2\delta E + J_r\Omega_{rc} + R(\delta E, \psi_r, J_r)\,,$$

where K_0 and K_2 are constants and Ω_{rc} is the frequency of the respective harmonic oscillator (Appendix B).

Neglecting the remainder $R(\delta E, \psi_r, J_r) = \mathscr{O}(\varepsilon^3)$ we could accurately describe quasi-circular orbits. However we would like to describe nearly all the bound orbits with sufficient precision, which is why we implement the canonical perturbation theory as discussed in the next section.

C. Tidally perturbed orbits

In this section we finish the construction of the approximative Hamiltonian system of a Schwarzschild with a ring in action-angle variables. First, we perform two normalization steps, as described in Sec. II B. This implies finding two generating functions ω_1 and ω_2 to be used in the Lie operators acting on the Hamiltonian $H_{\rm Schw(\lambda)}$

$$\exp(\mathscr{L}_{\omega_2})\exp(\mathscr{L}_{\omega_1})H_{\rm Schw(\lambda)} = H_{\rm NS}(J_r, J_\theta) + \mathscr{O}(\varepsilon^5)\,. \tag{35}$$

For the purposes of our study we deem approximation (35) to be sufficiently describing geodesic bound orbits around a Schwarzschild black hole, hence, we can now add the ring-like source.

Our initial Hamiltonian (28) can be naturally split into the Schwarzschild and the ring part as in the case of the linearly perturbed metric (23)

$$H_{\rm tot} = H_{\rm Schw(\lambda)} + QH_{\rm ring}\,. \tag{36}$$

The perturbation part is then transformed into the same coordinates as the Schwarzschild part

$$\exp(\mathscr{L}_{\omega_2})\exp(\mathscr{L}_{\omega_1})H_{\rm ring} = H_{Q1} + \mathscr{O}(\varepsilon^5)\,, \tag{37}$$

while the terms of higher order in ε are neglected. And, thus, the total Hamiltonian reads:

$$H_{\rm tot} = H_{\rm NS}(J_r, J_\theta) + QH_{Q1}(\psi_r, \psi_\theta, J_r, J_\theta) + \mathscr{O}(\varepsilon^5)\,. \tag{38}$$

The last step in our computation is to solve the homological equation for the function χ in order to eliminate the angles from H_{Q1}.[2] After this, the total Hamiltonian reads

$$\begin{aligned} H_{\rm tot} &= H_{\rm NS}(J_r, J_\theta) + QZ_{Q1}(J_r, J_\theta) + \mathscr{O}(Q^2) \\ &= H_{\rm N}(J_r, J_\theta) + \mathscr{O}(Q^2)\,. \end{aligned} \tag{39}$$

[1] For equatorial motion $J_\theta = 0$.

[2] Note that now Q is the perturbation parameter.

The original coordinates can be expressed using the Lie operators as functions of the new ones as follows:

$$\begin{aligned} r &= \exp(Q\mathscr{L}_\chi)\exp(\mathscr{L}_{\omega_2})\exp(\mathscr{L}_{\omega_1})r_0 = U(\omega_1,\omega_2,\chi)r_0, \\ p_r &= U(\omega_1,\omega_2,\chi)p_{r_0}, \\ \theta &= \exp(Q\mathscr{L}_\chi)\theta_0,\ p_\theta = \exp(Q\mathscr{L}_\chi)p_{\theta_0},\ \phi = \exp(Q\mathscr{L}_\chi)\phi_0 \end{aligned} \tag{40}$$

where $r_0, p_{r_0}, \theta_0, p_{\theta_0}$ and ϕ_0 are the original transformation functions given by Eqs. (B8), (B3), and (B4) respectively in the Appendix B.

Solving the homological equation (13) at each step is quite straightforward, the relatively difficult part is finding the generating function χ as it involves two degrees of freedom. By expanding the Hamiltonians in parameters ε and Q, the h_1 part of H_{Q1}, which is to be eliminated, takes form

$$h_1 = \sum_{k,l} a_{kl} e^{i(k\psi_r + l\psi_\theta)}, \tag{41}$$

where the coefficients a_{kl} are in fact functions of actions. The solution to Eq. (13) can then be expressed as:

$$\chi = \sum_{k,l} a_{kl} \frac{1}{i(k\Omega_{r0} + l\Omega_{\theta 0})} e^{i(k\psi_r + l\psi_\theta)} \tag{42}$$

where $\Omega_{r0} = \frac{\partial H_{\rm NS}}{\partial J_r}$ and $\Omega_{\theta 0} = \frac{\partial H_{\rm NS}}{\partial J_\theta}$ are the frequencies of the Schwarzschild Hamiltonian obtained in (35). When close to resonances the denominator of this expression tends to zero which causes the remainder to be large, thus making the approximation less accurate as we shall see in the following section.

All the above-mentioned calculations involving canonical perturbation theory are included in the first part of our Supplemental material [51].

The analytical formulas (40) can be plotted for fixed values of the actions to illustrate our result (Fig. 1). It is clear from the figure that nonequatorial motion is no longer planar since the ring (located in the $z = 0$ plane) breaks the spherical symmetry of the Schwarzschild spacetime.

D. Validity of the approximation

Knowing the explicit expressions (40) and the approximate normal form of our Hamiltonian $H_{\rm N}(J_i)$ (39) we have essentialy perturbatively solved the original equations of motion given by $H_{\rm tot}$. First we fix three of our new set of conserved actions and then compute the fourth so that the normalization condition

$$H_N(J_r, J_\theta, \delta E, J_\phi) = 0 \tag{43}$$

is satisfied. Then, we find the frequencies of motion for our new angles as well as the relation between the coordinate time t and λ

$$\frac{\mathrm{d}\psi_i}{\mathrm{d}\lambda} = \frac{\partial H_N}{\partial J_i} = \Omega_i(J_r, J_\theta, \delta E, J_\phi), \qquad \frac{\mathrm{d}t}{\mathrm{d}\lambda} = \frac{\partial H_N}{\partial \delta E}. \tag{44}$$

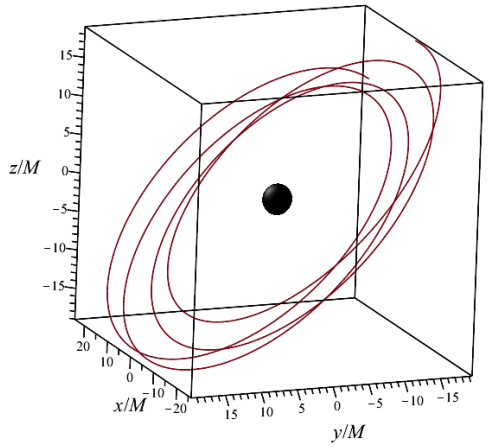

FIG. 1: Spatial representation of the approximate solution to the geodesic equation.
($Q = 10^{-6}M^{-2}, J_r = 0.1M, J_\theta = 1.5M, J_\phi = 3.5M$.)

Finally we substitute the angles and actions into Eq. (40) to get the coordinates and their respective momenta as explicit functions of Mino time λ ($x^i(\lambda), p_i(\lambda)$).

The evolution of the deviations from the exact solutions is governed by the remainder $R(\psi_i, J_i)$ which contains all the terms of the order $\mathscr{O}(\varepsilon^5)$ and $\mathscr{O}(Q^2)$. It is clear that the validity of our approximation not only depends on the fixed parameter Q describing the gravitational field of our ring-like source, but also on all our actions J_r, J_θ, J_ϕ. The most straightforward way to test our approximation would be plotting and comparing our analytical solution to the numerical one. This is certainly illustrating, nevertheless, it is still useful to have some quantity to describe the deviation from the exact solution. For this purpose we can use quantities denoted as δJ_i which measures the relative error of the conservations of actions. The errors δJ_i can then be expressed as functions of actions J_i in order to study the validity of the approximation (details are given in Appendix C).

In general, it can be said that the larger the value of J_r is the less accurate the approximation becomes. Apart from that the approximation depends on the perturbation parameter Q and the total angular momentum L. These two, however, are not independent from each other as increasing the value of L is equivalent to increasing Q. This comes from the fact that ν_Q is not bounded by a fixed value of Q instead we have $\nu_Q \sim r^2$ (see Eq. (24)) and $r \sim L^2$. We can, thus, conclude that it is the value of the quantity QL^4/M^2 that characterizes the entire strength of the perturbation.

The most general type of motion is the nonequatorial one, for which we have $J_\theta \neq 0$. The dependence of δJ_r and δJ_θ on actions is the same as in the equatorial motion, what is new

here, however, is the presence of the resonances of the form

$$k\Omega_{r0} + l\Omega_{\theta 0} = 0, \quad k,l \in \mathbb{Z} \setminus \{0\}, \tag{45}$$

where Ω_{r0} and $\Omega_{\theta 0}$ are the Schwarzschild frequencies. When the orbit is close to these resonances the approximation is no longer reliable because the denominators in the expression (42) tend to zero. These small divisors then prevent the convergence of the normalization procedure (see, e.g., [18]). In our particular case we only applied one generating function involving two degrees of freedom which is χ (used in Eq. (39)). From the analysis of the function χ and the Schwarzschild frequencies it becomes clear that the only ratios $\frac{\Omega_{r0}}{\Omega_{\theta 0}}$ present in the expansion (42) of χ are the $\frac{1}{2}$, $\frac{2}{3}$ and 1. This is illustrated in Fig. 2, which depicts the resonance sets in the J_r-J_θ plane for a fixed value of J_ϕ. It is important to stress at this point that even though Ω_{r0} depends explicitly on the total angular momentum $L = J_\theta + J_\phi$ it is correct to treat both angular actions separately. The same can be said for the dependence on Q, which is much more significant than that on L, e.g. smaller value of Q shifts the resonance curves to larger values of L. This dependence can be understood from the substitution of the energy from constraint (43) in Ω_{r0}, for which we have $E = E(Q,J_r,J_\theta,J_\phi) \neq E(Q,J_r,J_\theta+J_\phi)$. Namely, in total the expression for the radial frequency reads $\Omega_{r0} = \Omega_{r0}(E(Q,J_r,J_\theta,J_\phi),J_r,J_\theta+J_\phi)$.

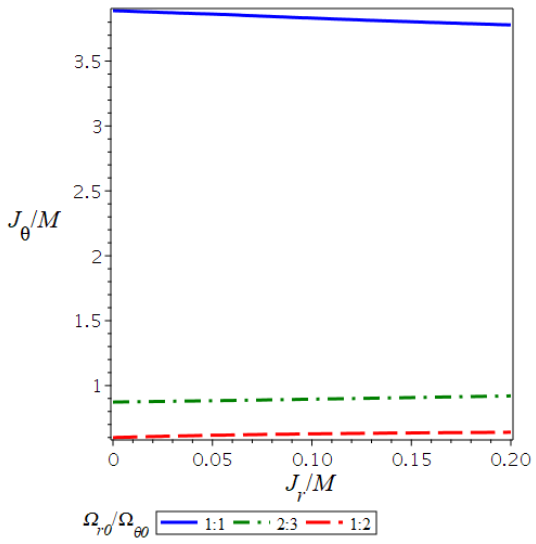

FIG. 2: Resonances in the J_r-J_θ plane for $J_\phi = 3M$, $Q = 10^{-5}M^{-2}$.

In summary, the geodesics obtained from the Hamiltonian (39) approximate the exact solution sufficiently well provided that the errors δJ_i are small and we are not close to resonances. However, the size of δJ_i unfortunately does not tell the whole story. The error in the evolution of (ψ_i, J_i) accumulates over time and it is up to us to fix the accuracy of the approximation, so the error does not become substantial for ε_m^{-1} number of orbital periods (Appendix C), where ε_m is the mass ratio.

To conclude this part we illustrate the advantages and the drawbacks of this approximation on the precession of near-circular and near-equatorial orbits. The precession rates of orbits can be expressed using fundamental frequencies as

$$\Delta\Psi_r = 2\pi\left(1 - \frac{\Omega_r}{\Omega_\phi}\right)\Big|_{r_{\rm circ.}}, \quad \Delta\Psi_\theta = 2\pi\left(1 - \frac{\Omega_\theta}{\Omega_\phi}\right)\Big|_{r_{\rm circ.}}, \tag{46}$$

where $\Delta\Psi_r$ corresponds to the pericenter precesion per one period of the azimuthal coordinate ϕ while similarly for the nodal precession rate we have defined the quantity $\Delta\Psi_\theta$. Of course the frequencies are functions of the integrals of motion (actions) and for a near-circular and near-equatorial orbits they need to be evaluated at $(\delta E = 0, J_r = 0, J_\theta = 0)$. The precession rates are then functions solely of J_ϕ, which itself can be expressed as a function of the radial coordinate r or rather the circular-orbit location r_c. For the Schwarzschild spacetime the precession rates (46) reduce to simple results

$$\Delta\Psi_r|_{Q=0} = 2\pi\left(1 - \sqrt{1 - \frac{6M}{r_c}}\right), \qquad \Delta\Psi_\theta|_{Q=0} = 0. \tag{47}$$

Alternatively instead of r_c we can use a dimensionless frequency parameter x

$$x = (M\Omega_\phi^{(t)})^{\frac{2}{3}}, \qquad \Omega_\phi^{(t)} = \Omega_\phi \frac{{\rm d}\lambda}{{\rm d}t}. \tag{48}$$

where the azimuthal frequency $\Omega_\phi^{(t)}$ is defined with respect to the coordinate time t (and not the Mino time λ). For Schwarzschild the frequency parameter x is related to r_c by a simple formula $x = \frac{M}{r_c}$. In the superposition background, however, the quantity x is not an injective function of r_c, which can be seen in Fig. 3 (right panel). The same figure also shows the relation between x and the precession rate of near-circular near-equatorial orbits. The nodal precession rate is in general nonzero and tends to grow (in absolute value) with the distance from the black hole, which can be expected since we are approaching the external gravitating ring that breaks the spherical symmetry. This in turn means that it is small for large values of x.

The left panel in Fig. 3 shows an unexpected divergence of $\Delta\Psi_r$ close to the innermost stable circular orbit[3] (ISCO). This we deem to be completely unphysical as it happens in the region dominated by the black hole. The divergence is in fact caused by the factor Ω_{rc}^{-1} present in the generating functions ω_1 and ω_2 as $\Omega_{rc} = 0$ for $r_c = 6M$. The sudden decrease of x at Schwarzschild ISCO is caused for the very same reason. One would be able to invert the function $x(r_c)$ if not for this unphysical part of the graph. The fact that $x(r_c)$ cannot be inverted can be also seen from the graph of $\Delta\Psi_r$. Actually, this effect is a consequence of the perturbation expansion we have chosen.

Had we used the expansion from the circular equatorial orbits of the superposition, the unphysical part of the graph

[3] Note that the ISCO is slightly shifted from the Schwarzschild value $r = 6M$

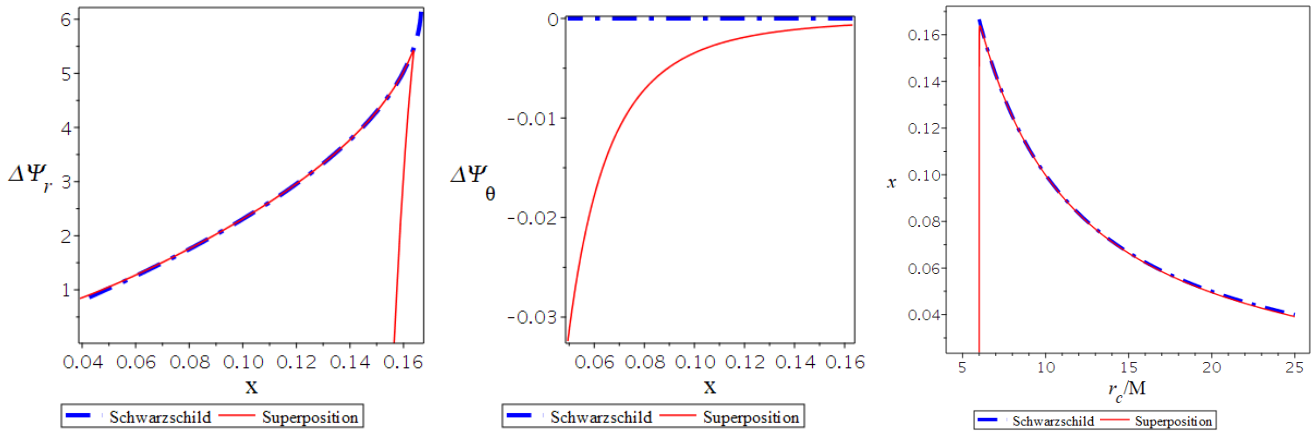

FIG. 3: The relation between pericenter (left panel) and the nodal (middle panel) precession rate of near-circular near-equatorial orbits and a frequency parameter x which itself can be expressed as a function of r_c (right panel), $Q = 10^{-6}M^{-2}$.

would not have appeared as the fundamental frequencies of the circular orbits are finite. In fact, we have checked this claim numerically. On the other hand the expansion scheme we have used is easier to perform due to the simplicity of the Schwarzschild Hamiltonian and it can also describe orbits with arbitrary inclination. Nevertheless, note that close to the Schwarzschild ISCO the approximation fails to describe the correct geodesic dynamics anyway.

IV. ADIABATIC INSPIRALS INTO THE PERTURBED BLACK HOLE

In this section we are going to present our model of an EMRI in the perturbed background field by using a basic prescription for radiation reaction. In the geodesic context we defined our Hamiltonian (28) using a four-momentum normalized to -1. To reintroduce the mass m of our "particle", we retain the original form of our Hamiltonian with actions and energy normalized to unit mass, $E = E^{(m)}/m$, $J_i = J_i^{(m)}/m$ instead of using the new coordinates $J_i^{(m)}$ and normalization to $-m^2$. Regardless of that, every not dimensionless quantity is still scaled with respect M as can be seen in all the figures presented in our paper.

A. Computation of the gravitational-wave fluxes

Following the general approach described in [4, 5], we can write down the equations of motion of an inspiraling binary as an expansion in the mass ratio ε_m

$$\frac{\mathrm{d}\psi_i}{\mathrm{d}t} = \Omega_i^{(t)}(\mathbf{J}) + \mathscr{O}(\varepsilon_m), \tag{49}$$

$$\frac{\mathrm{d}J_i}{\mathrm{d}t} = \varepsilon_m G_i(\psi,\mathbf{J}) + \mathscr{O}(\varepsilon_m^2), \tag{50}$$

where G_i corresponds to radiation reaction to the orbital elements of the binary, which drives the inspiral.

Note that the evolution equations (49) and (50) use the "internal" coordinate time t as the evolution parameter which is trivially redshifted by the ring with respect to the time T of observers at infinity. It is also important to note that equations (49) and (50) represent the action-angle form of the evolution equations of an exactly integrable system at zeroth order in ε_m. Examples of such integrable systems considered in the EMRI scenario include bound geodesics in the Schwarzschild or the Kerr spacetime. Using canonical perturbation theory, however, we can approximate a nearly-integrable system by an integrable one, which is exactly what we did in the previous section.

The global inspiral solution to the equations (49) and (50) can be naturally expanded with respect ε_m using a two-timescale analysis. The first timescale is the orbital timescale of the geodesic motion $\sim 1/\Omega$. Since this involves the evolution of the angles ψ_i these are then called "fast" variables. On the other hand we have the inspiral timescale which deals with the decays of the actions on the much longer time-scale $\varepsilon_M J/G \sim \varepsilon_M/\Omega$. The actions are thus classified as "slow" variables. The standard procedure is then to separate these two timescales by averaging the functions G_i over the fast variables, that is the n-dimensional invariant tori $\mathbb{T}^n$ parametrized by the angles

$$g_i(\mathbf{J}) = \langle G_i(\psi,\mathbf{J})\rangle = \int_{\mathbb{T}^n} G_i(\psi,\mathbf{J})\mathrm{d}^n\psi. \tag{51}$$

We can then first solve the equations for the actions

$$\frac{\mathrm{d}J_i(t)}{\mathrm{d}t} = \varepsilon_m g_i(\mathbf{J}(t)), \tag{52}$$

while the angles can be obtain simply by integrating the fundamental frequencies whose evolution is given by the actions $J_i(t)$

$$\psi_i(\tilde{t}) = \int_0^{\tilde{t}} \Omega_i^{(t)}(\mathbf{J}(t))\mathrm{d}t. \tag{53}$$

Let us now discuss the particular method we employed to compute the gravitational wave fluxes (i. e. the functions g_i).

For this purpose we employ the quadrupole formalism which is the lowest order expansion in the post-Newtonian theory. The limitations of this method in the context of strong-field inspirals are obvious, but this method is sufficient for a qualitative analysis, and computing the fluxes with more sophisticated approximations is beyond the scope of our work. Hence, the flux formulas for the energy and the components of the angular momentum read

$$\begin{aligned}\frac{\mathrm{d}E}{\mathrm{d}t} &= -\frac{1}{5}\sum_{i,j=1}^{3}\left\langle (\dddot{I}_{ij})^2 \right\rangle,\\ \frac{\mathrm{d}L_i}{\mathrm{d}t} &= -\frac{2}{5}\sum_{j,k,l=1}^{3}\varepsilon_{ijk}\left\langle (\dddot{I}_{jl}\ddot{I}_{kl}) \right\rangle,\end{aligned} \tag{54}$$

where the traceless quadrupole moment of our particle has the form

$$I^{ij}(t) = m\left(x^i(t)x^j(t) - \frac{1}{3}\delta^{ij}x^k(t)x_k(t)\right). \tag{55}$$

The functions $x^i(t)$ represent the orbital motion in Cartesian coordinates. Since we have so far used spherical-like coordinates, it is necessary to transform into the coordinates x^i, for that purpose we used the standard (flat-space) relations between spherical and Cartesian coordinates.

The time derivatives present in Eq. (54) are computed in accordance with the assumptions of the adiabatic approximation, which means that we neglect the change in the slow variables

$$\dot{x}^i(\psi(t),\mathbf{J}(t)) = \frac{\partial x^i}{\partial \psi_j}\frac{\mathrm{d}\psi_j}{\mathrm{d}t} + \frac{\partial x^i}{\partial J_j}\frac{\mathrm{d}J_j}{\mathrm{d}t} \approx \Omega_j^{(t)}\frac{\partial x^i}{\partial \psi_j}. \tag{56}$$

Note that the frequencies in the above expression are with respect to the coordinate time t while our fundamental frequencies are related to the Mino time λ. This is not a problem since we have

$$\Omega_j^{(t)} = \Omega_j\frac{\mathrm{d}\lambda}{\mathrm{d}t}. \tag{57}$$

In fact, we can exchange $t \to \lambda$ in higher time derivatives in the adiabatic approximation, since the differentiation of $\frac{\mathrm{d}\lambda}{\mathrm{d}t}$ with respect to time would involve terms proportional to the time derivatives of the actions which can be neglected as in (56). We can thus write

$$\frac{\mathrm{d}^n}{\mathrm{d}t^n} \approx \left(\frac{\mathrm{d}\lambda}{\mathrm{d}t}\right)^n\frac{\mathrm{d}^n}{\mathrm{d}\lambda^n}, \qquad \frac{\mathrm{d}t}{\mathrm{d}\lambda} = \frac{\partial H_N}{\partial \delta E}(\mathbf{J}). \tag{58}$$

We would like to remind the reader here that all quantities depending on $\mathbf{J}$ also depend on E (or δE), but the energy and the three actions are not independent, since we have the normalization condition (43), which is why the energy dependence is often omitted. Ideally the coordinate functions $x^i(t)$ can be expressed as a Fourier-like expansions, the same can then be said about expression for the fluxes. The averaging is then equivalent to eliminating all the oscillating terms

$$G = \sum_k c_{\mathbf{k}}(\mathbf{J})e^{i(\mathbf{k}\cdot\psi(t))} \;\Rightarrow\; \langle G\rangle = c_{\mathbf{0}}(\mathbf{J}), \qquad \mathbf{k}\in\mathbb{Z}^3. \tag{59}$$

In practice, however, this fully analytical approach is not feasible because of the number of terms present in Eq. (54), this is especially true for the non-equatorial orbits. It is easier to numerically integrate the function G. Instead of using a multidimensional integral like in Eq. (51), we can integrate over an orbit that densely covers the invariant torus determined by the actions. This implies integrating over a sufficiently long time Λ

$$\langle G(\psi(\lambda),\mathbf{J})\rangle = \frac{1}{\Lambda}\int_0^{\Lambda} G(\psi(\lambda),\mathbf{J})\mathrm{d}\lambda. \tag{60}$$

We now have to find the evolution equations for the three independent integrals of motion. It is straightforward to use the energy and the z-component of the angular momentum (J_ϕ) since we have explicit formulas (54) for them. The third integral will be the action J_θ, which can be written as

$$J_\theta = J_\theta^{(0)} - \delta J_\theta, \qquad \delta J_\theta = \{J_\theta,\chi_1\}, \tag{61}$$

where the action $J_\theta^{(0)}$ is the original one derived in Eq. (32), i.e. the one before applying the Lie operator with the generating function χ_1 (see Eq. (42)). Knowing the quadrupole fluxes for the angular momentum components we can compute its time derivative as

$$\frac{\mathrm{d}J_\theta^{(0)}}{\mathrm{d}t} = \frac{\vec{L}\cdot\frac{\mathrm{d}\vec{L}}{\mathrm{d}t}}{L} - \frac{\mathrm{d}J_\phi}{\mathrm{d}t}. \tag{62}$$

The components of the angular momentum can be expressed in terms of our original phase-space coordinates as

$$L_x = -\sin(\phi)\,p_\theta - \cos(\phi)\cot(\theta)J_\phi, \tag{63}$$

$$L_y = \cos(\phi)\,p_\theta - \sin(\phi)\cot(\theta)J_\phi. \tag{64}$$

Since the function δJ_θ contains only oscillating terms it does not survive the averaging

$$\left\langle\frac{\mathrm{d}J_\theta}{\mathrm{d}t}\right\rangle = \left\langle\frac{\mathrm{d}J_\theta^{(0)}}{\mathrm{d}t}\right\rangle, \qquad \left\langle\frac{\mathrm{d}\delta J_\theta}{\mathrm{d}t}\right\rangle \to 0 \quad \text{as} \quad \Lambda\to\infty. \tag{65}$$

We, thus, arrive at the complete system of evolution equations for three independent integrals of motion

These three equations can then be solved numerically, The radial action J_r can be computed at each time step from the normalization condition (43), while the evolution of the angles is given by the integrals of their respective fundamental frequencies (expression (53)).

The computation of the fluxes is detailed in the second Maple notebook [52]

V. RESULTS

In this section we present the adiabatic evolution in the general nonequatorial case. Let us again stress that our results provide essentially a qualitative analysis due to the approximative methods we have employed. This includes the particular values of various parameters we have used in this section,

some of which are not relevant for realistic EMRIs. For instance, the mass ratio we use in this section is $\varepsilon_m = 10^{-3}$, but it does not practically matter in our approach, since the equations which govern the adiabatic evolution of actions do not depend explicitly on the time; any other value of ε_m would just rescale the time variable in our solution. Another important parameter is the external quadrupole Q representing the ring, its value was intentionally chosen to be large ($Q = 10^{-6}$) in the following so that its effect is prominent in the figures. Lastly the ring radius is set to $r_{\rm r} = 50M$.

A. Phase shifts

First we investigate the effect of the ring perturbation on the orbital phases, i.e. the angle coordinates.

$$\delta\psi_i(t) = \psi_i(t) - \psi_i(t)|_{Q=0}, \tag{66}$$

where the evolution of $\psi_i(t)$ is given by Eq. (53). As the fundamental frequencies are in principle observable, it is natural to parametrize our orbits by them instead of the actions. Thus, we start from the same initial frequencies in both the perturbed and unperturbed cases so that not only $\delta\psi_i(0) = 0$, but also $\delta\dot{\psi}_i(0) = 0$. This matching of the frequencies was used in [53] in the case of a spinning particle in Kerr spacetime. Unlike in their case however our reference spacetime is Schwarzschild where $\Omega_\theta^{Schw} = \Omega_\phi^{Schw}$ which is a consequence of spherical symmetry while for $Q \neq 0$ we have $\Omega_\theta \neq \Omega_\phi$.

Despite the inability to match all the frequencies we can still choose two of them (in our case Ω_r and Ω_ϕ) and match them to their Schwarzschild counterparts for a fixed value of Q. In addition we can find the matches for different values of J_θ, which effectively means different initial inclinations.

When evolving the angles (or other quantities) one should use the proper time T of the asymptotic observer as an evolution parameter instead of t. This involves including the redshift factor z_{in} given by Eq. (22), which was absorbed into the coordinates t and r. This monopole term of the expansion (see Eq. (A6)) is necessary to include what is dynamically dominating; however, it is the non-constant quadrupole term which breaks the spherical symmetry. For this reason, we compute the phase shift only for the quadrupole perturbation which means using the definition (66) but with the time T. The phase shifts for the two matched frequencies are then plotted in the Fig. 4. It is interesting to see that $|\delta\psi_i|$ is smaller for larger values of J_θ, keep in mind that $\psi_i(t)|_{Q=0}$ remains unchanged as the evolution in the Schwarzschild spacetime does not depend on the initial inclination.

B. Inclination and eccentricity

When considering non-equatorial motion in a non-spherically symmetric spacetime one can study the behavior of orbital inclination i. This quantity is defined as an angle between the current orbital plane and the equatorial plane. In terms of our action variables it can be expressed as

$$i = \arccos\left(\frac{J_\phi}{J_\phi + J_\theta^{(0)}}\right). \tag{67}$$

When the quadrupole perturbation is present the inclination of a geodesic orbit does not remain constant, but it oscillates. The oscillations is caused by the δJ_θ term contained in $J_\theta^{(0)}$ (see Eq. (61)).

In order to show the effect of the adiabatic evolution on the inclination, it is useful to separate this geodesic evolution by defining the averaged inclination

$$I = \langle i \rangle = \arccos\left(\frac{J_\phi}{J_\phi + J_\theta}\right). \tag{68}$$

This inclination is constant in the geodesic case, since it depends only on the integrals of motion. During an inspiral, however, I shall evolve on the inspiral timescale and it is interesting to compare the geodesic oscillation of i to the EMRI evolution of I.

Fig. 5 shows that the geodesic oscillation of inclination for a particular choice of initial conditions is two orders of magnitude larger than the drift of I caused by radiation reaction. This difference of course depends on the strength of the perturbation (Q) which in our example is quite large, however, we must also keep in mind that the influence of the ring on the dynamics decreases as we approach the black hole. This is caused by the smaller value of the total angular momentum close to the ISCO, where the amplitude of the geodesic oscillations of i is comparable to the total change of I during the EMRI. The fact that the function I is decreasing is expected, as the dissipation of the constants of motion should, in principle, lead to the equatorial plane value $I = 0$. On the other hand, for some initial conditions we have seen an increase of I as the inspiral reaches ISCO, we should speculate this effect to be possibly of numerical origin. This growth is also present in the case of eccentricity, which can be defined as

$$e = \frac{r_1 - r_2}{r_1 + r_2} \tag{69}$$

where r_1 is the maximum value of $r(t)$ for a given geodesic while r_2 is the corresponding minimum. An evolution of the eccentricity during the inspiral can be seen in Fig. 6. The growth of eccentricity close to the ISCO was also found in other works (see, e.g., [54]), but it is questionable whether it has a physical significance or it is just a coordinate effect.

C. Waveforms

Finally let us conclude our results with some plots of gravitational waveforms. In our radiation-quadrupole formalism the components of the metric perturbation can be written in the TT gauge as

$$h_{ij}^{TT} = \frac{2}{R}\ddot{I}_{ij}^{TT}(u). \tag{70}$$

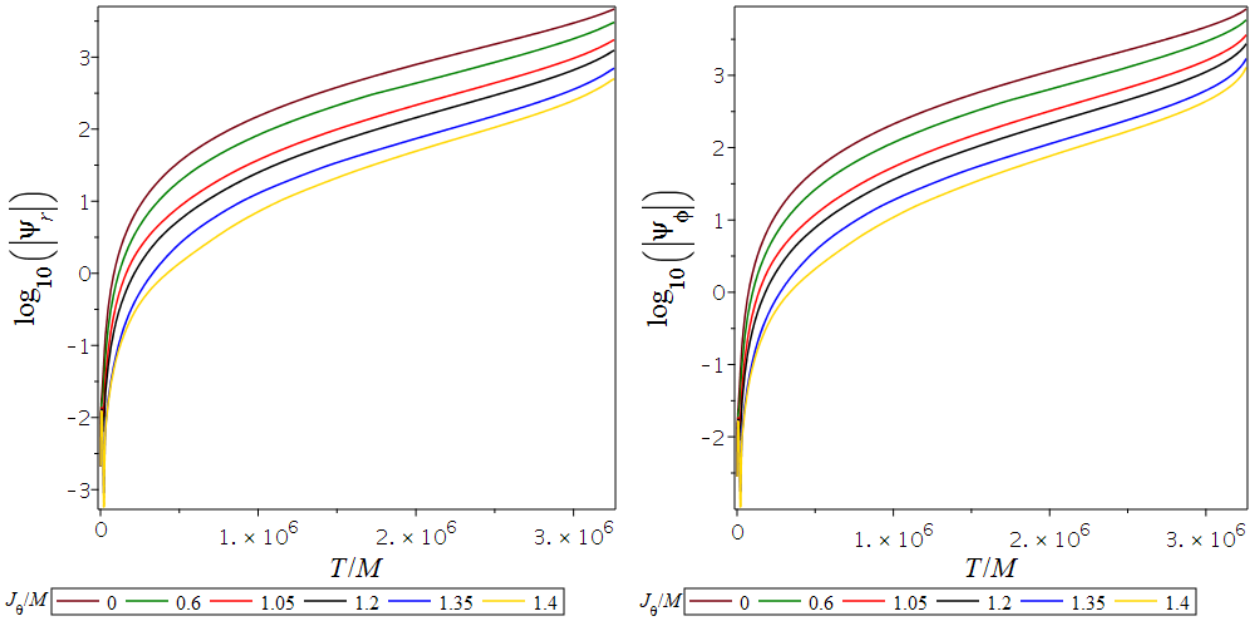

FIG. 4: The left panel shows logarithmic plot of the radial phase shift $\delta\psi_r(T)$ (left panel) and the right panel shows logarithmic plot of the azimuthal one $\delta\psi_\phi(T)$ for different initial value values of J_θ. For these plots we have used $Q = 10^{-6}M^{-2}$ and $r_{\rm r} = 50M$ while the initial frequencies are matched to the Schwarzschild ones with $J_r(0) = 0.1M, L(0) = 5M$. In all cases the phase shifts remain negative during the evolution.

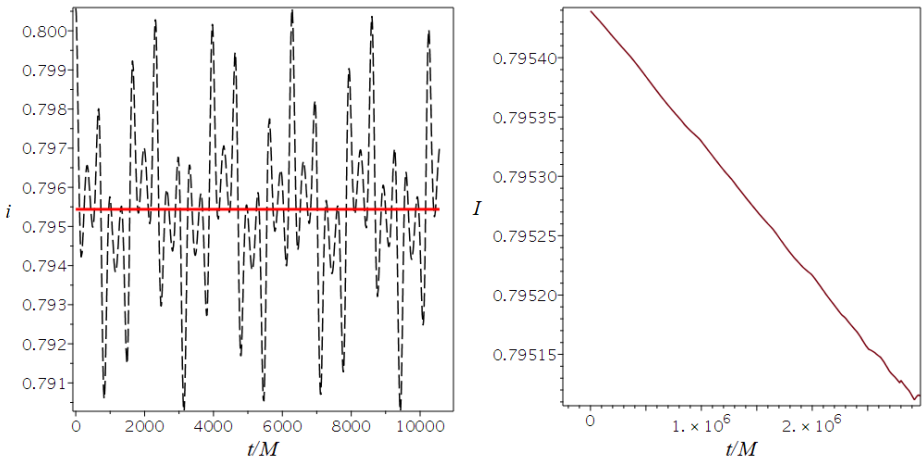

FIG. 5: The left panel shows the oscillation of the orbital inclination (dashed black) with respect to the averaged constant inclination (red continuous curve) for a geodesic orbit. The right panel shows the evolution of the averaged inclination I during the inspiral. For these plots we have used $Q = 10^{-6}M^{-2}, J_r(0) = 0.11M, J_\theta(0) = 1.5M, J_\phi(0) = 3.5M$.

where $u = T - R$ is the retarded time and I_{ij}^{TT} can be obtained from I_{ij} using projectors P_{ij} as

$$I_{ij}^{TT} = P_i^k I_{kl} P_j^l - \frac{1}{2} P_{ij} P^{kl} I_{kl}, \quad P_{ij} = \delta_{ij} - n_i n_j. \tag{71}$$

where n_i is a unit vector pointing from source to the observer. Naturally, as in the case of the calculations of the fluxes, I_{kl} depends on the coordinates of our particle. Their adiabatic evolution is determined by the evolution of actions and angles

$$x^i(T) = x^i(\psi(T), \mathbf{J}(T)). \tag{72}$$

In following we decompose h_{ij}^{TT} as it was done in [55]. For that we need to define two additional vectors $\vec{p}$ and $\vec{q}$ which together with $\vec{n}$ form an orthonormal basis in the 3D Euclidean space.

$$\vec{p} = \frac{\vec{n} \times \vec{L}}{|\vec{n} \times \vec{L}|}, \qquad \vec{q} = \vec{p} \times \vec{n}.$$

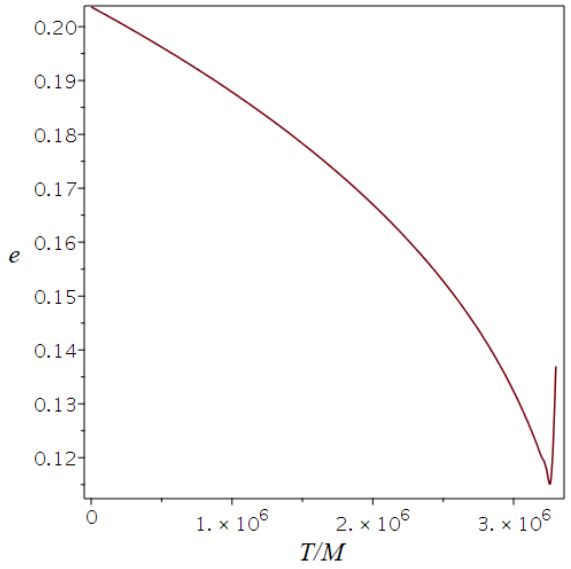

FIG. 6: The adiabatic evolution of eccentricity as a function of time T in the case of an equatorial inspiral ($Q = 10^{-6}M^{-2}, J_r(0) = 0.098M, J_\theta(0) = 0, J_\phi(0) = 5M.$).

The components of the angular momentum $\vec{L}$ can be computed from our action-angle variables as was the case in Eq. (63). The two independent polarizations have the form

$$h^{\{+,\times\}} = \frac{1}{2} H_{ij}^{\{+,\times\}} h_{TT}^{ij}, \tag{73}$$

where $H_{ij}^{\{+,\times\}}$ are defined as

$$H_{ij}^{+} = p_i p_j - q_i q_j, \qquad H_{ij}^{\times} = p_i q_j - q_i p_j. \tag{74}$$

With all the ingredients in place we can plot some waveforms. One such an example is depicted in Fig. 7, where we can see the component $h^{\{+\}}$ at the beginning of the evolution around $r \approx 21M$ and at a later time when $r \approx 9M$. Despite not having decomposed the signal into modes it is evident from the figure that the amplitudes and frequencies grow during the inspiral as expected.

In Fig. 8 we compare two waveforms to see the effect of the quadrupole term in our Hamiltonian. Although the initial radial and azimuthal frequencies are matched as above the phase shifts tend to grow rather quickly for the large value of Q we had chosen. In addition to that we can see a great difference in the amplitudes as well.

Throughout the Sec. V we included the value Q for each figure. It is, however, the quantity QL^4/M^2 which characterizes the strength of the quadrupole perturbation (as was mentioned in Sec. III D). The reason we chose Q over QL^4/M^2 is because the latter is not a constant during the inspiral as the total angular momentum L is a decreasing function of time. Namely, the effect of perturbation are lower as we get farther from the ring. On the other hand, it is important to point out that due to the expansion scheme we used the effects of the perturbation will again grow close to the Schwarzschild's ISCO, where the approximation breaks down as was demonstrated in Sec. III D for the precession rates. Nevertheless, the maximum strength of the perturbation is at the beginning of the adiabatic evolution, where we had $QL^2(0)/M^2 = 2.5 \cdot 10^{-5}$.

VI. SUMMARY AND DISCUSSION

This work showcased the advantages of using the Lie series approach to tackle the EMRI problem. For this purpose, we used a fairly complex background system, in which the primary black hole is surrounded by a matter distribution. In particular, we truncated a gravitating ring-like source up to its leading quadrupole term to introduce a quite generic tidal field around the primary Schwarzschild black hole. We wrote the Hamiltonian system providing the geodesic motion in the above background and noticed that it can be split into a part giving the motion in the Schwarzschild background, which correspond to an integrable system, and a perturbative part expressing the perturbation due to the quadrupole term.

By using the Mino time, we further split the Schwarzschild part of the Hamiltonian into a radial and angular part. After relatively simple manipulation we showed that the angular part can be written in action-angle variables, while for the radial part we perturbed it around a circular orbit as a harmonic oscillator and used a standard canonical transformation to get it into action-angle variables as well. To expand our scheme further from the circular orbit we applied two canonical transformations using the Lie series approach on the Schwarzschild part of the Hamiltonian. The same series of transformations were also applied on the perturbative part of the Hamiltonian leading to a Hamiltonian system in action-angle variables valid up to the separatrix. We tested the obtained Hamiltonian system and found that as far as we stay away from the $1:1$, $1:2$ and $2:3$ resonances between the radial and polar frequencies and ISCO the system is behaving sufficiently well.

After establishing the conservative part of our approximation to an EMRI, we addressed the dissipative part. To introduce dissipation into the system we used fluxes computed by the quadrupole formula. By averaging out the oscillating terms of the fluxes, we were able to provide the equations for the adiabatic radiative decay of the actions and evolve the inspirals. Since we derived the characteristic frequencies of the system, we were able to easily obtain the orbital phase shifts caused by the matter distribution. Moreover, we were able to compute the eccentricity and inclination changes as the inspiral evolves and the respective waveforms.

In the future, we would like to improve this work in a number of ways. First, it is necessary to also treat the case of a perturbed inspiral into a generic spinning black hole, that is the Kerr space-time. Second, our formalism breaks down near resonances, so we would like to implement a variant of the formalism sketched in Ref. [56] to evolve the inspiral faithfully through the resonances. Third, we have restricted to the case of a perfectly axially symmetric stationary cloud of matter. However, in astrophysically realistic scenarios the external matter sources are only approximately so. In particular, when the external matter consists of a halo of orbiting objects

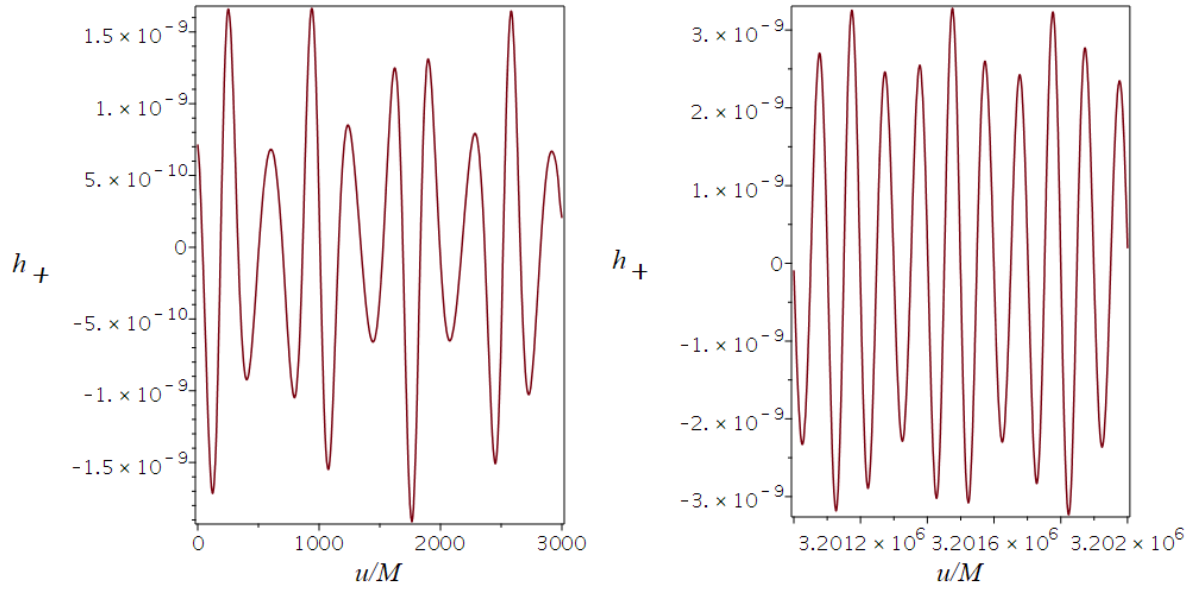

FIG. 7: The gravitational wave strain ($h^{\{+\}}$) of a single non-equatorial EMRI $(Q = 10^{-6}M^{-2}, J_r(0) = 0.11M, J_\theta(0) = 1.5M, J_\phi(0) = 3.5M)$ at two different instants: $u = 0$ (left panel) and $u = 3.2 \cdot 10^6 M$ (right panel)

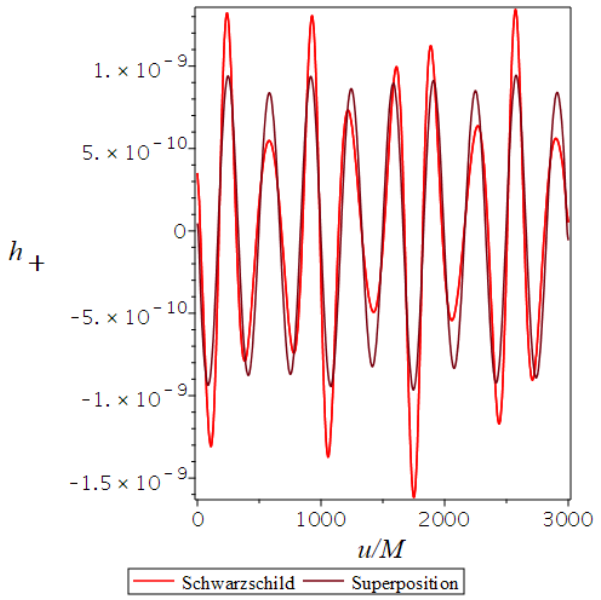

FIG. 8: A comparison of the unperturbed (red) and perturbed waveform for two matched frequencies in the equatorial plane $(Q = 10^{-6}M^{-2}, J_r(0) = 0.002M, J_\theta(0) = 0, J_\phi(0) = 5M.)$

such as stars, the largest deviations from stationarity and axisymmetry come from those objects that have either outstanding masses or are very close to the center [57]. Even though the question of resonances caused by such perturbations was already treated by Refs. [57, 58], we wish to systematically address the symmetry breaking within our formalism in the future.

The last, but perhaps most salient point we would like to improve upon in the future is the question of the gravitational-wave fluxes of energy and angular momentum. Rather obviously, it is necessary to include a strong-field flux computation using the Teukolsky equation or a similar method. However, the additional issue is that the tidal quadrupole perturbation also causes a perturbation to the Teukolsky equation. This perturbation then adds a Q-proportional contribution to the flux, which implies a comparable contribution to the inspiral phasing as the perturbation to the geodesics we have treated here. However, the perturbation makes the equation non-separable and will require a delicate analysis.

VII. ACKNOWLEDGEMENTS

LP and GLG have been supported by the fellowship Lumina Quaeruntur No. LQ100032102 of the Czech Academy of Sciences. VW was supported by by European Union's Horizon 2020 research and innovation programme under grant agreement No 894881. LP acknowledges support by the project "Grant schemes at CU" (reg.no.CZ.02.2.69/0.0/0.0/19 073/0016935).

[1] Stanislav Babak, Jonathan Gair, Alberto Sesana, Enrico Barausse, Carlos F. Sopuerta, Christopher P. L. Berry, Emanuele Berti, Pau Amaro-Seoane, Antoine Petiteau, and Antoine Klein.

Science with the space-based interferometer LISA. V. Extreme mass-ratio inspirals. *Phys. Rev. D*, 95(10):103012, May 2017.

[2] Leor Barack and Adam Pound. Self-force and radiation reaction in general relativity. *Reports on Progress in Physics*, 82(1):,, January 2019.

[3] Adam Pound and Barry Wardell. Black hole perturbation theory and gravitational self-force. *arXiv e-prints*, page arXiv:2101.04592, January 2021.

[4] Tanja Hinderer and Éanna É. Flanagan. Two-timescale analysis of extreme mass ratio inspirals in kerr spacetime: Orbital motion. *Phys. Rev. D*, 78:064028, Sep 2008.

[5] Jirair K Kevorkian and Julian D Cole. *Multiple scale and singular perturbation methods*, volume 114. Springer Science & Business Media, 2012.

[6] Vladimir I Arnold, Valery V Kozlov, and Anatoly I Neishtadt. *Mathematical aspects of classical and celestial mechanics*, volume 3. Springer Science & Business Media, 2007.

[7] W. Schmidt. Celestial mechanics in Kerr spacetime. *Classical and Quantum Gravity*, 19(10):2743–2764, May 2002.

[8] Steve Drasco and Scott A. Hughes. Rotating black hole orbit functionals in the frequency domain. *Phys. Rev. D*, 69(4):044015, February 2004.

[9] Saul A. Teukolsky. Perturbations of a rotating black hole. 1. Fundamental equations for gravitational electromagnetic and neutrino field perturbations. *Astrophys. J.*, 185:635–647, 1973.

[10] Maarten van de Meent. Conditions for sustained orbital resonances in extreme mass ratio inspirals. *Phys. Rev. D*, 89(8):084033, April 2014.

[11] Alexandre Le Tiec, Luc Blanchet, and Bernard F. Whiting. The First Law of Binary Black Hole Mechanics in General Relativity and Post-Newtonian Theory. *Phys. Rev. D*, 85:064039, 2012.

[12] Alexandre Le Tiec. First Law of Mechanics for Compact Binaries on Eccentric Orbits. *Phys. Rev. D*, 92(8):084021, 2015.

[13] Ryuichi Fujita, Soichiro Isoyama, Alexandre Le Tiec, Hiroyuki Nakano, Norichika Sago, and Takahiro Tanaka. Hamiltonian Formulation of the Conservative Self-Force Dynamics in the Kerr Geometry. *Class. Quant. Grav.*, 34(13):134001, 2017.

[14] Soichiro Isoyama, Ryuichi Fujita, Hiroyuki Nakano, Norichika Sago, and Takahiro Tanaka. "Flux-balance formulae" for extreme mass-ratio inspirals. *PTEP*, 2019(1):013E01, 2019.

[15] Ryuichi Fujita and Wataru Hikida. Analytical solutions of bound timelike geodesic orbits in Kerr spacetime. *Class. Quant. Grav.*, 26:135002, 2009.

[16] Maarten van de Meent. Analytic solutions for parallel transport along generic bound geodesics in Kerr spacetime. *Class. Quant. Grav.*, 37(14):145007, 2020.

[17] Vojtěch Witzany. Action-angle coordinates for black-hole geodesics I: Spherically symmetric and Schwarzschild. *arXiv e-prints*, page arXiv:2203.11952, March 2022.

[18] C. Efthymiopoulos. Canonical perturbation theory; stability and diffusion in Hamiltonian systems: applications in dynamical astronomy. *Workshop Series of the Asociacion Argentina de Astronomia*, 3:3–146, January 2011.

[19] John R Cary. Lie transform perturbation theory for Hamiltonian systems. *Physics Reports*, 79(2):129–159, 1981.

[20] V. I. Arnold. Proof of a Theorem of A. N. KOLMOGOROV on the Invariance of Quasi-Periodic Motions Under Small Perturbations of the Hamiltonian. *Russian Mathematical Surveys*, 18(5):9–36, October 1963.

[21] Jürgen Moser. New aspects in the theory of stability of hamiltonian systems. *Communications on Pure and Applied Mathematics*, 11(1):81–114, 1958.

[22] George Contopoulos. *Order and chaos in dynamical astronomy*. Astronomy and astrophysics library. Springer Science and Business Media, New York, 2002.

[23] Alessandro Morbidelli. *Modern celestial mechanics : aspects of solar system dynamics*. Advances in astronomy and astrophysics (Taylor and Francis) ;. CRC Press; 1st edition, London ; New York, 2002.

[24] Nadine Neumayer, Anil Seth, and Torsten Böker. Nuclear star clusters. *The Astronomy and Astrophysics Review*, 28(1):1–75, 2020.

[25] Reinhard Genzel, Frank Eisenhauer, and Stefan Gillessen. The galactic center massive black hole and nuclear star cluster. *Reviews of Modern Physics*, 82(4):3121, 2010.

[26] Otto A. Hannuksela, Kenny C. Y. Ng, and Tjonnie G. F. Li. Extreme dark matter tests with extreme mass ratio inspirals. *Phys. Rev. D*, 102(10):103022, November 2020.

[27] Caio F. B. Macedo, Paolo Pani, Vitor Cardoso, and Luís C. B. Crispino. Into the Lair: Gravitational-wave Signatures of Dark Matter. *Astrophys. J.*, 774(1):48, September 2013.

[28] Miguel C. Ferreira, Caio F. B. Macedo, and Vitor Cardoso. Orbital fingerprints of ultralight scalar fields around black holes. *Phys. Rev. D*, 96(8):083017, October 2017.

[29] David Merritt. *Dynamics and evolution of galactic nuclei*, volume 23. Princeton University Press, 2013.

[30] Werner M. Vieira and Patricio S. Letelier. Chaos around a Hénon-Heiles-Inspired Exact Perturbation of a Black Hole. *Phys. Rev. Lett.*, 76(9):1409–1412, February 1996.

[31] Alessandro P. S. de Moura and Patricio S. Letelier. Chaos and fractals in geodesic motions around a nonrotating black hole with halos. *Phys. Rev. E*, 61(6):6506–6516, June 2000.

[32] Werner M Vieira and Patricio S Letelier. Relativistic and newtonian core-shell models: analytical and numerical results. *The Astrophysical Journal*, 513(1):383, 1999.

[33] O Semerák and Petra Suková. Free motion around black holes with discs or rings: between integrability and chaos–i. *Monthly Notices of the Royal Astronomical Society*, 404(2):545–574, 2010.

[34] O Semerák and Petra Suková. Free motion around black holes with discs or rings: between integrability and chaos–ii. *Monthly Notices of the Royal Astronomical Society*, 425(4):2455–2476, 2012.

[35] P. Suková and O. Semerák. Free motion around black holes with discs or rings: between integrability and chaos - III. *"Monthly Notices of the Royal Astronomical Society"*, 436(2):978–996, December 2013.

[36] Vojtěch Witzany, Oldřich Semerák, and Petra Suková. Free motion around black holes with discs or rings: between integrability and chaos–iv. *Monthly Notices of the Royal Astronomical Society*, 451(2):1770–1794, 2015.

[37] L Polcar, P Suková, and O Semerák. Free motion around black holes with disks or rings: Between integrability and chaos–v. *The Astrophysical Journal*, 877(1):16, 2019.

[38] L Polcar and O Semerák. Free motion around black holes with discs or rings: Between integrability and chaos. vi. the melnikov method. *Physical Review D*, 100(10):103013, 2019.

[39] S. Wiggins. *Introduction to Applied Nonlinear Dynamical Systems and Chaos*. Second Edition. Springer-Verlag New York, Bristol, 2000.

[40] A. J. Lichtenberg and M. A. Lieberman. *Regular and Chaotic Dynamics*. Second Edition. Springer-Verlag New York, New York, 1983.

[41] A. Deprit. Canonical transformations depending on a small parameter. *Celestial Mechanics*, 1:12–30, 1969.

[42] Hans Thirring. Über die Wirkung rotierender ferner Massen in der Einsteinschen Gravitationstheorie. *Physikalische Zeitschrift*, 19:33, 1918.

[43] B. Mashhoon, F. W. Hehl, and D. S. Theiss. On the Gravitational effects of rotating masses - The Thirring-Lense Papers. *Gen. Rel. Grav.*, 16:711–750, 1984.

[44] Clifford M. Will. Perturbation of a Slowly Rotating Black Hole by a Stationary Axisymmetric Ring of Matter. I. Equilibrium Configurations. *Astrophys. J.*, 191:521–532, 1974.

[45] P. Čížek and O. Semerák. Perturbation of a Schwarzschild black hole due to a rotating thin disc. *Astrophys. J. Suppl.*, 232:14, 2017.

[46] Hermann Weyl. Zur Gravitationstheorie. *Annalen der Physik*, 359(18):117–145, 1917.

[47] Jerry B. Griffiths and Jiří Podolský. *Exact Space-Times in Einstein's General Relativity*. Cambridge Monographs on Mathematical Physics. Cambridge University Press, Cambridge, 2009.

[48] Brandon Carter. Global structure of the Kerr family of gravitational fields. *Phys. Rev.*, 174:1559–1571, 1968.

[49] Yasushi Mino. Perturbative approach to an orbital evolution around a supermassive black hole. *Physical Review D*, 67(8), Apr 2003.

[50] Subrahmanyan Chandrasekhar. *The mathematical theory of black holes*. 1985.

[51] L Polcar. Canonical perturbation theory. `https://github.com/LukasPolcar/EMRI-perturbation-theory`. Maple notebook.

[52] L Polcar. Gravitational-wave fluxes. `https://github.com/LukasPolcar/EMRI-perturbation-theory`. Maple notebook.

[53] Niels Warburton, Thomas Osburn, and Charles. R. Evans. Evolution of small-mass-ratio binaries with a spinning secondary. *Phys. Rev. D*, 96:084057, Oct 2017.

[54] Ollie Burke, Jonathan Gair, and Joan Simón. Transition from inspiral to plunge: A complete near-extremal trajectory and associated waveform. *Physical Review D*, 101(6), Mar 2020.

[55] Christopher J Moore, Alvin J K Chua, and Jonathan R Gair. Gravitational waves from extreme mass ratio inspirals around bumpy black holes. *Classical and Quantum Gravity*, 34(19):195009, Sep 2017.

[56] Georgios Lukes-Gerakopoulos and Vojtěch Witzany. *Nonlinear Effects in EMRI Dynamics and Their Imprints on Gravitational Waves*, pages 1–44. Springer Singapore, Singapore, 2020.

[57] Béatrice Bonga, Huan Yang, and Scott A. Hughes. Tidal Resonance in Extreme Mass-Ratio Inspirals. *Phys. Rev. Lett.*, 123(10):101103, September 2019.

[58] Priti Gupta, Béatrice Bonga, Alvin JK Chua, and Takahiro Tanaka. Importance of tidal resonances in extreme-mass-ratio inspirals. *Physical Review D*, 104(4):044056, 2021.

Appendix A: Derivation of perturbed black-hole field

To derive the tidally perturbed black hole field, we use the formulas for black hole fields surrounded by light ring-like sources at finite distances as recently presented by Čížek & Semerák [45] (see also the seminal work of Will [44]). They start from metrics of the form

$$\begin{aligned} \mathrm{d}s^2 = &-e^{2\nu}\mathrm{d}T^2 + R^2\left(1-\frac{M^2}{4R^2}\right)^2 e^{-2\nu}(\mathrm{d}\phi-\omega\mathrm{d}T)^2 \\ &+ e^{2\zeta-2\nu}(\mathrm{d}R^2+R^2\mathrm{d}\theta^2)\,, \end{aligned} \tag{A1}$$

where T,ϕ,R,θ are coordinates of the Carter-Thorne-Bardeen type, and ν,ω,ζ are unknown metric functions. The zeroth-order solution (isolated static black hole) is presented in this case by the metric functions

$$\nu_0 = \ln\left(\frac{2R-M}{2R+M}\right),\ \omega_0 = 0\,,\ \zeta_0 = \ln\left(1-\frac{M^2}{4R^2}\right). \tag{A2}$$

It can then be easily seen that R is the isotropic radius at zeroth order. The linear perturbations $\nu = \nu_0+\delta\nu$, $\omega = \omega_0+\delta\omega$ by a rotating ring are then obtained by using Green's functions $\mathscr{G}^\nu$ and $\mathscr{G}^\omega$ in equations (66) and (75) of Čížek & Semerák [45]. Specifically, for a ring of Komar mass $\mathscr{M}_\mathrm{r}$ and angular momentum $\mathscr{J}_\mathrm{r}$ we obtain

$$\delta\nu = -\frac{2\mathscr{M}_\mathrm{r}}{M}\mathscr{G}^\nu(x(R),\theta,x(R_\mathrm{r}),\pi/2)\,, \tag{A3}$$

$$\delta\omega = -\frac{8\mathscr{J}_\mathrm{r}}{M^3}\mathscr{G}^\omega(x(R),\theta,x(R_\mathrm{r}),\pi/2)\,, \tag{A4}$$

$$x(R) = \frac{R}{M}\left(1+\frac{M^2}{4R^2}\right). \tag{A5}$$

where $x(R)$ is the auxiliary dimensionless radius used by Čížek & Semerák. The perturbation to $\zeta = \zeta_0+\delta\zeta$ is then obtained by a particular line integral involving the gradient of ν. We expand the Green's function in the limit $R_\mathrm{r} \gg R \sim M$ to obtain

$$\begin{aligned} \mathscr{G}^\nu = &\frac{M}{2R_\mathrm{r}} \\ &+ \frac{M\left[(M^2+4R^2)^2-(3M^4+8M^2R^2+48R^2)\cos^2\theta\right]}{128R^2R_\mathrm{r}^3} \\ &+ \mathscr{O}(R_\mathrm{r}^{-4})\,, \end{aligned} \tag{A6}$$

$$\mathscr{G}^\omega = -\frac{M^3}{4R_\mathrm{r}^3}+\frac{3M^4}{4R_\mathrm{r}^4}+\mathscr{O}(R_\mathrm{r}^{-5})\,. \tag{A7}$$

Note that we consider the $\mathscr{G}^\omega$ expansion to order R_r^{-4} since it enters the metric multiplied by $\mathscr{J}_\mathrm{r} \sim R_\mathrm{r}^{1/2}$. Finally, we obtain for $\delta\zeta$

$$\delta\zeta = -\frac{\mathscr{M}_\mathrm{r}M\sin^2\theta\left(M^2+4R^2\right)}{4RR_\mathrm{r}^3}+\mathscr{O}(R_\mathrm{r}^{-4})\,. \tag{A8}$$

Now the transformation to the local Schwarzschild-like coordinates in which the metric attains the form (23) is given by

$$r = R\left(1+\frac{M}{2R}\right)^2(1+z_\mathrm{in}),\ \vartheta=\theta\,, \tag{A9}$$

$$t-t_0 = T(1-z_\mathrm{in})\,,\varphi-\varphi_0 = \phi-\Omega_\mathrm{in}T\,, \tag{A10}$$

where t_0, φ_0 are integration constants and the redshift and angular-velocity factors are

$$z_{\rm in} = \frac{\mathscr{M}_{\rm r}}{R_{\rm r}} = \frac{\mathscr{M}_{\rm r}}{r_{\rm r}}\left(1+\frac{M}{r_{\rm r}}\right) + \mathscr{O}(r_{\rm r}^{-3}), \tag{A11}$$

$$\Omega_{\rm in} = \frac{2\mathscr{J}_{\rm r}}{R_{\rm r}^3}\left(1-\frac{3M}{R_{\rm r}}\right) = \frac{2\mathscr{J}_{\rm r}}{r_{\rm r}^3} + \mathscr{O}(r_{\rm r}^{-5}). \tag{A12}$$

Appendix B: Schwarzschild in action-angle coordinates

In order to find the action-angle form of the Schwarzschild Hamiltonian we first have to separate its radial and angular parts which can be done by replacing the proper time as an evolution parameter using $\mathrm{d}\tau = r^2\mathrm{d}\lambda$. One can easily make sure that the Hamiltonian $H_{(\lambda)} = \frac{1}{2}r^2(2\,H+1) = \frac{1}{2}r^2(g^{\mu\nu}p_\mu p_\nu + 1)$ is the generator of evolution in λ

$$\begin{aligned}
\frac{dx^\mu}{d\lambda} &= \frac{\partial H_{(\lambda)}}{\partial p_\mu} = r^2\frac{\partial H}{\partial p_\mu} = r^2\frac{dx^\mu}{d\tau}, \\
\frac{dp_\theta}{d\lambda} &= -\frac{\partial H_{(\lambda)}}{\partial \theta} = -r^2\frac{\partial H}{\partial \theta} = r^2\frac{dp_\theta}{d\tau}, \\
\frac{dp_r}{d\lambda} &= -\frac{\partial H_{(\lambda)}}{\partial r} = -r^2\frac{\partial H}{\partial r} - r(2\,H+1) = r^2\frac{dp_r}{d\tau}.
\end{aligned}$$

The angular part of the Hamiltonian takes a simple form (33) with actions $J_\phi = p_\phi$ and $J_\theta = L - J_\phi$ (derived using the integral (32)) the angles can be found using generating function of second kind which is a solution to the corresponding Hamilton-Jacobi equation. We can take advantage of the separability of the Hamilton-Jacobi equation and write the generating function as

$$S = S_\theta(\theta, J_\theta, J_\phi) + S_\phi(\phi, J_\phi) = \int p_\theta(\theta, J_\theta, J_\phi)\mathrm{d}\theta + \phi J_\phi. \tag{B1}$$

From here it is straightforward to get the angles conjugated to actions J_θ and J_ϕ

$$\psi_\theta = \frac{\partial S}{\partial J_\theta}, \qquad \psi_\phi = \frac{\partial S}{\partial J_\phi}. \tag{B2}$$

These expressions can then be inverted to express the old coordinates in terms of the new. For the coordinates θ and p_θ we have

$$\theta = \pi - \arccos\left(\sqrt{1 - \frac{{J_\phi}^2}{\left(J_\phi + J_\theta\right)^2}}\sin(\psi_\theta)\right), \tag{B3}$$

$$p_\theta = \cos(\psi_\theta)\sqrt{\frac{J_\theta\left(J_\theta^3 + 4J_\theta^2 J_\phi + 5J_\theta J_\phi^2 + 2J_\phi^3\right)}{J_\theta^2\cos^2(\psi_\theta) + 2J_\theta J_\phi\cos^2(\psi_\theta) + J_\phi^2}},$$

while the coordinate ϕ can be written as

$$\phi = \psi_\phi - \psi_\theta + \frac{1}{2}\arctan\left(\frac{J_\phi\left(J_\phi + J_\theta\right)\sin(2\,\psi_\theta)}{\cos^2(\psi_\theta)\left(J_\theta^2 + 2J_\theta J_\phi + 2J_\phi^2\right) - J_\phi^2}\right). \tag{B4}$$

Of course one has to keep in mind that in this expression it is necessary to add factor $\pi/2$ each time the denominator inside arctan is zero so that the transformation is continuous. It is also worth noting that in the equatorial plane ($J_\theta = 0$) the equation (B4) is reduced to $\phi = \psi_\phi$.

The following step is to write the radial Hamiltonian (31) as a Taylor expansion from a stable circular orbit. The location of a circular orbit ($r = r_c$) is related to the total angular momentum $L = J_\theta + J_\phi$ as

$$r_c = \frac{L}{2M}\left(L + \sqrt{L^2 - 12M^2}\right). \tag{B5}$$

Our expansion parameter is ε. The order of ε is for the relevant quantities given by (34). In particular when expanding the energy one obtains

$$\begin{aligned}
E = E_c + \delta E &= E_c + \frac{\partial E}{\partial r}\Big|_{\substack{r=r_{\rm c}\\ p_r=0}}(r - r_{\rm c}) + \frac{\partial E}{\partial p_r}\Big|_{\substack{r=r_{\rm c}\\ p_r=0}}p_r + \mathscr{O}(\varepsilon^2) \\
&= E_c + \mathscr{O}(\varepsilon^2),
\end{aligned} \tag{B6}$$

where the partial derivatives vanish since our stable circular orbit has minimal energy, thus, we get $\delta E = \mathscr{O}(\varepsilon^2)$. The energy of the circular orbit is then

$$E_c = \frac{r_c - 2M}{\sqrt{r_c^2 - 3Mr_c}}. \tag{B7}$$

We can now expand the radial Hamiltonian, identify the harmonic oscillator terms and transform them into action-angle coordinates

$$\begin{aligned}
r &= r_{\rm c} + \sqrt{\frac{2J_r {r_{\rm c}}^2}{\Omega_{rc}}\left(1 - \frac{2M}{r_{\rm c}}\right)}\sin(\psi_r), \\
p_r &= \sqrt{\frac{2J_r\Omega_{rc}}{{r_{\rm c}}^2\left(1 - \frac{2M}{r_{\rm c}}\right)}}\cos(\psi_r),
\end{aligned} \tag{B8}$$

where the frequency of the harmonic oscillator can be written as

$$\Omega_{rc} = \sqrt{\frac{M(r_c - 6M)\,r_c}{r_c - 3M}}. \tag{B9}$$

After performing the transformation we arrive at the radial Hamiltonian in the form

$$\begin{aligned}
H_{\rm rad} = \frac{1}{2}\frac{M{r_{\rm c}}^2}{3M - r_{\rm c}} - \frac{{r_{\rm c}}^3\delta E}{\sqrt{r_{\rm c}\,(r_{\rm c} - 3M)}} + J_r\Omega_{rc} \\
+ R(\delta E, \psi_r, J_r).
\end{aligned} \tag{B10}$$

We can now employ the canonical perturbation theory to get farther from the circular orbit and closer to the separatrix. In our case we applied the Lie operator twice

$$\exp(\mathscr{L}_{\omega_2})\exp(\mathscr{L}_{\omega_1})H_{\rm Schw(\lambda)} = H_{NS}(J_r, J_\theta) + \mathscr{O}(\varepsilon^5). \tag{B11}$$

For instance the first generating function ω_1 can be written as

$$\omega_1 = \frac{4\sqrt{2}}{3\left(-r_c+2M\right)^4\Omega^2 f r_c}\Bigg\{\left(\left(-\frac{r_c}{2}+M\right)^4(M-r_c)\Omega^2+\frac{{r_c}^4 f^2 M^3 {E_c}^2}{4}\right)J_r e^{-3i\psi_r}+$$
$$+\left(3\left(-\frac{1}{2}r_c+M\right)^4(M-r_c)J_r\Omega^2-9{r_c}^4 f\left(-\frac{1}{2}r_c+M\right)^2\delta E\left(M-\frac{1}{3}r_c\right)E_c\Omega-\frac{9{r_c}^4 f^2 J_r M^3 {E_c}^2}{4}\right)e^{-i\psi_r}+$$
$$+\left(\left(-\frac{r_c}{2}+M\right)^4(M-r_c)\Omega^2+\frac{{r_c}^4 f^2 M^3 {E_c}^2}{4}\right)J_r e^{3i\psi_r}+$$
$$+3\left(\left(-\frac{1}{2}r_c+M\right)^4(M-r_c)J_r\Omega^2-3{r_c}^4 f\left(-\frac{1}{2}r_c+M\right)^2\delta E\left(M-\frac{1}{3}r_c\right)E_c\Omega-\frac{3}{4}{r_c}^4 f^2 J_r M^3 {E_c}^2\right)e^{i\psi_r}\Bigg\}\sqrt{\frac{J_r f}{\Omega}},$$

where f is the factor Schwarzschild factor

$$f = 1-\frac{2M}{r_c}. \tag{B12}$$

The normal form of the Schwarzschild Hamiltonian reads up to the $\mathcal{O}(\varepsilon^5)$ terms

$$H_{NS} = \frac{M{r_c}^2}{6M-2r_c}-\frac{{r_c}^3\delta E}{\sqrt{|r_c\left(3M-r_c\right)|}}+J_r\Omega+\frac{1}{2}\left(J_\theta+L_z\right)^2+$$
$$+\frac{1}{4r_c\Omega^4\left(-r_c+2M\right)^5}\Bigg\{48\left({J_r}^2M^2-\frac{4}{3}Mr_c{J_r}^2+\frac{2}{3}{r_c}^2\left(\delta E^2{r_c}^2+{J_r}^2\right)\right)\left(-\frac{r_c}{2}+M\right)^4\Omega^4-$$
$$-192E_c\left(M^2+\frac{1}{3}Mr_c-\frac{1}{6}{r_c}^2\right){r_c}^3\left(-\frac{r_c}{2}+M\right)^3\delta E J_r\Omega^3-$$
$$-96\left(-3M^2{r_c}^4\delta E^2+2Mr_c{}^5\delta E^2-\frac{1}{3}{r_c}^6\delta E^2+{J_r}^2M^4-2M^3r_c{J_r}^2\right){E_c}^2{r_c}^2\left(-\frac{r_c}{2}+M\right)^2\Omega^2-$$
$$-576{E_c}^3M^3\left(M-\frac{r_c}{3}\right){r_c}^5\left(-\frac{r_c}{2}+M\right)\delta E J_r\Omega+240M^6{E_c}^4{r_c}^4{J_r}^2\Bigg\}+\mathcal{O}(\varepsilon^5).$$

Appendix C: Limits of the approximation

In the flow generated by H_N the actions J_r and J_θ are conserved, which is not true in the case of the full Hamiltonian H. By inverting the coordinate transformations (40) we can express the actions in terms of our original phase space coordinates. This enables us to evolve actions J_i under H_{tot} and compute the relative error

$$\delta J_i = \max_\tau \frac{|J_i^0 - J_i(\tau)|}{J_i^0},$$

which tells us how the evolved actions $J_i(\tau)$ differ from their theoretical counterparts J_i^0. The maximum is computed for a sufficiently large value of proper time τ, which serves as our evolution parameter here. This relative error is the quantity we will use to test our approximation.

Before switching on the perturbation we should briefly examine the approximation for the Schwarzschild solution itself, for which the situation is fairly simple, since we have only one perturbation parameter ε. The Schwarzschild circular orbits are in our approximation represented exactly and from our expansion of the Schwarzschild Hamiltonian (40), it is clear that the farther we get from a fixed circular orbit the less accurate our approximation is. This "phase-space distance" is measured by the action J_r where $J_r = 0$ corresponds to a circular orbit. If our approximation is accurate enough we should approach the separatrix as we increase the value of J_r. When close to the separatrix the approximation should break down which is actually the case. The change of δJ_r with J_r and the total angular momentum L is illustrated in Fig. 9.

The value of L selects the circular orbit around which the expansion takes place. The minimum value of L, which can be chosen, is $L = 2\sqrt{3}M$ representing the ISCO located at $r = 6M$. When L is close to its ISCO value, while the value of J_r is large, we can get a bound orbit that can reach the phase-space region corresponding to the infalling orbits (for low r) leading to a direct contradiction with the exact dynamics. We can, thus, expect that for higher L the approximation is more

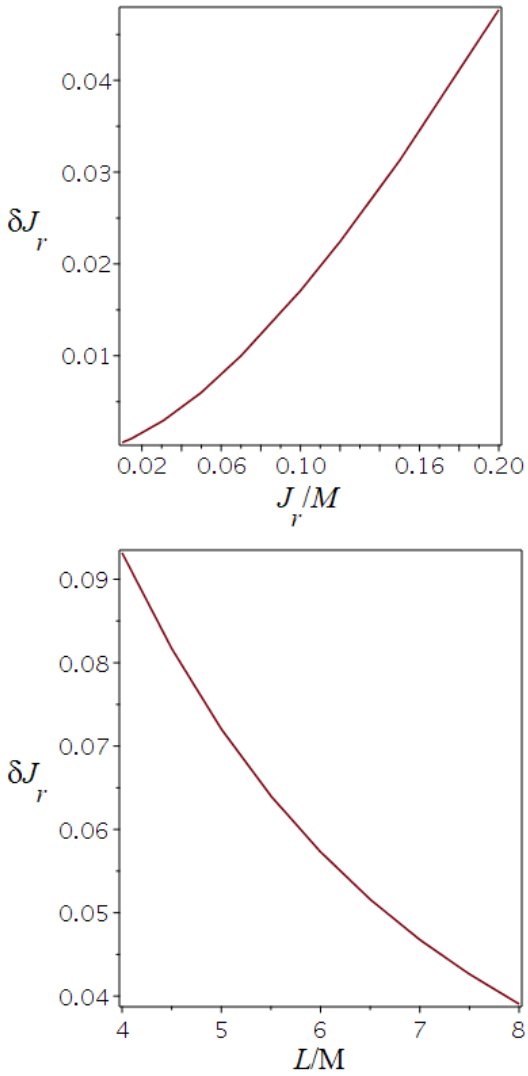

FIG. 9: The relative error of the radial action (δJ_r) in the Schwarzschild spacetime for fixed value of $L = 3.6M$ (top panel) and for $J_r = 0.3M$ (bottom panel).

precise, since the orbit is farther from ISCO, this is verified for example in Fig. 9.

Let us now switch on the perturbation. Even in the case of equatorial motion ($J_\theta = 0$) the situation is now slightly more complex than in the Schwarzschild case. As previously the larger the value of J_r the greater the approximation error is. Note that $J_r = 0$ still corresponds to circular orbits, however these are not represented exactly [4]. The other relevant action in this setting is J_ϕ. The approximation breaks down for large values of J_ϕ because we get farther from the black hole and closer to the ring-like source which is equivalent to increasing Q. The dependence $\delta J_r(J_r, J_\phi)$ is illustrated in Fig. 10.

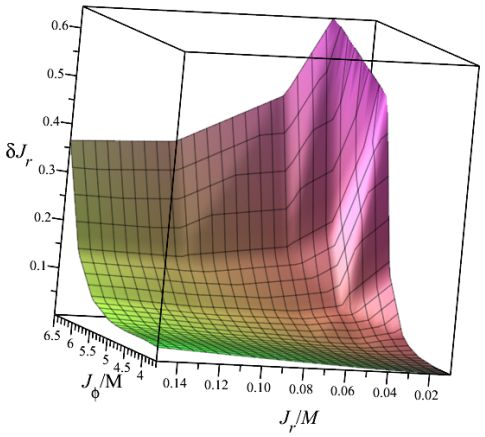

FIG. 10: δJ_r as a function of J_r and J_ϕ in the case of equatorial motion for $Q = 10^{-6}M^{-2}$.

In the non-equatorial motion the presence of the resonance of the form (45) has to be taken into account. Thus when plotting the relative errors of actions δJ_θ and δJ_r as functions of J_θ we get an increasing function except for the close neighborhood of the resonance curves where $\delta J_i \to \infty$. This corresponds to the two gaps in the graph 11 (resonances $1:2$ and $2:3$).

If we were to plot the functions $r(\tau)$ and $\theta(\tau)$ we would find that they even leave the domains they are defined on (for example $r < 0$). This is caused by the perturbative parts proportional to Q which become larger then the Schwarzschild parts. Alternatively we can plot the relative error of a coordinate as a function of proper time. For example for the radial coordinate we have

$$\delta r(\tau) = \frac{|r(\tau) - r^{(n)}(\tau)|}{r^{(n)}(\tau)} \tag{C1}$$

where $r^{(n)}(\tau)$ is the numerical solution to the geodesic equation. This error tends to grow over time and even to much larger (but finite) values than the action errors δJ_i. This growth is especially prevalent in the case of non-equatorial which can be seen in Fig. 12.

[4] The exact Schwarzschild circular orbits are shifted by the perturbation.

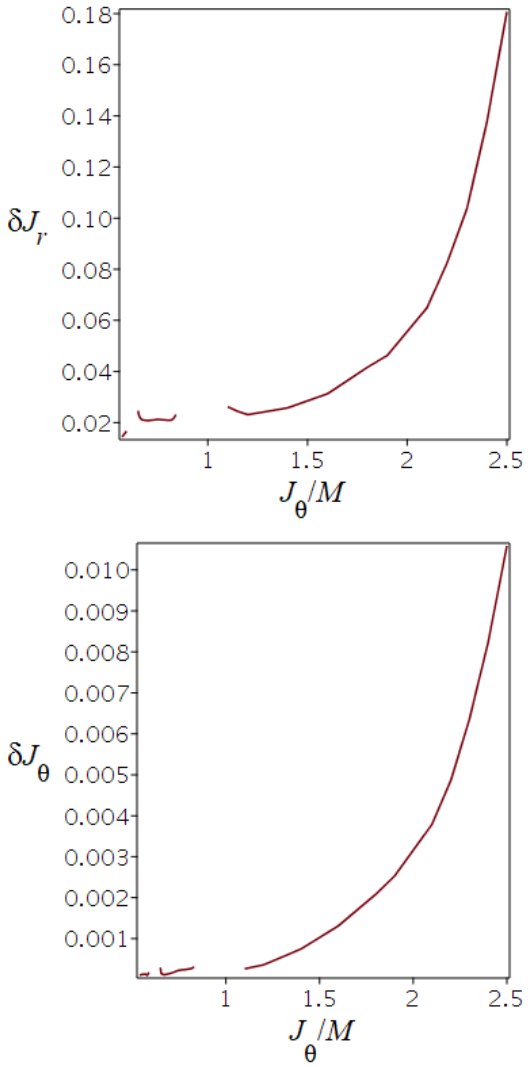

FIG. 11: Relative error δJ_r .(top panel) and relative error δJ_θ for $J_r = 0.1M$, $J_\phi = 3M$ and $Q = 10^{-6}M^{-2}$ (bottom panel).

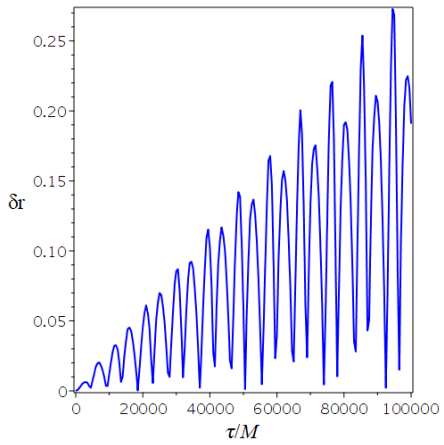

FIG. 12: Relative error of the radial coordinate as a function of proper time for a non-equatorial orbit

6. Action-Angle formalism for extreme mass ratio inspirals in Kerr spacetime (paper 3)

- Kerachian, M., Polcar, L., Skoupý, V., Efthymiopoulos, C., and Lukes-Gerakopoulos, G. Action-angle formalism for extreme mass ratio inspirals in Kerr spacetime, 2023. Accepted for publication in Physical Review D

This last chapter focuses on our publication [46] where we performed an approximate transformation of the Kerr Hamiltonian to action-angle coordinates. The theory relevant for this work is described in chapter 3 (Canonical perturbation theory and Teukolsky formalism).

This work was built upon our experience from [69] where we used the Lie series formalism for the first time. There are several key differences however between this paper and [69]. Firstly the background metric is different here, it is the well-known Kerr spacetime in which the geodesic motion is integrable. Secondly we cared much more about accuracy of the geodesic approximation which is why we applied more canonical transformations on the Hamiltonian and lastly we used the Teukolsky formalism for the calculation of the gravitational-wave fluxes and gravitational waveforms. Throughout the paper we compare our results to those obtained using the exact analytical formulas derived in [26]. These formulas contain elliptic integrals unlike ours which use only elementary functions, this then allowed us to evaluate geodesics faster during the calculation of the fluxes.

While our Hamiltonian and analytical formulas for geodesics are expressed in action-angle coordinates we nevertheless adopted the orbital parameters (p, e, x) (semi-latus rectum, eccentricity and inclination) instead of the actions (there is one-to-one correspondence between these parameters and actions) in our calculation as is common in the literature in which the exact formulas [26] are used. This is convenient in the Kerr spacetime where simple formulas relating the rate of change of (p, e, x) and the fluxes of integrals of motion exist. In a perturbed spacetime it is natural to use the actions directly like we did in [69] as simple analytical formulas using the orbital parameters (p, e, x) might not be available.

The accuracy of our geodesics is measured by the deviation of our approximate actions (which are not constants of motion if we do not neglect the remainder) from the exact ones calculated numerically. In addition to that we also compared the fluxes calculated using our perturbativelly obtained geodesics to those sourced by the exact formulas. By testing our results for different values of orbital parameters we concluded that our approximation is limited by eccentricity, for $e > 0.5$ the approximation breaks down. This is caused by the expansion in the radial part of the Kerr Hamiltonian which relies on the proximity to a stable fixed point in accordance with the Birkhoff normal form theorem.

If we were to successfully calculate an EMRI in Kerr or Schwarzschild spacetime surrounded by matter and include highly eccentric orbits we would have to include partially numerical approach to avoid the expansion from a stable fixed point as was demonstrated for example in [62] or use a completely different perturbation scheme.

Action-Angle formalism for extreme mass ratio inspirals in Kerr spacetime

Morteza Kerachian[1], Lukáš Polcar[1,2], Viktor Skoupý[1,2],
Christos Efthymiopoulos[3], and Georgios Lukes-Gerakopoulos[1*]
[1] *Astronomical Institute of the Czech Academy of Sciences, Boční II 1401/1a, CZ-141 00 Prague, Czech Republic*
[2] *Institute of Theoretical Physics, Faculty of Mathematics and Physics, Charles University in Prague, 18000 Prague, Czech Republic and*
[3] *Dipartimento di Matematica Tullio Levi-Civita, Università degli Studi di Padova, Via Trieste 63 35121 Padova, Italy*

We introduce an action-angle formalism for bounded geodesic motion in Kerr black hole spacetime using canonical perturbation theory. Namely, we employ a Lie series technique to produce a series of canonical transformations on a Hamiltonian function describing geodesic motion in Kerr background written in Boyer-Lindquist coordinates to a Hamiltonian system written in action-angle variables. This technique allows us to produce a closed-form invertible relation between the Boyer-Lindquist variables and the action-angle ones, while it generates in analytical closed form all the characteristic functions of the system as well. The expressed in the action-angle variable Hamiltonian system is employed to model an extreme mass ratio inspiral (EMRI), i.e. a binary system where a stellar compact object inspirals into a supermassive black hole due to gravitational radiation reaction. We consider the adiabatic evolution of an EMRI, for which the energy and angular momentum fluxes are computed by solving the Teukolsky equation in the frequency domain. To achieve this a new Teukolsky equation solver code was developed.

I. INTRODUCTION

An extreme mass ratio inspiral (EMRI) is a binary compact object system consisting of a secondary stellar body of mass μ inspiraling into a primary supermassive black hole of mass M, due to radiation reaction. The mass ratio $q = \mu/M$ of an EMRI lies in the range $10^{-7} \leq q \leq 10^{-4}$. EMRIs are one of the prominent sources for the planned space-based gravitational wave (GW) detectors like the Laser Interferometer Space Antenna (LISA) [1]. It is expected that we will be able to observe $\sim 10^4 - 10^5$ cycles in the sensitivity frequency range. This implies that for modelling an EMRI the accuracy during one cycle must be below the 10^{-5} order [1, 2].

The extreme difference in the mass ratio between the secondary and the primary allows us to treat the influence of the secondary as a perturbation to the primary's background spacetime [3, 4]. This background is expected to be sufficiently well described by a Kerr spacetime. Hence, perturbation theory in Kerr spacetime provides the means to model the radiation reaction driving an EMRI evolution.

The modelling of the evolution can be split into two timescales [5]: a slow one and a fast one. The slow timescale concerns the dissipation of energy and angular momentum due to the emission of gravitational waves, while the fast one concerns the orbital revolution of the secondary around the primary. In terms of celestial mechanics [6], the slow timescale deals with the actions of the system, while the fast one with the angles of the system. Realizing this one is compelled to express an EMRI system in action-angle (AA) variables.

Schmidt in his seminal work called "Celestial Mechanics in Kerr spacetime" [7] was able to provide the fundamental frequencies of bounded geodesic motion in Kerr by using elements of the action-angle formalism. This in turn allowed the frequency domain decomposition of the Teukolsky equation [8] providing the energy and angular momentum fluxes. The idea of using action-angle variables for EMRIs is now widely adapted [5, 9–13], and there are works [14, 15] providing transformations from and to action-angle variables for bounded geodesic motion in Kerr spacetime using integrals and special functions, but not in closed forms. Examples of how this non-closed form transformation can be implemented can be found in Ref. [16–18]. Closed-form transformations have been given in the Schwarzschild spacetime for the first time in [19] and [20] using different approaches. Ref. [19] used a Taylor series approach to provide a closed-form transformation to and from action-angle variables, while Ref. [20] used a technique coming from the canonical perturbation theory [6, 21] to achieve this. In particular, Ref. [20] employed the Lie series approach, which we follow also in this work in order to provide a closed-form transformation to and from action-angle variables for bound geodesic orbits in Kerr spacetime.

Perturbation theory has enjoyed many successes spanning from celestial mechanics [22], like the prediction of Neptune's existence by Urbain Le Verrier in the mid nineteenth century, to general relativity [3, 23]. In our work, we employ two branches of the perturbation theory: the canonical perturbation theory renowned for the Kolmogorov-Arnold-Moser theorem [24], which allows us to express the Hamiltonian system describing the geodesic motion in Kerr spacetime purely in action

* gglukes@gmail.com

terms; and the black hole perturbation one provided by Teukolsky in [25], which provides the action's fluxes due to gravitational radiation reaction. Combining these two perturbation theories we suggest in this work a scheme for adiabatic modelling of EMRIs aiming to contribute in the ongoing effort for more and more computationally efficient schemes [26–28]. The framework that we setup in this work could be expanded to other directions by adding more perturbative sources [16], like matter distribution around a black hole [20] or the extended body effects induced by the secondary body [29]. Actually, the latter is expected to be the main advantage of the Lie series approach over other techniques providing action-angle variables for the motion in a Kerr background, see, e.g.. Ref. [20] for the Schwarzschild case.

The rest of the article is organized as follows. Sec. II.1 briefs basic concepts and steps of the Lie series canonical perturbation approach. The application of this approach on the Kerr geodesic motion is discussed in Sec. III and an approximate Hamiltonian system is introduced in action-angle variables. Sec. IV provides adiabatic EMRI models using the introduced system in action-angle variables. Finally, Sec. V summarizes our work.

II. ACTION-ANGLE FORMALISM AND CANONICAL PERTURBATION THEORY

We use in this work AA formalism and two elements from the canonical perturbation theory: the Lie series mapping and the Birkhoff normal form. This section briefly introduces these elements and for more on them, the interested reader is referred to the literature [5, 21].

II.1. Action-angle formalism

For a Hamiltonian system which consists of a $2N$-dimensional differentiable manifold $\mathcal{M}$, there exists a symplectic coordinate system $\{q_n, p_n\}$ with $n = \{1, N\}$. This Hamiltonian system $H(\boldsymbol{q}, \boldsymbol{p})$ is called an integrable system in an open region $\mathcal{U}$, if there exist N integrals of motion which are independent and in involution at every point of $\mathcal{U}$. If the integrable Hamiltonian system is, moreover, compact and connected, then there should be a canonical transformation allowing us to write the system in *action-angle* (AA) variables $\{\psi_n, J_n\}$. For the angles, it holds that

$$\psi_m + 2\pi \equiv \psi_m, \qquad 1 \leq m \leq \kappa, \tag{1}$$

implying that either all ($\kappa = N$) or some ($\kappa < N$) of the angle variables are periodic [6, 30]; the J_m are the integrals of motion given by

$$J_i = \frac{1}{2\pi} \oint p_i dq_i, \tag{2}$$

where the path integral takes place over an irreducible circle. In AA variables an integrable system should read $H_{AA}(\boldsymbol{J})$, hence the Hamilton equations would be

$$\dot{\psi}_i = \frac{\partial H_{AA}(\boldsymbol{J})}{\partial J_i} \equiv \Upsilon_i(\boldsymbol{J}), \quad \dot{J}_i = -\frac{\partial H_{AA}(\boldsymbol{J})}{\partial \psi_i} = 0. \tag{3}$$

The solution to the above equations of motion is

$$\psi_i = \Upsilon_i \lambda + \psi_{i0}, \tag{4}$$
$$J_i = J_{i0}, \tag{5}$$

where J_{i0} and q_{i0} are initial conditions and λ is the evolution parameter.

In order to express $H(\boldsymbol{q}, \boldsymbol{p})$ in the AA variables, i.e. $H_{AA}(\boldsymbol{J})$, we need to know the canonical transformation from the $\{q_n, p_n\}$ coordinate system to the $\{\psi_m, J_m\}$ one. However, determining the exact canonical transformation is not an easy task for most of the Hamiltonian systems. Thus, we use the canonical perturbation theory to approximate the system by using a series of canonical transformations.

II.2. Lie Series

If χ is a generating function, a Lie derivative for a given function f is defined as

$$f \to \mathcal{L}_\chi f = \{f, \chi\}, \tag{6}$$

where $\{f, \chi\}$ is the Poisson bracket, i.e.

$$\{f, \chi\} = \sum_{i=1}^{N} \left(\frac{\partial f}{\partial q_i} \frac{\partial \chi}{\partial p_i} - \frac{\partial \chi}{\partial q_i} \frac{\partial f}{\partial p_i} \right). \tag{7}$$

The respective Lie series is defined as

$$\exp(\mathcal{L}_\chi) f = \sum_{k=0}^{\infty} \frac{1}{k!} \mathcal{L}_\chi^k f. \tag{8}$$

The Lie series transformation is a canonical one.

II.3. Birkhoff normal form theorem

To derive a Hamiltonian in the action form, we follow the Birkhoff normal form theorem. Here we explain the necessary steps that one has to follow to derive the Hamiltonian in the action up to the desired order.

Let's assume that we have a Hamiltonian in the form

$$H^{(0)} = Z_0(J_i^0) + \sum_{k=1}^{N} \epsilon^k H_k^{(0)}(\psi_i^0, J_i^0), \tag{9}$$

where the ϵ is called the book-keeping parameter and is used to keep track of the smallness of each term in the Hamiltonian. When all the calculations are done, the numerical value of the book-keeping parameter is set $\epsilon = 1$. Note that J_i^0 are not constants of motion for the whole Hamiltonian (9), but just for the Z_0 part.

By expanding the Hamiltonian (9) up to second order in ϵ we arrive at

$$H^{(0)} = Z_0(J_i^0) + \epsilon\left(Z_1^{(0)}(J_i^0) + h_1^{(0)}(\psi_i^0, J_i^0)\right) + \epsilon^2\left(Z_2^{(0)}(J_i^0) + h_2^{(0)}(\psi_i^0, J_i^0)\right) + \mathcal{O}(\epsilon^3), \quad (10)$$

where each $H_k^{(0)}(\psi_i^0, J_i^0)$ was split to the pure action part $Z_k^{(0)}(J_i^0)$ and the part $h_k^{(0)}(\psi_i^0, J_i^0)$, which still depends on angles, i.e.

$$H_k^{(0)}(\psi_i^0, J_i^0) = Z_k^{(0)}(J_i^0) + h_k^{(0)}(\psi_i^0, J_i^0).$$

For simplicity, we reduce the notation to $Z_k^{(0)}, h_k$ dropping the respective dependencies. In the following, we provide an example of the procedure up to $\mathcal{O}(\epsilon^2)$.

To remove the angle dependency in the first order in ϵ in the Hamiltonian (10), we apply the Lie series as follows

$$H^{(1)} = \exp(\mathcal{L}_{\chi_1})H^{(0)} = H^{(0)} + \mathcal{L}_{\chi_1}H^{(0)} + \frac{1}{2}\mathcal{L}_{\chi_1}^2 H^{(0)}, \quad (11)$$

where

$$\begin{aligned}\mathcal{L}_{\chi_1}H^{(0)} &= \{Z_0, \chi_1\} + \epsilon\{Z_1^{(0)} + h_1^{(0)}, \chi_1\} \\ &\quad + \epsilon^2\{Z_2^{(0)} + h_2^{(0)}, \chi_1\}, \\ \mathcal{L}_{\chi_1}^2 H^{(0)} &= \{\{Z_0, \chi_1\}, \chi_1\} + \epsilon\{\{Z_1^{(0)} + h_1^{(0)}, \chi_1\}, \chi_1\} \\ &\quad + \epsilon^2\{\{Z_2^{(0)} + h_2^{(0)}, \chi_1\}, \chi_1\}. \end{aligned} \quad (12)$$

We choose χ_1 to be a quantity of the order $\mathcal{O}(\epsilon)$; therefore,

$$Z_0 = \mathcal{O}(0), \quad (13)$$

$$\epsilon\left(Z_1^{(0)} + h_1^{(0)}\right) + \{Z_0, \chi_1\} = \mathcal{O}(\epsilon), \quad (14)$$

$$\epsilon^2\left(Z_2^{(0)} + h_2^{(0)}\right) + \epsilon\{Z_1^{(0)} + h_1^{(0)}, \chi_1\} + \frac{1}{2}\{\{Z_0, \chi_1\}, \chi_1\} = \mathcal{O}(\epsilon^2), \quad (15)$$

and in a similar way for $\mathcal{O}(\epsilon^3)$.

From Eq. (14) we see that to eliminate the angle dependency at order $\mathcal{O}(\epsilon)$, we have to define χ_1 as

$$\epsilon h_1^{(0)} + \{Z_0, \chi_1\} = 0. \quad (16)$$

This equation and the respective equations that eliminate the angle dependency for higher orders in ϵ are called homological equations. By substituting χ_1 from (16) into the Eq. (11), we can rewrite the Hamiltonian (11) in its normal form up to the $\mathcal{O}(\epsilon)$:

$$H^{(1)} = Z_0 + \epsilon Z_1^{(0)} + \epsilon^2\left(Z_2^{(1)} + h_2^{(1)}\right) + \mathcal{O}(\epsilon^3), \quad (17)$$

where

$$\epsilon^2\left(Z_2^{(1)} + h_2^{(1)}\right) = \epsilon^2\left(Z_2^{(0)} + h_2^{(0)}\right) + \epsilon\{Z_1^{(0)} + h_1^{(0)}, \chi_1\} + \frac{1}{2}\{\{Z_0, \chi_1\}, \chi_1\}. \quad (18)$$

To bring the Hamiltonian (17) normal form up to $\mathcal{O}(\epsilon^2)$, we have to apply another Lie series in a similar fashion as we did for $\mathcal{O}(\epsilon)$. We start from

$$H^{(2)} = \exp(\mathcal{L}_{\chi_2})H^{(1)} = H^{(1)} + \mathcal{L}_{\chi_2}H^{(1)} + \frac{1}{2}\mathcal{L}_{\chi_2}^2 H^{(1)}, \quad (19)$$

where

$$\begin{aligned}\mathcal{L}_{\chi_2}H^{(1)} &= \{Z_0, \chi_2\} + \epsilon\{Z_1^{(0)}, \chi_2\} + \epsilon^2\{Z_2^{(1)} + h_2^{(1)}, \chi_2\}, \\ \mathcal{L}_{\chi_2}^2 H^{(1)} &= \{\{Z_0, \chi_2\}, \chi_2\} + \epsilon\{\{Z_1^{(0)}, \chi_2\}, \chi_2\} \\ &\quad + \epsilon^2\{\{Z_2^{(1)} + h_2^{(1)}, \chi_2\}, \chi_2\}. \end{aligned} \quad (20)$$

By choosing χ_2 to be a quantity of $\mathcal{O}(\epsilon^2)$, the generating function χ_2 can be determined from the second homological equation

$$\epsilon^2 h_2^{(1)} + \{Z_0, \chi_2\} = 0. \quad (21)$$

Using the solution of Eq. (21) and apply it into the Hamiltonian (19) we arrive at the normal form

$$H^{(2)} = Z_0 + \epsilon Z_1^{(0)} + \epsilon^2 Z_2^{(1)} + \mathcal{O}(\epsilon^3), \quad (22)$$

The final step is to set $\epsilon = 1$. The $\mathcal{O}(\epsilon^3)$ part still depends on angles and it is called the remainder.

II.4. General formalism and benefit

In the previous section, we demonstrated in detail how to express a Hamiltonian in AA variables using the Lie canonical transformation up to the $\mathcal{O}(\epsilon^2)$. However, we can generalize this computation to an arbitrary order $H^{(n)}$ by applying n canonical transformations. The $H^{(n)}$ then reads

$$H^{(n)} = \exp(\mathcal{L}_{\chi_n})\exp(\mathcal{L}_{\chi_{n-1}})...\exp(\mathcal{L}_{\chi_2})\exp(\mathcal{L}_{\chi_1})H^{(0)}. \quad (23)$$

In Eq. (23) each χ_κ where $\kappa \in \{1, n\}$ comes from a solution of the respective homological equation, i.e.

$$\epsilon^\kappa h_\kappa^{(\kappa-1)} + \{Z_0, \chi_\kappa\} = 0. \quad (24)$$

The main benefit of using the Lie series is that we can always transform the original variables (sometimes we call them old variables) to the AA variables (new variables) and vice versa. The transformation from the old variables to the new ones for n transformations is given by a Lie series composition in the following way

$$X_{\text{new}} = \exp(\mathcal{L}_{\chi_n})\exp(\mathcal{L}_{\chi_{n-1}})...\exp(\mathcal{L}_{\chi_1})X_{\text{old}}, \quad (25)$$

and the transformation from new variables to old variables is given by

$$X_{\text{old}} = \exp(-\mathcal{L}_{\chi_1})...\exp(-\mathcal{L}_{\chi_{n-1}})\exp(-\mathcal{L}_{\chi_n})X_{\text{new}}, \quad (26)$$

where X can be any phase space quantity like action, angle, coordinate, or momentum.

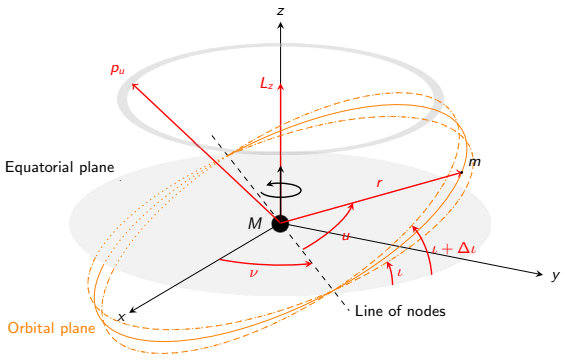

FIG. 1: This figure shows an off-equatorial motion of a secondary object with the mass m around the Kerr black hole with the mass M in the polar nodal coordinates. The radial distance of the secondary from the supermassive black hole is indicated by r, and the angle u represents the azimuth-like angle on the instantaneous orbital plane. Due to the spin of the black hole, the orbital plane itself precesses around the z-axis with the precession angle ν and its inclination ι oscillates slightly by $\Delta\iota$. The z component of the orbital angular momentum is conserved, while the orbital angular momentum, whose measure is denoted as p_u and which is perpendicular to the instantaneous orbital plane, is oscillating. The grey ring is the area that the p_u is swiping while the secondary object rotates around the black hole. The line of nodes is the intersection of the orbital plane and the equatorial plane.

III. EXPRESSING GEODESIC MOTION IN KERR IN AA VARIABLES

The Kerr line element in Boyer-Lindquist coordinates (t, r, θ, ϕ) reads

$$\begin{aligned} ds^2 =& -\left(1-\frac{2Mr}{\Sigma}\right)dt^2 + \frac{\Sigma}{\Delta}\,dr^2 + \Sigma\,d\theta^2 \\ &+\left(r^2+a^2+\frac{2Ma^2r}{\Sigma}\sin^2\theta\right)\sin^2\theta\,d\phi^2 \\ &-\frac{4Mar}{\Sigma}\sin^2\theta\,dt\,d\phi, \end{aligned} \tag{27}$$

where a is the Kerr parameter corresponding to the spin of the black hole and M is its mass, while

$$\Delta = r^2 - 2Mr + a^2, \qquad \Sigma = r^2 + a^2\cos^2\theta.$$

The stationarity and the axisymmetry of the spacetime provide two integrals of motion, the energy E and the angular momentum L_z along the symmetry axis z. The third integral is the Carter constant Q [31], which in the case of $a = 0$ is related to the projection of the angular momentum on the equatorial plane ($Q|_{a=0} = L_x^2 + L_y^2$). The equations of the geodesic motion in a spacetime, which is described by a metric tensor $g_{\mu\nu}$, can be provided by the Hamiltonian function

$$H = \frac{1}{2}g^{\mu\,\nu}p_\mu p_\nu. \tag{28}$$

For the Kerr spacetime, this Hamiltonian reads

$$\begin{aligned} H =& \frac{\Delta}{2\Sigma}p_r^2 + \frac{1}{2\,\Sigma}p_\theta^2 + \frac{(p_\phi + a\,\sin^2\theta p_t)^2}{2\,\Sigma\,\sin^2\theta} \\ &- \frac{\left(\left(r^2+a^2\right)\,p_t + a\,p_\phi\right)^2}{2\,\Sigma\,\Delta}, \end{aligned} \tag{29}$$

since the system is autonomous the Hamiltonian itself is an integral of motion. Having four independent and in involution constants in a four degrees of freedom system implies that the system is integrable and, as Carter showed, separable [31]. This suggests that, in principle, there should be a way to express the Hamiltonian system in AA variables through a canonical transformation.

Actually, the Hamiltonian (29) can be separated into a radial and an angular part by replacing the proper time τ with the Carter-Mino [31, 32] time λ, i.e. $d\tau = (r^2 + a^2\cos^2\theta)d\lambda$. Then, the Hamiltonian (29) transforms to

$$\begin{aligned} H_\lambda =& \frac{1}{2}\left(\Delta p_r^2 - \frac{((r^2+a^2)\,p_t + aL_z)^2}{\Delta} + \mu^2 r^2\right) \\ &+ \frac{1}{2}\left(p_\theta^2 + a^2\mu^2\cos^2\theta + \frac{(L_z + a\sin^2\theta p_t)^2}{\sin^2\theta}\right). \end{aligned} \tag{30}$$

The next step we take is to express Hamiltonian (30) in polar-nodal coordinates[1]. This choice of coordinates provides a good insight into the motion of the secondary, since the coordinates and their conjugate momenta are related to the orbital parameters. For instance, in the case of the Schwarzschild spacetime ($a = 0$), an orbit takes place on a single plane that has a fixed inclination angle ι, a fixed precession angle ν, and the orbital angular momentum of measure p_u is perpendicular to this orbital plane. Moreover, in the polar-nodal coordinates representation, the motion is split into two parts: the motion of the secondary on the orbital plane described by the coordinates r and u; and the motion of the orbital plane itself described by the angles ν and ι; in this set up $\{t, r, u, \nu\}$ are the coordinates and their conjugate momenta are $\{p_t, p_r, p_u, L_z\}$. Fig. 1 illustrates these variables.

The coordinate change is provided by a canonical

[1] For more on polar-nodal coordinates see Appendix A

transformation given by

$$\theta = \arccos\left(\sqrt{1-\frac{L_z^2}{p_u^2}}\sin u\right),$$
$$p_\theta = p_u\sqrt{1-\frac{L_z^2}{p_u^2-(p_u^2-L_z^2)\sin^2 u}}, \quad (31)$$
$$\phi = u+\nu+\arctan\left(\frac{(L_z/p_u-1)\cos u\sin u}{1+(L_z/p_u-1)\sin^2 u}\right),$$

where u is the azimuth-like angle in the inclined plane of the orbital motion. Note that the angular momentum L_z remains unchanged in this canonical transformation. With the help of p_u we can define the inclination angle as

$$\cos\iota = \frac{L_z}{p_u}. \quad (32)$$

Note that this definition is different than $\cos\iota = L_z/\sqrt{L_z^2+Q}$ given in [33]; since p_u is not constant in Kerr spacetime, the inclination angle oscillates.

Consequently, the Hamiltonian in the polar-nodal coordinate will be

$$H_{pn} = \frac{1}{2}\left(\Delta\, p_r^2 - \frac{((r^2+a^2)\,p_t + aL_z)^2}{\Delta} + \mu^2\, r^2\right) \quad (33)$$
$$+\frac{1}{2}\left(a^2p_t^2 + 2\,a\,L_z\,p_t + p_u^2 + \frac{a^2(\mu^2-p_t^2)\,(p_u^2-L_z^2)\sin^2 u}{p_u^2}\right),$$

We could apply the Lie series at this point, but we prefer to rewrite first the angular part in terms of the Carter constant as follows

$$H_{pn} = \frac{1}{2}\left(\Delta\, p_r^2 - \frac{((r^2+a^2)\,p_t + aL_z)^2}{\Delta} + \mu^2\, r^2\right)$$
$$+\frac{1}{2}\left((ap_t+L_z)^2+Q\right), \quad (34)$$

where

$$Q = \left(1-\frac{L_z^2}{p_u^2}\right)\left(p_u^2 + a^2\,(\mu^2-p_t^2)\,\sin^2 u\right) \quad (35)$$

is the Carter constant in the polar-nodal coordinates.

Since $H_{pn}=0$, we can get p_r as a function of $r,\ a,\ \mu$ and the constants of motion, where μ is the mass of test body; from Eq.(35) p_u can be written as a function of $u,\ a,\ \mu$ and the constants of motion. This leads to the following relations

$$p_t = -E,\ p_r = \pm\frac{\sqrt{V_r}}{\Delta},\ p_u = \sqrt{\frac{V_u}{2}},\ p_\nu = L_z. \quad (36)$$

The V_r and V_u are

$$V_r = [a\,L_z - (r^2+a^2)E]^2 - \Delta[\mu^2\,r^2 + (L_z - a\,E)^2 + Q],$$
$$V_u = v_u + \sqrt{4\,L_z^2\,(\mu^2-E^2)a^2\,\sin^2 u + v_u^2}, \quad (37)$$

where

$$v_u = L_z^2 + Q - (\mu^2-E^2)\,a^2\,\sin^2 u.$$

In polar-nodal coordinate, the four constants of motions are $\{\overline{J}_r, \overline{J}_u, \overline{J}_\nu, \overline{J}_t\}$ and their conjugate angle are denoted by $\{\overline{\psi}_r, \overline{\psi}_u, \overline{\psi}_\nu, \overline{\psi}_t\}$; here the over-line refers to the definition of the actions and the angles (2)- (4). These actions are defined from Eq. (2) as follows

$$\overline{J}_r = \frac{1}{2\pi}\oint\frac{\sqrt{V_r}}{\Delta}dr = \frac{1}{\pi}\int_{r_p}^{r_a}\frac{\sqrt{V_r}}{\Delta}dr, \quad (38)$$
$$\overline{J}_u = \frac{1}{2\pi}\oint\sqrt{\frac{V_u}{2}}du = \frac{1}{\pi}\int_0^{\pi}\sqrt{\frac{V_u}{2}}du, \quad (39)$$
$$\overline{J}_\nu = \frac{1}{2\pi}\oint p_\nu d\nu = L_z, \quad (40)$$
$$\overline{J}_t = \frac{1}{2\pi}\int_0^{2\pi} p_t dt = -E, \quad (41)$$

where $r_{p,a}$ are the periapsis and apoapsis which are related to the semi-latus rectum p and eccentricity e as

$$r_{p,a} = \frac{p}{1\pm e}. \quad (42)$$

We got numerical indications that $\overline{J}_u = \overline{J}_\nu + \overline{J}_\theta$, where $\overline{J}_\theta$ is the action related to the θ angle in the Boyer-Lindquist coordinates [5]. This implies that $\overline{J}_u$ is the action that reflects the total angular momentum. Note that in our work by assumption $L_z > 0$.

Hamiltonian (34) has been reduced to just one degree of freedom along the radius since the angular dependence is hidden in the Carter constant. We take advantage of the above split into radial and angular parts in the following sections.

III.1. Radial motion

In order to apply the Lie series to the Hamiltonian (34), we should convert it to the form of Eq. (9). To do that, we first have to choose a reference orbit around which we expand the system perturbatively. We choose to expand around a spherical orbit in Kerr [33], i.e. an orbit of constant radius. Since the Hamiltonian (34) corresponds to a system of one degree of freedom, a spherical orbit degenerates to a circular one. This orbit can be characterized by its radius r_c and angular momentum L_{zc}, where the index "c" refers to a circular orbit. The Carter constant and the energy can be derived by the following relations:

$$E_c = -p_{tc} = \frac{a^2\, L_{zc}^2\,(r_c - M) + r_c\,\Delta_c^2}{a\, L_{zc}\, M\,(r_c^2 - a^2) + \Delta_c\sqrt{r_c^5\,(r_c - 3\,M) + a^4\, r_c\,(r_c + M) + a^2 r_c^2\,(L_{zc}^2 - 2\,M\, r_c + 2\, r_c^2)}}, \tag{43}$$

$$Q_c = \frac{\big((a^2 + r_c^2)E_c - a\, L_{zc}\big)^2}{\Delta_c} - \left(r_c^2 + a^2\, E_c^2 - 2\, a\, E_c\, L_{zc} + L_{zc}^2\right), \tag{44}$$

where $\Delta_c = r_c^2 - 2\,M\, r_c + a^2$.

Now, from a fixed reference orbit, we parameterize the deviation from it as follows

$$\begin{aligned} &r = r_c + \epsilon\, d\hat{r}, \qquad p_r = \epsilon\, \hat{p}_r, \qquad L_z = L_{zc} + \epsilon^2\, J_\nu^0, \\ &p_t = p_{tc} + \epsilon^2\, J_t^0, \qquad Q = Q_c + \epsilon^2\, \tilde{Q}. \end{aligned} \tag{45}$$

Note that we expand around p_t instead of the energy.

The accuracy of the scheme highly depends on the choice of the position of the circular orbit r_c and how we set the small perturbation $d\hat{r}$. By trial and error, we have found that by using the canonical transformation

$$d\hat{r} = \delta dr, \qquad \hat{p}_r = \frac{\tilde{p}_r}{\delta}. \tag{46}$$

and appropriately choosing r_c and δ we could improve the accuracy of the scheme.

We substitute the transformations (45)- (46) into the Hamiltonian (34) and expand it with respect to the book-keeping parameter ϵ. This leads to

$$H_o = \left(\Omega_{t0} J_t^0 + \frac{1}{2}\,\tilde{Q} + \Omega_{z0} J_\nu^0 + \alpha\, dr^2 + \beta\, \tilde{p}_r^2\right)\epsilon^2 + \mathcal{O}(\epsilon^n), \tag{47}$$

where $n \geq 3$. Note that the zero and linear terms in ϵ vanished. The explicit formulas of Ω_{t0}, Ω_{z0}, α and β read

$$\begin{aligned} \Omega_{t0} &= -\frac{r_c}{\Delta_c}\big(p_{tc}(r_c^3 + a^2(2M + r_c)) + 2\, a\, M\, L_{zc}\big), \\ \Omega_{z0} &= \frac{r_c}{\Delta_c}\big(L_{zc}(r_c - 2\,M) - 2\, a\, M\, p_{tc}\big),\ \beta = -\frac{\Delta_c}{2\delta^2} \\ \alpha &= \frac{-\delta^2}{2\Delta_c}\Big(\mathfrak{A}_1\, p_{tc}^2 + 4\,\mathfrak{A}_2\, a\, M\, L_{zc}\, p_{tc} + \mathfrak{A}_3\, a^2\, L_{zc}^2 - \Delta_c^3\Big), \end{aligned} \tag{48}$$

where

$$\begin{aligned} \mathfrak{A}_1 &= \Delta_c^3 + 4\, M^2(a^4 - 3a^2 r_c^2 + 2\, M\, r_c^3) \\ \mathfrak{A}_2 &= r_c^3 + a^2(2M - 3r_c), \\ \mathfrak{A}_3 &= a^2(M^2 - a^2) + 3\Delta_c. \end{aligned}$$

Since in the part of the Hamiltonian (47) up to $\mathcal{O}(\epsilon^2)$ apart from the $(dr,\ \tilde{p}_r)$ pair all the other quantities are constants, this part of the Hamiltonian is basically describing a harmonic oscillator, where the mass and frequency can be given respectively as

$$m_c = \frac{1}{2\beta}, \qquad \Omega_{r0} = \sqrt{\frac{2\alpha}{m_c}}. \tag{49}$$

A harmonic oscillator can be expressed into AA variables by the well-known transformation

$$dr = \sqrt{\frac{2\, J_r^0}{m_c\, \Omega_{r0}}}\,\sin\psi_r^0, \tag{50}$$

$$\tilde{p}_r = \sqrt{2\, J_r^0\, m_c\, \Omega_{r0}}\,\cos\psi_r^0. \tag{51}$$

We substitute the above relations into Eq. (47) and, since the zero and linear terms have vanished in Eq. (47), we reduce the order of the Book-keeping parameter by 2. This results in

$$H^{(0)} = \left(\Omega_{t0}\, J_t^0 + \frac{1}{2}\,\tilde{Q} + \Omega_{z0}\, J_\nu^0 + \Omega_{r0}\, J_r^0\right) + \mathcal{O}(\epsilon^n), \tag{52}$$

where $n \geq 1$. Note that the Hamiltonian (52) is in the form of Eq. (9), since at order ϵ^0 the $\{J_t^0, J_\nu^0, J_r^0\}$ are the actions of the system. We denote their conjugate angles as $\{\psi_t^0, \psi_\nu^0, \psi_r^0\}$. Therefore, we can now apply the Lie series, derive the generating functions, and express the Hamiltonian (34) in terms of AA variables. Note that $\tilde{Q}$ is a constant, but not an action. We address this issue in the next section.

III.2. Angular motion

In the previous section, we expanded the Hamiltonian (34) around a spherical orbit in Kerr. In this section, we apply similar steps to express $\tilde{Q}$ in terms of the actions. For the Carter constant, however, we choose a circular orbit in Schwarzschild as a reference orbit and we expand the system around it perturbatively. This orbit is characterized by its radius $r_{c_{\rm sc}}$, total angular momentum p_{uc}, z-component of the angular momentum $\tilde{L}_{zc}$ and its energy $\tilde{E}_c = -\tilde{p}_{tc}$. By substituting $a = 0$ into the Eq. (43) and Eq (44) we get $E_c = \tilde{E}_c$ and $Q_c = p_{uc}^2 - \tilde{L}_{zc}^2$. The deviation from this reference orbit is parameterized as follows:

$$\begin{aligned} &p_u = p_{uc} + \epsilon^2\, J_u^0, \qquad L_z = \tilde{L}_{zc} + \epsilon^2 \tilde{J}_\nu^0, \\ &p_t = \tilde{p}_{tc} + \epsilon^2 \tilde{J}_t^0, \qquad a = \epsilon^2 \tilde{a}. \end{aligned} \tag{53}$$

The Carter constant (35) can be set as the Hamiltonian describing the angular motion. Having this in mind, we expand it with respect to ϵ to arrive at

$$Q = (p_{uc}^2 - \tilde{L}_{zc}^2) + 2(p_{uc}\, J_u^0 + \tilde{L}_{zc}\, \tilde{J}_\nu^0)\,\epsilon^2 + \mathcal{O}(\epsilon^n), \tag{54}$$

for $n \geq 3$. Since $p_{uc}^2 - \tilde{L}_{zc}^2$ is constant, we can remove it and define a new Hamiltonian $Q^{(0)} = Q - (p_{uc}^2 - \tilde{L}_{zc}^2)$. Furthermore, we can reduce the order of the Book-keeping parameter ϵ by 2. Hence, we arrive at

$$Q^{(0)} = 2(p_{uc}\, J_u^0 + \tilde{L}_{zc}\, \tilde{J}_\nu^0) + \mathcal{O}(\epsilon^n), \tag{55}$$

where $n \geq 1$. Now, the Carter constant (55) is in the form of (9), since at order ϵ^0 the $\{J_u^0, \tilde{J}_\nu^0\}$ are the actions of the system. Their conjugate angles are denoted by $\{\psi_u^0, \tilde{\psi}_\nu^0\}$, while $\tilde{\psi}_t^0$ is the conjugate angle to the action $\tilde{J}_t^0$. At this point, we can apply the Lie series to the system.

III.3. New Hamiltonian

By applying n canonical transformations, i.e. Lie series transformations, to the Hamiltonian (52) and n' canonical transformations to the Carter constant (55), the new Hamiltonian takes the form

$$H_{AA} = \mathcal{H}(J_t, J_\nu, J_r) + \frac{1}{2}\tilde{Q} + \mathcal{O}(\epsilon^{n+1}), \tag{56}$$

with

$$\tilde{Q} = \mathcal{Q}(J_u, \tilde{J}_t, \tilde{J}_\nu) + (p_{uc}^2 - \tilde{L}_{zc}^2) - Q_c + \mathcal{O}(\epsilon^{n'+1}), \tag{57}$$

where the $\{J_r, J_u, J_\nu, J_t\}$ are the actions of the new system[2]; the $\mathcal{O}(\epsilon^{n+1})$ and $\mathcal{O}(\epsilon^{n'+1})$ are the remainders. When we refer to the H_{AA} Hamiltonian from now on we consider it without the remainders. At this point, we set the book-keeping parameter $\epsilon = 1$ in the H_{AA}. The exact expression of Eq. (56) is extremely long to be provided in the text, thus we provide it in the supplemental material [34].

We have n generating functions for the radial transformation, i.e. χ_{r_i} where $i = \{1, n\}$, and n' generating functions for the angular transformation, i.e. χ_{u_j} where $j = \{1, n'\}$. The crucial question is how can we determine the n and n', namely how many times we should apply the canonical transformations? To find it out, we check if the new system H_{AA} converges to the original system H_{pn}, namely, we see how accurate is the new system. Therefore, we check if the new actions $\{J_t, J_r, J_u, J_\nu\}$ are converging to their theoretical expected constant values. The J_t and J_ν automatically converge, since the Hamiltonian does not explicitly depend on the respective angles. However, for the J_r and J_u we have to write them in terms of the original variables by applying the inverse Lie transformations, in the same fashion as shown in Eq. (26), i.e.

$$J_{r_{\rm old}} = \exp(-\mathcal{L}_{\chi_{r_1}}) \exp(-\mathcal{L}_{\chi_{r_2}}) ... \exp(-\mathcal{L}_{\chi_{r_n}})\, J_r, \tag{58}$$

$$J_{u_{\rm old}} = \exp(-\mathcal{L}_{\chi_{u_1}}) \exp(-\mathcal{L}_{\chi_{u_2}}) ... \exp(-\mathcal{L}_{\chi_{u_{n'}}})\, J_u. \tag{59}$$

In other words, by using the above transformations (58) and (59), we are able to express the new actions into the Boyer–Lindquist variables, i.e. $r(\lambda)$, $\theta(\lambda)$, L_z and etc.

As we mentioned earlier, the accuracy of the new system depends on the position of the reference orbit r_c and how we deviate the system from the reference orbit, i.e. $\delta\, dr$. We observed that by choosing

$$r_c = \frac{p}{1-e^2} + e(1 - 10\, e)M, \qquad \delta = r_c \frac{a}{e\, M^2} \tag{60}$$

the new system obtains better accuracy. However, we should mention that there isn't any general prescription on how one should set r_c and δ. Note that our scheme diverges when the Kerr parameter tends to zero. In the Schwarzschild limit one should follow the approach suggested in [20].

In Figs. 2-3 we illustrate the aforementioned comparison for different n and n'. To illustrate the $J_{r_{\rm old}}$ and $J_{u_{\rm old}}$, we use *KerrGeodesics* package of the *Black Hole Perturbation Toolkit* repository [35] since $J_{r_{\rm old}}$ and $J_{u_{\rm old}}$ are functions of $r(\lambda)$ and $\theta(\lambda)$ respectively. The numerical values for $\overline{J}_r$ and $\overline{J}_u$ are computed from (38)- (39) where we numerically integrate them for given values of E, L_z, and Q from the parameters $\{a, p, e, \iota_0\}$ [7, 36]. Figs. 2-3 show that by increasing the number of canonical transformations, the actions converge to their numerical values, indicating that the approximate system is converging to the original one. More precisely, applying more and more canonical transformations reduces the oscillations of the actions around their numerical values (see Fig. 2), while for the number of transformations shown in Fig. 3 the convergence appears to be exponential. Although the actions are converging, they have still a small oscillation around the value they converge to.

As mentioned in Sec. I, modeling an EMRI system requires accuracy below 10^{-5} during one cycle. Thus, in our approximation system, we require to have an error not greater than 10^{-5}. Therefore, we set 10 canonical transformations for the radial part and 7 canonical transformations for the angular part. For these numbers of canonical transformations, the oscillations of the actions compared to the numerical values are small enough. The accuracy of the radial part by setting $n = 10$ is in the range $\sim 10^{-11} - 10^{-9}$ for small eccentricity, i.e. ~ 0.1, and by increasing the eccentricity the accuracy is decreasing to $\sim 10^{-5}$ for eccentricity ~ 0.5; we observed that by increasing the numbers of canonical transformations for the radial part, the accuracy does not improve significantly. However, for the angular part for $n' = 7$ we

[2] We substitute $\tilde{J}_\nu = J_\nu + L_{zc} - \tilde{L}_{zc}$ and $\tilde{J}_t = J_t + p_{tc} - \tilde{p}_{tc}$ into the Eq. (57). Therefore, the Hamiltonian (56) is in terms of the $\{J_t, J_r, J_u, J_\nu\}$. Note that, the conjugate angles for this system are denoted by $\{\psi_r, \psi_u, \psi_\nu, \psi_t\}$.

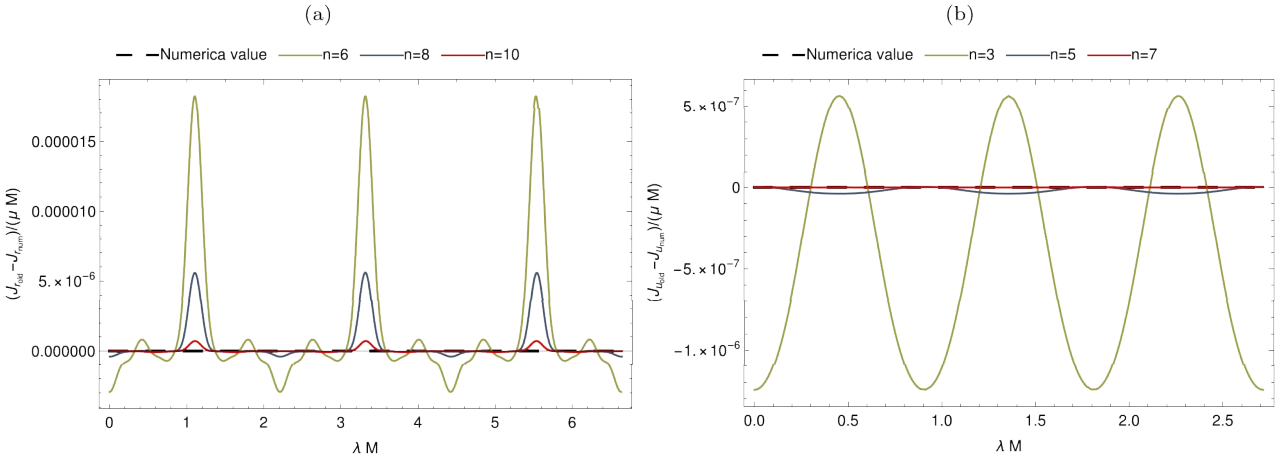

FIG. 2: These plots show by an increasing the number of transformations how the actions $J_{r_{\rm old}}$ and $J_{u_{\rm old}}$ are converging to their numerical values. For these figures we set $a = 0.99M$, $e = 0.3$, semilatus rectum $p = 10M$, and initial inclination $\iota_0 = \pi/8$.

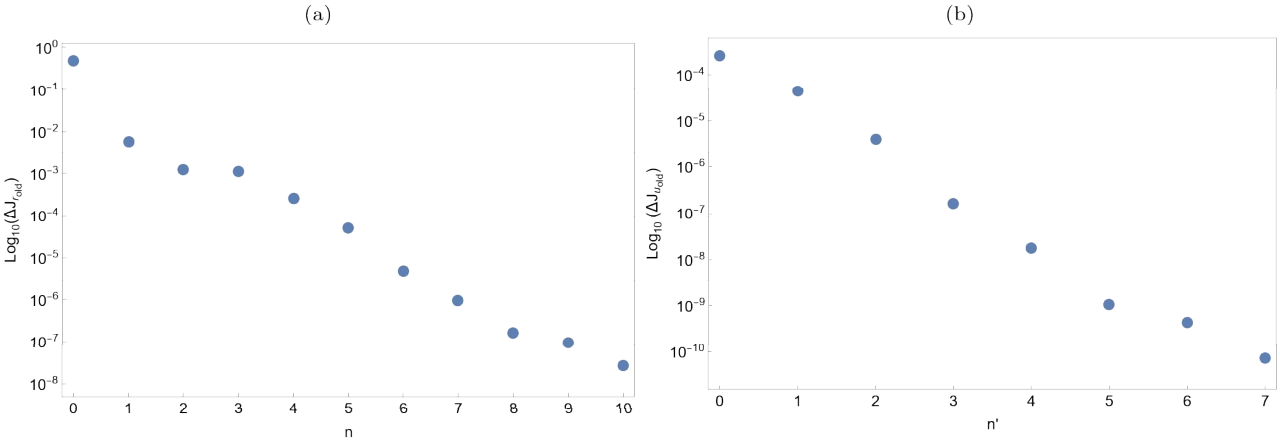

FIG. 3: These plots show $\Delta J_{r_{old}}$ and $\Delta J_{u_{old}}$, as defined in Eq. (61), at each order n and n' respectively of a canonical transformation. For these figures we set $a = 0.99M$, $e = 0.3$, semilatus rectum $p = 10M$, and initial inclination $\iota_0 = \pi/8$.

get the accuracy $\sim 10^{-14} - 10^{-9}$ for small eccentricities $e \sim 0.1$, while when the eccentricity is approaching to 0.5 the accuracy drops to $\sim 10^{-11} - 10^{-8}$. For a fixed eccentricity, the accuracy decreases as the Kerr parameter increases, while increasing the initial inclination does not have much influence on the accuracy of the system. Tables I and II show the accuracy of the resulting system for the radial part and tables III and IV show the accuracy achieved for the angular part for two different initial conditions. Table V shows a case of how the angular part depends on the inclination. In these tables, the Δ and δ correspond to the relative errors and are defined as

$$\Delta X = |1 - \frac{X_{\rm max}}{X_{\rm num}}|, \qquad \delta X = |1 - \frac{X_{\rm min}}{X_{\rm max}}|, \tag{61}$$

where the $X_{\rm max}$ and $X_{\rm min}$ are the maximum and the minimum values of the oscillation of each variable X and $X_{\rm num}$ denote its numerical value. In these tables, the actions are computed from Eqs. (58) and (59) and $\Upsilon_i = \partial H_{AA}/\partial J_i$; the numerical values of the frequencies $\Upsilon_{i_{\rm num}}$ are obtained from the *KerrGeodesics* package of the *Black Hole Perturbation Toolkit* repository.

TABLE I: Here we provide the order of the relative errors for quantities related with the radial motion. $\Delta J_{r_{\rm old}}$ represents the relative error of the maximum value of the $J_{r_{\rm old}}$ with respect to its numerical values; $\delta J_{r_{\rm old}}$ shows the relative error between the maximum and minimum values of the $J_{\rm old}$; and the $\Delta\Upsilon_r$ shows the relative error of the maximum Υ_r and its numerical value, i.e. $\Upsilon_{r_{\rm num}}$. The orbit has semi-latus rectum $p = 10M$ and inclination $\iota_0 = \frac{\pi}{8}$, and to approximate the system 10 canonical transformations have been applied. See Sec. III.3 for more details.

a	e	$\mathcal{O}(\Delta J_{r_{\rm old}})$	$\mathcal{O}(\delta J_{r_{\rm old}})$	$\mathcal{O}(\Delta\Upsilon_r)$
0.1	0.1	10^{-9}	10^{-9}	10^{-11}
	0.2	10^{-8}	10^{-8}	10^{-9}
	0.3	10^{-6}	10^{-6}	10^{-7}
	0.4	10^{-5}	10^{-5}	10^{-5}
	0.5	10^{-4}	10^{-4}	10^{-4}
0.3	0.1	10^{-10}	10^{-10}	10^{-12}
	0.2	10^{-8}	10^{-8}	10^{-9}
	0.3	10^{-6}	10^{-6}	10^{-7}
	0.4	10^{-5}	10^{-5}	10^{-6}
	0.5	10^{-4}	10^{-4}	10^{-5}
0.5	0.1	10^{-9}	10^{-9}	10^{-11}
	0.2	10^{-9}	10^{-7}	10^{-10}
	0.3	10^{-7}	10^{-7}	10^{-8}
	0.4	10^{-5}	10^{-5}	10^{-6}
	0.5	10^{-4}	10^{-4}	10^{-5}
0.7	0.1	10^{-7}	10^{-7}	10^{-10}
	0.2	10^{-7}	10^{-7}	10^{-8}
	0.3	10^{-7}	10^{-6}	10^{-8}
	0.4	10^{-6}	10^{-5}	10^{-7}
	0.5	10^{-5}	10^{-5}	10^{-5}
0.99	0.1	10^{-7}	10^{-7}	10^{-10}
	0.2	10^{-6}	10^{-6}	10^{-8}
	0.2	10^{-7}	10^{-7}	10^{-8}
	0.4	10^{-6}	10^{-6}	10^{-5}
	0.5	10^{-5}	10^{-5}	10^{-5}

III.4. Perturbed-Kerr trajectory

Up to here, we have just expressed up to a certain accuracy the Hamiltonian in the AA variables and the respective generating functions have been derived. In what follows we use the acquired system to generate the trajectories in AA variables.

In our approximative formalism, the evolution equations are given by

TABLE II: As in Table I, but for an orbit with semilatus rectum $p = 30M$ and inclination $\iota_0 = \frac{\pi}{3}$.

a	e	$\mathcal{O}(\Delta J_{r_{\rm old}})$	$\mathcal{O}(\delta J_{r_{\rm old}})$	$\mathcal{O}(\delta\Upsilon_r)$
0.1	0.1	10^{-11}	10^{-11}	10^{-10}
	0.2	10^{-8}	10^{-8}	10^{-7}
	0.3	10^{-6}	10^{-6}	10^{-6}
	0.4	10^{-5}	10^{-5}	10^{-5}
	0.5	10^{-3}	10^{-3}	10^{-4}
0.3	0.1	10^{-7}	10^{-7}	10^{-10}
	0.2	10^{-8}	10^{-8}	10^{-8}
	0.3	10^{-6}	10^{-6}	10^{-6}
	0.4	10^{-5}	10^{-5}	10^{-6}
	0.5	10^{-3}	10^{-3}	10^{-4}
0.5	0.1	10^{-7}	10^{-7}	10^{-10}
	0.2	10^{-7}	10^{-8}	10^{-8}
	0.3	10^{-6}	10^{-7}	10^{-6}
	0.4	10^{-5}	10^{-5}	10^{-5}
	0.5	10^{-3}	10^{-3}	10^{-4}
0.7	0.1	10^{-7}	10^{-7}	10^{-9}
	0.2	10^{-6}	10^{-6}	10^{-7}
	0.3	10^{-7}	10^{-7}	10^{-7}
	0.4	10^{-5}	10^{-5}	10^{-6}
	0.5	10^{-3}	10^{-3}	10^{-4}
0.99	0.1	10^{-5}	10^{-5}	10^{-8}
	0.2	10^{-6}	10^{-6}	10^{-7}
	0.3	10^{-5}	10^{-5}	10^{-6}
	0.4	10^{-4}	10^{-4}	10^{-5}
	0.5	10^{-3}	10^{-3}	10^{-4}

$$\Upsilon_r = \dot{\psi}_r = \frac{\partial H_{AA}}{\partial J_r}, \tag{62}$$

$$\Upsilon_u = \dot{\psi}_u = \frac{\partial H_{AA}}{\partial J_u}, \tag{63}$$

$$\Upsilon_\nu = \dot{\psi}_\nu = \frac{\partial H_{AA}}{\partial J_\nu}, \tag{64}$$

$$\Upsilon = \dot{\psi}_t = \frac{\partial H_{AA}}{\partial J_t}, \tag{65}$$

where Υ_i denotes the approximative Mino-time frequency and over-dot denotes the derivative with respect to the Mino time. The transformation (31) implies that $\Upsilon_u = \Upsilon_\theta$ for the Schwarzschild case. For the Kerr case, it's not so obvious that this relation should hold, we have confirmed, however, numerically that it does hold.

From the above equations of motion, we derive the trajectories in the AA phase space $\{J_r, J_u, J_\nu, J_t, \psi_r, \psi_u, \psi_\nu, \psi_t\}$. We apply the Lie series (25) to transform the above approximative trajectories in terms of the Boyer-Lindquist coordinates. In order to achieve this, we start from the point at which no Lie series has been applied yet, i.e. from the

TABLE III: Here we provide the order of the relative errors for quantities related to the angular motion. $\Delta J_{u_{\rm old}}$ represents the relative error of the maximum value of the $J_{u_{\rm old}}$ with respect to its numerical values; $\delta J_{u_{\rm old}}$ shows the relative error between the maximum and minimum values of the $J_{u_{\rm old}}$; and the $\Delta\Upsilon_u$ shows the relative error of the maximum Υ_u and its numerical value, i.e. $\Upsilon_{u_{\rm num}}$. The orbit has semilatus rectum $p = 10M$ and inclination $\iota_0 = \frac{\pi}{8}$ to approximate the system 7 canonical transformations have been applied. See Sec. III.3 for more details.

a	e	$\mathcal{O}(\Delta\Upsilon_u)$	$\mathcal{O}(\Delta Q)$	$\mathcal{O}(\Delta J_{u_{\rm old}})$	$\mathcal{O}(\delta J_{u_{\rm old}})$
0.1	0.1	10^{-11}	10^{-10}	10^{-9}	10^{-10}
	0.2	10^{-11}	10^{-10}	10^{-9}	10^{-10}
	0.3	10^{-11}	10^{-10}	10^{-10}	10^{-12}
	0.4	10^{-11}	10^{-10}	10^{-10}	10^{-11}
	0.5	10^{-11}	10^{-10}	10^{-10}	10^{-10}
0.3	0.1	10^{-12}	10^{-11}	10^{-11}	10^{-10}
	0.2	10^{-12}	10^{-11}	10^{-11}	10^{-11}
	0.3	10^{-12}	10^{-11}	10^{-11}	10^{-11}
	0.4	10^{-11}	10^{-11}	10^{-11}	10^{-11}
	0.5	10^{-10}	10^{-11}	10^{-11}	10^{-11}
0.5	0.1	10^{-11}	10^{-10}	10^{-10}	10^{-10}
	0.2	10^{-11}	10^{-10}	10^{-10}	10^{-10}
	0.3	10^{-11}	10^{-10}	10^{-10}	10^{-10}
	0.4	10^{-10}	10^{-10}	10^{-10}	10^{-10}
	0.5	10^{-9}	10^{-10}	10^{-10}	10^{-10}
0.7	0.1	10^{-10}	10^{-10}	10^{-10}	10^{-10}
	0.2	10^{-10}	10^{-10}	10^{-10}	10^{-10}
	0.3	10^{-10}	10^{-10}	10^{-10}	10^{-10}
	0.4	10^{-9}	10^{-10}	10^{-10}	10^{-10}
	0.5	10^{-9}	10^{-10}	10^{-10}	10^{-10}
0.99	0.1	10^{-9}	10^{-10}	10^{-9}	10^{-9}
	0.2	10^{-9}	10^{-10}	10^{-9}	10^{-9}
	0.3	10^{-10}	10^{-9}	10^{-9}	10^{-9}
	0.4	10^{-9}	10^{-9}	10^{-9}	10^{-9}
	0.5	10^{-8}	10^{-9}	10^{-9}	10^{-9}

Eqs. (31), (45), (50), in which we replaced u with ${\psi_u}^0$ and ν with ${\psi_\nu}^0$. Namely, in that step, the transformation

TABLE IV: As in Table III, but for an orbit with semilatus rectum $p = 30M$ and inclination $\iota_0 = \frac{\pi}{3}$.

a	e	$\mathcal{O}(\Delta\Upsilon_u)$	$\mathcal{O}(\Delta Q)$	$\mathcal{O}(\Delta J_{u_{\rm old}})$	$\mathcal{O}(\delta J_{u_{\rm old}})$
0.1	0.1	10^{-12}	10^{-12}	10^{-10}	10^{-10}
	0.2	10^{-12}	10^{-12}	10^{-10}	10^{-10}
	0.3	10^{-12}	10^{-12}	10^{-11}	10^{-11}
	0.4	10^{-12}	10^{-12}	10^{-11}	10^{-11}
	0.5	10^{-11}	10^{-12}	10^{-11}	10^{-11}
0.3	0.1	10^{-14}	10^{-14}	10^{-12}	10^{-13}
	0.2	10^{-11}	10^{-12}	10^{-11}	10^{-11}
	0.3	10^{-12}	10^{-11}	10^{-11}	10^{-11}
	0.4	10^{-11}	10^{-11}	10^{-11}	10^{-11}
	0.5	10^{-10}	10^{-11}	10^{-10}	10^{-10}
0.5	0.1	10^{-13}	10^{-13}	10^{-12}	10^{-12}
	0.2	10^{-13}	10^{-13}	10^{-12}	10^{-12}
	0.3	10^{-13}	10^{-13}	10^{-12}	10^{-12}
	0.4	10^{-11}	10^{-13}	10^{-13}	10^{-11}
	0.5	10^{-10}	10^{-11}	10^{-11}	10^{-10}
0.7	0.1	10^{-12}	10^{-12}	10^{-11}	10^{-11}
	0.2	10^{-12}	10^{-12}	10^{-11}	10^{-11}
	0.3	10^{-12}	10^{-12}	10^{-12}	10^{-11}
	0.4	10^{-11}	10^{-11}	10^{-11}	10^{-11}
	0.5	10^{-10}	10^{-11}	10^{-10}	10^{-10}
0.99	0.1	10^{-11}	10^{-11}	10^{-10}	10^{-10}
	0.2	10^{-11}	10^{-11}	10^{-10}	10^{-10}
	0.3	10^{-11}	10^{-11}	10^{-11}	10^{-11}
	0.4	10^{-11}	10^{-12}	10^{-11}	10^{-11}
	0.5	10^{-10}	10^{-10}	10^{-10}	10^{-10}

TABLE V: As in Table III, but for $\{a, p, e\} = \{0.99, 10, 0.5\}$ and different inclinations.

ι	$\mathcal{O}(\Delta\Upsilon_u)$	$\mathcal{O}(\Delta Q)$	$\mathcal{O}(\Delta J_{u_{\rm old}})$	$\mathcal{O}(\delta J_{u_{\rm old}})$
$\pi/8$	10^{-8}	10^{-9}	10^{-9}	10^{-9}
$\pi/7$	10^{-8}	10^{-9}	10^{-9}	10^{-9}
$\pi/6$	10^{-8}	10^{-9}	10^{-9}	10^{-9}
$\pi/5$	10^{-8}	10^{-9}	10^{-9}	10^{-9}
$\pi/4$	10^{-8}	10^{-9}	10^{-9}	10^{-9}
$\pi/3$	10^{-9}	10^{-9}	10^{-10}	10^{-9}

is given by

$$r_{\rm old} = r_c + \sqrt{\frac{2\,J_r^0}{m_c\,\Omega_{r0}}}\sin\psi_r^0, \tag{66}$$

$$\theta_{\rm old} = \arccos\left(\sqrt{1-\frac{(J_\nu^0+L_{zc})^2}{(J_u^0+p_{uc})^2}}\sin\psi_u^0\right), \tag{67}$$

$$\phi_{\rm old} = \psi_\nu^0+\psi_u^0 + \arctan\left(\frac{\left(\frac{J_\nu^0+L_{zc}}{J_u^0+p_{uc}}-1\right)\cos\psi_u^0\sin\psi_u^0}{1+\left(\frac{J_\nu^0+L_{zc}}{J_u^0+p_{uc}}-1\right)\sin^2\psi_u^0}\right), \tag{68}$$

$$t_{\rm old} = \psi_t^0. \tag{69}$$

Then the approximative trajectories in Boyer-Lindquist coordinates are determined from

$$r_{\rm new} = [\exp(\mathcal{L}_{\chi_{r_{10}}})\exp(\mathcal{L}_{\chi_{r_9}})...\exp(\mathcal{L}_{\chi_{r_1}})]\,r_{\rm old}, \tag{70}$$

$$\theta_{\rm new} = [\exp(\mathcal{L}_{\chi_{u_7}})\exp(\mathcal{L}_{\chi_{u_6}})...\exp(\mathcal{L}_{\chi_{u_1}})]\,\theta_{\rm old}, \tag{71}$$

$$\phi_{\rm new} = [\exp(\mathcal{L}_{\chi_{r_{10}}})\exp(\mathcal{L}_{\chi_{r_9}})...\exp(\mathcal{L}_{\chi_{r_1}})] \times[\exp(\mathcal{L}_{\chi_{u_7}})\exp(\mathcal{L}_{\chi_{u_6}})...\exp(\mathcal{L}_{\chi_{u_1}})]\,\phi_{\rm old}, \tag{72}$$

$$t_{\rm new} = [\exp(\mathcal{L}_{\chi_{r_{10}}})\exp(\mathcal{L}_{\chi_{r_9}})...\exp(\mathcal{L}_{\chi_{r_1}})] \times[\exp(\mathcal{L}_{\chi_{u_7}})\exp(\mathcal{L}_{\chi_{u_6}})...\exp(\mathcal{L}_{\chi_{u_1}})]\,t_{\rm old}. \tag{73}$$

By applying the above Lie series transformations we essentially express $r_{\rm new}$, $\theta_{\rm new}$, $\phi_{\rm new}$, $t_{\rm new}$ as functions of $\{J_r, J_u, J_\nu, J_t, \psi_r, \psi_u, \psi_\nu, \psi_t\}$. Note that, since the χ_{u_i} are independent of J_r^0 and ψ_r^0, Eq. (70) is independent of $\exp(\mathcal{L}_{\chi_{u_i}})$. In the same fashion Eq. (71) is independent of $\exp(\mathcal{L}_{\chi_{r_i}})$. On the other hand, both χ_{u_i} and χ_{r_i} depend on J_t^0 and J_ν^0, that is why we apply both Lie series transformations in the case of Eqs. (72), (73). In the latter case, the resulting equations for $\phi_{\rm new}$ and $t_{\rm new}$ have the following form

$$\phi_{\rm new} = \psi_\nu+\psi_u+\Delta\phi_r[\chi_{r_i}]+\Delta\phi_\theta[\chi_{u_i}], \tag{74}$$

$$t_{\rm new} = \psi_t+\Delta t_r[\chi_{r_i}]+\Delta t_\theta[\chi_{u_i}], \tag{75}$$

where $\Delta\phi_r[\chi_{r_i}]$ and $\Delta t_r[\chi_{r_i}]$ correspond to the parts of $\phi_{\rm new}$ and $t_{\rm new}$ derived from applying the radial generating functions χ_{r_i}; and the $\Delta\phi_\theta[\chi_{u_i}]$ and $\Delta t_\theta[\chi_{u_i}]$ are determine from applying the angular generating functions χ_{u_i}. Equations (74) and (75) are similar to the expressions given in Ref. [28]

$$\phi(\lambda) = \phi_0+\overline{\Upsilon}_\phi\lambda+\Delta\phi_r[r(\lambda)]+\Delta\phi_\theta[\theta(\lambda)], \tag{76}$$

$$t(\lambda) = t_0+\overline{\Upsilon}\lambda+\Delta t_r[r(\lambda)]+\Delta t_\theta[\theta(\lambda)], \tag{77}$$

where the over-line refers to the exact (not approximated) value of the frequencies. By comparing the Eq. (76) with the Eq. (74) we conclude that $\psi_\phi = \psi_\nu+\psi_u$ and this indicates that the orbital plane precession frequency is $\Upsilon_\nu = \Upsilon_\phi - \Upsilon_u$.

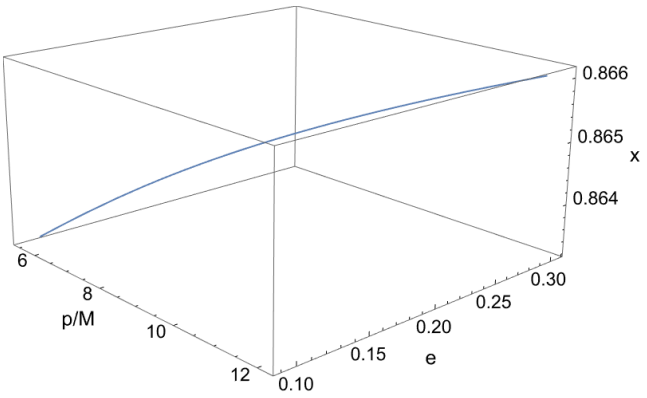

FIG. 4: Adiabatic evolution of the orbital parameters during an inspiral into Kerr black hole. The Kerr parameter is $a = 0.5M$ while the orbital parameters (p, e, x) drift gradually from $(12M, 0.3, 0.8660)$ to $(6.08413, 0.10579, 0.86357)$.

IV. GRAVITATIONAL WAVE FLUXES AND GENERIC ADIABATIC INSPIRAL

We now include gravitational backreaction into our scheme. In this case, the secondary is inspiraling, and now not only the angles but also the actions change during the evolution. The equations describing the respective motion can then be expanded in mass ratio q as

$$\frac{{\rm d}\psi_i}{{\rm d}t} = \Upsilon_i(\mathbf{J}) + q\,f_i^{(1)}(\psi_r,\psi_u,\mathbf{J})+\mathcal{O}(q^2), \tag{78}$$

$$\frac{{\rm d}J_i}{{\rm d}t} = q\,F_i^{(1)}(\psi_r,\psi_u,\mathbf{J})+\mathcal{O}(q^2), \tag{79}$$

where $f_i^{(1)}$ provides the instantaneous first-order corrections to the geodesic frequency, while $F_i^{(1)}$ provides the flux of the actions (or equivalently of the orbital parameters).

Based on the two timescale separation, i.e. on the fact that the orbital timescale corresponding to the periods of the geodesic motion (determined by frequencies Υ_i) is much smaller than the inspiral timescale, we can implement the adiabatic approximation. We average over the invariant torus parametrized by the angles in order to obtain averaged fluxes of the integrals of motion (actions) and hence the rate of change of the orbital parameters. The equations of motion at the leading order then read

$$\frac{{\rm d}\psi_i(t)}{{\rm d}t} = \Upsilon_i(\mathbf{J}(\mathbf{t})), \tag{80}$$

$$\frac{{\rm d}J_i(t)}{{\rm d}t} = q\langle F_i^{(1)}\rangle(\mathbf{J}(\mathbf{t})), \tag{81}$$

where the averaged functions $\langle F_i^{(1)}\rangle$ are the averaged fluxes.

To calculate the fluxes of (p, e, ι_0) we first have to calculate the fluxes of $\mathbf{C} = (E, L_z, Q)$. We employed the Teukolsky formalism to calculate the fluxes of the three

TABLE VI: Table of constants of motion fluxes through the horizon and to infinity for $a = 0.9M$, $p = 6M$.

e	ι_0	$(M/\mu)^2\left\langle \frac{dE^\infty}{dt}\right\rangle$	$(M/\mu)^2\left\langle \frac{dE^H}{dt}\right\rangle$	$M/\mu^2\left\langle \frac{dL_z^\infty}{dt}\right\rangle$	$M/\mu^2\left\langle \frac{dL_z^H}{dt}\right\rangle$	$1/(M\mu^2)\left\langle \frac{dQ^\infty}{dt}\right\rangle$	$1/(M\mu^2)\left\langle \frac{dQ^H}{dt}\right\rangle$
0.1	20°	5.87342×10^{-4}	-4.25247×10^{-6}	8.53698×10^{-3}	-6.71479×10^{-5}	5.24007×10^{-3}	-3.30062×10^{-5}
	40°	6.18311×10^{-4}	-3.94869×10^{-6}	7.63084×10^{-3}	-7.72832×10^{-5}	2.02268×10^{-2}	-1.04495×10^{-4}
	60°	6.83339×10^{-4}	-3.32657×10^{-6}	6.07821×10^{-3}	-1.11064×10^{-4}	4.32189×10^{-2}	-1.50541×10^{-4}
	80°	8.05842×10^{-4}	-9.49684×10^{-7}	3.6253×10^{-3}	-1.90003×10^{-4}	7.18506×10^{-2}	-8.40648×10^{-5}
0.3	20°	6.80194×10^{-4}	-5.86914×10^{-6}	8.62328×10^{-3}	-7.76597×10^{-5}	5.22018×10^{-3}	-4.45666×10^{-5}
	40°	7.26381×10^{-4}	-5.84039×10^{-6}	7.83838×10^{-3}	-9.98056×10^{-5}	2.04352×10^{-2}	-1.44068×10^{-4}
	60°	8.30438×10^{-4}	-5.17799×10^{-6}	6.49511×10^{-3}	-1.6471×10^{-4}	4.50611×10^{-2}	-2.12317×10^{-4}
	80°	1.08148×10^{-3}	4.96873×10^{-9}	4.36954×10^{-3}	-3.44232×10^{-4}	8.16276×10^{-2}	-8.57416×10^{-5}
0.5	20°	7.9204×10^{-4}	-7.75248×10^{-6}	8.28526×10^{-3}	-9.01706×10^{-5}	4.9126×10^{-3}	-5.82767×10^{-5}
	40°	8.65272×10^{-4}	-8.07832×10^{-6}	7.75244×10^{-3}	-1.35035×10^{-4}	1.97217×10^{-2}	-1.92668×10^{-4}
	60°	1.03918×10^{-3}	-6.50404×10^{-6}	6.83898×10^{-3}	-2.63457×10^{-4}	4.58815×10^{-2}	-2.84301×10^{-4}
	80°	4.63908×10^{-3}	4.06096×10^{-5}	1.5077×10^{-2}	-1.12034×10^{-3}	2.31186×10^{-1}	1.64899×10^{-4}

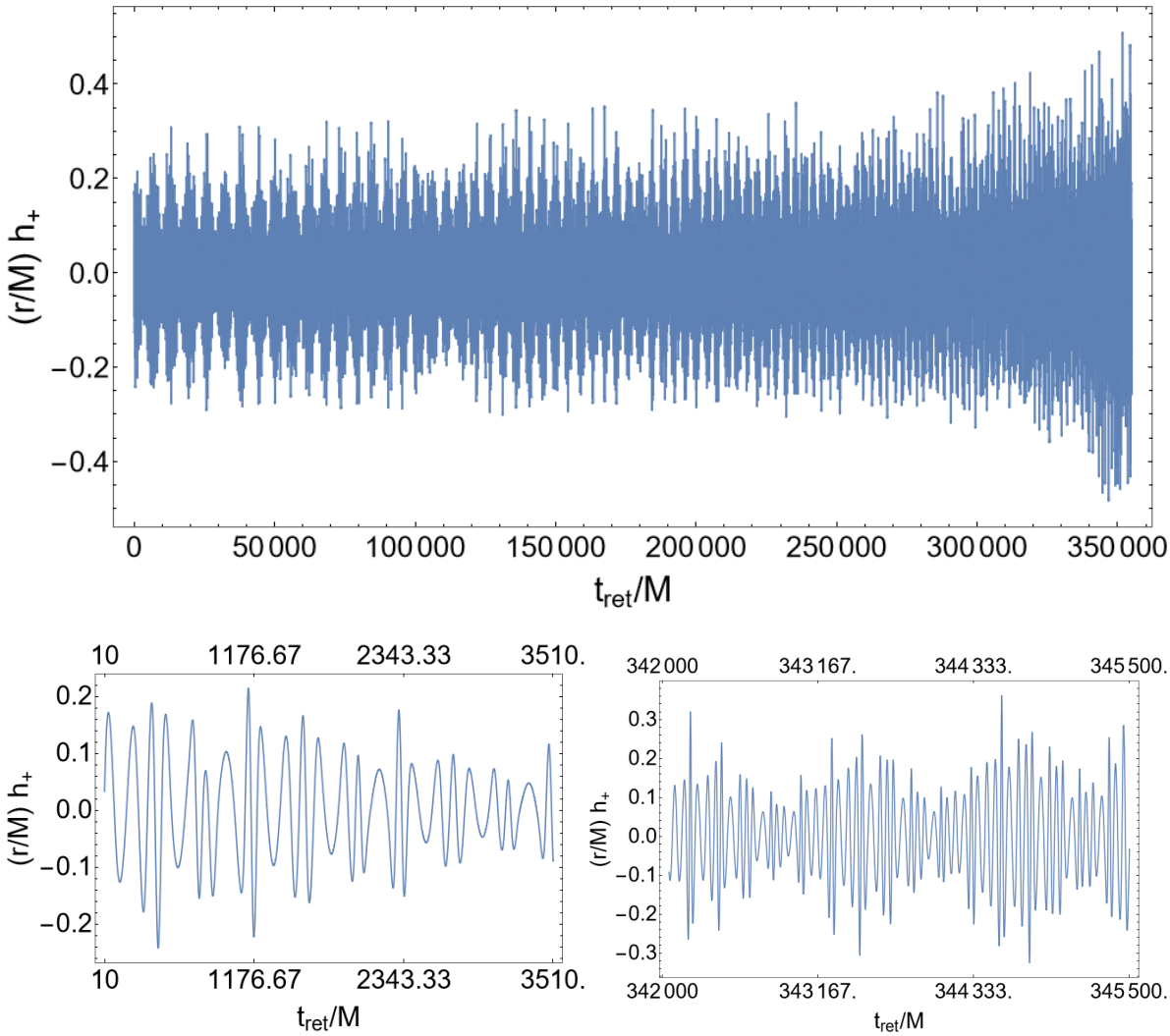

FIG. 5: The component h_+ of the waveform produced during the inspiral shown in Fig. 4 as observed from the equatorial plane. The complete waveform (top) is depicted in detail at the early stage (bottom left) and late stage (bottom right) of the modelled inspiral. The mass ratio is $q = 10^{-3}$.

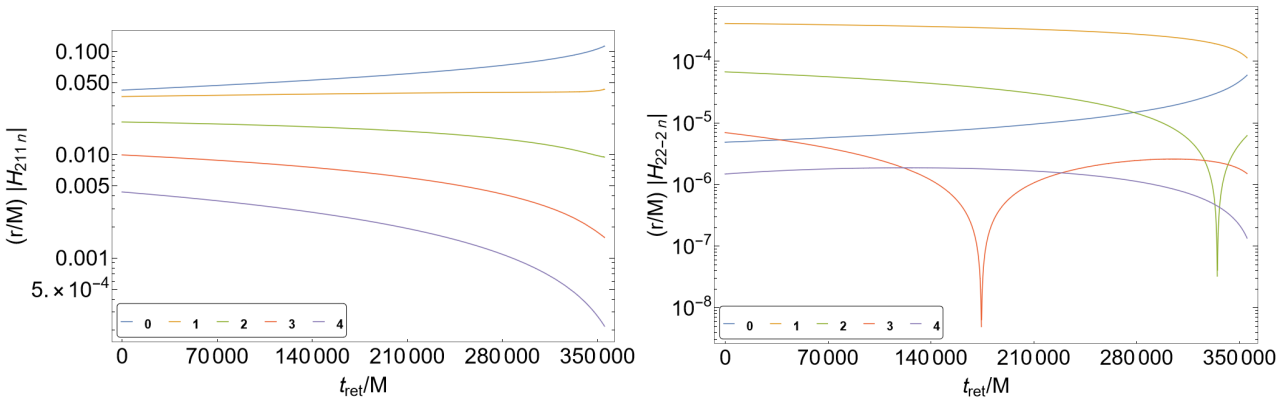

FIG. 6: Logarithmic plots of H_{211n} (left) and H_{22-2n} (right) during the inspiral shown in Fig. 4.

independent constants of motion C_i through the infinity and the primary's black hole horizon. This is in more detail described in Appendix D. In full analogy with [36] we present table VI with the flux values $\left\langle \frac{\mathrm{d}C_i^{\infty,H}}{\mathrm{d}t} \right\rangle$ for $a = 0.9M$, $p = 6M$.

It is difficult to determine the relative errors of the values in the table. It is clear, however, that the dominant contribution to the error comes from our approximation of the geodesic motion, this fact is more prominent for larger values of e. When discussing the results of the table VI we have to keep in mind that the values $a = 0.9M$, $p = 6M$ are extreme in the sense that $0.9M$ is a large value for our perturbation parameter a while $p = 6M$ means we are getting closer to the last stable spherical orbit. Hence, fluxes for larger values of p and/or smaller values of a would be more accurate.

Regardless of the comment in the previous paragraph, we can conclude that the error grows with eccentricity which is an expected result since our geodesics are derived using expansions from a Kerr spherical orbit and a Schwarzschild stable circular orbit. For $e = 0.5$ the values of the fluxes cease to be reliable, since in most cases only the first significant digit seems to be correct (see the respective table in [36].). An interesting aspect here is the dependence on the inclination that is non-trivial and it is relevant for high eccentricity and small semi-latus rectum, which can be seen particularly in the last row of the table VI, where the error magnitude is the largest. This has its source already at the geodesic level, where we checked numerically that our approximation scheme does not behave well when the trajectory passes close to the central body.

To better illustrate the error introduced by our geodesic approximation we created a table of relative errors VII corresponding to the Table VI; the relative error is computed with respect to the fluxes from exact geodesics calculated through the *KerrGeodesics* package) and using the same new code for the Teukolsky amplitudes. As already mentioned, the error depends on the eccentricity, for $e = 0.1$ the relative error is sufficiently small and comparable with realistic values of mass ratio. On the other hand, the errors for $e = 0.5$ show the limits of the approximation. The values in the last row of the Table VI corresponding to the inclination $\iota_0 = 80°$ are of a particular interest as the error is of the order of unity. This inclination dependence becomes noticeable only when close to the horizon. To be more specific it is the radial part of the geodesic motion which deviates substantially, for instance the relative error of the radial frequency is 0.18 while the angular part is well-behaved even for this highly inclined and eccentric orbit with error of the order 10^{-9} (see Table V.). In general, we expect that such large errors in the fluxes should not consist a problem for initially not very eccentric orbits $e < 0.5$, since by the time the inspiral would reach close to the horizon of the primary black hole the eccentricity will be sufficiently small. Details of how the errors in fluxes emerge are discussed in Appendix D.

Once the fluxes of constants of motion are calculated we can easily determine the rate of change of the three orbital parameters (p, e, x) where $x = \cos(\iota_0)$. For this, we have created a grid in the (p, e, x) space to interpolate the fluxes (see Appendix D). Solving the system of equations (81) is then a straightforward task with the result being the three parameters as functions of the coordinate (Boyer-Lindquist) time $(p(t), e(t), x(t))$.

We are now going to demonstrate our scheme on an inspiral with $a = 0.5M$ and initial condition

$$(p_{\rm ini}, e_{\rm ini}, x_{\rm ini}) = (12M, 0.3, \cos(30°)) = (12M, 0.3, 0.86602).$$

After adiabatically evolving the parameters we get

$$(p_{\rm fin}, e_{\rm fin}, x_{\rm fin}) = (6.08413, 0.10579, 0.86357),$$

at the coordinate time $t_{\rm insp} = 355M/q$. The evolution of this eccentric non-equatorial inspiral is depicted in Fig. 4. Note that the eccentricity of the inspiral becomes sufficiently small ($e \sim 0.1$) by the end of the computation, i.e. by the time it gets closer to the horizon.

TABLE VII: Table of relative errors of the total fluxes presented in table VI. The relative errors are calculated with respect to the fluxes sourced by exact formulas for Kerr geodesics.

e	ι_0	$\delta\left\langle\frac{\mathrm{d}E^\infty}{\mathrm{d}t}\right\rangle = \delta\dot{E}^\infty$	$\delta\dot{E}^H$	$\delta\dot{L}_z^\infty$	$\delta\dot{L}_z^H$	$\delta\dot{Q}^\infty$	$\delta\dot{Q}^H$
0.1	20°	4.27×10^{-7}	1.12×10^{-8}	3.88×10^{-7}	4.45×10^{-8}	5.05×10^{-8}	2.18×10^{-7}
	40°	6.17×10^{-7}	1.10×10^{-7}	5.39×10^{-7}	1.51×10^{-7}	4.01×10^{-7}	1.88×10^{-7}
	60°	6.90×10^{-8}	2.99×10^{-8}	8.35×10^{-8}	2.61×10^{-8}	6.77×10^{-8}	1.78×10^{-7}
	80°	5.54×10^{-7}	2.88×10^{-7}	4.82×10^{-7}	2.56×10^{-7}	3.37×10^{-7}	1.02×10^{-6}
0.3	20°	1.84×10^{-4}	9.51×10^{-5}	1.85×10^{-4}	5.41×10^{-6}	1.57×10^{-4}	1.84×10^{-4}
	40°	1.45×10^{-4}	1.78×10^{-4}	1.51×10^{-4}	7.07×10^{-4}	1.22×10^{-4}	1.54×10^{-4}
	60°	1.13×10^{-4}	2.95×10^{-4}	1.28×10^{-4}	3.41×10^{-4}	8.98×10^{-5}	1.49×10^{-4}
	80°	1.60×10^{-3}	4.32×10^{-1}	1.39×10^{-3}	1.02×10^{-3}	1.15×10^{-3}	6.19×10^{-4}
0.5	20°	8.17×10^{-3}	7.09×10^{-2}	7.06×10^{-3}	1.29×10^{-2}	6.66×10^{-3}	9.77×10^{-3}
	40°	1.01×10^{-2}	9.61×10^{-2}	8.30×10^{-3}	1.25×10^{-2}	8.25×10^{-3}	9.50×10^{-3}
	60°	1.83×10^{-2}	1.22×10^{-1}	1.56×10^{-2}	1.94×10^{-2}	1.43×10^{-2}	1.14×10^{-2}
	80°	1.77×10^{0}	1.40×10^{-2}	1.56×10^{0}	2.19×10^{-1}	1.28×10^{0}	3.84×10^{0}

Inspired by Ref. [28], we calculate the gravitational waveforms. The strain $h = h_+ + ih_\times$ can for $r \to \infty$ be written as a sum of individual modes

$$h = \frac{1}{r}\sum_{lmkn} H_{lmkn}(t_{\rm ret},\theta)e^{-i\Phi_{mkn}(t_{\rm ret})+im\phi}, \tag{82}$$

$$H_{lmkn}(t_{\rm ret},\theta) = -2\frac{C^+_{lmkn}(t_{\rm ret})}{\omega^2_{mkn}(t_{\rm ret})}{}_{-2}S_{lm}(\theta, a\omega_{mkn}(t_{\rm ret})), \tag{83}$$

where $t_{\rm ret}$ is the retarded time which can be at the infinity written as $t_{\rm ret} \approx t - r$. The amplitudes H_{lmkn} can be expressed in terms of the coefficients C^+_{lmkn}, which are calculated by solving the inhomogeneous Teukolsky equation (see Appendix D), while ${}_{-2}S_{lm}$ are the spin-weighted spheroidal harmonic functions.

The frequencies ω_{mkn} and the phases Φ_{mkn} read

$$\omega_{mkn} = n\Omega_r + k\Omega_u + m\Omega_\phi, \tag{84}$$

$$\Phi_{mkn}(t_{\rm ret}) = \int_{t_{ret0}}^{t_{\rm ret}} \omega_{mkn}(t)\mathrm{d}t, \tag{85}$$

where $\Omega_i = \Upsilon_i/\Upsilon$ are the fundamental frequencies with respect to the time t, which are calculated using Eqs. (62)-(65).

Knowing the trajectory in the parameter space $(p(t), e(t), x(t))$, we can adiabatically evolve the frequencies Ω_i and C^+_{lmkn}, since they are functions of the orbital parameters. The integration of frequencies in Eq. (85) is just a consequence of the adiabatic evolution of angles in Eq. (80).

Before plotting a waveform we have to fix the mass ratio q because in Eq. (82) both timescales are present, the rapidly oscillating phases Φ_{mkn} and the slowly changing amplitudes H_{lmkn}. In our case, we calculated the waveform from the generic inspiral provided in Fig. 4) and chose the mass ratio to be $q = 10^{-3}$, which is not realistic for an EMRI, but shortens the time of the calculation of the complete waveform whose component h_+ is shown in Fig. 5 for illustration. Similarly to [28], we plot the evolution of the amplitudes for given l, m, k and n to see how their contribution to the sum (82) changes over the time of the inspiral (Fig. 6).

V. CONCLUSION

Writing a Hamiltonian system in action-angle variables provides characteristic quantities of the system, like the fundamental frequencies, in closed form. The split in actions (constants of motion) and angles is a very convenient approach for modelling EMRIs, when adopting the two time-scale approximation. Having this in mind, we have used the Lie series transformation method to express the Hamiltonian giving the geodesic equation of motion in a Kerr spacetime in action angle variables. The advantage in this approach is that all the involved relations are in closed form and the transformation is invertible. Hence, one can go back and forth easily between the Boyer-Lindquist coordinates and the action-angle variables. The drawback is that the approach is perturbative and the Hamiltonian in action-angle variables only approximates the original Hamiltonian. However, one should keep in mind that every model is just an approximation of the real system and what is really required from a model is to be accurate enough for the purpose we need it to serve.

Taking advantage of the fact that the Mino-Carter time allows us to have a separable Hamiltonian for the original system, we split it into a radial part and an angular part. The Hamiltonian function can be expressed purely in the constants of motion and the radial coordinate along with its conjugate momentum, while the Carter constant can be expressed purely in the constants of motion E, L_z and the polar coordinate along with its conjugate momentum. This allowed us to use different perturbation schemes for

each part. Namely, for the radial part, we perturbed around a spherical geodesic orbit in Kerr spacetime, while for the angular we perturbed around an inclined geodesic circular orbit in Schwarzschild spacetime. The latter choice was inspired by the fact that for Schwarschild the inclination is constant and the introduction of the Kerr parameter essentially causes an oscillation around this plane. Actually, this is the reason we preferred to transform first the system from the Boyer-Lindquist coordinates to the polar nodal one before we started the perturbation procedure.

By applying the Lie series method we noticed that after a certain number of transformations, the actions ceased to converge fast to a constant value. This convergence saturation defined the number of transformations we employed to define our Hamiltonian function H_{AA} expressed purely in actions, which approximates the original system. We found that the approximation can be considered satisfactory for eccentricities $e \leq 0.5$; as expected the lower the eccentricity the better the approximation. We found also a weak dependency of the accuracy on the value of the inclination and the value of the Kerr parameter, but these dependencies are insignificant in comparison to the effect that eccentricity has on our approximation.

Having transformed the system in action-angle variables, we used it to model the adiabatic evolution of an EMRI as a showcase of what is possible. The first step for this was the calculation of the fluxes of the constants of motion at infinity and through the horizon of the primary black hole. We used a newly developed frequency domain solver. By comparing our approximative fluxes values with those given in [36] and those computed using the exact solutions of the geodesic orbits in Kerr, we found them to be in good agreement in the domain that our approximation is valid. However, the accuracy in the fluxes is significantly lower than the one reached on the level of the actions. In order to achieve better accuracy, further improvement in our approximative scheme of Kerr geodesics is needed. After this test, we provided an example of adiabatic evolution on a generic inspiral in the Kerr background.

Providing the Hamiltonian of geodesic motion in Kerr in actions and having the whole transformation in closed form allows for several useful applications apart from being able to evolve efficiently an EMRI in the adiabatic approximation. Namely, one can include several forms of perturbations to an EMRI system, like matter distribution around the primary black hole or another stellar compact object in the vicinity of the EMRI, and slightly extend the provided scheme, as was done in [20] for the Schwarzschild background, to be able to evolve and study EMRIs in perturbed systems as well.

ACKNOWLEDGEMENTS

MK, LP, VS and GLG have been supported by the fellowship Lumina Quaeruntur No. LQ100032102 of the Czech Academy of Sciences. L.P. and V.S. acknowledge support by the project "Grant schemes at CU" (reg.no. CZ.02.2.69/0.0/0.0/19_073/0016935). Computational resources were supplied by the project "e-Infrastruktura CZ" (e-INFRA CZ LM2018140) supported by the Ministry of Education, Youth and Sports of the Czech Republic. We would like to thank Vojtěch Witzany for his comments on our work.

[1] Stanislav Babak, Jonathan Gair, Alberto Sesana, Enrico Barausse, Carlos F. Sopuerta, Christopher P. L. Berry, Emanuele Berti, Pau Amaro-Seoane, Antoine Petiteau, and Antoine Klein. Science with the space-based interferometer LISA. V. Extreme mass-ratio inspirals. *Physical Review D*, 95(10):103012, May 2017.

[2] Steve Drasco, Éanna É. Flanagan, and Scott A. Hughes. Computing inspirals in Kerr in the adiabatic regime: I. The scalar case. *Classical and Quantum Gravity*, 22(15):S801–S846, August 2005.

[3] Leor Barack and Adam Pound. Self-force and radiation reaction in general relativity. *Reports on Progress in Physics*, 82(1):,, January 2019.

[4] Adam Pound and Barry Wardell. Black Hole Perturbation Theory and Gravitational Self-Force. page 38, 2022.

[5] Tanja Hinderer and Éanna É. Flanagan. Two-timescale analysis of extreme mass ratio inspirals in kerr spacetime: Orbital motion. *Phys. Rev. D*, 78:064028, Sep 2008.

[6] Vladimir I Arnold, Valery V Kozlov, and Anatoly I Neishtadt. *Mathematical aspects of classical and celestial mechanics*, volume 3. Springer Science & Business Media, 2007.

[7] W. Schmidt. Celestial mechanics in Kerr spacetime. *Classical and Quantum Gravity*, 19(10):2743–2764, May 2002.

[8] Steve Drasco and Scott A. Hughes. Rotating black hole orbit functionals in the frequency domain. *Phys. Rev. D*, 69(4):044015, February 2004.

[9] Maarten van de Meent. Conditions for sustained orbital resonances in extreme mass ratio inspirals. *Physical Review D*, 89(8):084033, April 2014.

[10] Alexandre Le Tiec, Luc Blanchet, and Bernard F. Whiting. The First Law of Binary Black Hole Mechanics in General Relativity and Post-Newtonian Theory. *Phys. Rev. D*, 85:064039, 2012.

[11] Alexandre Le Tiec. First Law of Mechanics for Compact Binaries on Eccentric Orbits. *Phys. Rev. D*, 92(8):084021, 2015.

[12] Ryuichi Fujita, Soichiro Isoyama, Alexandre Le Tiec, Hiroyuki Nakano, Norichika Sago, and Takahiro Tanaka. Hamiltonian Formulation of the Conservative Self-Force Dynamics in the Kerr Geometry. *Class. Quant. Grav.*, 34(13):134001, 2017.

[13] Soichiro Isoyama, Ryuichi Fujita, Hiroyuki Nakano, Norichika Sago, and Takahiro Tanaka. "Flux-balance formulae" for extreme mass-ratio inspirals. *PTEP*,

2019(1):013E01, 2019.
[14] Ryuichi Fujita and Wataru Hikida. Analytical solutions of bound timelike geodesic orbits in Kerr spacetime. *Class. Quant. Grav.*, 26:135002, 2009.
[15] Maarten van de Meent. Analytic solutions for parallel transport along generic bound geodesics in Kerr spacetime. *Class. Quant. Grav.*, 37(14):145007, 2020.
[16] Jonathan R. Gair, Éanna É. Flanagan, Steve Drasco, Tanja Hinderer, and Stanislav Babak. Forced motion near black holes. *Physical Review D*, 83(4):044037, February 2011.
[17] Maarten van de Meent and Niels Warburton. Fast self-forced inspirals. *Classical and Quantum Gravity*, 35(14):144003, July 2018.
[18] Philip Lynch, Maarten van de Meent, and Niels Warburton. Eccentric self-forced inspirals into a rotating black hole. *Classical and Quantum Gravity*, 39(14):145004, July 2022.
[19] Vojtěch Witzany. Action-angle coordinates for black-hole geodesics I: Spherically symmetric and Schwarzschild. *arXiv e-prints*, page arXiv:2203.11952, March 2022.
[20] Lukáš Polcar, Georgios Lukes-Gerakopoulos, and Vojtěch Witzany. Extreme mass ratio inspirals into black holes surrounded by matter. *Physical Review D*, 106(4):044069, August 2022.
[21] C. Efthymiopoulos. Canonical perturbation theory; stability and diffusion in Hamiltonian systems: applications in dynamical astronomy. *Workshop Series of the Asociacion Argentina de Astronomia*, 3:3–146, January 2011.
[22] Alessandro Morbidelli. *Modern celestial mechanics : aspects of solar system dynamics*. Advances in astronomy and astrophysics (Taylor and Francis) ;. CRC Press; 1st edition, London ; New York, 2002.
[23] Luc Blanchet. Gravitational Radiation from Post-Newtonian Sources and Inspiralling Compact Binaries. *Living Reviews in Relativity*, 17(1):2, December 2014.
[24] V. I. Arnold. Proof of a Theorem of A. N. KOLMOGOROV on the Invariance of Quasi-Periodic Motions Under Small Perturbations of the Hamiltonian. *Russian Mathematical Surveys*, 18(5):9–36, October 1963.
[25] Saul A. Teukolsky. Perturbations of a rotating black hole. 1. Fundamental equations for gravitational electromagnetic and neutrino field perturbations. *Astrophys. J.*, 185:635–647, 1973.
[26] Thomas Osburn, Niels Warburton, and Charles R. Evans. Highly eccentric inspirals into a black hole. *Physical Review D*, 93(6):064024, March 2016.
[27] Michael L. Katz, Alvin J. K. Chua, Lorenzo Speri, Niels Warburton, and Scott A. Hughes. Fast extreme-mass-ratio-inspiral waveforms: New tools for millihertz gravitational-wave data analysis. *Physical Review D*, 104(6):064047, September 2021.
[28] Scott A. Hughes, Niels Warburton, Gaurav Khanna, Alvin J. K. Chua, and Michael L. Katz. Adiabatic waveforms for extreme mass-ratio inspirals via multivoice decomposition in time and frequency. *Physical Review D*, 103(10):104014, May 2021.
[29] Viktor Skoupý and Georgios Lukes-Gerakopoulos. Adiabatic equatorial inspirals of a spinning body into a Kerr black hole. *Physical Review D*, 105(8):084033, April 2022.
[30] Emanuele Fiorani, Giovanni Giachetta, and Gennadi Sardanashvily. LETTER TO THE EDITOR: The Liouville-Arnold-Nekhoroshev theorem for non-compact invariant manifolds. *Journal of Physics A Mathematical General*, 36(7):L101–L107, February 2003.
[31] Brandon Carter. Global structure of the Kerr family of gravitational fields. *Phys. Rev.*, 174:1559–1571, 1968.
[32] Yasushi Mino. Perturbative approach to an orbital evolution around a supermassive black hole. *Physical Review D*, 67(8), Apr 2003.
[33] Scott A. Hughes. Evolution of circular, nonequatorial orbits of Kerr black holes due to gravitational-wave emission. *Physical Review D*, 61(8):084004, April 2000.
[34] Cpkerrgeodesics. Mathematica package.
[35] Black Hole Perturbation Toolkit. (bhptoolkit.org), 2022.
[36] Steve Drasco and Scott A. Hughes. Gravitational wave snapshots of generic extreme mass ratio inspirals. *Phys.Rev.*, D73:024027, 2006.
[37] Jesús Palacián. Closed-form normalizations of perturbed two-body problems. *Chaos Solitons and Fractals*, 13(4):853–874, March 2002.
[38] G. W. Hill. Motion of a system of material points under the action of gravitation. *Astronomical Journal*, 27:171–182, April 1913.
[39] Martin Lara. Analytical and Semianalytical Propagation of Space Orbits: The Role of Polar-Nodal Variables. In *Astrodynamics Network AstroNet-II*, volume 44 of *Astrophysics and Space Science Proceedings*, page 151, January 2016.

Appendix A: Polar-nodal coordinate

To describe the generic motion of a particle in a central force field a Cartesian coordinate system $\boldsymbol{x} = \{x, y, z\}$ originating at the position of the force centre is usually not the best choice. A coordinate system in which the coordinates and their conjugate moments can be related to the orbital parameter of the motion sounds as a better idea. Therefore, we are interested in the polar-nodal coordinate system and the Euler angles [37–39].

Let us assume a set of Cartesian coordinates $\boldsymbol{x} = \{x, y, z\}$ along with their conjugate momenta $\boldsymbol{p} = \{p_x, p_y, p_z\}$. In this set of variables, the total angular momentum vector is defined as $\boldsymbol{p_u} = \boldsymbol{x} \times \boldsymbol{p}$. We can decompose this vector as $\boldsymbol{p_u} = p_u \boldsymbol{n}$, where $p_u > 0$ is the measure of the angular momentum and the unit vector $\boldsymbol{n}$, i.e. $|| \boldsymbol{n} || = 1$, is perpendicular to the instantaneous orbital plane.

The inclination of the orbital plane denoted by ι, is determined from the angle between the orbital plane and the equatorial plane or $\boldsymbol{z} \cdot \boldsymbol{n} = \cos \iota$. The angle ν between the positive x axis and the lines of nodes is called the longitude of the ascending node. The line of nodes is the intersection of the orbital plane and the equatorial plane, while the nodes are those two points where the particle passes the equatorial plane. The ascending node is the node where the particle passes the equatorial plane from $-z$ to $+z$. The line of nodes lies along a vector $\boldsymbol{l}$ such that $\boldsymbol{z} \times \boldsymbol{n} = \boldsymbol{l} \sin \iota$. Finally, on the orbital plane, the angle between the ascending node and the particle is defined as the argument of the latitude u. The angles $\{\nu, u, \iota\}$ are known as the Euler angles and the three unit vectors

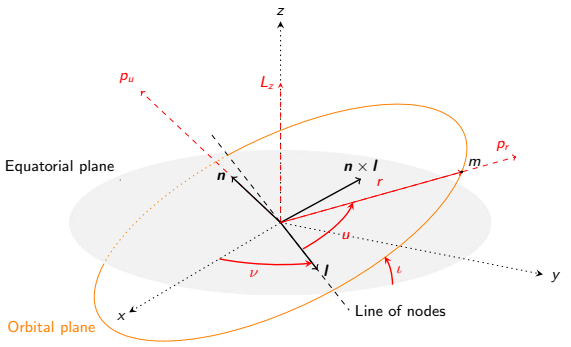

FIG. 7: This figure shows the Euler angles $\{\nu, u, \iota\}$, the nodal frame $\{\boldsymbol{n}, \boldsymbol{l}, \boldsymbol{n}\times\boldsymbol{l}\}$, and the polar-nodal variables $\{r, u, \nu, p_r, p_u, L_z\}$. The unit vector $\boldsymbol{n}$ is perpendicular to the instantaneous orbital plane while the unit vector $\boldsymbol{l}$ lies in the intersection of the equatorial plane and the orbital plane. From $\boldsymbol{n}$ and $\boldsymbol{l}$ the unit vector $\boldsymbol{n}\times\boldsymbol{l}$ which lies on the orbital plane, is defined. The motion of the orbiting body can be described by its radial distance from the central body r, the argument of the latitude u, and the longitude of the ascending node ν along with their conjugate moments p_r, p_u, and L_z respectively.

$\{\boldsymbol{n}, \boldsymbol{l}, \boldsymbol{n}\times\boldsymbol{l}\}$ define the nodal frame. Note that, both unit vectors $\boldsymbol{l}$ and $\boldsymbol{n}\times\boldsymbol{l}$ lie in the orbital plane.

The polar-nodal coordinate consists of the coordinates $\{r, u, \nu\}$ and their conjugate momenta $\{p_r, p_u, L_z\}$. Fig 7 illustrates these variables. The transformation between Cartesian and polar nodal coordinates are given by [38]

$$\begin{aligned}
x &= r\cos u\cos\nu - r\sin u\cos\iota\sin\nu,\\
y &= r\cos u\sin\nu + r\sin u\cos\iota\cos\nu,\\
z &= r\sin u\sin\iota,\\
p_x &= p'_x\cos\nu - p'_y\cos\iota\sin\nu,\\
p_y &= p'_x\sin\nu + p'_y\cos\iota\cos\nu,\\
p_z &= p'_y\sin\iota,
\end{aligned} \tag{A1}$$

where

$$\begin{aligned}
p'_x &= p_r\cos u - \frac{p_u}{r}\sin u,\\
p'_y &= p_r\sin u + \frac{p_u}{r}\cos u\\
\cos\iota &= L_z/p_u.
\end{aligned} \tag{A2}$$

Inverting the transformation (A1) results in

$$\begin{aligned}
r &= \sqrt{x^2+y^2+z^2},\\
\theta &= \arccos\frac{z}{r} = \arccos\left(\sqrt{1-\frac{L_z^2}{p_u^2}}\sin u\right),\\
\phi &= \arctan\frac{x}{y} = u+\nu+\arctan\left(\frac{(L_z/p_u-1)\cos u\sin u}{1+(L_z/p_u-1)\sin^2 u}\right),
\end{aligned} \tag{A3}$$

and also

$$\begin{aligned}
p_r &= \frac{1}{r}\boldsymbol{x}\cdot\boldsymbol{p},\\
p_u &= \sqrt{(\boldsymbol{x}\times\boldsymbol{p})^2},\\
p_\theta &= \sqrt{p_u^2-\frac{L_z^2}{\sin\theta^2}} = \pm p_u\sqrt{1-\frac{L_z^2}{p_u^2-(p_u^2-L_z^2)\sin^2 u}},\\
p_\phi &= L_z = xp_y - yp_x = p_u\cos\iota.
\end{aligned} \tag{A4}$$

From p_ϕ it's obvious that $\cos\iota = L_z/p_u$, in other words, the inclination angle ι is not an independent variable since it can be written in terms of p_u and L_z. This is why the inclination angle does not appear in the polar-nodal coordinates.

Appendix B: *CPKerrGeodesics* Package

This section provides some information regarding the *CPKerrGeodesics* package [34], i.e. *Canonically Perturbed Kerr Geodesics*.

This package provides the Hamiltonian, orbital frequencies, and trajectories in the AA variables once the parameters $\{a, p, e, \iota_0\}$, i.e. Kerr parameter, semilatus rectum, eccentricity and initial inclination respectively, are provided.

As we discussed in Sec. III.3, we set $n = 10$ and $n' = 7$, namely 10 canonical transformations for the radial part and 7 canonical transformations for the angular part to provide reliable orbital results for eccentricities smaller than 0.5. Then, we derive the explicit formula for the Hamiltonian (56) which is a function of $\{J_r, J_u, J_\nu, J_t\}$. Consequently, the frequencies are determined from Eqs. (62)- (65). The trajectories are determined from Eqs. (70)- (73) which are the functions of actions and angles, i.e. $\{J_r, J_u, J_\nu, J_t\}$ and $\{\psi_r, \psi_u, \psi_\nu, \psi_t\}$.

In order to determine the trajectories (70)- (73) in terms of the Mino-time λ then it does the following steps

- From the given input, i.e. $\{a, p, e, \iota_0\}$, the code determines numerically the actions $\{J_r, J_u, J_\nu, J_t\}$ from Eqs. (38)- (39) and L_z and E from [7].
- The numerical values of actions then determine the frequencies and consequently $\psi_i(\lambda) = \Upsilon_i\lambda$.

Thus, substituting these two steps into the Eqs. (70)- (73) determines the trajectories as a function of λ.

This package was inspired by *KerrGeodesics* package from the *Black Hole Perturbation Toolkit* [35]. The part of our package which calculates the constants of motion from the parameters $\{a, p, e, \iota_0\}$ was directly adopted from the *KerrGeodesics* package.

Appendix C: Two canonical transformations

In this section we provide an example of a Hamiltonian function expressed in AA variables after two canonical transformations are performed; the respective generating functions are provided as well. We also provide the trajectories in the AA variables when we applied one canonical transformation. In these relations, many constants appear; some of them are given in Eqs. (43), (44), and (48), and the others are given in Sec. .5.

.1. ***Initial conditions.*** For a given parameter set $\{a, p, e, \iota_0\}$, we set the radius of the circular orbit

$$r_c = \frac{p}{1-e^2} + e(1-10\,e)$$

and $\delta = r_c\,a/e$ as we mentioned in Sec. III.3. The L_{zc} is chosen in such a way that the relation $L_{zc} = \cot\iota_0\sqrt{Q_c}$ satisfies Eq. (44); and we set $\tilde{L}_{zc} = \cos\iota_0\,p_{uc}$.

.2. ***The Hamiltonian in AA variables.*** The Hamiltonian (56) for $n = 2$ and $n' = 2$ has the following form

$$\begin{aligned} H = &\left(\Omega_{t0}J_t + \frac{1}{2}\tilde{Q} + \Omega_{r0}J_r + \Omega_{z0}J_\nu\right) - \\ &\Big(\frac{3J_r^2(A_{rs}^2 + A_{s3}^2) + J_rA_{rs}A_{tzs}(J_t,J_\nu) + A_{tzs}^2(J_t,J_\nu)}{\Omega_{r0}} \\ &- J_r^2B_r - J_rB_{rtz}(J_t,J_\nu) - B_{tz}(J_t,J_\nu)\Big), \end{aligned} \tag{C1}$$

where

$$\begin{aligned} \tilde{Q} = 2\left(p_{uc}J_u - \tilde{L}_{zc}(J_\nu + L_{zc} - \tilde{L}_{zc})\right) - \big((J_\nu + L_{zc} - \tilde{L}_{zc})^2 \\ - J_u^2\big) + \frac{a^2}{p_{uc}^3}\big((J_t + p_{tc} - \tilde{p}_{tc})\tilde{p}_{tc}p_{uc}\left(\tilde{L}_{zc}^2 - p_{uc}^2\right) \\ + (J_\nu + L_{zc} - \tilde{L}_{zc})\tilde{L}_{zc}\left(\tilde{p}_{tc}^2 - 1\right)p_{uc} \\ - J_u\tilde{L}_{zc}^2\left(\tilde{p}_{tc}^2 - 1\right)\big) - Q_c, \end{aligned} \tag{C2}$$

and

$$A_{tzs}(J_t, J_\nu) = \frac{4\beta}{\alpha}^{1/4}(J_tb_t + J_\nu\,b_z), \tag{C3}$$

$$B_{rtz}(J_t, J_\nu) = \sqrt{\frac{\beta}{\alpha}}(c_zJ_\nu + c_tJ_t), \tag{C4}$$

$$B_{tz}(J_t, J_\nu) = c_{t^2}\,J_t^2 + c_{tz}\,J_t\,J_\nu + c_{z^2}\,J_\nu^2. \tag{C5}$$

Substituting Eqs. (C2)- (C5) into the Hamiltonian (C1) provides the approximate Hamiltonian in actions.

.3. ***Generating functions.*** The radial generating functions for this system read

$$\begin{aligned} \chi_{r1} &= -\epsilon\frac{\sqrt{J_r}}{3\Omega_{r0}}\left(3(A_{rs}J_r + A_{tzs})\cos\psi_r + A_{s3}J_r\cos(3\psi_r)\right), \\ \chi_{r2} &= \epsilon^2\frac{J_r}{8\Omega_{r0}}\Big[2\Omega_{r0}(2(B_{rc2}J_r - B_{rtz})\sin(2\psi_r) \\ &\quad + B_{rc4}J_r\sin(4\psi_r)) - (8A_{rs}A_{s3}J_r + 4A_{s3}A_{tzs})\sin(2\psi_r) \\ &\quad - A_{rs}A_{s3}J_r\sin(4\psi_r)\Big], \end{aligned} \tag{C6}$$

and the angular ones are

$$\begin{aligned} \chi_{u1} &= \frac{a^2\epsilon^2\left(\tilde{p}_{tc}^2 - 1\right)\left(p_{uc}^2 - \tilde{L}_{zc}^2\right)\sin(2\psi_u)}{8p_{uc}^3}, \\ \chi_{u2} &= \frac{a^2\epsilon^4\sin(2\psi_u)}{8p_{uc}^4}\Big[2\left(J_t + p_{tc} - \tilde{p}_{tc}\right)\tilde{p}_{tc}\,p_{uc}^3 \\ &\quad + J_u\left(\tilde{p}_{tc}^2 - 1\right)\left(3\tilde{L}_{zc}^2 - p_{uc}^2\right) \\ &\quad - 2\tilde{L}_{zc}\,p_{uc}\big((J_t + p_{tc} - \tilde{p}_{tc})\tilde{L}_{zc}\tilde{p}_{tc} \\ &\quad + (J_\nu + L_{zc} - \tilde{L}_{zc})(\tilde{p}_{tc}^2 - 1)\big)\Big]. \end{aligned} \tag{C7}$$

.4. ***Trajectories.*** The trajectories in terms of the AA variables determine from Eqs. (70)- (73). Here we apply only one canonical transformation[3], i.e. χ_{r_1} and χ_{u_1}, to derive the following trajectories

[3] Only for $t_{\rm new}$ we apply two canonical transformations, i.e. χ_{u1} and χ_{u_2} since χ_{u_1} does not depend on J_t and does not have any effect on it.

$$r_{\rm new} = \left(r_c + \delta\sqrt{\frac{2J_r}{m_c\Omega_{r0}}}\sin(\psi_r)\right) - \frac{\delta}{2\alpha\sqrt{\alpha\beta}}\Big[\sqrt{\alpha\beta}(b_t J_t + b_z J_z) + J_r(b_{p^2}\alpha + 3b_{r^2}\beta) + J_r(b_{p^2}\alpha + b_{r^2}\beta)\cos(2\psi_r)\Big],$$

$$\theta_{\rm new} = \arccos\left(\sqrt{1 - \frac{(J_\nu + L_{zc})^2}{(J_u + p_{uc})^2}}\sin\psi_u\right) + \frac{a^2(J_\nu + L_{zc})^2\left(\tilde{p}_{tc}^2 - 1\right)\left(\tilde{L}_{zc}^2 - p_{uc}^2\right)(\sin(\psi_u) - \sin(3\psi_u))}{8p_{uc}^3\,(J_u + p_{uc})^3\sqrt{1 - \frac{(J_\nu+L_{zc})^2}{(J_u+p_{uc})^2}}\sqrt{\sin^2(\psi_u)\left(\frac{(J_\nu+L_{zc})^2}{(J_u+p_{uc})^2} - 1\right) + 1}},$$

$$\phi_{\rm new} = \psi_\nu + \psi_u - \left[\frac{b_z\sqrt{J_r}\cos\psi_r}{\sqrt{2\alpha\sqrt{\alpha\beta}}}\right] + \left[\arctan\left(\frac{\left(\frac{J_\nu+L_{zc}}{J_u+p_{uc}} - 1\right)\cos\psi_u\sin\psi_u}{1 + \left(\frac{J_\nu+L_{zc}}{J_u+p_{uc}} - 1\right)\sin^2\psi_u}\right) + \right.$$
$$\left. + \frac{a^2(J_\nu + L_{zc})\left(\tilde{p}_{tc}^2 - 1\right)\left(p_{uc}^2 - \tilde{L}_{zc}^2\right)\sin(4\psi_u)}{8p_{uc}^3\left(\cos(2\psi_u)\left(J_u^2 + 2J_u p_{uc} - (J_\nu + L_{zc})^2 + p_{uc}^2\right) + J_u^2 + 2J_u p_{uc} + (J_\nu + L_{zc})^2 + p_{uc}^2\right)}\right],$$

$$t_{\rm new} = \psi_t - \left[\frac{b_t\sqrt{J_r}\cos\psi_r}{\sqrt{2\alpha\sqrt{\alpha\beta}}}\right] + \left[\frac{a^2\tilde{p}_{tc}\sin(2\psi_u)}{4p_{uc}} - \frac{a^2\tilde{L}_{zc}^2\tilde{p}_{tc}\sin(2\psi_u)}{4p_{uc}^3}\right].$$

.5. ***Constants.*** The constants which appeared in the Secs. .2, .3, and .4 are given by

$$A_{rs} = \sqrt{\frac{\alpha^{1/2}\beta^{3/2}}{2}}\left(\frac{b_{p^2}}{\beta} + 3\frac{b_{r^2}}{\alpha}\right), \tag{C8}$$

$$A_{s3} = \sqrt{\frac{\alpha^{1/2}\beta^{3/2}}{2}}\left(\frac{b_{p^2}}{\beta} - \frac{b_{r^2}}{\alpha}\right), \tag{C9}$$

$$B_r = \frac{3\,\beta\,c_{r^2}}{2\,\alpha} + \frac{1}{4}, \tag{C10}$$

$$B_{rc2} = -\frac{2\,\beta\,c_{r^2}}{\alpha}, \tag{C11}$$

$$B_{rc4} = \frac{\beta\,c_{r^2}}{2\,\alpha} - \frac{1}{4}, \tag{C12}$$

where

$$b_{r^2} = \frac{2\delta^3}{\Delta_c^4}\left(\mathfrak{B}_1\,p_{tc}^2 + \mathfrak{B}_2\,p_{tc}L_{zc} + \mathfrak{B}_3\,L_{zc}^2\right) \tag{C13}$$

$$b_t = -\frac{2\delta}{\Delta_c^3}\left(\mathfrak{B}_4 p_{tc} + \mathfrak{B}_5 L_{zc}\right), \tag{C14}$$

$$b_z = \frac{2a\delta}{\Delta_c^2}\left(M\left(r_c^2 - a^2\right)p_{tc} + a(r_c - M)L_{zc}\right), \tag{C15}$$

$$b_{p^2} = \frac{(r_c - M)}{\delta}, \tag{C16}$$

$$c_{r^2} = \frac{\delta^4}{2\Delta_c^5}\left(\mathfrak{C}_1\,p_{tc}^2 + \mathfrak{C}_2\,p_{tc}L_{zc} + \mathfrak{C}_3\,L_{zc}^2\right) \tag{C17}$$

$$c_t = \frac{\delta^2}{\Delta_c^3}\left(\mathfrak{C}_4\,p_{tc} + \mathfrak{C}_5\,L_{zc}\right) \tag{C18}$$

$$c_{t^2} = -\frac{r_c}{2\Delta_c}\left(a^2(2M + r_c) + r_c^3\right), \tag{C19}$$

$$c_{z^2} = \frac{r_c(r_c - 2M)}{2\Delta_c}, \tag{C20}$$

$$c_{tz} = -\frac{2aMr_c}{\Delta_c}, \tag{C21}$$

where

$$\mathfrak{B}_1 = 2M^2\left(-a^4(M - 2r_c) - 2a^2r_c^3 + Mr_c^4\right) \tag{C22}$$

$$\mathfrak{B}_2 = aM\left(a^4 + a^2\left(-4M^2 + 8Mr_c - 6r_c^2\right) + r_c^4\right), \tag{C23}$$

$$\mathfrak{B}_3 = a^2(M - r_c)\left(a^2 - 2M^2 + 2Mr_c - r_c^2\right), \tag{C24}$$

$$\mathfrak{B}_4 = \left(a^2 + r_c^2\right)\left(a^2(M + r_c) + r_c^2(r_c - 3M)\right), \tag{C25}$$

$$\mathfrak{B}_5 = aM(a - r_c)(a + r_c), \tag{C26}$$

and

$$\begin{aligned}
\mathfrak{C}_1 &= 4M^2\left(-a^6 + 2a^4\left(2M^2 - 5Mr_c + 5r_c^2\right) - 5a^2r_c^4 + 2Mr_c^5\right),\\
\mathfrak{C}_2 &= 4aM\left(a^4(5r_c - 4M) + 2a^2\left(4M^3 - 10M^2r_c + 10Mr_c^2 - 5r_c^3\right) + r_c^5\right),\\
\mathfrak{C}_3 &= a^2\left(a^4 - 2a^2\left(6M^2 - 10Mr_c + 5r_c^2\right) + 16M^4 - 40M^3r_c + 40M^2r_c^2 - 20Mr_c^3 + 5r_c^4\right),\\
\mathfrak{C}_4 &= \Delta_c^3 + 4M^2\left(a^4 - 3a^2r_c^2 + 2Mr_c^3\right),\\
\mathfrak{C}_5 &= 2aM\left(a^2(2M - 3r_c) + r_c^3\right).
\end{aligned} \tag{C27}$$

Appendix D: Gravitational-wave fluxes

In this section, we describe our approach of calculating gravitational-wave fluxes using Teukolsky equation [25] for geodesic orbits in the Kerr spacetime using action-angle formalism.

In the Teukolsky equation's framework, gravitational waves are treated as perturbations of the Kerr spacetime using Newmann-Penrose (NP) formalism. In this formalism, we calculate a perturbation of the NP scalar $\psi_4 = -C_{\alpha\beta\gamma\delta} n^\alpha \bar{m}^\beta n^\gamma \bar{m}^\delta$, where $C_{\alpha\beta\gamma\delta}$ is the Weyl tensor and n^μ and $\bar{m}^\mu$ are Kinnersley tetrad legs

$$n^\mu = \left(r^2 + a^2, -\Delta, 0, a\right)/(2\Sigma)\,, \tag{D1}$$

$$\bar{m}^\mu = -\left(ia\sin\theta, 0, -1, i/\sin\theta\right)/(\sqrt{2}\zeta) \tag{D2}$$

with $\zeta = r - ia\cos\theta$. This ψ_4 is governed by the Teukolsky equation [25], which we solve in frequency domain.

Because the radial and polar motion are recurrent, the strain at infinity $h = h_+ - ih_\times$ can be written as a sum over discrete frequencies

$$h = -\frac{2}{r}\sum_{lmkn} \frac{C^+_{lmkn}}{\omega^2_{mkn}} {}_{-2}S^{a\omega}_{lm}(\theta) e^{-i\omega_{mkn}u + im\phi}\,, \tag{D3}$$

where the frequencies are $\omega_{mkn} = m\Omega_\phi + k\Omega_\theta + n\Omega_r$, ${}_{-2}S^{a\omega}_{lm}(\theta)$ is the spin-weighted spheroidal harmonic function, $u = t - r^*$ is the retarded coordinate and the amplitudes can be expressed as two-dimensional integral [36]

$$C^+_{lmkn} = \frac{1}{2\pi\Upsilon}\int_0^{2\pi} \mathrm{d}\psi_r \int_0^{2\pi} \mathrm{d}\psi_\theta I^+_{lmkn}(r(\psi_r), \theta(\psi_\theta), u^r(\psi_r), u^\theta(\psi_\theta)) \times e^{i(k\psi_\theta + \omega_{mkn}\Delta t_\theta(\psi_\theta) - m\Delta\phi_\theta(\psi_\theta))} \times e^{i(n\psi_r + \omega_{mkn}\Delta t_r(\psi_r) - m\Delta\phi_r(\psi_r))}\,, \tag{D4}$$

where

$$I^+_{lmkn} = \frac{\Sigma}{W}\sum_{i=0}^{2}(-1)^i A_i \frac{d^i R^-_{lm\omega_{mkn}}}{dr^i}\,. \tag{D5}$$

$W = (R^+_{lm\omega}\partial_r R^-_{lm\omega} - R^-_{lm\omega}\partial_r R^+_{lm\omega})/\Delta$ is the invariant Wronskian and $R^\mp_{lm\omega}$ are the solutions of homogeneous radial Teukolsky equation satisfying ingoing (upgoing) boundary conditions (see, e.g., Eqs. (92) in [4]). The functions A_i are

$$A_0 = u_n^2 f^{(0)}_{nn} + u_n u_{\bar{m}} f^{(0)}_{n\bar{m}} + u^2_{\bar{m}} f^{(0)}_{\bar{m}\bar{m}}\,, \tag{D6}$$

$$A_1 = u_n u_{\bar{m}} f^{(1)}_{n\bar{m}} + u^2_{\bar{m}} f^{(1)}_{\bar{m}\bar{m}}\,, \tag{D7}$$

$$A_2 = u^2_{\bar{m}} f^{(2)}_{\bar{m}\bar{m}}\,, \tag{D8}$$

where u_n, $u_{\bar{m}}$ are projections of the four-velocity to the Kinnersley tetrad legs and the functions are

$$f^{(0)}_{nn} = -\frac{2\zeta^2}{\Delta^2}\left(\mathcal{L}^\dagger_1\mathcal{L}^\dagger_2 - 2ia\zeta^{-1}\sin\theta\mathcal{L}^\dagger_2\right)S\,, \tag{D9}$$

$$f^{(0)}_{n\bar{m}} = \frac{2\sqrt{2}\zeta^2}{\bar{\zeta}\Delta}\left(\left(\frac{iK}{\Delta} + \zeta^{-1} + \bar{\zeta}^{-1}\right)\mathcal{L}^\dagger_2 - a\sin\theta\frac{K}{\Delta}\left(\bar{\zeta}^{-1} - \zeta^{-1}\right)\right)S\,, \tag{D10}$$

$$f^{(1)}_{n\bar{m}} = \frac{2\sqrt{2}\zeta^2}{\bar{\zeta}\Delta}\left(\mathcal{L}^\dagger_2 + ia\sin\theta\left(\bar{\zeta}^{-1} - \zeta^{-1}\right)\right)S\,, \tag{D11}$$

$$f^{(0)}_{\bar{m}\bar{m}} = \frac{\zeta^2}{\bar{\zeta}^2}\left(i\partial_r\left(\frac{K}{\Delta}\right) - 2i\zeta^{-1}\frac{K}{\Delta} + \left(\frac{K}{\Delta}\right)^2\right)S\,, \tag{D12}$$

$$f^{(1)}_{\bar{m}\bar{m}} = -\frac{2\zeta^2}{\bar{\zeta}^2}\left(\zeta^{-1} + i\frac{K}{\Delta}\right)S\,, \tag{D13}$$

$$f^{(2)}_{\bar{m}\bar{m}} = -\frac{\zeta^2}{\bar{\zeta}^2}S\,, \tag{D14}$$

where $S = {}_{-2}S^{a\omega_{mkn}}_{lm}(\theta)$, $K = (r^2 + a^2)\omega - am$ and

$$\mathcal{L}^\dagger_s = \frac{\partial}{\partial\theta} - \frac{m}{\sin\theta} + a\omega\sin\theta + s\cot\theta\,. \tag{D15}$$

Thanks to the flux-balance laws, the rate of loss in E and L_z is equal to the GW fluxes of energy and angular momentum to infinity and through the horizon. Similar law holds for the Carter constant Q. Explicit expressions can be found e.g. in Eqs. (3.26)-(3.32) of [28].

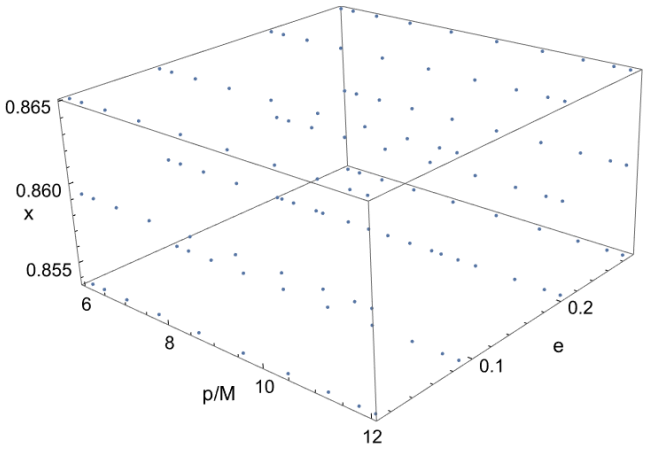

FIG. 8: Grid for interpolating the fluxes in the (p, e, x) space, $p \in (6, 12)$, $e \in (0, 0.3)$ and $x \in (\cos(31.5°), \cos(30°))$.

We have developed a new code in Mathematica which solves the inhomogeneous Teukolsky equation in the frequency domain. The transformation relations between BL coordinates and the phases $r(\psi_r)$ and $\theta(\psi_\theta)$ as well as the oscillating parts $\Delta t_{r,\theta}$ and $\Delta\phi_{r,\theta}$ are provided in the *CPKerrGeodesics* package. For the integration in Eq. (D4), the midpoint rule was employed since the integrand is periodic in ψ_r and ψ_θ and, therefore, it has exponential convergence. To find the homogeneous solutions of the radial and angular Teukolsky equation $R^{\pm}_{lm\omega}$ and ${}_{-2}S^{a\omega}_{lm}$ we used the Black Hole Perturbation Toolkit [35].

1. Flux Grid

Let us now briefly comment on the calculation of the total fluxes of the constants of motion. The averaged rate of change of a constant of motion C is given by the corresponding fluxes to infinity and horizon

$$\left\langle \frac{\mathrm{d}C}{\mathrm{d}t} \right\rangle = -\Big(F^{\infty} + F^{H}\Big). \tag{D16}$$

The fluxes can be in the same fashion as the strain (D3) expressed as sum of individual modes

$$F = \sum_{l,m,k,n} F_{lmkn}. \tag{D17}$$

Each of the F_{lmkn} is determined by the amplitudes $C^{\pm}_{lmkn}$ discussed above. During our calculation, we use the symmetry $F_{lmkn} = F_{l-m-k-n}$. We, thus, sum only the modes with $\omega_{mkn} > 0$ and then multiply the result by 2.

Our summation algorithm starts from the dominant F_{220n} modes where we start by calculating the contributions for growing n. We stop this procedure at some n_0 once F_{220n} stops converging to zero and starts oscillating as shown in Fig. 9. This happens for higher values of n and the exact value of n_0 depends on the eccentricity; for higher eccentricities, we have to sum more modes so n_0 is larger for larger e. This error is introduced by our perturbative approximation to geodesics. All the modes with contribution smaller than $F^{\infty}_{220n_0} + F^{H}_{220n_0}$ are omitted in the subsequent summation. We then sum over k

$$F_{22} = \sum_{k=-3}^{3} F_{22k}, \quad F_{22k} = \sum_{n} F_{22kn}$$

For the $m = 2$ mode, we sum over l from 2 to 10.

To shorten the time of the calculation for the other modes, it is useful to estimate the maximum value $\max_k F_{lmk} = F_{lmk_{\max}}$ with $F_{lmk} = \sum_n F_{lmkn}$, when summing over k for fixed m and l. F_{lmk} for fixed m and l seems to have a maximum when $k_{\max} = l - m$. In our summation the index k, then goes from $k_{\max} - 3$ to $k_{\max} + 3$. Having settled the summation over k, we then sum over m from -3 to 6 with l going from $\max(2, |m|)$ to 10. Regardless of our summation scheme, it is important to stress again that the deviation from the correct values of fluxes is dominantly caused by our approximation of the geodesics and not by neglecting higher modes.

Even if this was already discussed, it is useful to compare the partial fluxes F_{lmkn} computed using our perturbatively derived geodesics to those calculated from the exact geodesics using the same Teukolsky solver just like we did in Sec. IV for the total fluxes. If we fix the indices l, m, k, the expected behaviour would be $F_{lmkn} \to 0$ as $n \to \infty$. When looking at the logarithmic plots 9 depicting the dominant modes F_{220n}, we can indeed see that the partial fluxes decrease with n but due to numerical errors even the fluxes calculated using the KerrGeodesics package eventually start oscillating around a small but non-zero value. When close to the spherical orbits we can see that this happens for small n but this is not an issue as the higher modes barely contribute to the sum (for an exact spherical orbit there is no sum over n). For eccentric orbits more n-modes need to be summed and here there is a clear difference between the exact geodesics and our approximation. As the oscillations start sooner (for $n = n_0$) when using the approximation, we are forced to neglect all modes with $n > n_0$ which is the primary source of deviation from the correct values of the total fluxes. By adding more generating functions, we can push n_0 to higher values which is illustrated in Fig. 9 (5 versus 10 generating functions). For higher modes the integrand in Eq. (D4) has more and more oscillations which tend to cancel each other, leaving us with a very small resulting number, which means that even a small deviation in the integrand can create a large error in the Teukolsky amplitude and consequently in the partial fluxes.

To calculate the fluxes we used a grid and Chebyshev interpolation like in [29]. In particular, we created a $10 \times 4 \times 3$ grid in the (p, e, x) space for $a = 0.5M$

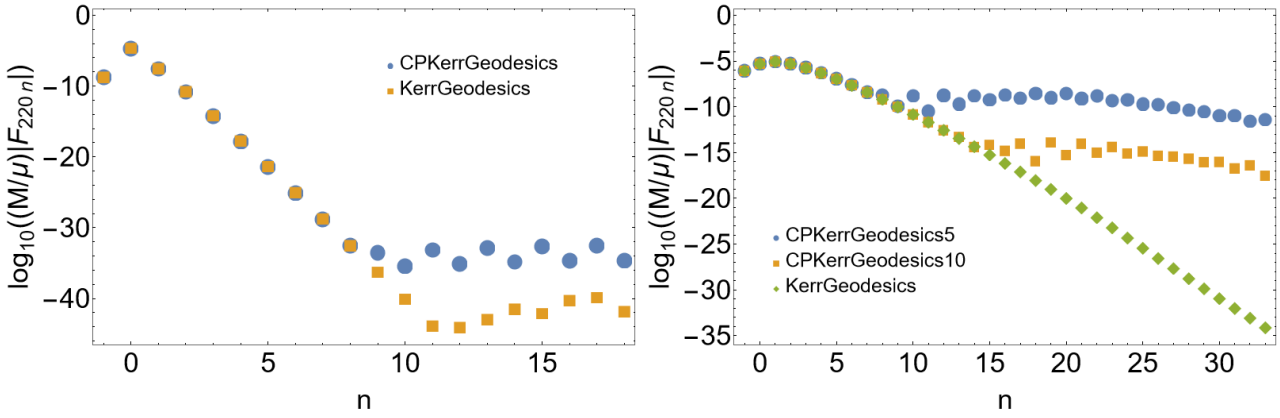

FIG. 9: Logarithmic plots comparing the convergence of partial fluxes F_{220n} (more specifically, the energy fluxes to infinity) for the KerrGeodesics package with our CPKerrGeodesics package. The orbital parameters are $a = 0.5M$, $p = 10M$, $\iota_0 = \pi/6$ with eccentricities $e = 0.01$ (left) and $e = 0.3$ (right).

(see Fig. 8) with the interpolation points located at the Chebyshev nodes. Note that the grid is simpler than in [29] since we do not come very close to the separatrix. The relative error of the Chebyshev interpolation is of the order 10^{-3} which is similar to the relative errors of the fluxes themselves. Since there are analytical formulas $C_i = C_i(p, e, x)$ linking the constants of motion to the orbital parameters, it is possible to differentiate them and transform the fluxes of C_i to fluxes of (p, e, x), this is in detail described in [28].

Conclusion

The results presented in this thesis belong to two distinct areas of gravitational physics, however in both cases the starting point of our work was a stationary axially symmetric spacetime.

The first part of our work focused on Weyl solutions constructed from "particles" and "rods" which can be extended to solutions with scalar field using the symmetries of the field equations. While investigating these solutions and various generating techniques like the Janis-Newman algorithm, a particular solution captured our mind which we then studied in detail in our publication [68]. This spherical Curzon-Chazy solution has several uncommon properties, it is a wormhole which is not symmetric with respect to its throat, it possesses a non-scalar curvature singularity. While its asymptotic structure may seem unremarkable at first sight (it resembles Minkowski spacetime), it is a one-directional time machine allowing geodesic observers to reach future timelike infinity in a finite proper time. The mass-energy content of the spacetime was also widely discussed which enabled us to interpret the solution partly from the Newtonian perspective.

The other direction of research pursued in this thesis was in the area of gravitational waves and extreme mass ratio inspirals. This work resulted in two papers, [69] and [46] (the paper [46] is not yet published at the time of writing this thesis but it has been accepted for publication in a scientific journal). While the inspirals were calculated only at the adiabatic order, the novelty of our work lay in the use of the canonical perturbation theory to solve the geodesic part of the problem. The main motivation was to obtain precomputed analytical expression for the geodesics that would allow for a computationally effective calculation of gravitational-wave fluxes while at the same time enable us to replace standard orbital parameters with action-angle coordinates in perturbed spacetimes which do not have a complete set of integrals of motion.

The difference between the papers [69] and [46] lay in the spacetime in which the inspiral was studied and the method used to calculate the fluxes of the constants of motion. In the first paper the spacetime was a Schwarzshild black hole perturbed by a distant matter. This set-up proved to be more complicated then in the case of Kerr spacetime used in the second paper as the geodesic motion is non-integrable in the first case. On the other hand in the first paper we used a simple quadrupole formalism (a post-Newtonian approach) for the computation of gravitational-wave fluxes and waveforms while in the Kerr spacetime we employed the black hole perturbation theory, namely the Teukolsky formalism. In our future work we would like to combine the strengths of both of these papers, which means calculating an EMRI in a perturbed black-hole spacetime while simultaneously use a fully relativistic approach for the fluxes.

Bibliography

[1] Abbott, B. P., et al. Observation of gravitational waves from a binary black hole merger. *Phys. Rev. Lett.*, 116:061102, Feb 2016.

[2] Abraham, R. and Marsden, J. *Foundations of Mechanics*. AMS Chelsea publishing. AMS Chelsea Pub./American Mathematical Society, 2008.

[3] Amaro-Seoane, P., et al. Astrophysics with the laser interferometer space antenna. *Living Reviews in Relativity*, 26(1), Mar 2023.

[4] Antonowicz, M. On the freedom of choice of the action-angle variables for Hamiltonian systems. *Journal of Physics A: Mathematical and General*, 14 (5):1099, May 1981.

[5] Arnold, V., Iacob, A., Kozlov, V., and Neishtadt, A. *Mathematical Aspects of Classical and Celestial Mechanics*. Number sv. 3 in Dinamicheskie sistemy. Springer Berlin Heidelberg, 2013.

[6] Arnold, V. I. *Mathematical methods of classical mechanics*, volume 60. Springer Science & Business Media, 2013.

[7] Arnowitt, R., Deser, S., and Misner, C. W. Republication of: The dynamics of general relativity. *General Relativity and Gravitation*, 40(9):1997–2027, Aug 2008.

[8] Asada, H. and Futamase, T. Chapter 2. post-Newtonian approximation. *Progress of Theoretical Physics Supplement*, 128:123–181, 1997.

[9] Barack, L. and Pound, A. Self-force and radiation reaction in general relativity. *Reports on Progress in Physics*, 82(1):016904, Nov 2018.

[10] Belinfante, F. J. On the current and the density of the electric charge, the energy, the linear momentum and the angular momentum of arbitrary fields. *Physica D: Nonlinear Phenomena*, 7:449–474, 1940.

[11] Bini, D., Cherubini, C., Jantzen, R. T., and Ruffini, R. Teukolsky master equation: de Rham wave equation for gravitational and electromagnetic fields in vacuum. *Progress of Theoretical Physics*, 107(5):967–992, May 2002.

[12] Blanchet, L. Gravitational radiation from post-Newtonian sources and inspiralling compact binaries. *Living Reviews in Relativity*, 17(1), feb 2014.

[13] Blanco, F. M. and Flanagan, É . É. Particle motion under the conservative piece of the self-force is hamiltonian. *Physical Review Letters*, 130(5), feb 2023.

[14] Bojowald, M. *Canonical Gravity and Applications: Cosmology, Black Holes, and Quantum Gravity*. Cambridge University Press, 2010.

[15] Brown, J. D. and York, J. W. Quasilocal energy and conserved charges derived from the gravitational action. *Physical Review D*, 47(4):1407–1419, feb 1993.

[16] Damour, T. The general relativistic two body problem and the effective one body formalism. In *General Relativity, Cosmology and Astrophysics*, pages 111–145. Springer International Publishing, 2014.

[17] Deprit, A. Canonical transformations depending on a small parameter. *Celestial Mechanics*, 1(1):12–30, March 1969.

[18] Drake, S. P. and Szekeres, P. Uniqueness of the Newman–Janis algorithm in generating the Kerr–Newman metric. *General Relativity and Gravitation*, 32(3):445–457, Mar 2000.

[19] Drasco, S. and Hughes, S. A. Gravitational wave snapshots of generic extreme mass ratio inspirals. *Physical Review D*, 73(2), Jan 2006.

[20] Drummond, L. V. and Hughes, S. A. Precisely computing bound orbits of spinning bodies around black holes. II. generic orbits. *Physical Review D*, 105(12), jun 2022.

[21] Efthymiopoulos, C. Canonical perturbation theory; stability and diffusion in Hamiltonian systems: applications in dynamical astronomy. *Workshop Series of the Asociacion Argentina de Astronomia*, 3:3–146, January 2011.

[22] Čížek, P. and Semerák, O. Perturbation of a Schwarzschild black hole due to a rotating thin disk. *The Astrophysical Journal Supplement Series*, 232 (1):14, sep 2017.

[23] Ellis, G. F. R. and Schmidt, B. G. Singular space-times. *Gen. Rel. Grav.*, 8: 915–953, 1977.

[24] Erbin, H. Janis–Newman algorithm: Generating rotating and NUT charged black holes. *Universe*, 3(1):19, Mar 2017.

[25] Flanagan, É . É. and Hughes, S. A. The basics of gravitational wave theory. *New Journal of Physics*, 7:204–204, sep 2005.

[26] Fujita, R. and Hikida, W. Analytical solutions of bound timelike geodesic orbits in Kerr spacetime. *Classical and Quantum Gravity*, 26(13):135002, jun 2009.

[27] Gad, R. M. On Møller energy-momentum complex of a static axially symmetric vacuum space-time. *Astrophysics and Space Science*, 314(4):369–369, apr 2008.

[28] Gambini, R., Mato, E., Olmedo, J., and Pullin, J. Classical axisymmetric gravity in real Ashtekar variables. *Classical and Quantum Gravity*, 36(12): 125009, May 2019.

[29] Gambini, R., Mato, E., and Pullin, J. Axisymmetric gravity in real Ashtekar variables: the quantum theory. *Classical and Quantum Gravity*, 37(11): 115010, May 2020.

[30] Geroch, R., Held, A., and Penrose, R. A space–time calculus based on pairs of null directions. *J. Math. Phys. (N.Y.), v. 14, no. 7, pp. 874-881.*

[31] Gibbons, G. W. Phantom matter and the cosmological constant. *arXiv:0302199*, 2003.

[32] Gibbons, G. W. and Volkov, M. S. Weyl metrics and wormholes. *Journal of Cosmology and Astroparticle Physics*, 2017(05):039–039, May 2017.

[33] Giorgilli, A. and Locatelli, U. Kolmogorov theorem and classical perturbation theory. *Z. Angew. Math. Phys.*, 48(2):220–261, Mar 1997.

[34] Grébert, B. Birkhoff Normal Form and Hamiltonian PDEs. In de France, S. M., editor, *Partial differential equations and applications.*, Séminaires et Congrès, pages 1–46. Société Mathématique de France, 2007. 55 pages.

[35] Griffiths, J. B. and Podolský, J. *Exact Space-Times in Einstein's General Relativity*. Cambridge Monographs on Mathematical Physics. Cambridge University Press, 2009.

[36] Harms, E., Bernuzzi, S., Nagar, A., and Zenginoğ lu, A. A new gravitational wave generation algorithm for particle perturbations of the Kerr spacetime. *Classical and Quantum Gravity*, 31(24):245004, Nov 2014.

[37] Hayward, S. A. Dynamic wormholes. *International Journal of Modern Physics D*, 08(03):373–382, Jun 1999.

[38] Hinderer, T. and Flanagan, É . É. Two-timescale analysis of extreme mass ratio inspirals in Kerr spacetime: Orbital motion. *Physical Review D*, 78(6), sep 2008.

[39] Hughes, S. A. Computing radiation from Kerr black holes: Generalization of the Sasaki-Nakamura equation. *Physical Review D*, 62:044029, 2000.

[40] Hughes, S. A. Evolution of circular, nonequatorial orbits of Kerr black holes due to gravitational-wave emission. II. inspiral trajectories and gravitational waveforms. *Physical Review D*, 64(6), Aug 2001.

[41] Hughes, S. A., Warburton, N., Khanna, G., Chua, A. J., and Katz, M. L. Adiabatic waveforms for extreme mass-ratio inspirals via multivoice decomposition in time and frequency. *Physical Review D*, 103(10), May 2021.

[42] Isaacson, R. A. Gravitational radiation in the limit of high frequency. i. the linear approximation and geometrical optics. *Phys. Rev.*, 166:1263–1271, Feb 1968.

[43] Isaacson, R. A. Gravitational radiation in the limit of high frequency. ii. nonlinear terms and the effective stress tensor. *Phys. Rev.*, 166:1272–1280, Feb 1968.

[44] Jaramillo, J. L. and Gourgoulhon, E. Mass and angular momentum in general relativity. In *Mass and Motion in General Relativity*, pages 87–124. Springer Netherlands, 2009.

[45] Katz, J., Lynden-Bell, D., and Bičák, J. Gravitational energy in stationary spacetimes. *Classical and Quantum Gravity*, 23(23):7111–7127, Oct 2006.

[46] Kerachian, M., Polcar, L., Skoupý, V., Efthymiopoulos, C., and Lukes-Gerakopoulos, G. Action-angle formalism for extreme mass ratio inspirals in Kerr spacetime, 2023. Accepted for publication in Physical Review D.

[47] Komar, A. Covariant conservation laws in general relativity. *Phys. Rev.*, 113:934–936, Feb 1959.

[48] Krikorian, R. On the divergence of Birkhoff normal forms. *Publications mathématiques de l'IHÉS*, 135:1–181, 04 2022.

[49] Lichtenberg, A. and Lieberman, M. *Regular and Chaotic Dynamics*. Applied Mathematical Sciences. Springer New York, 2013.

[50] Lynch, P., van de Meent, M., and Warburton, N. Eccentric self-forced inspirals into a rotating black hole. *Classical and Quantum Gravity*, 39(14): 145004, jun 2022.

[51] Lynden-Bell, D., Katz, J., and Bičák, J. Energy and angular momentum densities of stationary gravitational fields. *Phys. Rev. D*, 75:024040, 2007.

[52] Mars, M. and Senovilla, J. M. M. Axial symmetry and conformal Killing vectors. *Classical and Quantum Gravity*, 10(8):1633–1647, Aug 1993.

[53] Maselli, A., Franchini, N., Gualtieri, L., and Sotiriou, T. P. Detecting scalar fields with extreme mass ratio inspirals. *Physical Review Letters*, 125(14), sep 2020.

[54] McLeod, R. J. A brief review Noether's theorems and their application to general relativity. *arXiv: 2106.04393*, 2021.

[55] Mino, Y. Perturbative approach to an orbital evolution around a supermassive black hole. *Phys. Rev. D*, 67:084027, Apr 2003.

[56] Mirshekari, S. and Abbassi, A. M. Energy-momentum Prescriptions in General Spherically Symmetric Space-times. *Mod. Phys. Lett. A*, 24:747–758, 2009.

[57] Misner, C. W., Thorne, K. S., and Wheeler, J. A. *Gravitation*. W. H. Freeman, San Francisco, 1973.

[58] Møller, C. On the localization of the energy of a physical system in the general theory of relativity. *Annals of Physics*, 4(4):347–371, 1958.

[59] Moore, C. J., Chua, A. J. K., and Gair, J. R. Gravitational waves from extreme mass ratio inspirals around bumpy black holes. *Classical and Quantum Gravity*, 34(19):195009, sep 2017.

[60] Morris, M. S. and Thorne, K. S. Wormholes in space-time and their use for interstellar travel: A tool for teaching general relativity. *Am. J. Phys.*, 56: 395–412, 1988.

[61] Newman, E. T. and Janis, A. I. Note on the Kerr spinning particle metric. *J. Math. Phys.*, 6:915–917, 1965.

[62] Pan, Z., Yang, H., Bernard, L., and Bonga, B. Resonant dynamics of extreme mass-ratio inspirals in a perturbed Kerr spacetime, 2023.

[63] Pazos-Avalos, E. and Lousto, C. O. Numerical integration of the Teukolsky equation in the time domain. *Physical Review D*, 72(8), oct 2005.

[64] Peters, P. C. Gravitational radiation and the motion of two point masses. *Phys. Rev.*, 136:B1224–B1232, Nov 1964.

[65] Poisson, E. and Will, C. M. *Gravity: Newtonian, Post-Newtonian, Relativistic*. Cambridge University Press, 2014.

[66] Polcar, L. and Semerák, O. Free motion around black holes with discs or rings: Between integrability and chaos. VI. the Melnikov method. *Physical Review D*, 100(10), Nov 2019.

[67] Polcar, L., Suková , P., and Semerák, O. Free motion around black holes with disks or rings: Between integrability and chaos–V. *The Astrophysical Journal*, 877(1):16, May 2019.

[68] Polcar, L. and Svítek, O. Phantom scalar field counterpart to Curzon–Chazy spacetime. *Classical and Quantum Gravity*, 39(18):185002, Aug 2022.

[69] Polcar, L., Lukes-Gerakopoulos, G., and Witzany, V. Extreme mass ratio inspirals into black holes surrounded by matter. *Physical Review D*, 106(4), Aug 2022.

[70] Pound, A. and Poisson, E. Osculating orbits in Schwarzschild spacetime, with an application to extreme mass-ratio inspirals. *Physical Review D*, 77 (4), feb 2008.

[71] Pound, A. and Wardell, B. Black hole perturbation theory and gravitational self-force. In *Handbook of Gravitational Wave Astronomy*, pages 1–119. Springer Singapore, 2021.

[72] Robinson, D. C. Uniqueness of the Kerr black hole. *Phys. Rev. Lett.*, 34: 905–906, Apr 1975.

[73] Robinson, I. On the Bel - Robinson tensor. *Classical and Quantum Gravity*, 14(1A):A331, Jan 1997.

[74] Sago, N., Tanaka, T., Hikida, W., Ganz, K., and Nakano, H. Adiabatic evolution of orbital parameters in Kerr spacetime. *Progress of Theoretical Physics*, 115(5):873–907, May 2006.

[75] Sasaki, M. and Nakamura, T. Gravitational Radiation from a Kerr Black Hole. I. Formulation and a Method for Numerical Analysis. *Progress of Theoretical Physics*, 67(6):1788–1809, 06 1982.

[76] Sasaki, M. and Tagoshi, H. Analytic black hole perturbation approach to gravitational radiation. *Living Reviews in Relativity*, 6(1), Nov 2003.

[77] Schmidt, W. Celestial mechanics in Kerr spacetime. *Classical and Quantum Gravity*, 19(10):2743–2764, apr 2002.

[78] Semerák, O. Static axisymmetric rings in general relativity: How diverse they are. *Physical Review D*, 94(10), Nov 2016.

[79] Skoupý , V. and Lukes-Gerakopoulos, G. Adiabatic equatorial inspirals of a spinning body into a Kerr black hole. *Physical Review D*, 105(8), apr 2022.

[80] Speri, L. and Gair, J. R. Assessing the impact of transient orbital resonances. *Physical Review D*, 103(12), jun 2021.

[81] Stephani, H., Kramer, D., MacCallum, M., Hoenselaers, C., and Herlt, E. *Exact Solutions of Einstein's Field Equations*. Cambridge Monographs on Mathematical Physics. Cambridge University Press, 2 edition, 2003.

[82] Swanson, M. S. *Classical Field Theory and the Stress–Energy Tensor (Second Edition)*. 2053-2563. IOP Publishing, 2022.

[83] Szabados, L. B. Quasi-Local Energy-Momentum and Angular Momentum in General Relativity. *Living Rev. Rel.*, 12:4, 2009.

[84] Szekeres, P. and Morgan, F. H. Extensions of the Curzon metric. *Commun. Math. Phys.*, 32:313–318, 1973.

[85] Taylor, J. P. W. Unravelling directional singularities. *Class. Quant. Grav.*, 22:4961–4971, 2005.

[86] Teukolsky, S. A. and Press, W. H. Perturbations of a rotating black hole. III - Interaction of the hole with gravitational and electromagnet ic radiation. *Astrophys. J.*, 193:443–461, 1974.

[87] Teukolsky, S. A. Perturbations of a rotating black hole. 1. Fundamental equations for gravitational electromagnetic and neutrino field perturbations. *Astrophys. J.*, 185:635–647, 1973.

[88] van de Meent, M. and Shah, A. G. Metric perturbations produced by eccentric equatorial orbits around a Kerr black hole. *Physical Review D*, 92(6), sep 2015.

[89] Virbhadra, K. S. Naked singularities and Seifert's conjecture. *Phys. Rev. D*, 60:104041, Oct 1999.

[90] Wald, R. M. *General Relativity*. Chicago Univ. Pr., Chicago, USA, 1984.

[91] Wardell, B. and Warburton, N. Applying the effective-source approach to frequency-domain self-force calculations: Lorenz-gauge gravitational perturbations. *Physical Review D*, 92(8), oct 2015.

[92] Will, C. M. Perturbation of a Slowly Rotating Black Hole by a Stationary Axisymmetric Ring of Matter. I. Equilibrium Configurations. *apj*, 191:521–532, July 1974.

[93] Zerilli, F. J. Gravitational field of a particle falling in a Schwarzschild geometry analyzed in tensor harmonics. *Phys. Rev. D*, 2:2141–2160, Nov 1970.

List of publications

1. Kerachian, M., Polcar, L., Skoupý, V., Efthymiopoulos, C., and Lukes-Gerakopoulos, G. Action-angle formalism for extreme mass ratio inspirals in Kerr spacetime, 2023. Accepted for publication in Physical Review D

2. Polcar, L., Lukes-Gerakopoulos, G., and Witzany, V. Extreme mass ratio inspirals into black holes surrounded by matter. *Physical Review D*, 106(4), Aug 2022

3. Polcar, L. and Svítek, O. Phantom scalar field counterpart to Curzon–Chazy spacetime. *Classical and Quantum Gravity*, 39(18):185002, Aug 2022

4. Polcar, L. and Semerák, O. Free motion around black holes with discs or rings: Between integrability and chaos. VI. the Melnikov method. *Physical Review D*, 100(10), Nov 2019

5. Polcar, L., Suková , P., and Semerák, O. Free motion around black holes with disks or rings: Between integrability and chaos–V. *The Astrophysical Journal*, 877(1):16, May 2019